UNIVERSIDADE DE PASSO FUNDO

PROGRAMA DE PÓS-GRADUAÇÃO
EM ENGENHARIA CIVIL E AMBIENTAL

Área de concentração: Infraestrutura e Meio Ambiente

Tese de Doutorado

MATERIAL ASFÁLTICO FRESADO ESTABILIZADO COM LIGANTE ÁLCALI-ATIVADO ALTERNATIVO: DESEMPENHO MECÂNICO, MICROESTRUTURAL, DURABILIDADE E LIXIVIAÇÃO

Deise Trevizan Pelissaro

Passo Fundo

2023

CIP – Catalogação na Publicação

P384m Pelissaro, Deise Trevizan
Material asfáltico fresado estabilizado com ligante álcali-ativado alternativo: [recurso eletrônico] : desempenho mecânico, microestrutural, durabilidade e lixiviação / Deise Trevizan Pelissaro. – 2023.
5.5 MB ; PDF.

Orientador: Prof. Dr. Francisco Dalla Rosa.
Tese (Doutorado em Engenharia) – Universidade de Passo Fundo, 2023.

1. Pavimentos de asfalto. 2. Resíduos agrícolas - Reaproveitamento. 3. Geopolímeros. I. Dalla Rosa, Francisco, orientador. II. Título.

CDU: 625.8

Catalogação: Bibliotecária Juliana Langaro Silveira - CRB 10/2427

Material asfáltico fresado estabilizado com ligante álcali-ativado alternativo: desempenho mecânico, microestrutural, durabilidade e lixiviação

Deise Trevizan Pelissaro

Tese de Doutorado apresentada ao Programa de Pós-Graduação em Engenharia Civil e Ambiental da Universidade de Passo Fundo, como parte dos requisitos para obtenção do título de Doutor em Engenharia Civil.

Orientador: Prof. Dr. Francisco Dalla Rosa

Comissão Examinadora

Prof.ª Dra. Kamilla Vasconcelos Savasini

Prof. Dr. Eduardo Pavan Korf

Prof. Dr. Pedro Domingos Marques Prietto

Prof. Dra. Gladis Camarini

Passo Fundo, maio de 2023.

RESUMO

Do ponto de vista social e ambiental, a utilização de resíduos industriais e da construção civil se mostra como uma alternativa para a preservação e reutilização dos recursos naturais. Na pavimentação, o uso de material asfáltico fresado (RAP) na reciclagem de pavimentos consiste em uma alternativa de recuperação estrutural e funcional da rodovia. Apesar das vantagens técnicas, econômicas e ambientais do método, frequentemente o RAP necessita ser estabilizado por algum material com propriedades cimentantes, usualmente o cimento Portland. No entanto, devido às altas taxas de CO_2 emitidas durante a sua produção, os materiais álcali-ativados se apresentam como uma alternativa para a substituição de materiais cimentícios tradicionais. O processo de álcali-ativação consiste na mistura de um mineral aluminossilicato (precursor) e uma solução altamente alcalina (ativador). Um dos ativadores mais utilizados é o silicato de sódio, que apesar do seu bom desempenho também apresenta um processo de produção com significativas emissões de dióxido de carbono. Nesse sentido, a cinza de casca de arroz (CCA) é um resíduo rico em sílica com potencial para desenvolvimento de ativadores alternativos. Assim, o objetivo desta pesquisa consiste na avaliação da viabilidade técnica de um sistema álcali ativado de CCA, metacaulim e hidróxido de sódio na reciclagem profunda de pavimentos. Para atingir esse objetivo foi realizado inicialmente um estudo paramétrico da produção do ligante álcali ativado alternativo (LAA) de modo a reduzir o impacto ambiental e energético do ligante. Posteriormente diversas proporções de RAP e LAA foram avaliadas em termos de desempenho mecânico e microestrutural, durabilidade, desempenho a longo prazo, lixiviação de álcalis e degradação por fadiga. Os resultados demonstraram que o LAA se apresenta como uma opção adequada para uso na reciclagem de RAP. Do ponto de vista ambiental, os resultados deste estudo mostram que a técnica traz perspectivas positivas, juntamente com tecnologias inovadoras, para o desenvolvimento de pavimentos sustentáveis.

Palavras-chave: Reciclagem profunda de pavimentos; Álcali-ativação; Silicato de sódio; Cinza de casca de arroz.

ABSTRACT

From a social and environmental point of view, the use of industrial and civil construction waste is an alternative for the preservation and reuse of natural resources. In paving, the use of Reclaimed. Asphalt Pavement (RAP) in the recycling of pavements is an alternative for the structural and functional recovery of the highway. Despite the technical, economic and environmental advantages of the method, RAP often needs to be stabilized by some material with cementing properties, usually Portland cement. However, due to the high rates of CO_2 emitted during their production, alkali-activated materials are presented as an alternative to replace traditional cementitious materials. The alkali-activation process consists of mixing an aluminosilicate mineral (precursor) and a highly alkaline solution (activator). One of the most used activators is sodium silicate, which despite its good performance also has a production process with significant carbon dioxide emissions. In this sense, rice husk ash (RHA) is a residue rich in silica with potential for the development of alternative activators. Thus, the objective of this research is to evaluate the technical viability of an alkali activated system of RHA, metakaolin and sodium hydroxide in the deep recycling of pavements. To achieve this objective, a parametric study of the production of the alternative activated alkali binder (AAB) was initially carried out in order to reduce the environmental and energy impact of the binder. Subsequently, various ratios of RAP and AAB were evaluated in terms of mechanical and microstructural performance, durability, long-term performance, alkali leaching and fatigue degradation. The results demonstrated that the AAB presents itself as a suitable option for use in the recycling of RAP. From an environmental point of view, the results of this study show that the technique brings positive perspectives, together with innovative technologies, for the development of sustainable pavements.

Keywords: Depth pavement recycling; Alkali-activation; Sodium silicate; Rice husk ash.

SUMÁRIO

1. INTRODUÇÃO

Neste capítulo faz-se uma contextualização da relevância da pesquisa e da problemática envolvida, explicitando as razões que motivaram seu desenvolvimento. Além disso, são apresentados os objetivos que nortearam a realização da investigação e a estrutura de organização do trabalho.

1.1 Relevância da Pesquisa

A indústria da construção é um dos setores mais movimentados do mundo e frequentemente é utilizada como um indicador do nível de desenvolvimento de algumas regiões (RIVERA *et al.*, 2021). Particularmente o setor de infraestrutura rodoviária compreende 21 milhões de quilômetros em todo o mundo (WORLD BANK GROUP, 2018), e os setores industriais relacionados são considerados responsáveis por 24% das emissões globais de Gases de Efeito Estufa em todo o mundo (PLATI, 2019; IEA, 2019). No Brasil, 61% do transporte de carga e 95% do transporte de passageiros é realizado pelo modal rodoviário (CNT, 2019), evidenciando, a consolidação deste modal ao longo dos anos e mostrando a importância da infraestrutura rodoviária para o desenvolvimento econômico do país. Apesar da alta demanda por esse modal de transporte, apenas 12,4% (213.453 km) das rodovias são pavimentadas, mostrando que ainda existe uma grande quantidade de investimentos a serem destinados para este setor e, portanto, a necessidade também de grandes quantidades de materiais de pavimentação. Os agregados naturais são uma fonte não renovável e um dos principais componentes dos pavimentos, onde qualquer pequena ação de reciclagem pode reduzir significativamente o impacto ambiental do setor de infraestrutura.

Dessa forma avaliar novas tecnologias e alternativas se torna extremamente importante do ponto de vista econômico e ambiental. No âmbito econômico, para diminuir os custos elevados de manutenção, pesquisadores e gestores vêm buscando encontrar novas opções para o aproveitamento dos materiais, diminuir o consumo de energia, agilizar as intervenções de restauração, entre outros. Enquanto que em relação ao setor ambiental, busca-se minimizar o consumo de agregados naturais, as movimentações de terras, os combustíveis utilizados, entre outros (PIRES, 2014).

Atualmente, as ações de sustentabilidade em pavimentos compreendem o emprego de diversos tipos de agregados reciclados, sendo mais comuns o concreto reciclado (KISKU *et al.*,

2017), escória (HUANG *et al*., 2007), resíduos de areia de fundição (YAZOGHLI-MARZOUK *et al*., 2014), resíduos de vidro (JAMSHIDI *et al*., 2016), tijolo triturado (MOHAMMADINIA *et al*., 2017) e pavimento asfáltico fresado (RAP) (ANTUNES *et al*., 2019). O RAP é um resíduo produzido durante a reabilitação de pavimentos e uma quantidade muito elevada desse material ainda não é reciclada sendo descartada em aterros. Alguns estudos afirmam que a reciclagem de material asfáltico fresado pode reduzir o custo geral das seções do pavimento em 40% - 46% (SINGH *et al*., 2018; DEBBARMA *et al*., 2019). Além disso, recentemente foi publicada no Brasil a Resolução n° 14, de 8 de julho de 2021 que dispõe que todas as obras de restauração, adequação de capacidade e ampliação do Departamento Nacional de Infraestrutura de Transportes (DNIT) devem incluir o reaproveitamento do RAP.

A implementação do RAP como material de construção de pavimentos se destaca quando se trata das camadas de base, uma vez que são mais espessas e, portanto, podem consumir maiores volumes de materiais reciclados. No entanto, o uso de grandes quantidades de agregados reciclados representa, em geral, uma perda de propriedades que precisa ser compensada com o uso de ligantes ou estabilizadores, ou seja, agentes que aumentam a resistência à compressão e ao impacto e a integridade geral das camadas (AVIRNENI e SARIDE, 2016; ARULRAJAH *et al*., 2014). Para a estabilização química, tem-se empregado materiais com características aglomerantes, como a cal hidratada ou o cimento Portland, sendo largamente utilizados para camadas como solos-cal e solos-cimentos (INGLES; METCALF, 1972). O estabilizador mais usado para camadas de base é o cimento Portland, um material com uma grande contribuição na emissão de gases de efeito estufa, que são liberados durante sua fabricação (PATEL e SHAH, 2018). Cada tonelada de cimento produz aproximadamente 0,87 tonelada de dióxido de carbono, que é responsável por aproximadamente 6%-7% das emissões antropogênicas de CO_2, além de uma redução significativa dos recursos naturais (APRIANTI *et al*., 2015).

Em paralelo a necessidade de minimizar o consumo de energia e as emissões de gases do efeito estufa na atmosfera, existe uma preocupação crescente em relação ao armazenamento e descarte de materiais residuais ou subprodutos industriais (SCHARFF, 2014). Dessa forma, uma das possíveis alternativas ao cimento Portland são os materiais álcali ativados, que podem reduzir a pegada de carbono em até 80% (DUXSON *et al*., 2007) e mesmo assim apresentar boas propriedades mecânicas e durabilidade. Esses ligantes são produto da reação entre um mineral de aluminossilicato (precursor), com uma solução alcalina (ativador) (PROVIS e BERNAL, 2014). A denominação de produtos álcali-ativados é atribuída aos sistemas

produzidos com materiais com a presença de Al_2O_3, SiO_2 e um elevado conteúdo de CaO, enquanto que materiais com reduzido teor de CaO são chamados de geopolímeros. Embora exista essa diferença na nomenclatura os dois grupos de materiais são frequentemente utilizados sem distinção, gerando discordâncias na literatura.

Esta classe de materiais é muito versátil devido à grande variedade de matérias-primas e formas de produção. Inúmeros subprodutos industriais, resíduos agrícolas, e outros produtos residuais podem ser utilizados como fonte de materiais aluminossilicatos, como por exemplo cinza volante, escória granulada de alto forno, cinza de casca de arroz (CCA) e cinza de óleo de palma (YANG *et al*., 2013; DAVIDOVITS, 2008; DUXSON *et al*., 2007). Além disso, os materiais aluminossilicatos não reagem com água e por isso necessitam de soluções aquosas com elevado pH, identificadas como precursor e usualmente produzidas a partir de uma mistura entre hidróxidos, silicatos e água (LONGHI, 2019). Os ativadores alcalinos mais usados são o silicato de sódio, hidróxido de sódio, carbonato de sódio, hidróxido de potássio e silicato de potássio (RASHAD, 2013).

Embora os materiais álcali ativados apresentem emissões de CO_2 menores que cimento Portland, o uso de silicato sódio comercial como ativador também contribui para a emissão de gases antrópicos na atmosfera durante seu processo de fabricação em temperaturas relativamente altas da ordem de 1200-1400 °C (VILLAQUIRÁN-CAICEDO *et al*., 2017). A produção de silicato sódio comercial emite aproximadamente 1.514 kg de CO_2/kg (TCHAKOUTÉ *et al*., 2016a), além de contribuir significativamente para a poluição do ar. Dessa forma, o ativador deve ser capaz de ativar o precursor dentro do tempo desejado e deve estar disponível a baixo custo e com baixo impacto ambiental. Portanto, métodos alternativos, como processo hidrotérmico são empregados na produção de silicato de sódio com subprodutos agrícolas como a cinza de casca de arroz (TCHAKOUTÉ *et al*., 2017). A casca de arroz é considerada um dos resíduos agrícolas mais abundantemente disponíveis e seu uso pode ser uma alternativa para o aproveitamento de resíduos agrícolas, redução da emissão de gases do efeito estufa e redução no custo dos materiais álcali ativados (RAJAN *et al*., 2021). A produção mundial de arroz em 2019/20 foi de 496,11 milhões de toneladas (USDA, 2020). Assumindo a combustão de tais quantidades, aproximadamente 22,5 milhões de toneladas de CCA são produzidas em todo o mundo (VILLAQUIRÁN-CAICEDO *et al*., 2017; FAO, 2019). Segundo o IBGE, em 2019 o Brasil produziu 10,37 milhões de toneladas de arroz com casca, sendo estimado um aumento de 0,9% para a safra de 2020 e o estado do Rio Grande do Sul responsável por aproximadamente 70% da produção (7,17 milhões de toneladas).

O uso de CCA na síntese do ativador alcalino apresenta desempenho comparável e até mesmo superior ao silicato de sódio comercial podendo ser utilizado como fonte complementar de sílica na produção de materiais álcali ativados (BERNAL *et al*., 2015a). Este método alternativo pode reduzir a emissão de CO_2 em até 50% em comparação com os materiais álcali ativados sintetizados a partir de silicato de sódio comercial e hidróxido de sódio (MELLADO *et al*., 2014). Dessa forma, com o processo de utilização da CCA na produção de silicato de sódio, os impactos ambientais associado à produção de silicato de sódio comercial podem ser reduzidos, resultando em materiais álcali ativados ecológicos (VILLAQUIRÁN-CAICEDO *et al*., 2017).

1.2 Problemática e justificativa

Atualmente, na área de álcali ativação, tem-se uma grande quantidade de trabalhos publicados. Apesar disso, a utilização desses materiais com a finalidade de reciclagem das camadas de base e sub-base de pavimentos contendo RAP ainda é escassa. Os poucos estudos desenvolvidos até o momento abordam a reciclagem de RAP utilizando cinza volante e/ou escória como precursores e hidróxido de sódio e/ou silicato de sódio como ativadores (AVIRNENI *et al.*, 2016; HOY *et al*., 2016a; HOY et *al*., 2016b; MOHAMMADINIA *et al*., 2016a; MOHAMMADINIA *et al*., 2016b; SARIDE *et al*., 2016; HORPIBULSUK *et al*., 2017; HOY *et al*., 2018; JALLU *et al*., 2020; SARIDE e JALLU, 2020).

No entanto, além da utilização de fontes alternativas para os precursores, se faz necessário também o desenvolvimento de fontes alcalinas alternativas. Dentre os ativadores disponíveis, o silicato de sódio pode ser elencado, de um modo geral, como o ativador com melhor desempenho, principalmente quando se trata de cura em temperatura ambiente. Porém, a produção de silicato de sódio demanda um elevado consumo energético e apresenta grande impacto ambiental para sua produção (HABERT *et al*., 2011). Apesar da valiosa contribuição dos trabalhos desenvolvidos envolvendo a produção de silicato de sódio alternativo a base de CCA (BERNAL *et al*., 2012; HE *et al*., 2013; MEJÍA *et al*., 2013; BOUZÓN *et al*., 2014; BERNAL *et al*., 2015; TCHAKOUTÉ *et al*., 2016a; TCHAKOUTÉ *et al*., 2016b; MEJÍA *et al*., 2016; STURM *et al*., 2016; KAMSEU *et al*., 2017; GERALDO *et al*., 2017; PASSUELLO *et al*., 2017; HAJIMOHAMMADI e VAN DEVENTER, 2017; TONG *et al*., 2018; LUUKKONEN *et al*., 2018), percebe-se que não existe um consenso a respeito do processo de produção, além de que muitos fatores necessitam de uma maior compreensão. Logo, este

trabalho busca agregar contribuições a lacuna de conhecimento relacionada a padronização e influência de parâmetros relacionados ao processo de produção de um silicato de sódio alternativo a base de CCA.

Além disso, dentre as lacunas deixadas pela literatura também não se tem registro da utilização de silicato de sódio alternativo para a reciclagem de RAP em camadas de base e sub-base de pavimentos. O setor de infraestrutura anseia utilizar tecnologias e metodologias inovadoras de maneira a contribuir para novas alternativas que provejam soluções mais econômicas e sustentáveis, aliada à mitigação dos impactos ambientais causados pelas indústrias. Uma perspectiva que vem sendo sobrelevada, consiste na reutilização de resíduos industriais que, até então, não apresentam monetização expressiva e são considerados como material de descarte. Neste contexto, julga-se imprescindível que novas pesquisas sejam realizadas na área de desenvolvimento de materiais de pavimentação, com o intuito de buscar diretrizes seguras para o emprego e aproveitamento com qualidade dos dois resíduos envolvidos na presente pesquisa: o RAP e a CCA. Dessa forma com esta pesquisa, anseia-se aprimorar o conhecimento sobre o comportamento de um sistema álcali ativado de cinza de casca de arroz, metacaulim e hidróxido de sódio na reciclagem profunda de pavimentos.

1.3 Objetivo Geral

O objetivo geral deste estudo é avaliar a viabilidade técnica de um sistema álcali ativado de cinza de casca de arroz, metacaulim e hidróxido de sódio na reciclagem profunda de pavimentos asfálticos.

1.3.1 Objetivos específicos

De modo a alcançar o objetivo geral são definidos os seguintes objetivos específicos:

a) Determinar as condições de produção de um ativador alcalino alternativo baseado na dissolução de cinza de casca de arroz que maximizem o comportamento mecânico e microestrutural das pastas álcali-ativadas;
b) Avaliar a influência das diferentes proporções de agregados e solução álcali ativadora no comportamento mecânico e microestrutural das misturas de material asfáltico

fresado reciclado e ligante álcali ativado à base de metacaulim e silicato de sódio alternativo;

c) Avaliar a influência das condições de cura no comportamento mecânico e microestrutural das misturas de material asfáltico fresado reciclado e ligante álcali ativado à base de metacaulim e silicato de sódio alternativo;
d) Avaliar a durabilidade, comportamento mecânico a longo prazo e lixiviação de álcalis das misturas de material asfáltico fresado reciclado e ligante álcali ativado à base de metacaulim e silicato de sódio alternativo;
e) Avaliar a resistência a tração e o comportamento flexural estático e cíclico (fadiga) das misturas de material asfáltico fresado reciclado e ligante álcali ativado à base de metacaulim e silicato de sódio alternativo.

1.4 Estrutura da pesquisa

O presente documento divide-se em quatro capítulos, cujos conteúdos são apresentados sumariamente a seguir. No primeiro capítulo é apresentada uma breve introdução sobre as demandas do setor de infraestrutura, uma contextualização em relação a necessidade de uma alternativa ao cimento Portland e a utilização de materiais álcali ativados, além da menção à alguns trabalhos já desenvolvidos, apresentando as lacunas do conhecimento. De modo a direcionar e delimitar o desenvolvimento da pesquisa são apresentados neste capítulo também os objetivos e a estrutura da pesquisa.

No capítulo dois a fundamentação teórica é apresentada com cinco seções. A primeira reflete as conceitualizações acerca da restauração e reciclagem de pavimentos flexíveis. A segunda seção explora os aspectos inerentes a geração de material asfáltico fresado, bem como suas propriedades. Em seguida, são apresentados os conceitos relativos à estabilização de material asfáltico fresado. Posteriormente na seção 4 são abordados o processo de álcali ativação, as matérias primas utilizadas e o processo de produção de um silicato de sódio alternativo. Esse capítulo se encerra com uma revisão de trabalhos já desenvolvidos a respeito da estabilização de material asfáltico fresado através da álcali-ativação.

Após os dois capítulos iniciais, é apresentado o capitulo de resultados, onde cada objetivo específico representa uma seção do capítulo contendo um artigo submetido à periódicos. A Figura apresenta a estrutura organizacional da pesquisa, onde é exposto o título de cada artigo/seção.

Figura 1 - Estrutura da pesquisa

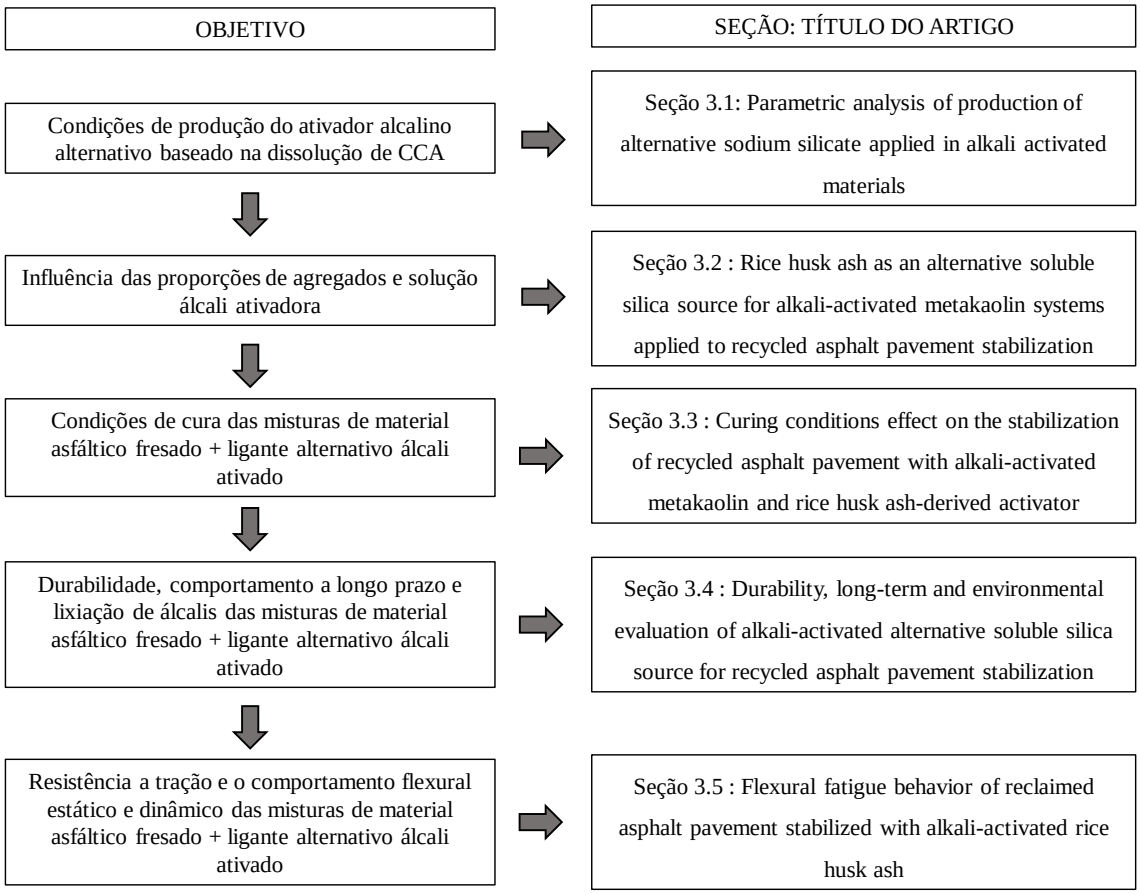

Fonte: Autor (2023)

De modo geral, o desenvolvimento da tese foi dividido em 5 tópicos de pesquisa. O primeiro aborda a produção de silicato de sódio alternativo a base de CCA e o segundo a sua aplicação em diversas proporções de agregados e solução álcali ativadora de CCA. O terceiro envolve as condições de cura e no quarto são avaliadas as questões relacionadas a durabilidade e lixiviação de álcalis. Por fim no quinto tópico a análise está voltada para o comportamento desses materiais quando submetidos a carregamentos cíclicos e consequentemente ao fenômeno de fadiga dos pavimentos. Na Figura 2 é apresentado um fluxograma geral da metodologia utilizada no presente estudo, na sequência é realizada uma abordagem geral sobre os procedimentos metodológicos adotados e informações mais detalhadas sobre a metodologia são apresentadas em cada artigo na seção de resultados.

Figura 2 – Fluxograma metodólogico da pesquisa

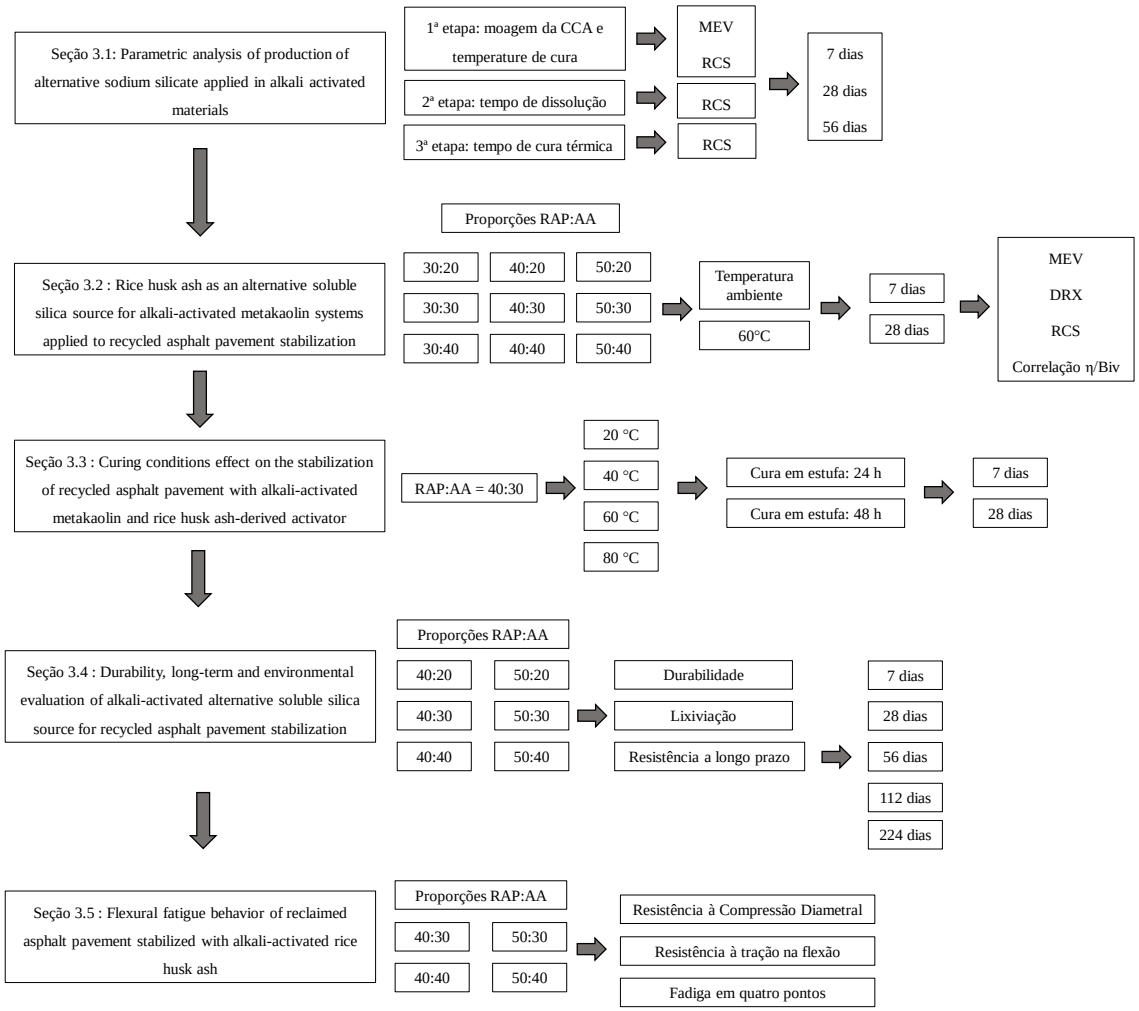

Fonte: Autor (2023)

No item 3.1, o processo de produção de silicato de sódio a base de CCA é avaliado em três etapas. Na primeira etapa são avaliados o tempo de moagem da CCA e a temperatura de cura. A segunda etapa se desenvolve frente a adoção dos melhores parâmetros evidenciados na etapa 1, buscando a otimização do tempo de dissolução. Na última etapa, de modo a obter uma economia de energia, é avaliado o tempo de cura térmica. As propriedades das pastas produzidas em cada etapa foram mensuradas a partir de resultados de resistência a compressão simples, além da utilização de DRX e MEV para uma melhor compreensão da influência da granulometria da CCA. Por fim, foram elencados os resultados de cada etapa e produzidas pastas que foram comparadas com pastas produzidas a partir de silicato de sódio comercial . Para a avaliação da eficiência do silicato de sódio alternativo foram utilizados, além dos ensaios mecânicos, a análise das características microestruturais das pastas álcali ativadas através de ensaios de DRX e termogravimetria.

No item 3.2 foi avaliada a aplicação do silicato de sódio alternativo para reciclagem de RAP através da álcali-ativação. Diferentes percentuais de RAP (30, 40 e 50%) foram combinados com diferentes teores de material álcali ativado (20, 30 e 40%) a fim de avaliar as proporções com maior potencial para utilização do material como camada de base de pavimentos. O método experimental consistiu na avaliação das propriedades físicas e mecânicas através dos ensaios de compactação e resistência a compressão simples. De modo a melhor compreender o comportamento mecânico das misturas foram ainda realizados ensaios microestruturais (DRX e MEV).

A partir da revisão bibliográfica desenvolvida observou-se que apesar dos estudos já existentes na área de reciclagem de RAP a partir da álcali-ativação, as condições de cura ainda não são compreendidas por não terem sido avaliadas como objetivo principal destes trabalhos. Dessa forma, no item 3.3, a proporção RAP:AA = 40:30 que apresentou um bom desempenho como camada de base de pavimentos, foi submetida a diferentes temperaturas (20°C, 40°C, 60°C, 80°C) por tempos distintos. As variáveis de resposta estão concentradas na análise da resistência a compressão simples e nas propriedades microestruturais através de MEV e DRX, aos 7 e 28 dias de cura. O objetivo desse capítulo foi compreender a influência das condições curas através das propriedades mecânicas e microestruturais, buscando um menor consumo de energia e aplicabilidade em campo da reciclagem de RAP a partir da álcali ativação a base de CCA.

A durabilidade é definida como uma condição desejada para garantir a resistência dos materiais aos processos de intemperismo, erosão e uso de tráfego. No âmbito da pavimentação, especialmente quando se trata de solo-cimento, procura-se garantir a permanência da coesão da mistura compactada, quando solicitado pela ação do trafego ou pelos esforços provenientes de variação de temperatura e de umidade. Dessa forma, com a definição das melhores composições e condições de cura ideais obtidas nos dois itens anteriores, no item 3.4 as amostras foram avaliadas segundo critérios de durabilidade quando submetidas a ciclos de molhagem e secagem e quanto a lixiviação de álcalis. De forma a simular as variações sazonais em campo, os corpos de prova foram submetidos a processos de imersão em água e secagem em estufa contemplando 12 ciclos. A resistência a compressão simples foi avaliada ao final do 3°, 7° e 12° ciclo, assim como a perda de massa e análise visual em todos os ciclos. Além disso, a fim de verificar a permanência do estabilizador/ativador sob a ação da infiltração da chuva foram realizados ensaios de lixiviação e sua classificação como material como perigoso.

Além disso, os materiais que compõem as camadas do pavimento estão submetidos a carregamentos cíclicos, sendo que a deformação elástica ou recuperável destes materiais está associada ao processo de fadiga. O fenômeno de fadiga é um dos principais processos que determina a longo prazo de pavimentos flexíveis com inclusão de bases cimentadas e constitui um dos mecanismos de falha que limita o dimensionamento deste tipo de estrutura. Desta forma, o estudo da degradação causada pelo fenômeno de fadiga é importante para finalidades de projeto. Portanto no item 3.5, os corpos de prova que atingiram bons resultados no item anterior foram submetidos a ensaios resistência a compressão diametral, de resistência à tração na flexão e fadiga em quatro pontos.

Por fim, é apresentado o capítulo 4, com as conclusões de cada artigo, apresentando as principais contribuições e recomendações para futuras pesquisas.

2. FUNDAMENTAÇÃO TEÓRICA

2.1 Restauração e reciclagem de pavimentos flexíveis

De acordo com pesquisa da Confederação Nacional de Transportes – CNT (2019), em uma extensão de mais de 108.863 km de rodovias no Brasil, 59% das rodovias apresentam algum problema relacionado às características do pavimento, sinalização ou geometria da via. A avaliação do item condição do pavimento aponta 52,4% das rodovias com problemas, sendo 38,6% considerados em ótimo estado; 9,0%, bom; 35%, regular; 13,7%, ruim; e 3,7%, péssimo. Essa mesma pesquisa aponta casos de pavimentos implantados, projetados para durar cinco anos, que chegam a apresentar problemas de desgaste em menos de sete meses e que são necessários R$ 38,60 bilhões para reconstrução e restauração das rodovias brasileiras. Dessa forma, para a melhoria no nível da malha é necessário que se façam intervenções de restauração e reabilitação dos pavimentos.

Segundo o Manual de Restauração de Pavimentos Asfálticos do DNIT (2006) o termo recuperação de pavimento está associado à recuperação dos atributos funcionais e estruturais do pavimento, através de intervenções físicas na rodovia que são intituladas de Restauração e/ou Reabilitação de pavimentos. Nesse sentido, o manual define o termo “Restauração de Pavimento” como a recuperação de um pavimento que se apresenta deteriorado, mas cujo grau de deterioração não compromete a sua habilitação. Nesse estágio de deterioração, que ainda não é qualificado como crítico, as medidas de conservação de caráter preventivo e/ou corretivo já se tornam praticamente ineficazes e/ou anti-econômicas. Já o termo “Reabilitação do Pavimento” é definido como a recuperação de um pavimento que, em decorrência do alto grau de deterioração alcançado, perdeu a sua habilitação e como solução envolve a reconstrução do pavimento.

Dentre as técnicas disponíveis, a fresagem é uma técnica constantemente aplicada como parte do processo de restauração de pavimentos com problemas funcionais e/ou estruturais. A fresagem de pavimentos é definida como o corte ou desbaste de uma ou mais camadas do pavimento, com espessura pré-determinada, por meio de processo mecânico realizado a quente ou a frio (BONFIM, 2011). O autor classifica ainda o tipo da fresagem de acordo com a espessura do corte: superficial, rasa ou profunda, e quanto à rugosidade resultante na pista: padrão, fina e microfresagem. A fresagem superficial destina-se apenas à correção de defeitos existentes na superfície do pavimento. Em contrapartida a fresagem rasa atinge as camadas

superiores do pavimento, podendo chegar à camada de ligação, atingindo uma profundidade de corte da ordem de 5 cm. Quando a técnica alcança, além da camada de revestimento, as camadas de ligação, de base e até sub-base de pavimento, é chamada de fresagem profunda. Em relação a rugosidade resultante na pista, a fresagem padrão é utilizada para o desbaste da camada especificada em projeto, visando aplicação em nova camada de revestimento. Já a fresagem fina é utilizada em regularização de vias, possibilitando melhores condições de trafegabilidade aos usuários. E por fim a microfresagem consiste na remoção de uma camada muito delgada do revestimento, visando a adequação do perfil longitudinal ou retirada das faixas de sinalização horizontal das pistas, para alteração do layout viário (BONFIM, 2011).

No que diz respeito a técnica utilizada, Bonfim (2011) destaca que a fresagem pode ser realizada a frio ou a quente. Na fresagem a frio ocorre uma alteração granulométrica, proveniente da quebra dos grãos realizada a temperatura ambiente. Já na fresagem a quente é gerada apenas uma desagregação do material, resultante de um processo de pré-aquecimento do revestimento e posterior escarificação da camada.

De acordo com Fedrigo et *al.* (2019), as rodovias de muitos países desenvolvidos e em desenvolvimento estão se aproximando do fim de sua vida útil e exigindo restauração e/ou reabilitação. Em paralelo a este cenário, a maioria desses países também enfrenta a falta de recursos naturais e tradicionais usados nas atividades de engenharia civil. Enormes quantidades de recursos naturais são consumidas pelas indústrias de pavimentação, as quais são responsáveis por 30% da poluição global do ar e produção de gases efeito estufa e contribuem para aproximadamente um quarto do consumo total de combustíveis fósseis em todo o mundo (MALLICK e VEERARAGAVAN, 2010).

Nesse contexto, o tijolo triturado e o material asfáltico fresado estão entre os maiores contribuintes de resíduos de construção e demolição de muitos países (SERRES et *al.*, 2016; SARIDE et *al.*, 2010). Dessa forma, utilizar métodos mais econômicos e ecológicos, como substituir recursos naturais através da reciclagem de pavimentos pode reduzir significativamente a pegada de carbono das rodovias (ARULRAJAH *et al.*, 2015; PAIGE-GREEN e WARE, 2006).

De acordo com Bernucci *et al*. (2008), a técnica de reciclagem de pavimentos consiste em reutilizar materiais triturados existentes para reconstrução total ou parcial da estrutura. A reutilização dos agregados do pavimento degradado para os serviços de reconstrução, restauração e conservação, propiciam uma diminuição da demanda de novos materiais e das

respectivas distâncias de transporte, prolongando o tempo de exploração das ocorrências existentes. Isso é particularmente benéfico devido as restrições impostas pela legislação de proteção ao meio ambiente e pela crescente valorização dos sítios de ocorrências de jazidas (DNIT, 2006). Nesse contexto, foi ainda recentemente aprovada a Resolução N° 14, de 8 de julho de 2021, que dispõe que todos os projetos de engenharia de restauração, adequação de capacidade e ampliação de obras viárias do Departamento Nacional de Infraestrutura de Transportes – DNIT devem incluir o reaproveitamento de material asfáltico fresado eventualmente produzido no empreendimento.

De acordo com o DNIT (2006), a reciclagem de pavimentos pode ser realizada a quente ou a frio, de acordo com as necessidades de restauração do pavimento. A reciclagem a quente pode corrigir deficiências de misturas betuminosas e pode ser utilizada para aumentar a capacidade estrutural, podendo ser usada antes de um recapeamento. Enquanto que a mistura final da reciclagem a frio pode ser utilizada em camada de base, que deverá ser revestida com um tratamento superficial ou uma mistura asfáltica antes de ser submetida a ação direta do tráfego. Os processos dos dois tipos de reciclagem consistem em remover toda ou parte da estrutura do pavimento e reduzir a dimensões apropriadas para depois ser misturada a frio no próprio local ou em usina, ou a quente no próprio local (in situ) ou em usina estacionária. Quando o objetivo da reciclagem é a correção de defeitos de superfície, exclusivamente de classe funcional, a reciclagem é realizada sem remover do local o material a ser reciclado. Já a reciclagem a quente permite melhorias estruturais significativas, devido principalmente à adição de asfalto ao material removido da pista e a posterior reposição na mesma espessura.

2.2 Material asfáltico fresado

O material asfáltico fresado removido de um pavimento existente é um material totalmente reciclável (EAPA, 2014; AAPA, 2018). Sendo composto por dois valiosos recursos não renováveis, ou seja, aproximadamente 95% em peso de agregados e 5% em peso de ligante betuminoso envelhecido, pode ser reutilizado em novas misturas asfálticas, reduzindo a demanda por agregados virgens e betume, ou como agregados reciclados para produzir camadas não ligadas de pavimentos (SABITA, 2019). Essa composição faz com que o material asfáltico fresado esteja no topo da hierarquia de materiais recicláveis com aplicações de engenharia, por não ser reduzido como simplesmente agregado (SABITA, 2019) e, portanto, reduzir significativamente os custos globais dos novos produtos betuminosos (BRETT *et al*., 2019).

O material asfáltico fresado tem sido usado em misturas de asfalto desde 1915 por razões ambientais e econômicas (Kennedy *et al.*, 1998). No Brasil, as obras de pavimentação rodoviária tiveram um grande incremento nos anos 50, quando, fruto do intenso intercâmbio de técnicos do extinto DNER, produziu-se uma grande transferência de tecnologia oriunda dos Estados Unidos da América do Norte (DNIT, 2006). No entanto o uso de pavimento asfáltico fresado foi particularmente atraente durante a década de 1970, especialmente com o aumento do preço do petróleo durante a restrição do petróleo árabe. Como consequência, os tecnólogos de pavimentação asfáltica foram forçados a desenvolver métodos de reciclagem que são capazes de reduzir a demanda por aglutinante de asfalto, reduzindo assim o custo das misturas de pavimentação asfáltica (MILAD *et al*., 2020).

Além disso recentemente entrou em vigor no Brasil a Resolução n° 14, de 8 de julho de 2021 que dispõe sobre o reaproveitamento do RAP (Reclaimed Asphalt Pavement) nas obras de restauração, adequação de capacidade e ampliação do Departamento Nacional de Infraestrutura de Transportes – DNIT.

> Art. 1º DISPOR que todos os projetos de engenharia de restauração, adequação de capacidade e ampliação de obras viárias do Departamento Nacional de Infraestrutura de Transportes - DNIT, desenvolvidos no âmbito da Sede e Superintendências Regionais, deverão incluir o reaproveitamento do RAP (Reclaimed Asphalt Pavement) eventualmente produzido no empreendimento.
>
> Art. 2º O RAP deverá ser aplicado nas camadas do pavimento a serem construídas ou na execução de novos concretos asfálticos.

Atualmente o material asfáltico fresado representa um dos produtos de construção mais reutilizados no mundo todo. Em 2018, aproximadamente 88% em peso e 72% em peso de material asfáltico fresado foram usados nos EUA e na Europa, respectivamente, como agregados para misturas de asfalto quente, quente e frio e para camadas não ligadas (TARSI *et al.*, 2020).

De acordo com Babashamsi *et al.* (2016), a análise do custo do ciclo de vida de pavimentos incorporando material asfáltico fresado mostrou que pode ser alcançada uma economia de $ 58.000/km em misturas asfálticas contendo 30% a 50% de material asfáltico fresado. Essa economia se deve à substituição de uma parte dos agregados virgens e ao menor custo de transporte. As pedras britadas convencionais são geralmente mais caras do que os materiais reciclados. Em 2014, a National Asphalt Pavement Association (NAPA) informou

que cerca de 71,9 milhões de toneladas de material asfáltico fresado foram utilizadas na construção de novos pavimentos nos Estados Unidos. Isso significa uma economia de cerca de US$ 2,5 bilhões a cada ano (GEORGE *et al*., 2019). Além disso, em 2018, mais de 100 milhões de toneladas de material asfáltico fresado foram coletadas para reutilização nos Estados Unidos, economizando cerca de 61,4 milhões de jardas cúbicas em aterros sanitários (SONG et *al*., 2018). Dessa forma, a reciclagem e/ou a reutilização de material asfáltico fresado é um exemplo de desenvolvimento sustentável no setor de infraestrutura. O incentivo ao seu uso reflete a tendência mundial de enfrentar as questões ambientais existentes, buscando aumentar o uso eficiente de recursos e reduzir a emissão de carbono (UNITED NATIONS, 2015).

Apesar da importância e das vantagens da reciclagem de pavimentos, o maior desafio no uso de material asfáltico fresado se deve ao fino revestimento de betume envelhecido na superfície do agregado (SARIDE *et al*., 2016; ARULRAJAH *et al.*, 2014). A camada de asfalto na superfície do agregado é responsável pela água baixa absorção do material e a fraca ligação entre o agregado e a argamassa cimentícia (SARIDE *et al*., 2016; SINGH *et al.*, 2017; SU *et al*., 2014; BRAND e ROESLER, 2017). De acordo com Saride *et al*. (2016), processos de beneficiamento podem ajudar na remoção parcial ou total do revestimento de asfalto, mas são considerados caros e inviáveis (SINGH *et al*., 2017).

A idade também pode desempenhar um papel importante nas propriedades dos agregados do material asfáltico fresado. Singh *et al*. (2018) observou que agregados de pavimento mais novos obtiveram menor trabalhabilidade e piores propriedades que agregados originados de pavimentos mais antigos. Brand e Roesler (2017) sugerem que o material com maior idade ou armazenado por muito tempo em pilhas sofre oxidação química que modifica a química do asfalto superficial levando a uma melhor aderência da pasta de cimento.

Dessa forma, o desempenho do material asfáltico fresado pode ser melhorado através da mistura com agregados virgens e/ou adição de agentes rejuvenescedores, ligantes asfálticos novos, espuma de asfalto, emulsões asfálticas e até cimento Portland ou outro aditivo químico (BERNUCCI *et al*., 2008). Nesse sentido, preocupações relacionadas à resistência dos materiais residuais reciclados levaram a uma extensa investigação na estabilização de agregados reciclados usando uma variedade de ligantes, como cimento Portland, cal, escória, resíduo de carboneto de cálcio e cinzas volantes (PUPPALA *et al*., 2011; SARIDE *et al*., 2015; GNANENDRAN e PIRATHEEPAN, 2010; HORPIBULSUK *et al*., 2015).

2.3 Estabilização de material asfáltico fresado

Aliada a técnica de reciclagem de pavimentos, métodos de estabilização dos materiais são comumente utilizados e necessários na construção das novas camadas de pavimentos. Para Yoder e Witczack (1975) os fatores que determinam a estabilidade granulométrica de misturas são a distribuição granulométrica, o formato das partículas, a densidade relativa e o atrito interno. Dentre esses fatores a distribuição granulométrica é o aspecto mais influente fazendo com que a estabilização granulométrica sirva como controle de qualidade e homogeneidade dos agregados de material asfáltico fresado (WANG *et al*., 2012). Para bases de pavimentos as misturas onde o contato grão-a-grão seja garantido são as preferenciais, desde que atendam as faixas granulométricas especificadas em norma. Uma das características do agregado que influencia a estabilização é a resistência mecânica do agregado, que deve ser suficiente para reter aproximadamente a mesma distribuição granulométrica durante a compactação e a posterior utilização pelo tráfego. O fator determinante no sucesso do emprego da estabilização granulométrica é a correta compactação do material, o que lhe confere grande resistência aos esforços verticais de compressão (BALBO, 2007; BERNUCCI *et al*., 2008; YODER e WITCZACK, 1975).

Geralmente, o material asfáltico fresado removido apresenta alto teor de partículas finas, devido às operações de fresagem das camadas do pavimento e/ou aos processos de britagem para redução do tamanho dos agregados, principalmente quando o material é proveniente de remoção total de pavimento (WANG, 2016; AL-QADI *et al*., 2007). A quantidade de partículas finas pode limitar a quantidade máxima de material asfáltico fresado, uma vez que os requisitos de graduação da mistura final podem não ser atendidos (AL-QADI et *al*., 2007). As partículas mais finas contêm também maior quantidade de aglutinante envelhecido, devido à sua maior área superficial (SHU et *al.*, 2008). Além disso o próprio material asfáltico fresado não possui drenagem como agregados virgens (WANG, 2016; AL-QADI *et al*., 2007) e a presença de partículas mais finas tendem a reter ainda mais a umidade (WANG, 2016; CHATTI e ZABAAR, 2012). Segundo Bonfim (2007), o contrário ocorre com a curva granulométrica do fresado constituído pelos grumos, ou seja, sem a extração do betume, em que o percentual de finos é muito pequeno, uma vez que estes estarão envoltos pelo cimento asfáltico de petróleo (CAP).

Todos esses aspectos devem ser levados em consideração para o gerenciamento correto e projeto de mistura do material asfáltico fresado. A qualidade dos materiais asfálticos

removidos dos pavimentos depende da fresadora, sua velocidade e profundidade de fresagem, em particular, o último fator é importante porque o material de uma única camada tem propriedades homogêneas: tipo de agregado e curva de granulometria, características e quantidade de betume (AL-QADI *et al*., 2007; SILVA *et al*., 2012).

No entanto quando um material ou uma combinação de materiais com estabilidade mecânica adequada não pode ser obtida, Ingles e Metcalf (1972) aconselham considerar a estabilização por meio da adição de estabilizantes químicos. Dellabianca (2004) afirma que a estabilização química quando utilizada em materiais granulares, tem a função de propiciar a melhora da resistência ao cisalhamento, causado pelo atrito produzido pelos contatos das superfícies das partículas. Conforme Bernucci *et al.* (2008), os materiais utilizados nas camadas do pavimento são usualmente constituídos por: agregados, solos e, eventualmente, aditivos como cimento, cal, emulsão asfáltica, entre outros, podendo ser classificados segundo o seu comportamento frente aos esforços em: granulares e solos, estabilizados quimicamente ou cimentados e materiais asfálticos. Como a camada de base encontra-se perto do revestimento, esta deve possuir elevada resistência de deformação, a fim de resistir às altas pressões que lhe são impostas. Sendo assim estas camadas podem ser executadas com algum tipo de estabilização química para melhorar seu desempenho.

Dellabianca (2004) afirma também que a presença do ligante asfáltico envolvendo os agregados facilita o deslizamento de uma partícula sobre a outra, diminuindo, assim, o atrito e consequentemente a resistência. Dessa forma o uso de agentes estabilizadores também tem como objetivo proporcionar um aumento na resistência da mistura.

Segundo Wirtgen (2012) existem uma série de agentes estabilizadores que podem ser empregados, mas todos têm a função de fazer a ligação dos agregados com o objetivo de aumentar a resistência e a rigidez e/ou aumentar a impermeabilidade e durabilidade dos materiais. Yoder e Witczack (1975) complementam que o processo de estabilização também envolve questões econômicas, como qualquer projeto de engenharia, sendo necessário escolher adequadamente o tipo de estabilização mais adequado para cada finalidade. A cal, o cimento e combinações desses produtos com cinzas volantes, escórias de altos-fornos e outros materiais pozolânicos são os agentes estabilizadores mais comumente usados. Exceto pelos primeiros experimentos dos romanos com a cal como agente, o cimento tem sido o elemento usado há mais tempo (WIRTGEN, 2012, INGLES E METCALF, 1972; YODER e WITCZACK, 1975).

2.3.1 Estabilização química com cimento Portland

A reciclagem de pavimentos com cimento Portland é uma técnica que consiste na fresagem *in situ* e posterior mistura com cimento das camadas superiores existentes de um pavimento danificado, principalmente a camada de revestimento e a base. A mistura resultante é então compactada para formar uma nova camada que aumentará a capacidade estrutural do pavimento (KATSAKOU e KOLIAS, 2007; PORTLAND CEMENT ASSOCIATION, 2005).

O processo de estabilização de solos com cimento é dividido por Ceratti e Casanova (1988) em duas fases. Na primeira fase ocorre uma diminuição da mobilidade da fase líquida seguida de uma forte floculação, ocasionadas pela reação de hidrólise do cimento, onde é gerada cal (*in situ*) com aumento do pH. A segunda fase é caracterizada pela formação de substâncias cimentantes que ficam dispostas sobre a superfície das partículas de argila ou em sua vizinhança, causando assim, cimentação dos grãos floculados nos seus pontos de contato.

De acordo com Cardoso *et al*. 1997, as características mecânicas de uma mistura de solo-cimento dependem do grau de compactação e sobretudo do tempo, uma vez que se realizada após a hidratação do cimento apresenta resultados ineficientes. Núñez (1991) aponta também a influência de do tipo de cura: altas temperaturas são favoráveis ao acréscimo de resistência, enquanto que a imersão não apresenta aspectos positivos. Dellabianca (2004) menciona ainda que a interação entre o cimento e as partículas granulares do solo é diferente do que ocorre em partículas finas, sendo a primeira similar ao que ocorre no concreto. A única diferença é que a cimentação em solos granulares ocorre apenas nos pontos de contato das partículas, enquanto que a pasta de cimento no concreto preenche os vazios dos agregados.

No entanto o RAP apresenta comportamento diferente dos materiais convencionais estabilizados com cimento. O material fresado consiste em uma mistura de agregados revestidos com aglomerante asfáltico e aglomerados de finos unidos por aglomerante asfáltico (FEDRIGO *et al*., 2019). A quantidade desses materiais na mistura depende da espessura da camada de revestimento e altera significativamente as propriedades da camada reciclada (KOLIAS et *al*., 2001). O comportamento mecânico de material asfáltico fresado estabilizado com cimento foi alvo de vários estudos (DALLA ROSA *et al*., 2015; DIXON *et al*., 2012; GRILLI *et al*., 2013a; MALLICK *et al*., 2002a, 2002b; MOHAMMADINIA *et al*., 2015; PUPPALA *et al*., 2011), assim como a durabilidade dessas misturas (FEDRIGO *et al*., 2017a; GUTHRIE *et al*., 2007; SUDDEEPONG *et al*., 2018; YUAN *et al*., 2011) e o desempenho das mesmas em campo

(AMARH *et al*., 2017; BESSA *et al*., 2016; GODENZONI *et al*., 2018; SANTOS *et al*., 2017; TATARANNI *et al*., 2017; WU *et al*., 2015).

Jasienski e Rens (2001) relataram que o uso de reciclagem de pavimento com adição de cimento começou na década de 1950, tendo os EUA e a França como pioneiros. O Brasil usa a técnica de reciclagem de pavimentos com cimento há cerca de três décadas (FEDRIGO *et al*., 2020). Segundo Paiva *et al*. (2013), a técnica já recuperou milhões de metros quadrados de pavimentos, com destaque para os estados de São Paulo e Minas Gerais.

Em relação aos aspectos ambientais, técnicos e econômicos, a literatura (PCA, 2005; IECA, 2013; MINGUELA, 2011; WIRTGEN, 2012) destaca as principais vantagens da reciclagem de pavimentos com cimento:

a) Permite a reabilitação de um pavimento deteriorado gerando uma camada homogênea, estável e espessa, proporcionando melhores características mecânicas;
b) Reciclagem e melhoraria dos materiais existentes que geralmente não possuem características técnicas adequadas;
c) Redução da necessidade de transportes (no caso da execução in situ), diminuindo consequentemente as emissões de CO_2 e outros poluentes, assim como os custos;
d) Perturbação mínima pelo tráfego de construção em função do ciclo rápido de construção e da pequena quantidade de volume de material transportado para dentro ou para fora. Além disso o tráfego é parcialmente interrompido, uma vez que o mesmo é geralmente permitido em uma faixa da estrada enquanto a construção ocorre na outra faixa;
e) Ampla aceitação e disponibilidade de cimento Portland pela indústria da construção;
f) Redução da tensão de compressão vertical no subleito e da tensão de tração horizontal na parte inferior do revestimento.

Apesar da série de vantagens elencadas, Minguela (2011) cita também como desvantagens e limitações da reciclagem de pavimentos com cimento, o fato de o pavimento antigo possuir uma estrutura muito heterogênea ao longo de sua extensão fazendo com que pavimento reabilitado também se apresente mais heterogêneo. O autor ainda menciona que a reciclagem de faixas individuais pode, ocasionalmente, causar o aparecimento de trincas longitudinais, caso precauções não sejam adotadas para garantir uma ligação adequada entre os materiais de vias adjacentes. PCA (2005) e Wirtgen (2012) trazem também como desvantagem o trincamento por contração e o aumento da rigidez resultando em fratura por fadiga precoce da camada. O primeiro problema pode ser minimizado através de métodos adequados de cura,

enquanto que o segundo pode ser tratado pela execução de camadas mais espessas com menos resistência (cerca de 2% de cimento).

Além disso, embora o custo da reciclagem de pavimentos com cimento seja mais barato que outras técnicas de reabilitação, estudos recentes (BRAHAM, 2016) avaliando o custo do ciclo de vida mostram que essa técnica pode ser mais cara. Ademais, se tratando de aspectos ambientais, os mesmos geralmente não são considerados na análise do ciclo de vida. No entanto, a fabricação de cimento Portland consome uma grande quantidade de energia e matérias-primas e ao mesmo tempo emite altas taxas de CO_2 responsável pelo aquecimento global (MEHTA, 2001). De acordo com Singh e Middendorf (2020), devido a essa necessidade de minimizar as emissões de CO_2 das indústrias de cimento, nos últimos anos ligantes álcali ativados/cimento geopolimérico parecem ser uma alternativa ao concreto convencional. Essa alternativa pode ser dada pela ativação alcalina de subprodutos industriais contendo fases de aluminossilicato com pouco impacto negativo no meio ambiente, resolvendo assim os problemas da indústria da construção e da geração de resíduos.

2.3.2 Comportamento mecânico de camadas de pavimento tratadas com agentes cimentantes

A adição de agentes cimentantes nas camadas dos pavimentos atua de forma a proporcionar maiores resistências à compressão e à tração (WIRTGEN, 2012), sendo estabelecido o critério mínimo de resistência à compressão de 2,1 MPa aos 7 dias de cura (DNIT, 2013). No entanto, além desses parâmetros, o Módulo de Resiliência (MR) também é considerado apropriado para medir a rigidez de materiais, sendo fundamental para o dimensionamento mecanístico ou mecanístico-empírico de pavimentos (AHMED e KHALID, 2011). Diferente do módulo de elasticidade de Young, que é definido por receber carregamento monotônico e sofrer pequenos deslocamentos, as camadas dos pavimentos são submetidas a carregamentos cíclicos e apresentam deformação elástica ou recuperável, e por isso a deformação resiliente é mais adequada. Dessa forma o MR é definido como a relação entre a tensão axial repetida aplicada e a deformação axial resiliente com a aplicação de n vezes a carga axial (Equação 1). Esse parâmetro é influenciado principalmente pelos estados de tensões utilizados no ensaio, pela energia de compactação do corpo de prova, pelo teor de umidade e pela granulometria (WERK, 2000, TAKEDA, 2006, MEDINA e MOTTA, 2015).

$$MR = \frac{\sigma_d}{\varepsilon_r} \quad (1)$$

Onde:

σ_d = tensão desvio $(\sigma_1 - \sigma_3)$

ε_r = deformação recuperável (elástica)

Na prática a maioria dos materiais de pavimentação acumulam pequenas deformações plásticas após a aplicação da carga, não apresentando um comportamento puramente elástico. Apesar disso, se a carga aplicada for baixa em relação a resistência do material e for aplicada várias vezes, a deformação decorrente de cada repetição da carga é predominantemente recuperável e proporcional a carga, podendo ser considerada elástica (HUANG, 1993).

De acordo com Medina (1997), quando as cargas de roda estão distantes, o estado de tensões em um dado elemento do pavimento é nulo. No entanto à medida que as cargas oriundas do tráfego se aproximam desse elemento, são geradas tensões normais verticais e horizontais e tensões de cisalhamento nos planos verticais e horizontais. Quando a carga está atuando exatamente acima desse elemento, as tensões cisalhantes se tornam nulas e, portanto, as tensões normais são máximas e principais. Esse estado de tensões principais pode ser determinado em laboratório pelo ensaio de cargas repetidas a compressão triaxial através de uma tensão confinante (σ_3), que representa a pressão confinante atuando nas três direções, e uma tensão desvio axial ($\sigma_d = \sigma_1 - \sigma_3$) repetida que simula a carga vertical uniformemente distribuída gerada pela ação do tráfego. Uma disparidade do ensaio de cargas repetidas a compressão triaxial em relação ao que ocorre no pavimento sob ação do tráfego é que no equipamento triaxial as tensões atuam sempre na mesma direção, enquanto no pavimento à medida que a roda se aproxima e se afasta do elemento, as tensões principais mudam suas direções (BOYCE, 1976). A magnitude das tensões normais evolui formando um pulso cuja duração depende da velocidade do veículo e da profundidade do elemento no interior do pavimento (Huang, 1993). Em laboratório a simulação é realizada com um pulso de carga com duração de 0,1 s a cada 0,9s, totalizando 1 ciclo/s (ou 1 Hz) (DNIT 134/2010).

Behak (2013) afirma que o ensaio de carga repetida na compressão triaxial é mais utilizado para solos, enquanto que para misturas asfálticas e materiais cimentados utiliza-se o

ensaio de carga repetida na compressão diametral. Os solos apresentam um comportamento resiliente dependente das tensões principais, sendo que nos solos finos é função da tensão desvio e nos solos granulares é função da tensão volumétrica. Os materiais cimentados apresentam um comportamento resiliente independente do estado de tensões, sendo o MR considerado um valor constante.

Apesar dos benefícios já mencionados, a cimentação das camadas dos pavimentos gera mecanismos de degradação como trincamento por fadiga, deformação permanente e trincamento térmico (GNANENDRAN e PIRATHEEPAN, 2010). A fadiga dos materiais cimentícios é causada pelas sucessivas flexões das camadas do pavimento, produzida pelas tensões e deformações repetidas, devido ao tráfego e por fatores ambientais, que resultam no surgimento de trincas e sua propagação e que são consideradas como mecanismo primário de ruptura de pavimentos com camadas de materiais cimentados (LITTLE e YUSUF, 2001).

De acordo com Bernucci *et al*. (2010), a vida de fadiga é definida em termos de vida da fratura, que presenta o número total de aplicações de carga necessário para a ruptura completa, ou vida de serviço, que indica o número de aplicações desta mesma carga necessário para redução do desempenho ou da rigidez do pavimento a um nível aceitável.

No dimensionamento mecanístico, o parâmetro de controle de fadiga é a deformação a tração na fibra inferior da camada cimentada. Em laboratório geralmente são utilizados ensaios de flexão simples de vigotas de seção retangular carregadas em três pontos (EPPS e MONISMITH, 1969) e de tração a compressão diametral (SAID, 1997). Os ensaios de fadiga podem ser realizados a tensão controlada, onde a magnitude da carga é mantida constante ao longo do ensaio, ou deformação controlada, onde a magnitude do deslocamento é mantida constante. O ensaio de flexão da vigota é um exemplo típico de ensaio de deformação controlada, enquanto que o ensaio de tração por compressão diametral é um típico ensaio de carga controlada (BEHAK, 2013). Os ensaios de tensão controlada reproduzem melhor as condições de tráfego de materiais estabilizados e, portanto, considerados mais adequados no dimensionamento a fadiga (KHALID, 2000).

O ensaio de fadiga a flexão em quatro pontos consiste em submeter um corpo de prova em formato prismático biapoiado a cargas localizadas no terço médio do vão, originando um estado de tração uniforme nessa região, zona onde o momento fletor constante e as tensões cisalhantes são nulas, fato que reduz a variação dos resultados (LÓPEZ, 2016). O ensaio segue as recomendações da Austroads (2012) que define um pulso do tipo semi-seno-verso

(*haversine*) com uma duração de 0,25 s aplicando ciclos de carregamento com uma frequência de 5 Hz, de forma a reduzir ao máximo o tempo de descanso. Com relação aos níveis de tensão aplicados, as normas australianas indicam que devem ser aplicadas tensões que gerem deformações de 50 a 100 microstrains, que refletem em uma faixa de 60% a 90% da resistência a tração na flexão para os ensaios fadiga a quatro pontos, causando a degradação do material.

Baburamani (1999) afirma que geralmente o número de ciclos de carga do eixo padrão requerido para causar trincas significativas em serviço é muito maior do que o número de ciclos do ensaio de fadiga de laboratório. Essa diferença se deve as condições de carga (tipo de veículo e configuração do eixo), período de repouso entre cargas de veículo, intensidade do tráfego, velocidade dos veículos, compactação e fatores ambientais como variação sazonal de temperatura e gradientes de temperatura diária. As funções de transferência são utilizadas para levar em consideração essas diferenças para estimativa de vida de fadiga em laboratório.

Apesar dos inúmeros benefícios já mencionados, o potencial de substituição de agentes cimentícios tradicionais por materiais aglomerantes alternativos, possibilita a instauração de metodologias que fazem alusão à sustentabilidade. Uma forma de aproveitamento de resíduos industriais como substituinte de agentes cimentícios convencionais é na produção de ligante álcali-ativado por meio do processo de ativação alcalina, que será abordada na próxima seção.

2.4 Álcali-ativação

Materiais álcali ativados são cada vez mais utilizados e amplamente estudados mundialmente (LIU *et al*., 2019; PROVIS e BERNAL, 2014; SHI et *al*., 2011). Esses materiais foram desenvolvidos como uma alternativa para substituição Cimento Portland, utilizado em concretos, argamassas e pastas, sendo considerados menos agressivos do ponto de vista ambiental, devido à menor emissão de CO_2 atmosférico quando comparada à produção de cimento Portland (KUA *et al*., 2019; ZHUANG *et al*., 2016).

De acordo com Davidovits (1994), materiais álcali-ativados são produto de uma reação entre um ativador alcalino e uma fonte de aluminossilicato. Samarakoon et *al*. (2019) afirmam que dentro da classe de ligantes álcalis ativados existe um subgrupo chamados geopolímeros. O termo "geopolímero" foi utilizado pela primeira vez em 1978 (Davidovits, 2008), no entanto os conceitos de álcali-ativação já eram utilizados desde 1908, onde se tem registro de uma das primeiras utilizações da combinação entre álcali e um aluminossilicato para produzir um ligante

cimentício a partir de uma patente relacionada à álcali-ativação da escória de alto forno (Kuehl, 1908).

Ainda existem discordâncias quanto a terminologia mais adequada para o produto da reação entre um ativador alcalino e uma fonte de aluminossilicato, fazendo com que alguns autores utilizem as duas terminologias indistintamente. Mendes et *al*. (2021) afirmam que geopolímeros e materiais álcali ativados se diferenciam pelas reações desenvolvidas e os produtos finais dessas reações, que variam de acordo com a composição do precursor e a concentração da solução alcalina.

Materiais geopoliméricos ou álcali-ativados são uma classe de materiais muito versátil devido à grande variedade de matérias-primas, formas de produção e redução potencial das emissões de CO_2 em comparação com o uso de produtos à base de cimento Portland (PROVIS, 2018). De acordo com Turner e Collins (2013), para cada quilo de cimento processado, cerca de 0,66 kg a 0,82 kg de CO_2 é liberado. A fabricação de concreto a partir de geopolímeros pode resultar em uma redução nas emissões de CO_2 de 26% a 45% em relação à produção de cimento Portland. Além disso, as matérias-primas utilizadas são geralmente subprodutos industriais, com pouco ou nenhum impacto ambiental atribuído e baixo custo. Além disso, podem apresentar propriedades e características como alta resistência mecânica, resistência ao fogo, baixa retração e baixa condutividade térmica (DUXSON *et al*., 2007; MA *et al.*, 2018). São os mecanismos de reação que determinam o comportamento de um material cuja formação é oriunda de um processo de reações químicas (PACHECO-TORGAL *et al*., 2015) e, portanto, serão abordados na próxima seção.

2.4.1 Mecanismos de reação

De acordo com Severo *et al*., (2013), os mecanismos de reação se relacionam aos processos químicos de dissolução alcalina e precipitação de um precursor. Esses mecanismos são ainda responsáveis pelo endurecimento e pelas propriedades dos materiais álcali-ativados. Duxson *et al*. (2007) afirmam que o conteúdo de cálcio na composição de um ligante álcali-ativado, se apresenta como um dos fatores que determina o grau de polimerização das estruturas de silicato.

Quando o precursor dos materiais álcali-ativados é essencialmente composto de Si, Al e grandes quantidades de Ca, os mesmos são conhecidos como sistemas com alto teor de cálcio.

Esses materiais exigem de baixa a média concentração de ativador para sua síntese (PALOMO *et al*., 1999). Os produtos da reação entre escórias ricas em cálcio e hidróxidos alcalinos ou silicatos são geralmente o gel de silicato de sódio/potássio e alumínio hidratado (N (K) -A-S-H) e o gel sílico-aluminato de cálcio hidratado (C-A-S-H). Este último tem uma estrutura semelhante ao gel resultante da hidratação do cimento Portland (C-S-H), mas com menor teor de Ca e mais substituições de alumínio em conjuntos tetraédricos (SAMARAKOON *et al*., 2019; PROVIS e BERNAL, 2014).

Já os aluminossilicatos tridimensionais sintetizados por uma alta concentração de solução alcalina (hidróxido ou silicato), que utilizam como precursores materiais ricos em Si e Al com baixo ou nenhum conteúdo de cálcio são conhecidos como sistemas de baixo teor de cálcio (Palomo, *et al*. 2014), ou ainda geopolímeros (Palomo *et al*., 1999). Argilas calcificadas (por exemplo, metacaulim), cinzas volantes e rejeitos de mineração com altas porcentagens de sílica e alumina podem ser aplicadas como matérias-primas. Os materiais com estas características necessitam de condições mais agressivas para iniciar as reações, condições de um meio alcalino forte e cura em temperaturas elevadas, entre 60º a 200ºC (Lodeiro, *et al*. 2013). Segundo Davidovits (1991) e Davidovits (1987), o produto resultante desse processo é uma matriz amorfa cujo componente principal é um gel aluminossilicato conhecido como N-A-S-H, onde N representa o cátion alcalino, ou como precursor zeolítico. Bernal *et al*. (2011) afirmam ainda que os géis C-A-S-H e N-A-S-H podem coexistir em misturas de precursores com baixo e alto teor de cálcio, embora a estabilidade da coexistência do gel em alta alcalinidade já seja discutida por Gartner e Macphee (2011) e García-Lodeiro *et al*. (2011).

A primeira tentativa de descrever o mecanismo para a ativação alcalina de materiais contendo sílica e alumina reativa foi proposta por Glukhovsky (1959) através de um modelo composto por quatro fases: dissolução, precipitação de espécies ativas, condensação e re-solidificação. Ao longo do tempo outros autores elaboraram e estenderam a teoria de Glukhovsky aplicando os conhecimentos sobre a síntese de zeólitas a fim de explicar o processo de geopolimerização como um todo (FERNÁNDEZ-JIMÉNEZ *et al*., 2005; FERNÁNDEZ-JIMÉNEZ *et al*., 2006; PROVIS *et al*., 2005; PROVIS *et al*., 2006; VAN DEVENTER *et al*., 2006).

O modelo conceitual do processo de geopolimerização proposto por Duxson *et al*. (2007) é apresentado na Figura 2 e os mecanismos da síntese de geopolímeros são detalhados a seguir.

Figura 3 - Modelo conceitual do processo de geopolimerização

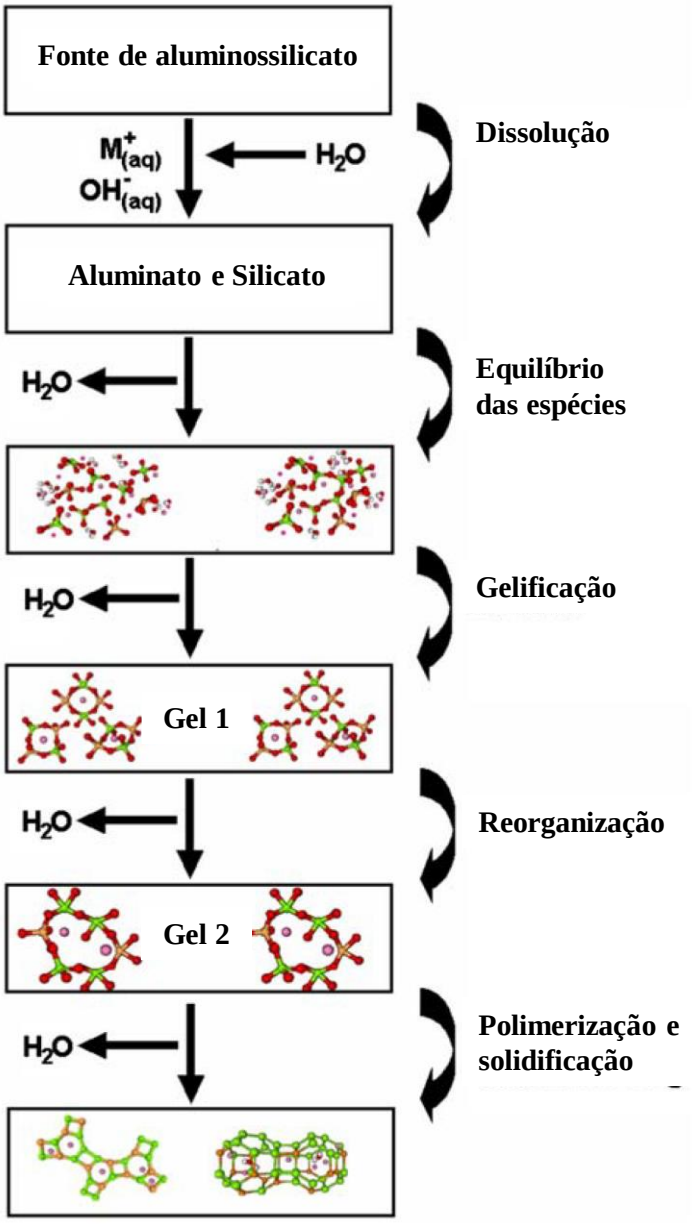

Fonte: Adaptado de Duxson *et al*. (2007)

O processo de dissolução de Si e Al dos materiais sólidos aluminossilicatos em solução aquosa altamente alcalina ocorre através da lixiviação. Dessa forma as espécies silicato e aluminato começam a se distribuir para a fase aquosa, que por sua vez, pode conter silicato na solução de ativação, e formar espécies aquosas por meio da ação dos íons hidróxidos, completando o processo de dissolução. Segundo Weng e Sagoe-Crentsil (2007), as ligações Al-

O apresentam menor energia de ligação e, portanto, são as primeiras a serem rompidas na fase de dissolução, enquanto que as ligações Si-O necessitam de mais tempo e maior alcalinidade para sua ruptura.

Além disso, em soluções aquosas, a dissolução química de minerais Al-Si é favorecida para altos valores de pH, visto que a taxa de dissolução desses materiais aumenta significativamente à medida que o pH da solução aumenta. A dissolução de aluminatos amorfos é rápida para valores elevados de pH e isto cria uma solução supersaturada, resultando na formação de um gel onde os oligômeros na fase aquosa formam grandes redes por condensação. Este processo libera a água que foi consumida durante a dissolução. Como tal, a água funciona como meio de reação, mas fica retida nos poros. Dessa forma a estrutura de gel é designada como sendo do tipo bi-fásica, contendo ligante aluminosilicato e água, que constituem as duas fases.

Giannopoulou e Panias (2007) afirmam que a taxa de dissolução de materiais sólidos de Al-Si depende fortemente do tamanho e da área de superfície específica das partículas. O tempo para a solução supersaturada de aluminossilicato formar um gel varia consideravelmente de acordo com condições de processamento da matéria-prima e a composição da solução e condições de síntese (AIELLO *et al*., 1991; IVANOVA *et al*., 1994). Após a gelificação, o sistema continua a se reorganizar, à medida que a conectividade da rede de gel aumenta, resultando na rede tridimensional de aluminossilicato comumente atribuída aos geopolímeros. Isso é apresentado na Figura 5 pela presença de múltiplos estágios de "gel", consistente com observações experimentais (FERNÁNDEZ-JIMÉNEZ *et al*., 2006, PROVIS e VAN DEVENTER, 2006) e modelagem numérica para geopolímeros baseados em metacaulim e cinza volante (PROVIS, 2006). A dissolução do material aluminossilicato e formação do polímero, é altamente dependente da termodinâmica e parâmetros cinéticos e engloba as duas primeiras etapas propostas por Glukhovsky. O crescimento é o estágio em que os núcleos atingem um tamanho crítico e os cristais começam a desenvolver. Esses processos de reorganização estrutural determinam a microestrutura e a distribuição dos poros do material, que são críticos na determinação muitas propriedades físicas (DUXSON *et al*., 2005).

Por fim, uma vez que a estrutura geopolimérica é desenvolvida na fase aquosa, ela se depara com os grupos de partículas sólidas ativas, onde é possível reagir ligando as partículas não dissolvidas na estrutura geopolimérica final. De acordo com Duxson *et al*. (2005), diferente das etapas de secagem e endurecimento da zeólita, na solidificação da matriz polimérica não ocorre reação química, apenas a evaporação da água que gera materiais duráveis e resistentes.

Ante ao exposto, é possível notar que as características dos produtos de reação do processo de álcali ativação dependem de muitos fatores, mas principalmente do tipo e da qualidade da matéria-prima utilizada como precursor e o tipo de ativadores alcalinos implementados para sua fabricação (KEULEN *et al*., 2018; ŠPAK e RASCHMAN, 2018; BONDAR *et al*., 2011; BUMANIS *et al*., 2017; FERNÁNDEZ-JIMÉNEZ *et al*., 2005). Dessa forma a subseção seguinte busca explorar tal influência.

2.4.2 Matérias primas utilizadas no processo de álcali ativação

Como já exposto anteriormente, ligantes álcalis ativados são definidos como materiais produzidos através da reação de uma fonte de aluminossilicato com um ativador alcalino (PROVIS, 2014). Além de ser ricos em alumina (Al_2O_3) e sílica (SiO_2), os materiais precursores, tanto na sua forma natural como na forma de resíduo industrial ou outra matéria-prima de baixo valor agregado, devem preferencialmente apresentar características amorfas reativas. Esses precursores de aluminossilicato requerem soluções de ativação alcalina que geralmente consistem em uma solução aquosa de hidróxidos, silicatos, carbonatos ou sulfatos alcalinos (ALANAZI *et al*., 2016; VARGAS *et al*., 2011; HU *et al*., 2009).

Zhang et *al*. (2013) classificam os materiais precursores em calcinados (cinzas volantes, escória, resíduos de construção e resíduos pozolânicos) e não calcinados (caulinita, feldspato, argilas e rejeitos de processamento mineral). Os autores explicam que o processo de calcinação aumenta a reatividade dos materiais, através da alteração da estrutura cristalina em amorfa. Dessa forma, precursores calcinados apresentam taxa de dissolução mais rápida e, portanto, maior resistência à compressão inicial quando comparados à precursores não calcinados que apresentam aumentos mais significativos da resistência mecânica nos estágios posteriores à reação de álcali-ativação.

Mais de 65% da crosta terrestre consiste de materiais à base de Al-Si e uma grande gama destes materiais podem servir como fonte para a síntese de materiais álcali ativados (XU e VAN DEVENTER, 2000). Os primeiros estudos e aplicações de materiais álcali ativados utilizaram principalmente precursores como como escória de alto forno, cinza volante e metacaulim (SHI *et al*., 2006; PROVIS *et al*., 2014; MAJIDI, 2009). No entanto atualmente os materiais álcali ativados são também uma maneira efetiva de reciclar e reutilizar vários subprodutos da indústria através da inclusão de por exemplo, cinzas volantes (OH *et al*., 2010; AYDIN e BARADAN, 2012; GIASUDDIN *et al*., 2013), escória à base de argila (YUSUF *et al*., 2014; RANJBAR *et*

al., 2014), cinza de casca de arroz (He *et al*., 2013), para torná-los mais sustentáveis em termos de meio ambiente, disponibilidade e economia.

O fato de esses materiais precursores serem produzidos por indústrias em todo o mundo torna os materiais álcali ativados sustentáveis também em termos de disponibilidade. São produzidas mundialmente 780 milhões toneladas/ano de cinza volante (BAKRI *et al*., 2013; DUAN *et al*., 2015), 11 milhões de toneladas/ano cinzas de óleo de palma (VAKILI *et al*., 2015), 20 milhões de toneladas/ano de cinza de casca de arroz (SINULINGGA *et al*., 2014; KAMSEU *et al*., 2016), 120 milhões de toneladas/ano de lama vermelha de alumina (DUAN *et al.*, 2015; YE *et al*., 2016, além da existência de enormes depósitos de caulim (YUN-MING *et al*., 2016; ZHANG *et al*., 2016).

Em relação ao ativador alcalino, Duxson *et al*. (2007) afirmam que seu objetivo principal consiste no fornecimento de cátions de metais alcalinos, de modo a aumentar o pH da mistura e acelerar a dissolução do precursor sólido. Um meio altamente alcalino é essencial para uma apropriada ativação do silício e alumínio existentes no material precursor, propiciando a transformação de uma estrutura parcial ou totalmente vítrea em um material bastante compacto (EDUOK, 2016).

Segundo Robayo-Salazar e Gutiérrez (2018), os ativadores alcalinos geralmente empregados são constituídos por hidróxidos (ROH, $R(OH)_2$), ácidos fortes (Na_2SO_4, $CaSO_{4.2}H_2O$), ácidos fracos (R_2CO_3) e sais de sílica ($R_2O(n)SiO_2$), onde o "R" pode ser assumido por K, Na ou Li. Os autores afirmam ainda que múltiplos parâmetros da solução ativadora influenciam nas propriedades do material geopolimérico, como o pH, solubilidade, concentração, o tipo do metal alcalino e a sua natureza (líquido ou sólido).

Embora possam ser empregados quaisquer metais da Família IA, os mais utilizados são os hidróxidos de sódio (NaOH) e o hidróxido de potássio (KOH). Já a solução de silicato tem a função de complementar o silício da mistura, a fim de obter as proporções de SiO_2/Al_2O_3 para cada tipo de utilidade ou propriedade desejada, onde os mais utilizados são silicato de sódio ($nSiO_2Na_2O$) e silicato de potássio ($nSiO_2K_2O$) (SEVERO *et al*., 2013).

Os ativadores mais utilizados são composições entre silicatos (líquido ou sólido dissolvido em água) e hidróxidos (diluídos) (CRIADO *et al*., 2005). Os mais comuns são os hidróxidos de Na, Ca, K e os silicatos de Na e K (PROVIS e BERNAL, 2014). Por ser o mais econômico e de maior disponibilidade, o NaOH, também conhecido como soda cáustica, é o hidróxido mais utilizado como ativador, entretanto devido a sua natureza corrosiva requer

equipamentos e manuseio apropriados para sua utilização (PROVIS e VAN DEVENTER, 2009). De um modo geral a resistência mecânica de materiais álcali ativados produzidos com NaOH apresentam menor resistência que os produzidos com outros silicatos (PROVIS *et al*., 2005).

Segundo Duxson *et al*. (2007b) estruturas mais densas e compactas são formadas em tempo menor ao adicionar silicatos solúveis nos ativadores. A presença de sílica monomérica (Si(OH)4) presente no ativador possibilita uma maior alcalinidade, acelerando a cinética das reações (PROVIS e VAN DEVENTER, 2007). Provis e Bernal (2014) explicam que a baixa reatividade de materiais álcali ativados produzidos com NaOH antes do endurecimento, leva à formação de uma solução rica em álcalis em uma matriz geopolimérica porosa que propicia a formação de eflorescência.

Soluções com o hidróxido de potássio (KOH) exibem maior potencial de reação devido ao tamanho do seu raio de hidratação e ao alto número de moléculas H_2O associados ao íon K^+ (PROVIS e VAN DEVENTER, 2009). Dessa forma, materiais precursores ativados com KOH, em maior parte, demonstram melhores resistências à compressão em comparação com materiais álcali ativados que utilizam solução de NaOH como ativadores (DUXSON *et al*., 2007). Também, a maior resistência à compressão apresentada por materiais álcali ativados sintetizados com KOH, pode ser explicada pelo tamanho do cátion do K^+. O cátion Na^+ apresenta tamanho menor que o cátion de K^+, portanto, forma pares com menores oligômeros de silicato. Atenta-se que quanto maior o tamanho do cátion, é favorecida a geração de oligômeros de silicato maiores, na qual o aluminato ($Al(OH)^{-4}$) prefere ligar-se (SEVERO *et al*., 2013).

No entanto, o uso comercial em larga escala de materiais álcali-ativados permanece extremamente pequeno devido a obstáculos tecnológicos relacionados a alta emissão de energia e CO_2 decorrente do processo de produção dos ativadores alcalinos. O uso de soluções de ativador alcalino é frequentemente considerado como uma das principais deficiências práticas de materiais álcali-ativados, porque tais soluções ativadoras são caras, corrosivas e prejudiciais ao meio ambiente (LUUKKONEN *et al*., 2018). Um estudo recente de Scrivener et *al*. (2018) afirmou que a pegada de CO_2 do ativador de silicato de sódio deve ser reduzida pelo menos pela metade para obter uma tecnologia escalonável de materiais álcali-ativados.

Dessa forma, há uma necessidade premente de desenvolvimento sustentável e ativadores de baixo custo que podem melhorar substancialmente as perspectivas de uso de materiais álcali-

ativados. As subseções porvindouras, exploram as ideias e conceitos inerentes à produção de ligantes álcali-ativados a partir de silicato de sódio alternativo.

2.4.3 Silicato de sódio alternativo

Materiais álcali ativados são uma nova alternativa ao cimento Portland principalmente no que diz respeito às emissões de CO_2 para o meio ambiente. Porém, para obter essa vantagem, é imprescindível o uso de ativadores que sejam produzidos de forma limpa e sustentável, o que não é o caso de produtos comerciais como NaOH ou silicato de sódio (MENDES *et al*., 2021). O silicato de sódio é um precursor do dióxido de silício, que é essencialmente necessário em síntese de geopolímero. A presença de íons de sódio favorece a dissolução, pois reage de forma mais eficaz para formar oligômeros e também melhora as propriedades mecânicas e químicas em comparação com outros íons, como por exemplo o potássio (ABDUL *et al*., 2015; XU, 2000). Tradicionalmente, os silicatos de sódio de grau laboratorial são preparados pela fusão de quartzo e pó de carbonato de sódio (Na_2CO_3) em alta temperatura (≈ 1300 °C) (OWOEYE, 2017), configurando um processo de produção que consome muita energia e que contribuiu com uma quantidade significativa nas emissões de dióxido de carbono. McLellan *et al*. (2011) afirmam que o silicato de sódio é o componente de maior impacto do ponto de vista energético e da emissão de CO_2 demandando 63,4% da energia total para produção do material. Duxson *et al*. (2007) estimam também que são emitidos 1,514 kg de CO_2 para a produção de um quilograma de silicato de sódio.

Como um subproduto agrícola, a CCA está disponível em abundância na maior parte dos países produtores de arroz, sendo obtido após o processo de queima da casca de arroz e contendo teor extremamente alto de sílica (IBRAHIM *et al*., 1980). A eliminação do restante da CCA é ainda uma grande preocupação, pois se não for descartado de forma adequada, as partículas transportadas pelo ar podem causar doenças respiratórias humanas graves e podem ser um risco potencial de incêndios em aterros sanitários (TSEN *et al*., 2020). Nesse sentido, Villaquirán-Caicedo e Gutiérrez (2018) afirmam que ativadores alcalinos a base de CCA geram uma emissão de cerca de 572,3 kg/m³ de geopolímero produzido, representando cerca de 48% a menos que o silicato de potássio por exemplo e, portanto, sendo considerados uma alternativa ecologicamente mais correta. Portanto, diversos estudos têm sido realizados a fim de utilizar a CCA em várias aplicações, inclusive na produção de silicato de sódio para posterior utilização em materiais álcali ativados (KALAPATHY *et al*., 2000; FOLETTO *et al*., 2006; ZIVICA,

2006; DETPHAN e CHINDAPRASIRT, 2008; BERNAL *et al*., 2012; LONGHI, 2015; GERALDO, 2017; TCHAKOUTÉ *et al*., 2016 a e b; APOLÔNIO, 2017; KAMSEU *et al*., 2017; AVILA, 2018; LIMA, 2018).

Apesar das crescentes pesquisas sobre ativadores alcalinos sustentáveis e econômicos (VINAI e SOUTSOS, 2019) e do potencial da CCA para ser utilizada como tal (ROSCHAT *et al*., 2016), os procedimentos de produção ainda não são bem estabelecidos. Nesse contexto, na próxima seção são sintetizados alguns parâmetros inerentes a produção ativadores alcalinos a base de CCA.

2.4.4 Processo de produção do silicato alternativo

De forma a progredir em relação a ativadores alcalinos mais sustentáveis, soluções alternativas com base na dissolução da sílica de resíduos têm sido promovidas de modo a produzir um ativador de silicato alcalino comparável ao comercial (ALNAHHAL *et al*., 2021). A CCA é um dos resíduos ricos em sílica mais comumente utilizados e os pesquisadores aplicam diferentes métodos de extração da sílica para desenvolver ativadores alternativos (TONG *et al*., 2018; BOUZÓN *et al*., 2014). O processo hidrotérmico é comumente utilizado para produzir um ativador alternativo na forma líquida, uma vez que geralmente consome menos energia em comparação com os outros métodos (FAVER *et al*., 1999), mas seu uso ainda requer mais pesquisas acerca dos processos envolvidos. Na Tabela 1 são apresentados alguns fatores envolvidos na produção de silicato de sódio alternativo a base de CCA para uso em materiais álcali ativados. A taxa de dissolução da sílica foi avaliada através do teor de sílica, temperatura, tempo de processamento, alcalinidade da solução e tamanho das partículas.

Tabela 1 - Parâmetros envolvidos na produção de silicato de sódio alternativo a base de CCA

Referência	Precursor	Condições de dissolução				Características da CCA	
		Fonte alcalina	Temperatura	Tempo de dissolução	Molaridade	(%) SiO_2	Tamanho da partícula
Bernal et al., 2012	Metacaulim/escória	NaOH	Ambiente	10 min	-	68	> 1 µm e < 60 µm
Geraldo et al., 2017	Metacaulim/lodo de tratamento de água	NaOH	Ambiente e 90 °C	30 min	-	89,51	20,4 µm
Tchakouté et al., 2016a	Metacaulim	NaOH	80°C	2 h	-	93,49	-
Tchakouté et al., 2016b	Metacaulim	NaOH	100°C	2 h	-	83,05	< 90 µm
Kamseu et al., 2017	Metacaulim	NaOH	Ambiente	40 min	8, 10 e 12 M	-	< 45 µm
Mejía et al., 2013	Metacaulim/cinza volante	NaOH	Ambiente	24 h	-	90,91	5 µm
Bernal et al., 2015	Escória	NaOH	Ambiente	24 h	2 e 4 M	68	> 1 µm e < 60 µm
Mejía et al., 2013	Escória/cinza volante	NaOH	Ambiente	-	-	94	36,9 µm e 39,5 µm
Tong et al., 2018	Escória /cinza volante	NaOH	Ambiente, 60°C, 80°C, 90°C e 100°C	1, 3, 5, 7 e 15 h	1, 2, 3.2, 4.9 e 6.5 M	90,5	6,82 µm
Passuello et al., 2017	Lodo de caulim	NaOH	100°C	1 h	-	97,3	-
He et al., 2013	Lama vermelha	NaOH	Ambiente	15 min	2, 4 e 6 M	91,5	25 µm e 32 µm
Bouzón et al., 2014	Resíduo de catalisador de craqueamento catalítico fluído	NaOH	100°C	5 - 240 min	-	85,58	20 µm e 62 µm
Luukkonen et al., 2018	Escória	NaOH	Ambiente	4 h	0.1, 1 e 10 M	88,46	20µm, 30µm, 172µm e 199 µm
Hajimohammadi e Van De	Metacaulim	$NaAlO_2$	Ambiente	-	-	56,22	8 µm
Sturm et al., 2016	Aluminato de sódio	$NaAlO_2$	Ambiente	-	-	88,49	11,1 µm

Fonte: Autor (2023)

O tempo de processamento e a temperatura são fatores importantes que afetam a dissolução da sílica. Apesar de não serem eficientes em termos de consumo de energia, os processos de aquecimento e agitação geralmente aumentam a taxa de dissolução de sílica assim como a cinética de reações químicas que geralmente aumentam com a temperatura e um estímulo externo (ALAM *et al*., 2019). Conforme a Tabela 1, o tempo de processamento e temperatura variaram de 5 min a 24 h e da temperatura ambiente a 100 ◦C. Bouzón *et al*. (2014) obtiveram a máxima dissolução da CCA utilizando um tempo de processamento de 60 min a 100°C, enquanto que Tong *et al*. (2018) mostraram ser necessário um tempo maior de processamento variando de três a seis horas. A variação no tempo de processamento pode ser atribuída à natureza e reatividade da fonte de sílica e a porção restante não dissolvida indica a presença de carbono não queimado e pequenas quantidades de outros resíduos insolúveis (ALNAHHAL *et al*., 2021).

A sílica amorfa é conhecida por ter um valor relativamente alto de energia de ativação (MARAGHECHI *et al*., 2016) e temperaturas de até 80 ◦C são essenciais para aumentar a taxa de dissolução no processo hidrotérmico de ativação da sílica em soluções alcalinas, não sendo observada nenhuma dissolução significativa adicional em temperaturas de processamento mais altas (TONG *et al*., 2018). Nesse sentido Geraldo *et al*. (2017) também verificaram um efeito significativo da temperatura representado por um aumento de 50% na quantidade de sílica dissolvida devido ao aquecimento a 90°C. No entanto, Passuelo *et al*. (2017) alertam sobre a possibilidade de evaporação da água em altas temperaturas, recomendando que o processo seja conduzido em um sistema fechado durante a dissolução da sílica. Alam et *al*. (2019) mostram que temperaturas baixas, incluindo a temperatura ambiente, também são eficientes no processo de dissolução, mas requerem um tempo maior de processamento, por exemplo 72 h para alcançar a eficiência de extração de 45%.

Em relação ao tamanho da partícula da fonte sílica, embora alguns estudos mostrem que as partículas menores se dissolvem mais rápido, os resultados de alguns estudos apresentados na Tabela 1 sugerem que a dissolução é independente do tamanho da partícula. Bouzón *et al*. (2014) observaram uma solubilidade semelhante para as partículas de CCA com tamanho médio de 20 μm e 62 μm. Em conformidade, Luukkonen, *et al*. (2018) também apontaram que os tamanhos de partícula de CCA têm um impacto insignificante sobre a quantidade de sílica dissolvida. O efeito insignificante do tamanho da partícula na solubilidade da sílica pode ser explicado ao efeito de reagregação das partículas muito finas (HAJIMOHAMMADI e VAN DEVENTER, 2016).

No que se refere às propriedades mineralógicas dos materiais na dissolução da sílica, Mejía *et al*. (2013) investigaram dois tipos de CCA e apontaram que ambas exibiram boa solubilidade quando misturados com NaOH, independentemente do teor de sílica amorfa, mas que a alcalinidade deve ser adequadamente ajustada para cada CCA. Uma das CCA foi produzida sob incineração controlada por laboratório a 600 ◦C por 3 h e obteve 94,4% de SiO_2 amorfo dos 94,7% totais, enquanto que a outra CCA foi coletada diretamente da fabrica de arroz e apresentou 27,7% de SiO_2 amorfa de um total de 94,1%. No entanto os autores afirmam que a CCA com maior conteúdo amorfo exigiu menos tempo e menor temperatura de aquecimento para a dissolução. Dessa forma as propriedades mineralógicas ajudam a identificar o tempo de processamento e temperatura adequados, e assim, a otimização do uso da energia.

Se tratando da concentração molar, Luukkonen, *et al.* (2018) observaram que a dissolução da sílica aumentou quando a concentração de NaOH aumentou de 1M para 10M. Isso pode ser atribuído à maior liberação de sílica em altas concentrações alcalinas (ANDREOLA *et al*., 2019). Tong *et al*. (2018) também relataram que baixas concentrações de NaOH (menores de 2 M) não são adequadas para maximizar a quantidade de sílica dissolvida, sugeriram que a molaridade ideal seria de 3 M.

Por fim, vários estudos apresentados nessa seção mostraram potenciais promissores para sintetização de ativadores usando subprodutos ricos em sílica. No entanto, como não existe um consenso sobre o processo de extração otimizado, são essenciais uma compreensão abrangente e uma seleção cuidadosa dos processos adotados afim de otimizar o uso de energia durante o processo de extração de sílica da CCA.

2.4.5 Cinza de casca de arroz

Resíduos agroindustriais são geralmente reintroduzidos no processo do agronegócio que os gerou, como compostagem ou como fonte de energia para fornos de secagem. A combustão de biomassa gera cinzas que vêm chamando atenção por décadas, já que sua composição química os qualifica como pozolanas ou como uma fonte eficaz de aluminossilicatos, especialmente adequada para a síntese de materiais álcali-ativados (RIVERA *et al*., 2021). Um dos resíduos agroindustriais mais utilizado em materiais álcali-ativados é a cinza de casca de arroz (CCA) caracterizada por possuir mais de 95% de SiO_2 em sua composição, com a maior parte desta sílica presente de forma amorfa (DELLA *et al.*, 2002). A casca de arroz corresponde a aproximadamente 20% a 25% do grão, não é digerível e, portanto, deve ser removida do grão.

Basicamente, é usada como combustível no processo de secagem do arroz, resultando em aproximadamente 18% de seu volume inicial em cinzas. Dependendo do tipo de arroz, o clima e o tipo de tecnologia de combustão, 1 tonelada de arroz produz aproximadamente 45 kg de CCA (RIVERA *et al*., 2021). Além disso, a CCA gera grande preocupação por causa da riscos potenciais da inalação deste mineral (SANJAYAN *et al*., 2015).

A produção mundial de arroz em 2019/20 foi de 496,11 milhões de toneladas (USDA, 2020). Assumindo a combustão de tais quantidades, aproximadamente 22,5 milhões de toneladas de CCA foram produzidas no mundo todo (VILLAQUIRÁN-CAICEDO *et al*., 2017; FAO, 2019). Segundo o IBGE, em 2019 o Brasil produziu 10,37 milhões de toneladas de arroz com casca, sendo estimado um aumento de 0,9% para a safra de 2020 e o estado do Rio Grande do Sul responsável por aproximadamente 70% da produção (7,17 milhões de toneladas).

O arroz possui grandes quantidades de sílica, especialmente na sua casca que consiste em uma capa lenhosa, dura e altamente silicosa e é composta por 50% de celulose, 30% de lignina e 20% de sílica (base anidra) (METHA, 1992). A quantidade, conteúdo cristalino e composição química da sílica produzida depende do projeto do forno e das temperaturas de queima (ZAIN *et al*., 2011), podendo assumir formas estruturais diferentes durante a combustão: amorfa e/ou cristalina (MEHTA, 1977).

A sílica cristalina pode ocorrer na natureza de três formas: quartzo, tridimita e cristobalita, sendo que a primeira ocorre mais frequentemente que as demais (KINGERY *et* al., 1976). Já a sílica amorfa é um material de fácil moagem e que se apresenta altamente reagente ao ser moída em processos de queima rápida a baixas temperaturas, inferiores a 700° C (POUEY, 2006). De acordo com Silveira (2007) a maior parte dos trabalhos desenvolvidos no Brasil utiliza cinzas residuais sem controle efetivo de tempo e temperatura de queima e mesmo exibindo picos cristalinos apresentam desempenho satisfatório. Pouey (2006) afirma também que além do simples processo de combustão, a sílica reativa pode ser obtida através de tratamentos físico-químicos da casca, seguido de queima e processo microbiológico.

Devido às suas propriedades, o uso de CCA como alternativa ao cimento na indústria de concreto torna-se cada vez mais comum (ALNAHHAL *et al*., 2017; ANTIOHOS *et al*., 2014; ZIEGLER *et al*., 2016; HABEEB e MAHMUD, 2010; HE *et al*., 2013; JUNAID *et al*., 2014; MEHTA, 1977; RAHEEM *et al*., 2013; SARAVANAN e SIVARAJA, 2016; SHALINI *et al*., 2016).

A CCA tem sido utilizada também como intensificadora da relação molar SiO_2/Al_2O_3 na síntese de materiais álcali-ativados, e também como um precursor na produção de soluções de silicato de sódio, devido ao seu alto teor de sílica (DETPHAN e CHINDAPRASIRT, 2009;

MEJÍA *et al*., 2016). Vários autores (VILLAQUIRÁN-CAICEDO *et al*., 2017; BERNAL *et al*., 2015; BOUZÓN *et al*., 2014) mostraram que o desenvolvimento de soluções ativadoras a base de CCA é uma alternativa viável para a substituição de ativadores alcalinos comerciais, conforme os resultados obtidos, em termos de resistência e microestrutura, que são muito semelhantes às dos silicatos comerciais.

Além disso, a CCA tem sido utilizada como material precursor para o desenvolvimento de materiais álcali-ativados pelo método "one-part", exigindo apenas a adição de água para o início da álcali-ativação (HAJIMOHAMMADI e VAN DEVENTER, 2017; LUUKKONEN *et al*., 2018; HAJIMOHAMMADI *et al*., 2008). A síntese em uma etapa elimina os riscos de manipulação das soluções ativadoras corrosivas e diminuindo as restrições de armazenamento e transporte. No entanto, os estudos são ainda muito limitados em comparação com os materiais álcali ativados por síntese em duas etapas que já foram desenvolvidos com sucesso para fins estruturais (GLASBY *et al*., 2015; ALDRED e DAY, 2012).

2.4.5 Parâmetros importantes no processo de álcali ativação

Como mencionado anteriormente, as reações do processo de álcali ativação ocorrem entre fontes de aluminossilicato e um ativador alcalino. No entanto Duxson *et al*. (2007) afirmam que nem todos os materiais constituídos de sílica e alumina apresentam potencial para álcali ativação, uma vez que parâmetros como teor de material amorfo, superfície específica do material, teor de fase vítrea e tamanho da partícula também determinam o comportamento reativo dos materiais. Nas últimas décadas, experiências práticas e muitos estudos em andamento apoiaram os fundamentos de materiais alcalinos ativados, ou seja, matérias-primas, requisitos, química e mineralogia, estrutura e propriedades de engenharia, fatores de controle, processamento, vida útil e durabilidade de materiais álcali-ativados (PACHECO-TORGAL *et al*. 2014; PROVIS e VAN DEVENTER, 2014). Os parâmetros que exercem influência no processo de álcali ativação apresentam-se como o alicerce para a criação de produtos economicamente e ambientalmente vantajosos. Dessa forma, os itens subsequentes exploram as ideias e conceitos inerentes aos parâmetros relacionados ao processo de álcali ativação.

a) Calcinação e tamanho de partícula dos precursores

A calcinação e o tamanho da partícula dos materiais precursores impactam no desempenho dos materiais álcali-ativados em termos de taxa de reação, resistência, quantidade de água e uniformidade. A dissolução e gelificação no processo de álcali-ativação são mais rápidas em precursores calcinados como cinzas volantes, metacaulim, escória, resíduos de construção e resíduos pozolânicos, o que eventualmente reduz a probabilidade de trincas devido ao maior ganho de resistência nas primeiras idades (DAVIDOVITS, 1991; KRIVENKO e SKURCHINSKAYA, 1991; PALOMO *et al*., 1999). Já os precursores não calcinados como caulinita, minerais de rocha aluminossilicatos, feldspatos e rejeitos de mina exibem maior ganho de resistência no estágio posterior à geopolimerização (XU e VAN DEVENTER, 2000; XU et *al*., 2001). Os precursores à base de argila possuem partículas lamelares que aumentam sua demanda por água e, portanto, resultam em misturas com alta porosidade e baixa durabilidade. Dessa forma, geralmente é necessária a calcinação em altas temperaturas para minerais de argila se tornarem reativos durante os processos de álcali ativação (HE *et al*., 2013; ZHANG *et al*., 2012).

Em relação ao tamanho da partícula observa-se que quanto maior a finura maior a área de superfície específica, acelerando o processo de polimerização e tornando a microestrutura mais densa (NAZARI *et al*., 2011). Esse comportamento tem impacto positivo em produtos à base de argila caulinita (AL-SHATHR e AL-ATTAR, 2015). Apesar de as cinzas volantes apresentarem essa mesma tendência (TEMUUJIN *et al*., 2009; KUMAR e KUMAR, 2011), suas partículas são muito heterogêneas, em termos de propriedades físicas e químicas, podendo resultar em materiais álcali ativados com configurações variáveis para cinzas volantes de origens diferentes (DIAZ–LOYA *et al*., 2015). Esse comportamento também é evidenciado em misturas como cinza volante e CCA (DETPHAN e CHINDAPRASIRT, 2009), lama vermelha e CCA (FERDOUS *et al*., 2015), escória e cinza volante (YANG e SONG, 2009).

b) Relação entre os óxidos

Apesar de a composição e a reatividade do material precursor desempenhar um papel importante na definição das propriedades dos materiais álcali-ativados (VAN JAARSVELD *et al.*, 2002), durante o processo de álcali-ativação o teor de Si na matriz determina se a condensação ocorre entre Al-Si ou Si-Si (DAVIDOVITS, 1991). Para baixas razões Si/Al, a condensação ocorre principalmente entre as espécies Al-Si, resultando na estrutura do polímero de poli (sialato), porém com o aumento da razão Si/Al, aumentam as espécies de Si devido à

hidrólise de SiO_2 formando silicatos oligoméricos por condensação entre si (WENG *et al*., 2002). Em geral, o alto teor de Si reativo é responsável por impactar significativamente a formação de grande quantidade de gel alcalino aluminossilicato (WENG *et al*., 2002), enquanto a quantidade de Al presente no precursor governa o tipo de estrutura química e a formação de rede (DAVIDOVITS, 2014). No entanto, o papel de Si e Al na síntese de geopolímero estão inter-relacionados e, portanto, expressos na razão Si/Al. A relação Si/Al ideal para desenvolvimento de geopolímero com as melhores propriedades de resistência variam principalmente com o tipo e composição do material de origem (FARHAN *et al*., 2020). Na maioria dos trabalhos de pesquisa envolvendo geopolímero de metacaulim, relações Si/Al na faixa de 3,0 a 3,8 forneceram as melhores propriedades mecânicas (DUXSON *et al*., 2005). É importante ainda ressaltar que além da relação molar SiO_2/Al_2O_3 intrínseca dos precursores é possível variar a mesma a partir da adição de um silicato solúvel, que afeta na cinética das reações e melhora as propriedades físicas dos geopolímeros (RODRÍGUEZ, 2012). Se tratando particularmente de cinzas volantes devido a sua heterogeneidade, a influência da relação Si/Al é bastante obscura. Algumas pesquisas indicam redução na resistência à compressão com aumento na razão Si/Al (CHINDAPRASIRT *et al*., 2012), enquanto outros indicam o contrário (GUNASEKARA *et al*., 2014) e ainda outras que demonstram que a relação Si/Al não tem qualquer relação com a resistência à compressão (ANTONIE *et al*., 2016a; ANTONIE *et al*., 2016b).

O óxido de cálcio como precursor também exerce influência no processo de geopolimerização, mas ainda não há uma concordância sobre seu efeito sobre o processo. De acordo com algumas pesquisas, a presença de grande quantidade de óxidos de cálcio atua como um impedimento no processo de geopolimerização (GOURLEY, 2003; LLOYD e RANGAN, 2010), enquanto que outras sugerem a influência positiva do aumento de CaO na resistência à compressão (CHINDAPRASIRT *et al*.,2012; WONGPA *et al*., 2010).

Outra relação importante é a Na_2O/SiO_2, uma vez que o grau de polimerização está conectado com a mesma, podendo estes materiais serem provenientes do precursor ou em alguns casos do ativador (LONGHI, 2015). Criado *et al*. (2008) constataram que com o aumento desta relação a variação de estruturas de silicato monomérico em dímeros, trímeros cíclico e linear, consequentemente um maior grau de polimerização. A relação Na_2O/Al_2O_3 é similar à Na_2O/SiO_2, mas tem como parcela sólida a alumina, que normalmente é encontrada em precursores em menores teores que a sílica, esta relação tem grande importância nos

geopolímeros por controlar algumas reações (DUXSON *et al*., 2006; FERNANDEZ-JIMENEZ *et al*., 2006).

c) Condições de cura

A cura adequada é um pré-requisito para a dissolução completa e condensação de espécies de Si e Al e é amplamente dependente da reatividade e das proporções dos precursores utilizados (KOMNITSAS e ZAHARAKI, 2007). Por estar relacionada com o processo de geopolimerização, a cura influencia na resistência mecânica e na porosidade do geopolímero formado (XU, 2002). Xu *et al*. (2010) afirmam que altas temperaturas são favoráveis para geopolímeros de cinza volante devido a reatividade relativamente baixa do precursor, mas que para geopolímeros de metacaulim são requeridas temperaturas menores. Já para geopolímeros a base de lama vermelha, sob condições de temperatura moderada, geralmente são necessárias pelo menos três semanas para sua estabilização, enquanto que os geopolímeros de cinza volante estabilizam em apenas alguns dias sob altas temperaturas (SOMNA *et al*., 2011; HE *et al*., 2012). No entanto, apesar de o calor ativar o processo de reação de geopolimerização, temperaturas elevadas por muito tempo podem resultar na redução da resistência e propriedades de durabilidade (PANGDAENG *et al*., 2015). O motivo é o rápido desenvolvimento da matriz de geopolímero na superfície que desacelera ou até mesmo impede a lixiviação dos aluminossilicatos (ZUHUA *et al*., 2009)

A pré-cura precedida por cura convencional exerce influência positiva na resistência dos geopolímeros (KANI e ALI, 2009). Kim e Kim (2013) recomendam a pré-cura a 75°C por 3 h e após cura à temperatura ambiente por 28 dias para produção geopolímeros de metacaulim de alta resistência. Nazari *et al.* (2011) utilizou a pré-cura por 24 h antes da aplicação da cura em estufa de 50°C a 90°C por 36 h. O estudo encontrou 80° C como temperatura ideal para todas as misturas aos 7 e 28 dias. O aumento da temperatura de cura além de 90°C resultou na redução da resistência. Muñiz-Villarreal *et al*. (2011) submeteram geopolímeros a base de metacaulim a uma cura inicial de 40°C por 2 h e posteriormente a uma segunda cura sob temperaturas que variavam de 30 a 90°C por 24 h. Os resultados mostraram que a temperatura de 60°C é ideal e que para temperaturas superiores a esta ocorre aumento da porosidade e redução na resistência a compressão. Em contrapartida, alguns trabalhos relataram que o aumento da temperatura inicial de cura pode resultar em cristalização rápida, particularmente para matriz ativada por NaOH que diminui o poder da reação (Provis *et al*., 2005)

Ainda se tratando das condições de cura vale ressaltar que o tempo de cura aquecida também é um parâmetro que exerce influência no produto final. Lloyd e Rangan (2010) variaram o tempo de cura de 4h a 96 h e concluíram que após 24 h os acréscimos de resistência são moderados e que em termos práticos não é conveniente ultrapassar esse limite de tempo.

Em relação ao ambiente de cura, Kusbiantoro *et al*. (2012) observaram que para álcali ativação a partir de cinza volante e CCA, a cura em estufa resultou em maiores resistências que as curas em exposição externa e em estufa. O aumento de temperatura proporciona um acréscimo na dissolução da sílica e alumina das cinzas volantes devido à polarização do íon hidróxido que por sua vez resulta em maiores resistências (TEOREANU, 1991). Zuhua *et al*. (2009) relataram que materiais álcali-ativados curados a 20 °C ou 40 °C mostraram melhores resultados de resistência à compressão do que amostras curadas em água a 20 ± 2 °C, evidenciando que a água lixivia as espécies dissolvidas. Wang *et al*. (2008) também relataram que a umidade excessiva (imersão na água) não trouxe nenhum benefício, o que também foi observado por Perera *et al*. (2007) e Zhang *et al*. (2009). No entanto, a perda abrupta de água em caso de cura a seco, especialmente em amostras moldadas abertas podem resultar em grande retração e desenvolvimento de microfissuras, que pode causar um efeito prejudicial (ZHANG *et al.*, 2009).

2.5 Álcali ativação aplicada a estabilização de material asfáltico fresado

No decorrer dos anos, diversas pesquisas avaliaram o potencial de incorporação do material fresado às camadas de base e sub-base de pavimento. No entanto, observa-se que para altos teores de substituição ocorrem reduções nas propriedades mecânicas, que podem ser compensadas pelo uso de estabilizadores. É possível utilizar materiais como cal, cimento, cinzas volantes, escória de alto forno, cinza de casca de arroz, cinza de bagaço de cana-de-açúcar, entre outros (SINGH *et al.*, 2018; ADHIKARI *et al*., 2019, CONSOLI *et al*., 2018, POLTUE *et al*., 2019). Materiais álcali-ativados surgiram nas últimas duas décadas como materiais de construção sustentáveis em substituição ao cimento Portland e mais recentemente esses novos ligantes tem sido estudados como estabilizadores em camadas de base e sub-base em combinação com material asfáltico fresado (COSTA *et al*., 2020). A literatura sobre o assunto ainda é limitada e na Tabela 2 são apresentados alguns estudos evidenciando os precursores e ativadores utilizados, bem como as proporções de agregados virgens (AV), os

percentuais de substituição de material asfáltico fresado, a temperatura de cura, os parâmetros avaliados e a faixa de valores de resistência a compressão simples (RCS) obtida nos mesmos.

Jallu *et al*. (2020) investigaram o comportamento da fadiga à flexão de pavimento asfáltico reciclado estabilizado com cinza volante ativada alcalinamente. Os maiores valores de resistência a compressão e módulo de resiliência foram obtidos para a combinação $Na_2SiO_3 : NaOH$ = 70:30. Também foram avaliadas amostras de vigas reforçadas com geogrelhas biaxiais e triaxiais, onde as vigas reforçadas com a geogrelha triaxial apresentaram vida à fadiga 1,66 vezes maior que as reforçadas com geogrelha biaxial e 2,54 vezes maior que as amostras de controle. Os autores identificaram um grande potencial na estabilização de material fresado a partir de um geopolímero a base de cinza volante como material de base de pavimento.

Hoy *et al*. (2016) avaliaram a estabilização de material fresado com cinza volante ativada alcalinamente por uma solução de hidróxido de sódio e silicato de sódio em diversas proporções. Os resultados evidenciam que a resistência aumenta à medida que a razão $NaOH/Na_2SiO_3$ diminui tanto para a temperatura ambiente quanto para cura a 40°C. As análises microscópicas indicam baixa geopolimerização quando é utilizado apenas NaOH ($NaOH/Na_2SiO_3$ = 100: 0) como solução alcalina, mas com o aumento do tempo de cura e da temperatura ocorre uma maior dissolução da sílica e alumina presente na cinza volante aumentando a resistência.

Como complemento do trabalho de Hoy *et al*. (2016a), Hoy *et al*. (2016b) avaliaram a capacidade de lixiviação de metais pesados para a estabilização de material fresado tanto com cinza volante ativada alcalinamente quanto para apenas cinza volante. Os resultados mostraram que não há risco ambiental para duas as misturas e que o ligante geopolimérico reduz a lixiviação de metais pesados, aumentando ainda mais as vantagens na aplicação de materiais reciclados de maneira sustentável na construção de estradas. Horpibulsuk *et al*. (2017) também chegaram nas mesmas conclusões, identificando que acima de seis ciclos de molhagem e secagem a resistência começa a diminuir.

Saride *et al*. (2016) investigaram o uso de cinza volante (20% e 30%) com e sem a ativação de uma solução de hidróxido nas proporções de 2% e 4%. O grande diferencial do trabalho é que os resultados são apresentados em função da área de superfície exposta do material fresado, uma vez que os agregados são revestidos com uma camada de asfalto amorfo que influenciam na formação de compostos pozolânicos.

Tabela 2 - Resumo dos estudos de estabilização de material asfáltico fresado a partir da álcali- ativação

Referência	Precursores	% Precursor	Ativadores	NaOH : Na2SiO3	Molaridade	% RAP	% AV*	Resistencia (MPa)	Temperatura de cura	Parâmetros avaliados
Avirneni et al. (2016)	Cinza Volante	20 e 30%	NaOH	-	1 e 2 M	80 e 60	20 e 40	1,5 a 5,5	Ambiente	RCS, durabilidade, microestrutura e
Hoy et al. (2016)	Cinza Volante	10, 20 e 30%	NaOH e Na2SiO3	100:0, 90:10, 60:40 e 50:50	10 M	100	-	1,9 a 7,0	Ambiente e 40°C	RCS e microestrutura
Hoy et al. (2016)	Cinza Volante	20%	NaOH e Na2SiO3	100:0, 90:10, 60:40 e 50:50	10 M	100	-	1,9 a 5,6	Ambiente	RCS, microestrutura e lixiviação
Hoy et al. (2018)	Escória	10 e 20 %	NaOH e Na2SiO3	100:0, 70:30, 60:40 e 50:50	8 M	100	-	0,75 a 3,0	Ambiente	RCS e microestrutura
Mohammadinia et al. (2016a)	Cinza Volante e Escória	2 e 4%	NaOH e Na2SiO3	-	8 M	100	-	1,0 a 2,2	Ambiente	RCS, módulo de elasticidade e de
Mohammadinia et al. (2016b)	Cinza Volante	4, 8 e 16%	NaOH e Na2SiO3	-	8 M	100	-	1,0 a 2,2	Ambiente e 40°C	RCS e módulo de resiliência
Saride et al. (2016)	Cinza Volante	20 e 30%	NaOH	-	1 e 2 M	80 e 60	20 e 40	1,5 a 6,5	Ambiente	RCS e microestrutura
Horpibulsuk et al. (2017)	Cinza Volante	20 e 30%	NaOH e Na2SiO3	100:0, 90:10, 60:40 e 50:50	10 M	100	-	1,9 a 6,0	Ambiente	RCS, durabilidade, microestrutura e
Jallu et al. (2020)	Cinza Volante	20%	NaOH e Na2SiO3	70:30 e 50:50	3 M	60	40	1,5 a 6,5	Ambiente	Fadiga na flexão
Saride e Jallu (2020)	Cinza Volante	20%	NaOH e Na2SiO3	100:0, 70:30, 50:50, 30:70 e 10:90	0,5; 1; 3M	60	40	0,200 a 6,5	27°C	RCS, módulo de resiliência e durabilidade

Fonte: Autor (2023)

Avirneni *et al*. (2016) submeteram misturas de material asfáltico fresado com cinza volante ativada alcalinamente a variações severas de umidade e temperatura afim de verificar a perda do revestimento asfáltico dos agregados de material fresado e/ou lixiviação do estabilizador das misturas. Os resultados dos testes de durabilidade e lixiviação indicaram que as perdas de resistência das misturas são mínimas e são consideradas adequadas para as aplicações na camada de base.

Mohammadinia *et al*. (2016) compararam o desempenho de três materiais reciclados de construção e demolição: tijolo triturado, agregado triturado reciclado e material asfáltico fresado estabilizados com geopolímeros produzidos a partir de cinza volante e escória de alto forno granulada moída. Os ligantes pozolânicos foram utilizados separadamente no teor de 4% e juntos em iguais teores de 2% e foram comparados com cimento Portland. Tanto o módulo de resiliência quanto a resistência à compressão aumentaram com uso do geopolímero para todos os materiais, no entanto para o agregado triturado reciclado a estabilização foi mais eficaz. O geopolímero a base de escória se mostrou mais eficiente que o a base de cinza volante. Todas as misturas de material fresado com geopolímero se mostraram suficientes para aplicação em sub-base de rodovias aos 7 dias, no entanto apenas o uso de 4% de geopolímero de escória aos 28 dias proporcionou os requisitos para base de pavimento. Geopolímeros à base de escória foram estudados também por Hoy *et al*. (2018) que evidenciaram ser essencial a utilização de Na_2SiO_3 para aplicação em base de rodovias aos 7 dias. No entanto os autores ressaltam que o uso de Na_2SiO_3 em excesso retardou a taxa de geopolimerização, levando à redução da resistência.

Mohammadinia *et al.* (2016b) também avaliaram a resistência e o módulo de resiliência para os mesmos resíduos de construção e demolição, mas para apenas o geopolímero de cinza volante em ambiente alcalino de silicato de sódio e hidróxido de sódio. Os resultados mostram que o uso de geopolímeros aumenta consideravelmente o módulo de resiliência, a resistência a compressão cresce com o aumento da quantidade de cinza e que o tratamento térmico aumenta a taxa de reação e consequentemente a resistência também. Por fim os autores afirmam que é possível utilizar agregado triturado reciclado e material asfáltico fresado com adição de 8% e 16% respectivamente de cinza volante para base de pavimento para as condições de cura a 40°C e por 7 dias.

Adhikari *et al*. (2018) propuseram um modelo de regressão para avaliar a sensibilidade das variáveis envolvidas na estabilização de dois solos com geopolímero de cinza volante e material asfáltico fresado. Teores mais altos de cinza volante e material asfáltico fresado produziram misturas com maiores resistências. O teor ideal de silicato de sódio depende do tipo

de solo e da porcentagem de cinza volante e material asfáltico fresado. As propriedades mecânicas e de durabilidade da mistura ótima foram melhores ou semelhantes às misturas do solo-cimento convencional.

Os estudos supramencionados revelam a possibilidade de aplicação do processo de álcali-ativação na reciclagem de material asfáltico fresado. No entanto, a quantidade de pesquisas sobre estabilização de material asfáltico fresado a partir da álcali ativação é ainda limitada e a maioria dos estudos utilizou apenas cinza volante como um precursor, e ainda pouco se sabe sobre as propriedades mecânicas e de durabilidade. Além disso, os estudos até então existentes se baseiam na utilização de hidróxido e/ou silicato de sódio, destacando melhorias consideráveis no desempenho dos produtos finais devido a ação do silicato. Apesar disso o silicato de sódio apresenta um elevado consumo energético e uma considerável emissão de CO_2, o que justifica o emprego de materiais locais que podem incluir resíduos industriais e agrícolas.

Nesse contexto, se faz necessária a produção de um silicato alternativo, que apresente benefícios econômicos e ambientais e viabilize a aplicação a longo prazo de matérias álcali ativados em grande escala, como é o caso da área de infraestrutura. Apesar de já existirem estudos a respeito do desenvolvimento de silicato alternativo baseado na dissolução da CCA, não se tem um amplo conhecimento sobre o processo completo de produção do mesmo.

O uso da álcali-ativação na estabilização de material asfáltico fresado é muito promissor na construção das camadas de base e sub-base de pavimentos, devido ao aumento de resistência proporcionado pelos ligantes álcali-ativados e pelo baixo impacto ambiental quando utilizadas soluções alternativas ao silicato de sódio comercial. Nesse sentido, percebe-se uma grande lacuna de conhecimento no que diz respeito à álcali-ativação com a utilização de silicato de sódio alternativo. Assim como nas pesquisas já realizadas se faz necessária a compreensão do comportamento mecânico e microestrutural para diferentes proporções de agregados e solução álcali ativadora, assim como a avaliação das propriedades de durabilidade e lixiviação de álcalis. Outro fator importante a ser considerado são as condições de cura, que até então não foram objetivo principal dos trabalhos mencionados neste item e serão abordadas no presente trabalho.

3. RESULTADOS

A seguir são apresentados os resultados, onde cada seção desse capitulo representa um objetivo específico que é apresentado no formato de artigo. Na seção 3.1 é apresentado o artigo intitulado “Parametric analysis of production of alternative sodium silicate applied in alkali activated materials” que foi submetido ao periódico “Advances in Cement Research – Qualis A3 (2017 -2020) e atualmente encontra-se revisado, segundo as considerações dos revisores do periódico, aguardando decisão final.

Na seção 3.2 é apresentado o artigo intitulado “Rice husk ash as an alternative soluble silica source for alkali-activated metakaolin systems applied to recycled asphalt pavement stabilization” que foi submetido e aprovado pelo periódico “Transportation Geotechnics – Qualis A2 (2017 -2020).

Na seção 3.3 é apresentado o artigo intitulado “Curing conditions effect on the stabilization of recycled asphalt pavement with alkali-activated metakaolin and rice husk ash-derived activator” que foi submetido ao periódico “Road Materials and Pavement Design – Qualis A2 (2017 -2020) e até o presente momento não foi obtido nenhum retorno.

Na seção 3.4 é apresentado o artigo intitulado “Durability, long-term and environmental evaluation of alkali-activated alternative soluble silica source for recycled asphalt pavement stabilization” que foi submetido ao periódico “Journal of Materials in Civil Engineering – Qualis A2 (2017 -2020) e atualmente encontra-se revisado, segundo as considerações dos revisores do periódico, aguardando decisão final.

Por fim, na seção 3.5 encontra-se o artigo intitulado “Flexural fatigue behavior of reclaimed asphalt pavement stabilized with alkali-activated rice husk ash” que ainda não foi submetido a nenhum periódico.

3.1 Parametric analysis of the production of alternative sodium silicate applied in alkali-activated materials

Abstract

Although alkali-activated materials are considered potential substitutes for Portland cement, they still present elevated costs and significant emissions of CO_2. One way to partially overcome this disadvantage is the development of alternative activators, such as a sodium silicate (SS) based on the dissolution of rice husk ash (RHA). However, to maximize the mechanical performance of alkali-activated materials, the production of RHA-based sodium silicates needs to be fully understood. This article investigates the production process of an alternative RHA-based sodium silicate activator through the experimental evaluation of the following parameters: RHA grinding time, RHA dissolution time, thermal curing temperature and time. The mechanical performance was evaluated through compressive strength tests carried out on alkali-activated pastes made up of metakaolin, as a precursor, and two types of activators (RHA-based sodium silicate and commercial sodium silicate). Microstructural features were evaluated by performing X-Ray Diffraction, Scanning Electron Microscopy, and Thermogravimetry analyses. The optimized production was obtained for a grinding time of 30 minutes, a thermal curing temperature of 40°C, a dissolution time of 6 hours, and a thermal curing time of 8 hours. The results show the efficiency of the alternative alkaline activator, which may represent a technically viable solution for the larger-scale application of alkali-activated materials.

Keywords: Alkaline activation; sodium silicate; rice husk ash; production process.

1. Introduction

Alkali-activated materials are a new alternative to Portland cement, mainly regarding CO_2 emissions into the environment. However, it is essential to use activators that are produced sustainably, which is not the case with commercial products such as sodium hydroxide or sodium silicate (Mendes et al., 2021). Sodium silicate (SS) is a precursor to silicon dioxide, which is needed in geopolymer synthesis. The presence of sodium ions favors dissolution, as it reacts more effectively to form oligomers, resulting in improved mechanical and chemical properties as compared to other ions, such as potassium (Rahim et al., 2015; Xu and Van Deventer, 2000).

Traditionally, laboratory-grade sodium silicates are prepared by melting quartz and sodium carbonate powder (Na_2CO_3) at elevated temperature (≈ 1300 °C) (Samuel Owoeye, 2017), configuring an energy-intensive production process that has contributed with significant amount of carbon dioxide emissions. Sodium silicate is the component with the greatest impact from the energy consumption and CO_2 emission point of view, requiring 63.4% of the total energy for its production (McLellan et al., 2011). It is esteemed that 1,514 kg of CO_2 are emitted to produce one kilogram of sodium silicate (Duxson et al., 2007).

As an agricultural by-product, rice husk ash (RHA) is abundantly available in most rice producing countries. RHA is obtained from the burning of rice husks and contains high levels of silica. Inadequate disposal of the remainder of the RHA is still a major environmental concern, since airborne particles can cause serious human respiratory illness and can be a potential cause of fires in landfills (Tsen et al., 2020). In this sense, alkaline activators based on RHA generate an emission of about 572.3 kg/m³ of CO_2 in the production of geopolymers, representing about 48% less when compared to potassium silicate, for example, being considered a more environmentally friendly alternative (Villaquirán-Caicedo et al., 2017). Therefore, several studies have been conducted to use RHA in various applications, including the production of sodium silicate for use in alkali-activated materials (Bernal et al., 2012; Detphan and Chindaprasirt, 2009; Foletto et al., 2006; Geraldo et al., 2017; Kalapathy et al., 2001; Kamseu et al., 2017; Hervé K Tchakouté et al., 2016; Hervé Kouamo Tchakouté et al., 2016; Živica, 2006).

Despite the growing research on sustainable and economical alkaline activators (Vinai and Soutsos, 2019) and the potential use of RHA (Roschat et al., 2016), the production procedures are still not well established. The hydrothermal process is commonly used to produce an activator in liquid form, as it consumes less energy compared to other methods, but its use still requires further research. Table 3.1 presents some of the factors involved in the production of alternative sodium silicates based on RHA for use in alkali-activated materials. The parameters evaluated for the determination of the silica dissolution rate were silica content, temperature, processing time, alkalinity of the solution, and particle size.

Table 3.1. Parameters involved in the production of alternative sodium silicate from RHA

Reference	Precursor	Dissolution conditions				RHA	
		Alkaline source	Temperature	Dissolution time	Molarity	(%) SiO_2	Particle size (μm)
(Bernal et al., 2012)	Metakaolin/slag	NaOH	RT	10 min	-	68	>1 and <60
(Geraldo et al., 2017)	Metakaolin/ water treatment sludge	NaOH	RT and 90°C	30 min	-	89.51	20.4
(Hervé K Tchakouté et al., 2016)	Metakaolin	NaOH	80°C	2 h	-	93.49	-
(Hervé Kouamo Tchakouté et al., 2016)	Metakaolin	NaOH	100°C	2 h	-	83.05	<90
(Kamseu et al., 2017)	Metakaolin	NaOH	RT	40 min	8, 10 and 12 M	-	<45
(Mejía et al., 2016)	Metakaolin/fly ash	NaOH	RT	24 h	-	90.91	5
(Bernal et al., 2015)	Slag	NaOH	RT	24 h	2 and 4 M	68	>1 and <60
(Mejía et al., 2013)	Slag/fly ash	NaOH	RT	-	-	94	36.9 and 39.5
(Tong et al., 2018)	Slag/fly ash	NaOH	RT, 60, 80, 90, 100°C	1, 3, 5, 7, 15 h	1, 2, 3.2, 4.9 and 6.5 M	90.5	6.82
(Passuello et al., 2017)	Kaolin sludge	NaOH	100°C	1h	-	97.3	-
(He et al., 2013)	Red mud	NaOH	RT	15 min	2, 4, 6 M	91.5	25 and 32
(Bouzón et al., 2014)	Fluid catalytic cracking catalyst residue	NaOH	100°C	5 - 240 min	-	85.58	20 and 62
(Luukkonen et al., 2018)	Slag	NaOH	RT	4 h	0.1, 1 and 10 M	88.46	20, 30, 172 and 199
(Hajimohammadi and van Deventer, 2017)	Metakaolin	$NaAlO_2$	RT	-	-	56.22	8
(Sturm et al., 2016)	Sodium aluminate	$NaAlO_2$	RT	-	-	88.49	11.1

*RT = room temperature

The studies reported in Table 3.1 show a promising potential for synthesizing activators using silica-rich byproducts. The work by Tong et al. (2018) stands out for evaluating a wide range of parameters involved in the production process of an RHA-based sodium silicate, however, the authors use slag and fly ash as precursors. Alkali-activated materials produced with metakaolin are seen as a model system, not involving the complexity of industrial by-products, which may vary depending on how they are obtained and possible contamination. Therefore, a comprehensive understanding and a careful selection of the processes adopted are

essential to optimize the silica extraction process, especially in alkali-activated materials that use metakaolin as a precursor. This fact justifies the innovative character of this research and shows a research gap to be studied. Thus, this work aims to investigate the process to produce sodium silicate based on RHA, focusing on the optimization of the mechanical performance of alkali-activated materials based on metakaolin. The experimental program was developed based on a wide range of laboratory tests that initially covered different RHA grinding times and thermal curing temperatures of alkali-activated pastes. Subsequently, the dissolution times of RHA in NaOH and thermal curing conditions were evaluated. Finally, the best results found were compared to those obtained for a commercial sodium silicate.

2. Materials and Methods

2.1 Rice Husk Ash

The RHA used in this study comes from the São Sepé thermoelectric plant, located in the central region of Rio Grande do Sul – Brazil. The temperature burning process varies from 800 °C to 900 °C. The RHA has a high silica content according to X-ray fluorescence (XRF) results presented in Table 3.2. The X-ray diffraction (XRD) Fig. 3.1, show that the RHA has a significant amorphous phase and the presence of some crystalline SiO_2, possibly formed during incineration at elevated temperatures. However, if the alkalinity conditions are properly adjusted, both the amorphous and the crystalline silica present in the RHA have the possibility to participate in the alkaline activation process (Mejía et al., 2013).

Table 3.2. Chemical composition of the materials

	SiO_2 (%)	Al_2O_3 (%)	Fe_2O_3 (%)	CaO (%)	MgO (%)	Na_2O (%)	K_2O (%)	TiO_2 (%)
MK	54.72	40.80	1.80	0.10	0.10	0.18	0.21	2.09
RHA	89.33	0.62	1.53	3.84	2.51	-	2.18	-

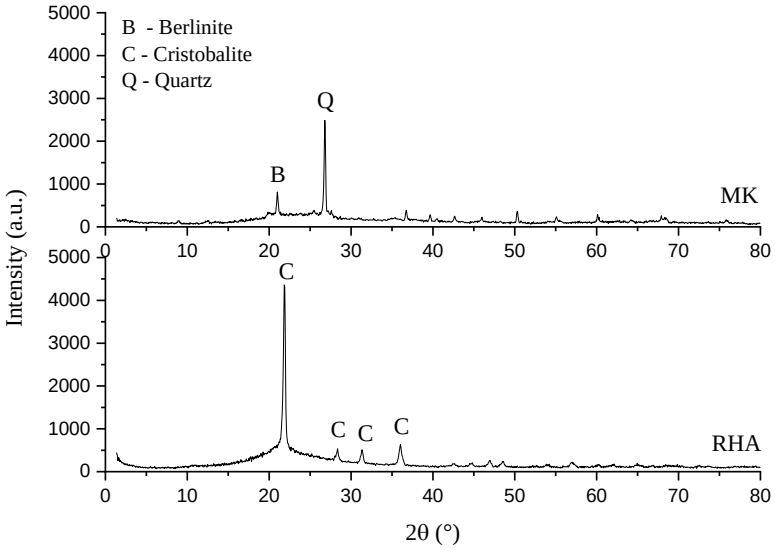

Figure 3.1. MK and RHA X–Ray Diffraction

2.2 Precursor and activators

The precursor used in this work was metakaolin (MK), which has a particle density of 2.64 g/cm³ and chemical composition as shown in Table 3.2. The mineralogical composition of metakaolin was determined by XRD Fig. 3.1, indicating that the main crystalline phases found were quartz and berlinite. The commercial sodium hydroxide used has a purity of 99% and the solution with the required concentration was prepared by dissolving the NaOH and RHA in distilled water. A commercially available sodium silicate solution (Na_2O = 8.55% and SiO_2 = 27.8%) was used as a control activator solution.

2.3 Methods

Due to the coarse and heterogeneous particle size distribution, and the fact that the size of the particles interferes with the kinetic reactions (Xu et al., 2015), the RHA was subjected to dry grinding in a ceramic vessel mill with alumina balls and a constant rotation speed of 200 rpm. A mass ratio of balls to ash of 3:1 was used, with 20mm, 10mm, and 5mm diameter alumina balls. The milling duration was investigated for various grinding times (10 min, 30 min, 60 min, 90 min, and 120 min). After each milling interval, the samples were submitted to both Scanning Electron Microscopy (SEM) and X-Ray Diffraction (XRD). The unconfined compressive strength (UCS) of alkali-activated pastes, at curing periods of 7, 28, and 56 days,

was used to evaluate the effect of different parameters on the production of the alternative sodium silicate. Fig. 3.2 presents the testing program carried out in this study.

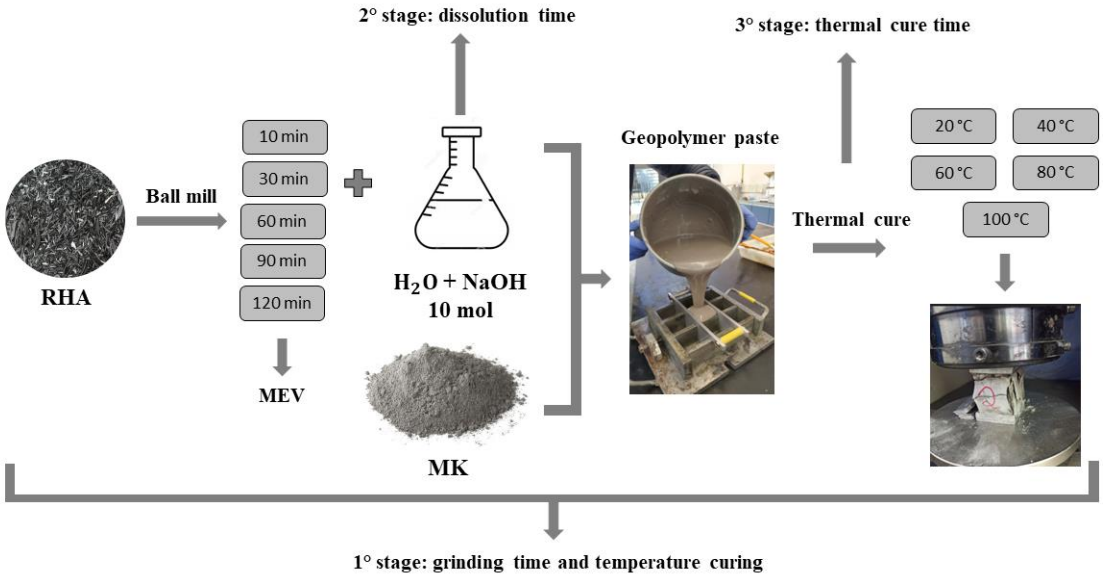

Figure 3.2. Summary of testing program developed

For a first set of tests, different grinding times of RHA and thermal curing temperatures of the alkali-activated pastes were evaluated. Seeking to reduce the energy consumption for the production of alternative silicate, the dissolution time of RHA in NaOH (1 h, 3 h, 6 h, 12 h and 24 h) and the thermal curing time (4 h, 8 h, 12 h, 16 h, 20 h and 24 h) were included as variables in the second and third phases of the study, respectively. The degree of crystallinity of the RHA is a limiting factor and affects its dissolution conditions since it is more difficult to break the SiO_2 crystal structure under hydrothermal conditions (Tong et al., 2018). Thus, the sodium silicate solution was produced by a hydrothermal method, dissolving the RHA in a NaOH solution with a concentration of 10 M, for the granulometry that presented the best result. By dissolving NaOH in water, the mixture reaches a temperature of 80°C, which was kept in a thermostatic container for different heating times, as mentioned earlier. The efficiency of the dissolution process was evaluated from unconfined compression tests performed on alkali-activated pastes produced with the alternative sodium silicate with different thermal curing times.

Finally, the best results found in the previous steps were compared with the results obtained for the specimens molded with commercial sodium silicate. For this step, the unconfined compressive strength tests were performed on cubic specimens, three for each mix, on an EMIC DL 20000 hydraulic press, with a coupled load cell of 200 kN with a precision of

1N, and a displacement rate of 0.5 mm/min. Also, the microstructural features were evaluated to understand the mechanisms involved in the alkali-activation process. The microstructural characterization was performed on the pastes through XRD, SEM, and thermogravimetric analysis (TG). XRD analyses were performed using pure copper-K-Alpha 1 radiation with a wavelength of 1.54 Å. The X-ray generator was set to 40 kV and 40 mA; the recorded angular range was 5 to 80° (2θ) with a step close to 0.017°. SEM analyses were performed using a Zeiss microscope, model EVO LS25. To cover the surface of the samples with gold, a Quorum metallizer SC 7620 was used and the micrographs were obtained at a voltage of 10 KV. TG analyses were performed using an equipment PerkinElmer, Model Sta 6000, under the following conditions: 10°C/min in a nitrogen atmosphere with a nitrogen flow rate of 100ml/min and temperatures between 20°C and 900°C.

The NaOH concentration of 10M and the SiO_2/Al_2O_3 ratio = 4 were kept constant and selected based on other studies (e.g. Juengsuwattananon et al., 2019). The Table 3.3 summarize the parameters evaluated in each stage of this study. It is important to emphasize that all the tests were performed on cubic specimens, three for each parameter evaluated as it is showing Table 3.

Table 3.3. Parameters evaluated in each stage.

	RHA grinding time	Curing temperature	RHA dissolution time	Thermal curing time	Curing time	Tests
1st stage	10 min 30 min 60 min 90 min 120 min	20 °C 40 °C 60 °C 80 °C 100 °C	24 h	24 h	7, 28 and 56 days	UCS and SEM
2st stage	30 min	40 °C	1 h 3 h 6 h 12 h 24 h	24 h	7, 28 and 56 days	UCS
3st stage	30 min	40 °C	6 h	4 h 8 h 12 h 16 h 20 h	7, 28 and 56 days	UCS

				24 h		
SS x RHA	30 min	40 °C	6 h	8 h	7 and 28 days	UCS, XRD, TG and DTG

Mix proportions for the RHA-derived alkali-activated pastes and the control alkali-activated pastes produced with the commercially available activator are shown in Table 3. According to the results reported by Tong et al. (2018), for alkaline solutions with concentrations greater than 2-3 M, about 95% of the silica present in the RHA is dissolved and is available for the alkali activation reaction. This information was considered in defining the quantities in Table 3.4 so that the amounts of silica available in the commercial solution and in the RHA-based solution were comparable. The pastes were prepared in a planetary mixer for 5 minutes. After mixing, they were transferred to 40x40x40 mm molds (Cheng et al., 2018), covered with a plastic film to prevent evaporation, and then cured at different temperatures. After these procedures, the samples were kept in a temperature-controlled chamber, at room temperature (23 - 25°C), until the testing date.

Table 3.4. Mix proportions for the alkali-activated pastes.

Constituent	RHA alkali-activated pastes	SS alkali-activated pastes
MK (kg/m³)	1562.5	1562.5
RHA (kg/m³)	402.3	-
NaOH (kg/m³)	416.8	274.1
SS (kg/m³)	-	1292.7
Water (kg/m³)	1041.9	685.3

2.4 Statistical method for the analysis of results

Statistical significance analyzes were performed on the results of unconfined compression strength by applying the analysis of variance method – ANOVA (e.g., Montgomery, 2001; Box et al., 1978), with a 5% significance level (α). The results of the ANOVA are expressed, for each effect evaluated, through the so-called P-value, which is a probability indicating the margin of error assumed by rejecting the null hypothesis, i.e., by concluding that the effect under analysis is statistically significant. Therefore, any effect is

assumed to be statistically significant if the P-value is lesser than α, or P-value < 0.05 for the present study.

3. Results and discussions

a) Step 1: Influence of grinding time and curing temperature

The influence of RHA grinding time and thermal curing temperature were investigated through unconfined compressive strength tests and the results are shown in Fig. 3.3.

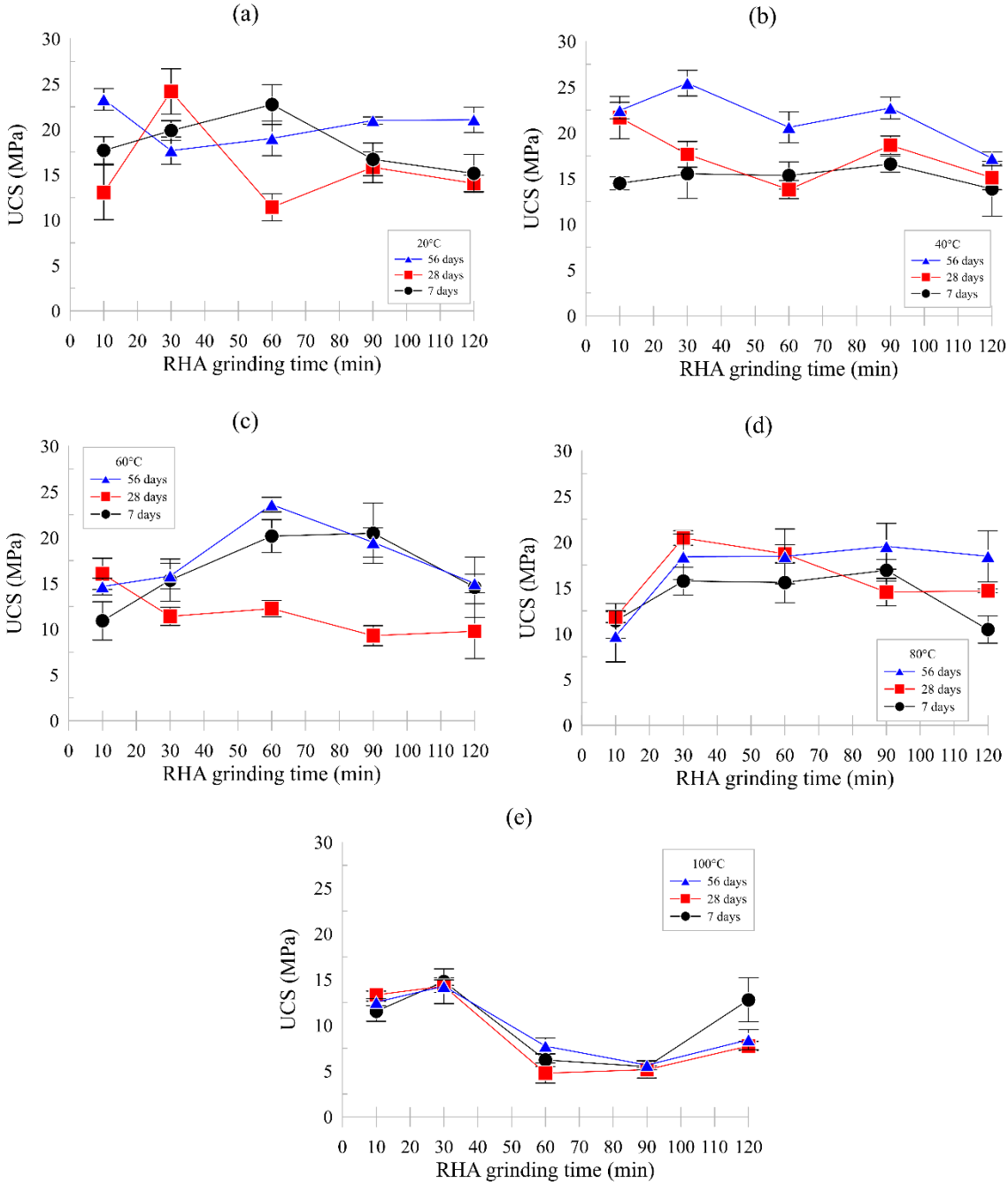

Figure 3.3. Compression strength of alkali-activated pastes for different grinding times and thermal curing at (a) 20°C (b) 40°C (c) 60°C (d) 80°C, and (e) 100°C

It can be observed that the shortest grinding time (10 min) does not present a well-defined pattern of increase, reduction, or even maintenance of strength over time. This variability might be explained by the irregular shape of the particles as observed in the SEM analysis presented in Fig. 3.4a.

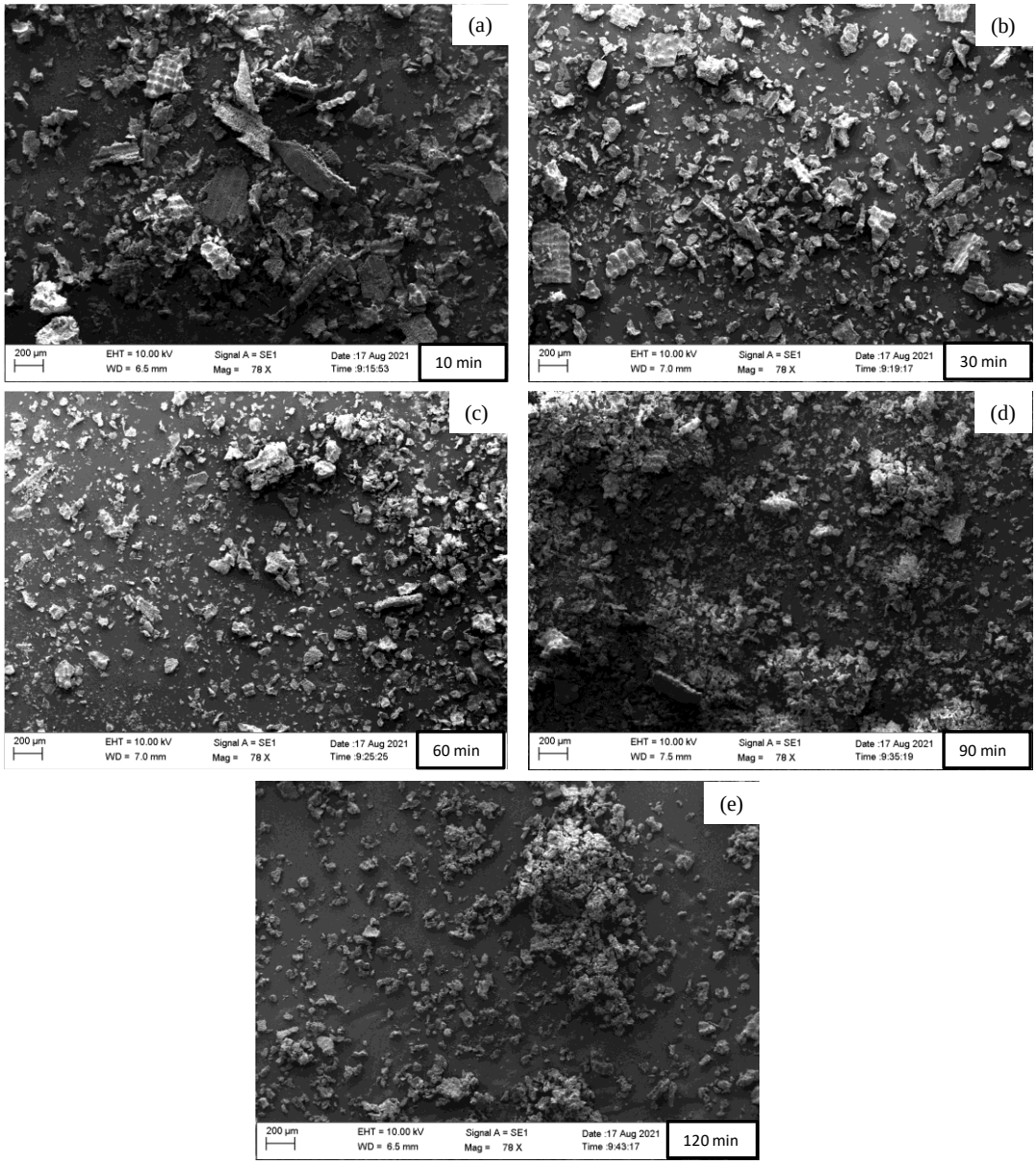

Figure 3.4. RHA SEM for different grinding times (a) 10 min (b) 30 min (c) 60 min (d) 90 min and (e) 120 min

The pozzolanic properties of the RHA, which makes it a potential substitute for Portland cement due to its high silica content (Ganesan et al., 2008; Mehta, 1998), were evidenced

mainly for the samples subjected to 30 minutes of grinding, which in general, except for the temperature of 60°C, yielded the highest strengths (see Fig 3.3b). For the 56-day curing period, higher strength values were achieved, most clearly at the temperature of 40°C, for all grinding times.

In general, it can be observed that the RHA grinding time significantly affects the unconfined compression strength (P-value < 0.048) However, for times above 60 minutes, grinding did not have a significant influence on mechanical strength. According to the literature, studies evaluating the fineness of the RHA, when used as a partial replacement of Portland cement, show that there is a linear relationship between the duration of grinding and the fineness of RHA, that is, the longer the grinding, the greater the degree of fineness and, consequently, the better the pozzolanic activity (Chindaprasirt et al., 2007; Chindaprasirt and Rukzon, 2008; Habeeb and Fayyadh, 2009). The increase in the specific area obtained by grinding, as a result of the reduction in particle sizes, will increase the pozzolanic activity in such a way that, depending on the intensity of grinding, it may turn materials with or without pozzolanic activity into materials suitable for use as pozzolans (Cordeiro et al., 2008). The increase in grinding time leads to changes in some factors, such as particle fracture, particle shape, and particle agglomeration (Flores et al., 2017). In the present study, the tendency of increasing strength with increasing milling time was not observed (Fig. 3.4), indicating that excessive milling can cause particle aggregation.

Previous studies report that for metakaolin-based systems, the curing temperature affects the compressive strength, indicating improvements of almost 100% when the samples are cured at 50°C and 80°C in relation to room temperature (Khalil and Merz, 1994). Although the RHA used in this study has a similar chemical structure for different milling times, the variation in curing temperature induces significant changes in the mechanical performance of the pastes produced by alkali activation of RHA, as observed in Fig. 3.3. It is important to highlight, however, that the compressive strength for samples cured at room temperature (20°C) does not show high values and that, on the other hand, high temperatures (100°C) can impair the mechanical performance of pastes activated by alkali.

In this study, curing at 40° and 80°C positively affects the development of compressive strength, mainly for the RHA prepared with a grinding time of 30 minutes and in the sense that there is no significative reduction in the strength values over time. Interestingly, the higher curing temperature Fig. 3.3 appears to weaken the structure, suggesting that small amounts of structural water need to be retained in order to reduce cracking and maintain structural integrity

(Jaarsveld et al., 2002). This reduction in compressive strength is also reported by Khalil and Merz (Khalil and Merz, 1994), who state that elevated temperatures break the mixture structure during the alkali-activation synthesis, resulting in dehydration and excessive shrinkage. transform into a more semi-crystalline form. A second factor influencing the reduction in compressive strength is the presence of water in metakaolin-based alkali-activated systems, which is present mainly as unbound or adsorbed water within the pore structure rather than in the hydrate phases. This free or unbound water can evaporate from the aluminosilicate gel, resulting in microcracks with consequent loss of strength (Kuenzel et al., 2012).

Evaluating the temperature range from 40°C to 80°C, it is observed that the intermediate temperature of 60°C is critical, since there is a sudden reduction in strength in the first curing times, stabilizing at 56 days. The curing temperature of 80°C showed a tendency of strength reduction at 56 days for shorter grinding times and an inversion of this behavior for grinding times longer than 60 minutes. For the temperature of 40°C, higher strengths were achieved with short grinding periods, without showing a strength reduction over time for all evaluated intervals.

The results obtained indicate that the ideal process parameters for the production of alkali-activated pastes through the alkaline activation of RHA are curing temperature of 40°C and grinding time of RHA of 30 minutes. With obvious positive impacts on economic and environmental performances, these parameters were used in the second stage of the study to evaluate the influence of dissolution time of RHA in NaOH.

b) Step 2: Influence of dissolution time

To investigate the influence of SiO_2 dissolution time, RHA ground for 30 minutes was dissolved in NaOH and water at a concentration of 10M, reaching a temperature of 80°C. This temperature was kept constant for five separate times: 1 h, 3 h, 6 h, 12 h, and 24 h. The corresponding results of unconfined compressive strength are presented in Fig. 3.5, indicating a significant increase in SiO2 dissolution (P-value = 0,044) as the unconfined strength increased up to 12 hours for the 7 and 28 days curing periods, but mostly up to 6 hours. For longer curing periods (56 days), a tendency for strength reduction is observed after 6 hours of dissolution. Overall, considering all thermal curing periods, the observed response for the unconfined compressive strength does not justify dissolution times greater than 6 hours.

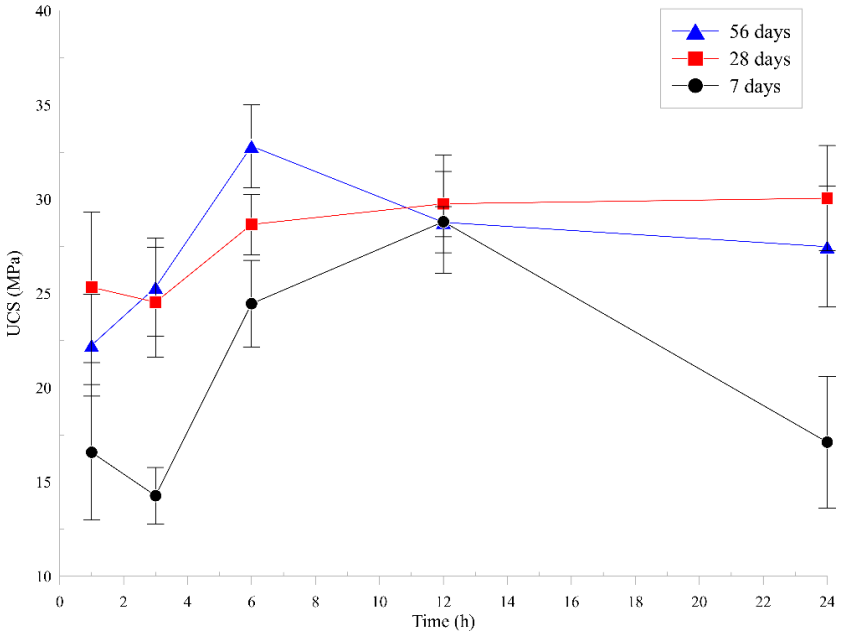

Figure 3.5. Compressive strength of alkali-activated pastes for different dissolution times

The results obtained so far indicate that the ideal parameters for the production of alkali-activated pastes from an alternative sodium silicate derived from RHA are: RHA grinding time of 30 minutes, curing temperature of 40°C and dissolution time of 6 hours.

c) Step 3: Influence of thermal curing time

The process parameters found as the best combination in section b) were fixed (grinding time of 30 minutes, curing temperature in an oven of 40°C) and the effect of different initial thermal curing times (4 h, 8 h, 12 h, 16 h, 20 h, and 24 h) on the unconfined compressive strength was evaluated, as shown in Fig. 3.6.

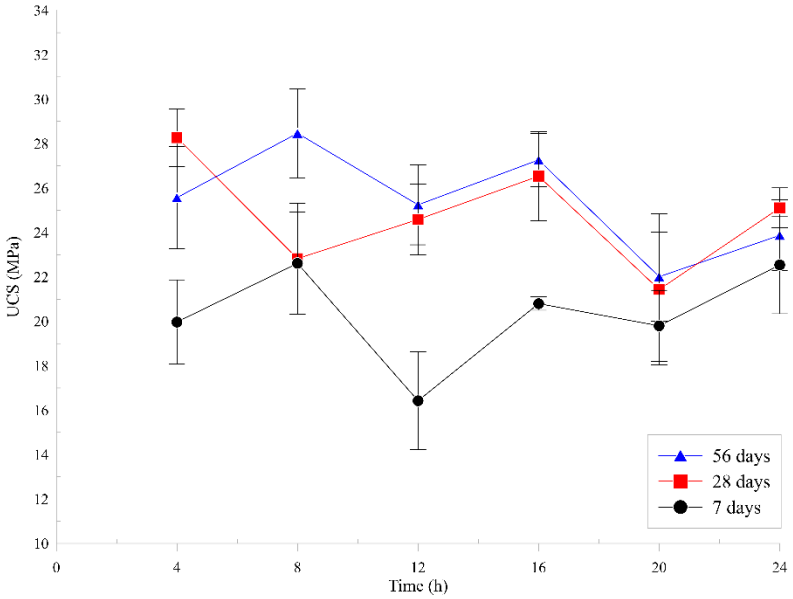

Figure 3.6. Compressive strength of alkali-activated pastes for different thermal curing times

The thermal curing time at an elevated temperature (40°C) does not seem to have a major influence on the final product (P-value = 0,245). Only the initial thermal curing time of 20 h stands out, which can be considered critical because it presents a reduction in strength for all curing periods evaluated. Previous studies (Sturm et al., 2016; Van Jaarsveld et al., 1998) show that longer curing times do not affect the crystalline part of the alkali-activated material, indicating that the changes responsible for the differences in compressive strength originate and occur within the amorphous of the structure. As observed in Fig. 3.6, the curing times at high temperatures that showed the best behavior were 8h, 16h, and 24h. According to Kürklü (2016), the first 24 hours of thermal curing are important because gels form and fill the pores of the material, making it more resistant.

3.3 Efficiency of alternative sodium silicate based on RHA

The evaluation of the effects of the factors involved in the production of the alternative silicate allowed the selection of a set of parameters that led to a better performance, when considering the pastes produced from it. Higher resistance values were obtained with relatively low environmental and economic costs. The efficiency of the alternative sodium silicate based on RHA was evaluated in relation to a commercially available activator through UCS, XRD, Thermogravimetry (TG and DTG).

3.3.1 Unconfined compressive strength

The unconfined compressive strength results of the alkali-activated pastes considering the two types of activators (RHA-based sodium silicate and commercial sodium silicate) are shown in Fig. 3.7. The compressive strength of pastes prepared with commercial sodium silicate (SS) increased by 21% from 7 days to 28 days, while for those with the RHA-based sodium silicate it was only 9.2%. Despite this increase in strength over time, a statistical analysis indicates that there is no significant difference in curing time for the two silica sources evaluated in this study.

Although the pastes produced with RHA show a slower reaction rate, they presented higher values at all curing ages. Sodium silicate solutions that use RHA as a source of silica present coarser molecular compounds that contribute to the formation of denser structures with high strength (Kamseu et al., 2017). Although some authors indicate a pre-treatment for filtration of silicate produced from RHA (Geraldo et al., 2017; Hervé K Tchakouté et al., 2016; Hervé Kouamo Tchakouté et al., 2016), the objective of the present study was centered on reducing its production costs and, therefore, filtration and calcination. This approach caused the undissolved residue to remain in the matrix acting as a filler or contributing to interfacial reactions (Kamseu et al., 2017). The results are consistent with the literature (Sturm et al., 2016), which evidenced that alternative sodium silicate solutions obtained simply by dissolving RHA in NaOH are able to achieve good strength and density because they have larger colloidal particles.

In contrast to the results obtained here, previous studies (Bernal et al., 2015) suggest that RHA-based alkali-activated pastes are expected to have a lower dissolved silica content when compared to those prepared with commercial sodium silicate. A probable reason is that the amount of silica present in the RHA studied by these authors is lower than that used in the present work. In this way, some amorphous products are partially dissolved during the first 24 h, during which the solution equilibrium occurs, decelerating the availability of SiO_2 in the system and, therefore, resulting in lower mechanical strength. However, other authors have also observed reduced and similar strength to this study in samples produced with commercially available sodium silicate (Apolonio et al., 2020; Lima et al., 2021).

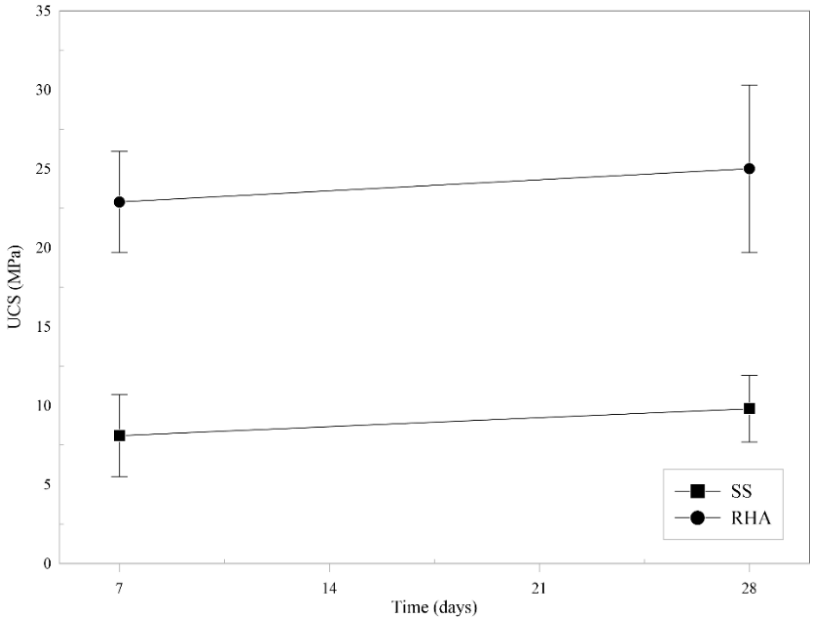

Figure 3.7. Compression strength of alkali-activated pastes with different activators: RHA-based and commercial sodium silicate (SS)

3.3.2 X-Ray Diffractometry

The XRD results obtained at 7 and 28 days are shown in Fig. 3.8. The main peak identified in all samples is quartz (SiO_2). Graphite appears in smaller amounts and only in the pastes produced from RHA. It is also observed that these minerals did not change over time, which is consistent with the TG results.

The intensity of the peaks associated with crystalline quartz was lower at 28 days for both pastes, suggesting a dissolution of quartz and, therefore, an increase in strength for longer curing times (Tong et al., 2018). The presence of significant amorphous phases in the samples suggest higher compressive strengths and denser matrices (Ramadhansyah et al., 2012), as observed in this study.

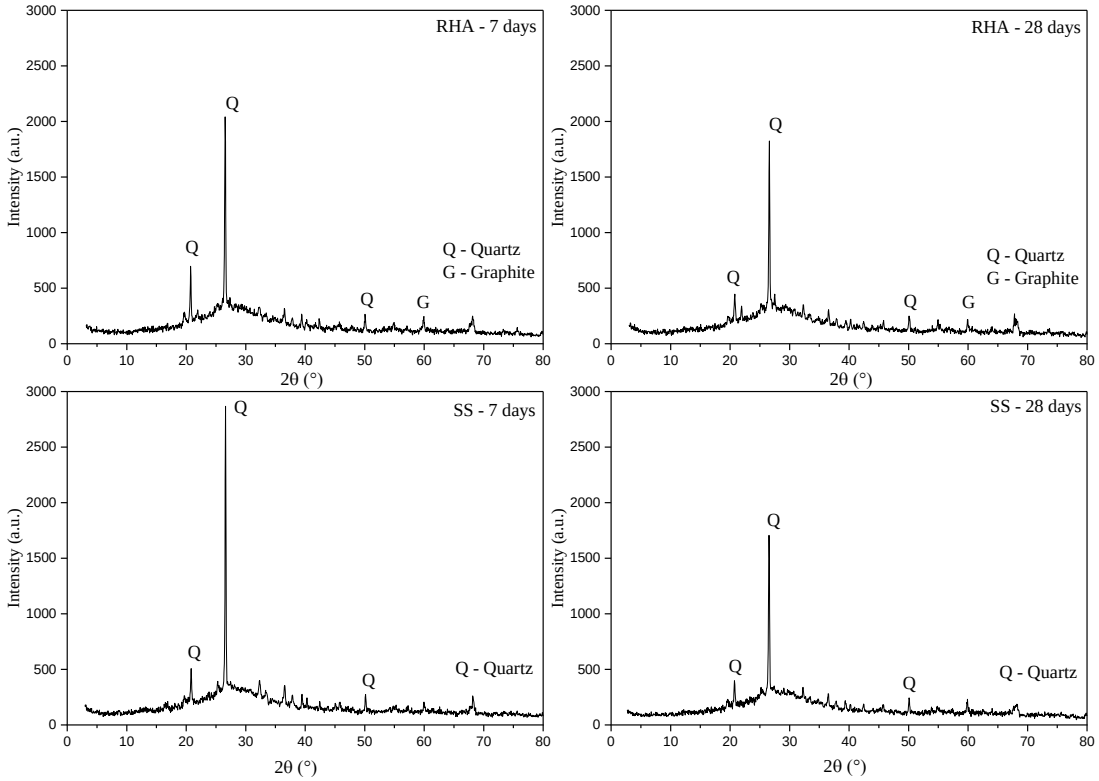

Figure 3.8. DRX of alkali-activated pastes with different activators: RHA-based and commercial sodium silicate (SS)

3.3.3 Thermogravimetry

The results of mass loss in relation to the heating temperature of alkali-activated pastes are shown in Fig. 3.9. The main losses occurred up to the temperature of 180°C, removing the absorption water or free water, a process that can occur in low heating rate conditions (Rosas-Casarez et al., 2014). The second thermal degradation occurs between 180°C and 350°C and is specifically associated with the presence of the sodium aluminosilicate gel (Rosas-Casarez et al., 2014). The remaining mass loss between 350°C and 650°C can be attributed to the remaining bound water that results from the condensation of silanol or aluminol groups (Mehta, 1998). This last mass loss is due to the dihydroxylation of the OH groups, and subsequent polycondensation in Si-O-Si siloxo bond, binding to the neighboring geopolymer micelles (Davidovits, 2020).

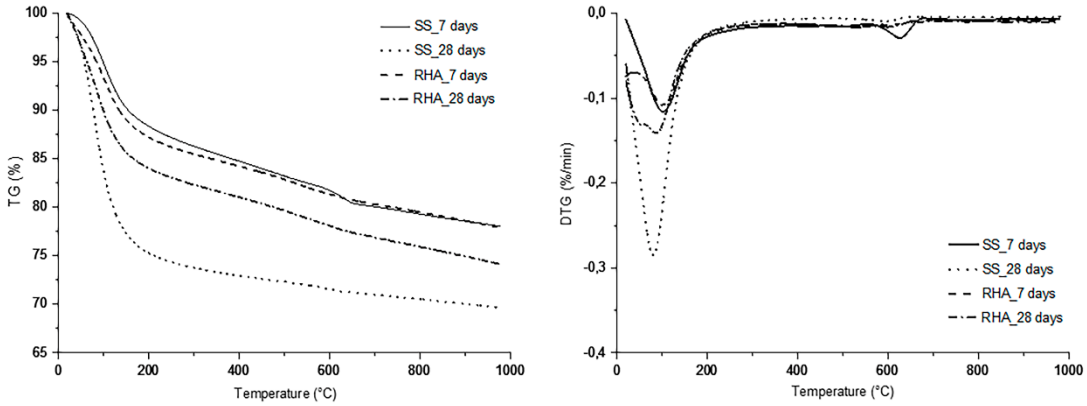

Figure 3.9. Thermogravimetry curves of alkali-activated pastes with different activators: RHA-based and commercial sodium silicate (SS)

The total mass losses at 7 days were around 22.5% for the two pastes, while at 28 days the values diverged reaching 25% and 30% for the pastes based on RHA and commercial sodium silicate, respectively. These results are not consistent with the literature (Hervé K Tchakouté et al., 2016) which reports that slower mass losses indicate lower dissolution and, therefore, lower strengths.

Slurries produced with the alternative sodium silicate showed lower mass losses over time when compared to slurries produced with commercial sodium silicate. This result suggests that the amount of C-S-H gel did not show much variation over time for the slurries with alternative sodium silicate. This observation is consistent with the compressive strength results that showed a smaller increase in strength over time for the pastes produced from RHA.

Although at 7 days the two pastes showed similar mass losses, suggesting that they have the same amount of C-S-H gel, the results of compressive strength for the RHA pastes showed higher values, ranging from 7 MPa to 22.9 MPa. This comparison confirms the hypothesis that the higher compressive strength observed for the RHA-based pastes is due to the presence of RHA particles that form denser structures.

After curing for 28 days, it is observed from the DTG that the pastes produced with the commercial sodium silicate show a peak centered at 100°C. This can be explained by the “water damming effect”, in which part of the water does not chemically react with the internal hydrates, but is physically bound to the surface of the materials they form as alkali-activated masses (Xu et al, 2023).

4. Conclusions

With the objective of optimizing the mechanical performance, the present study sought to establish a process to produce sodium silicate based on RHA. The following conclusions for the evaluated parameters were established:

- Grinding time: the grinding time of RHA has significantly influenced the unconfined compressive strength of the pastes. The optimum grinding time to produce sodium silicate based on RHA was found to be around 30 minutes.

- Thermal curing temperature: the variation in the thermal curing temperature resulted in changes in the compressive strength of the alkali-activated pastes, but not always representing a better mechanical response. Curing at 40°C and 80°C positively affected the development of strength, in the sense that there was no reduction and/or randomness in the values over time. An optimum curing temperature of around 40°C was found to produce a better response.

- Dissolution time: the compressive strength results for heating periods longer than 6 hours did not indicate an increase in SiO_2 dissolution, and therefore, a sufficient dissolution time of 6 hours was established.

- Thermal curing time at elevated temperature: in general, this factor did not have a major influence, except for the thermal curing time of 20 h, which can be considered critical because it presents reductions in strength for all curing periods. The thermal curing time of 8 hours was found to be the optimal condition, as it presents the highest strength at 56 days, which results in positive economic and environmental impacts.

Finally, the pastes produced from the production process established in this work showed a slower reaction rate and higher strengths than the pastes produced with commercial sodium silicate. From a technical point of view, the results of this study show that the optimization of the production process of alternative sodium silicate based on RHA brings positive perspectives, in the sense of promoting the use of alkaline activation in practice.

3.2 Rice husk ash as an alternative soluble silica source for alkali-activated metakaolin systems applied to recycled asphalt pavement stabilization

Abstract

Alkali-activated binders have been shown as a viable alternative to ordinary Portland cement. However, the development of lower carbon emission activators for this process is still a research-gap. The goal of this research was to analyze the stabilization of recycled asphalt pavement (RAP) mixtures with a metakaolin-based binder, alkali-activated by rice husk ash synthetized sodium silicate. Compaction, unconfined compressive strength (UCS), scanning electron microscopy (SEM), and X-ray diffraction (XRD) tests were conducted in stabilized RAP mixtures, submitted to different curing periods and temperatures. Also, results were correlated with the porosity/binder content index. Compaction results showed a reduction in dry unit weight as the RAP content increased for non-stabilized mixtures and a non-linear behavior for stabilized ones. For the UCS tests, the increase in binder content led to an increase in strength for all mixtures. High curing temperatures prevented the efflorescence phenomenon, however reduced strength due to crack formation. XRD analyzes showed the formation of minerals rich in silica and alumina, indicating the formation of geopolymerization products. Finally, the porosity/binder index was shown to be a viable dosage method to predict the strength of stabilized RAP mixtures.

Keywords: Recycled asphalt pavement; alkali-activated cement; alternative silica source; industrial waste; rational dosage methodology

1. Introduction

Recycled Asphalt Pavement (RAP) is a type of waste obtained during the rehabilitation of highways (Rahman et al., 2014), majorly composed of aged bituminous aggregates and additives (Hoy, Horpibulsuk e Arulrajah, 2016). This material can be reused in pavements base and subbase layers, reducing the overall cost of pavement sections up to 46% (Debbarma, Ransinchung e Singh, 2019; Singh et al., 2018), as well as significantly reducing environmental impacts in the infrastructure sector (Costa et al., 2020). Although its clear practical applicability, one of the main challenges in reusing RAP consists in the lack of adhesion of its grains, normally compensated by utilizing cementing agents.

Ordinary Portland cement (OPC) has been widely applied as a stabilizing material in pavement design, acting in the connection of particles through cementitious reactions, increasing strength and stiffness while reducing strain and improving permeability (Nawaz, Heitor e Sivakumar, 2020). Nevertheless, the manufacturing process of OPC is linked to high consumptions of energy and non-renewable resources, in addition to a large generation of carbon dioxide (CO_2) (Zhang et al., 2020). Thus, alternative materials to OPC are a current necessity.

Alkali-activated binders are rapidly becoming effective options, considering their lower carbon dioxide emission compared to OPC (Queiróz et al., 2022). Alkali-activation can be defined as the chemical reaction between an amorphous/semi-crystalline aluminosilicate source and an activator, generating cementitious structures similar to the ones found in OPC. This process is interesting from an environmental perspective, considering that during its production process several industrial by-products/wastes can be incorporated: fly ash (Phoo-ngernkham et al., 2015; Zhuang et al., 2016), blast furnace slag (Awoyera e Adesina, 2019), water treatment sludge (Geraldo, Fernandes e Camarini, 2017), sugarcane bagasse ash (Bruschi, Santos, dos, et al., 2021; Bruschi, Santos, et al., 2021; Pereira dos Santos et al., 2022), carbide lime (Bruschi et al., 2022; Carvalho Queiróz et al., 2022; Queiróz et al., 2022), eggshell lime (Consoli, Tonini de Araújo, et al., 2021; Tonini de Araújo et al., 2021), and rice husk ash (Bernal et al., 2012; Luukkonen et al., 2018; Mejía, Mejía de Gutiérrez e Puertas, 2013; Sturm et al., 2016; Tchakouté et al., 2016; Tong, Vinai e Soutsos, 2018). As for the activators, the most common include sodium or potassium hydroxides and/or silicates, while aluminosilicates may include suitable raw materials and by-products/wastes produced from various industrial processes (Torres-Carrasco, Palomo e Puertas, 2014).

Although alkali-activated binders (AA) are considered a more sustainable option when compared to OPC, it is important to highlight that the production process of several alkaline activators also contributes for CO_2 generation; considering that manufacturing processes are energy-intensive, involving temperatures up to 1400°C (Villaquirán-Caicedo, Mejia De Gutiérrez e Gallego, 2017). For instance, in the production of 1kg of commercial sodium silicate more than 1.5 kg of CO_2 is generated (Tchakouté et al., 2016). Previous researchers have studied alternative ways to incorporate glass waste to synthetize sodium silicate (Puertas e Torres-Carrasco, 2014; Torres-Carrasco, Palomo e Puertas, 2014; Torres-Carrasco e Puertas, 2015). However, products such as brine, ammonia and calcined limestone were utilized to enhance the silica dissolution process, once again utilizing energy-intensive materials.

In such way, alternative silica sources for the synthetization of sodium silicate are emerging as an attractive choice. Rice husk ash (RHA) has the potential to become a competitive option for this synthetization process, as this material is majorly composed by silica in an amorphous state (Consoli et al., 2019). Several studies have been carried with RHA as a precursor in the development of activating solutions (Bernal et al., 2015; Bouzón et al., 2014; Tchakouté et al., 2016; Villaquirán-Caicedo, Mejia De Gutiérrez e Gallego, 2017); results were shown to be similar to commercial silicates, both in terms of strength and microstructure.

As for paving applications, alkali-activated binders were already utilized as a stabilizing agent in combination with RAP (Adhikari, Khattak e Adhikari, 2020; Al-Hdabi, 2016; Avirneni, Peddinti e Saride, 2016; Edeh, Onche e Osinubi, 2012; Horpibulsuk et al., 2017; Hoy et al., 2018; Jallu et al., 2020; Kang, Ge, et al., 2015; Kang, Kang, et al., 2015; Saride, Avirneni e Challapalli, 2016; Sukprasert et al., 2021; Syed, GuhaRay e Goel, 2022; Tabyanga et al., 2021). However, the utilization of RAP alongside with alternative activators for the alkali-activation process is still a research-gap. The development of lower carbon emission activators is highly desirable and could lead to a significant reduction in the global warming potential of alkali-activated binders. Thus, the objective of this research was to stabilize RAP mixtures with a metakaolin-based binder, alkali-activated by rice husk ash synthetized sodium silicate. To that extent, compaction, unconfined compressive strength, scanning electron microscopy, and X-ray diffraction tests were conducted. In addition, all results were correlated with the porosity/binder content index to create a rational dosage methodology for the stabilized mixtures.

2. Materials and Method

2.1 Materials

The materials utilized in this research were reclaimed asphalt pavement (RAP), stone powder (SP), gravel (G), metakaolin (MK), rice husk ash (RHA), and sodium hydroxide (NaOH). RAP was acquired from ERS - 135 highway, located in city of Coxilha in southern Brazil. RHA is the waste of a rice processing industry and was collected directly from the company in Rio Grande do Sul, Brazil. On the other hand, SP, G, MK, and NaOH were all purchased from local manufacturers in Rio Grande do Sul, Brazil.

Materials physical characterization (Figure 2.1 and Table 2.1) was evaluated by determining their grain size distribution (ASTM, 2017a) and specific weight of grains (ASTM, 2014). For RAP, the bitumen content was determined in accordance with ASTM D 2172 (ASTM, 2018);

the specific gravity for coarse aggregate of RAP was determined according to NBR NM 53 (ABNT, 2009a), while for the fine aggregate NBR NM 52 (ABNT, 2009b).

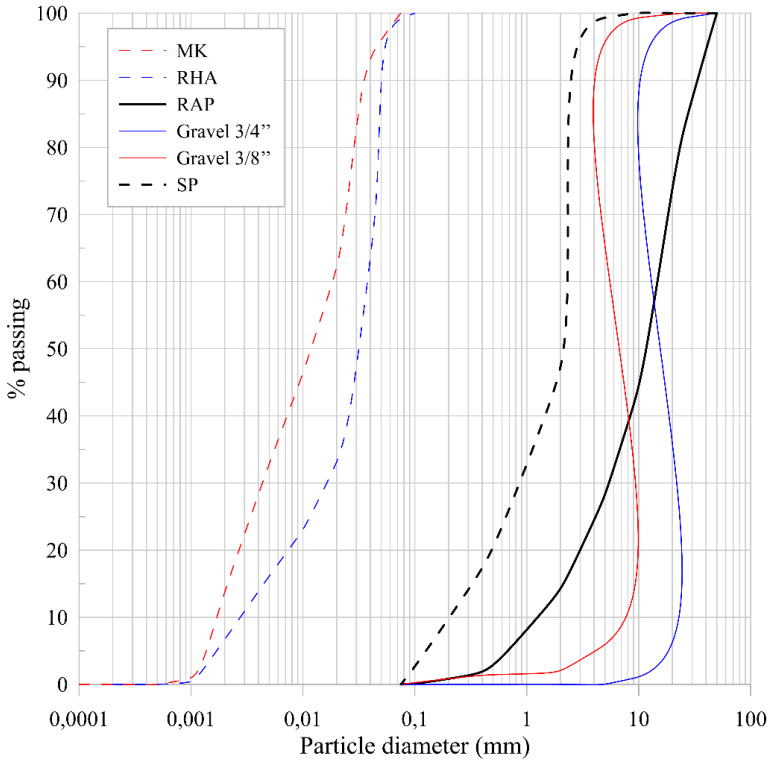

Figure 2.1. Materials grain size distribution.

Table 2.1. Materials physical properties.

Property	RAP	MK	RHA	SP	Gravel 3/4’’	Gravel 3/8”
Specific unit weight of grains (g/cm^3)	2.42	2.64	2.23	2.80	2.85	2.8
Bitumen content (%)	5.8	-	-	-	-	-
Gravel (4.75mm < diameter) (%)	72	0	0	0	100	94
Sand (0.06mm < diameter < 4.75mm) (%)	28	0	10	88	0	6
Silt (0.002mm < diameter < 0.06mm) (%)	0	86	82	22	0	0
Clay (diameter < 0.002mm) (%)	0	14	8	0	0	0
USCS classification	GW	SM	SM	SW	GP	GP

The mineralogical composition (Figure 2.2) was determined through an X-ray diffraction (XRD) test, the analysis was performed on a Shimadzu X-ray diffractometer, model XRD-6000 (θ-2θ), operating at 40 kV and 30 mA in the primary beam and curved graphite monochromator in the secondary beam. X-ray fluorescence spectrometry (XRF) was utilized to determine the elemental composition (Table 2), through a quantitative analysis with a calibration curve based on tabulated rock patterns from Geostandards. Scanning electron microscopy (SEM) analysis (magnifications of 4000 times) was utilized to study the microstructural characteristics of the

raw materials. In addition, an environmental classification was carried out on the RHA, following the procedures of NBR 10004 (ABNT, 2004a), NBR 10005 (ABNT, 2004b), and NBR 10006 (ABNT, 2009c). Metal concentrations were measured by inductively coupled plasma atomic emission spectrometry (Shimadzu-branded ICP-AES).

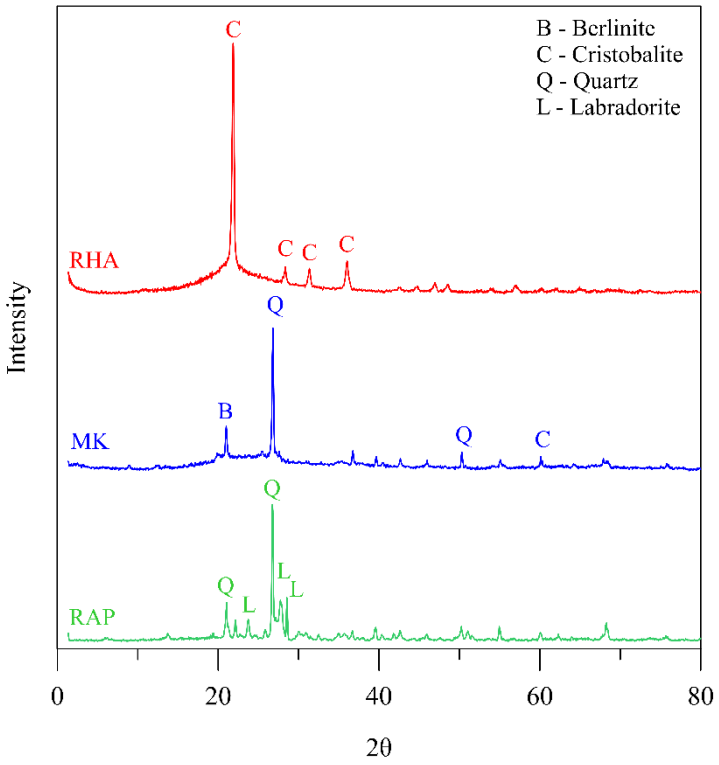

Figure 1.2. Mineralogical composition of RAP, MK and RHA.

Table 2.2. Materials chemical composition.

	SiO_2 (%)	Al_2O_3 (%)	Fe_2O_3 (%)	CaO (%)	MgO (%)	SO_2 (%)	Na_2O (%)	K_2O (%)	P_2O_5 (%)	TiO_2 (%)	ZnO (%)
RAP	64.39	14.65	1.16	4.10	<0.10	7.68	-	5.55	1.65	<0.10	<0.10
MK	54.72	40.80	1.80	0.10	0.10	-	0.18	0.21	-	2.09	-
RHA	89.33	0.62	1.53	3.84	2.51	-	-	2.18	-	-	-

RAP was classified as GW (well-graded gravel), while MK and RHA as SM (sand with fines) in accordance with the Unified Soil Classification System (USCS) (ASTM, 2017b). Regarding the mineralogical composition (Figure 2.2), RAP presented a crystalline structure composed by quartz (SiO_2) and labradorite [$(Ca,Na)(Al,Si)_4O_8$]; MK presented quartz (SiO_2), cristobalite (SiO_2), and berlinite ($AlPO_4$); and RHA was predominantly amorphous, with few sharp diffraction peaks of cristobalite (SiO_2). Crystalline silica has three polymorphic forms, cristobalite being obtained when subjected to burning temperatures between 981-991°C, as in the case of the RHA of this research. As for the chemical composition, RAP and MK majorly

consisted of silica and alumina, while RHA was mainly composed of silica. It is important to highlight that in its natural condition, RHA presents non-uniform particle size and therefore in this research it was subjected to grinding in a laboratory ball mill for 1 hour and then sieved in a sieve with an opening of 150 μm. RHA morphology after processing and in natura is shown in Figure 2.3a e Figure 2.3b respectively, indicating that the particles have an irregular, porous and finer shape after processing.

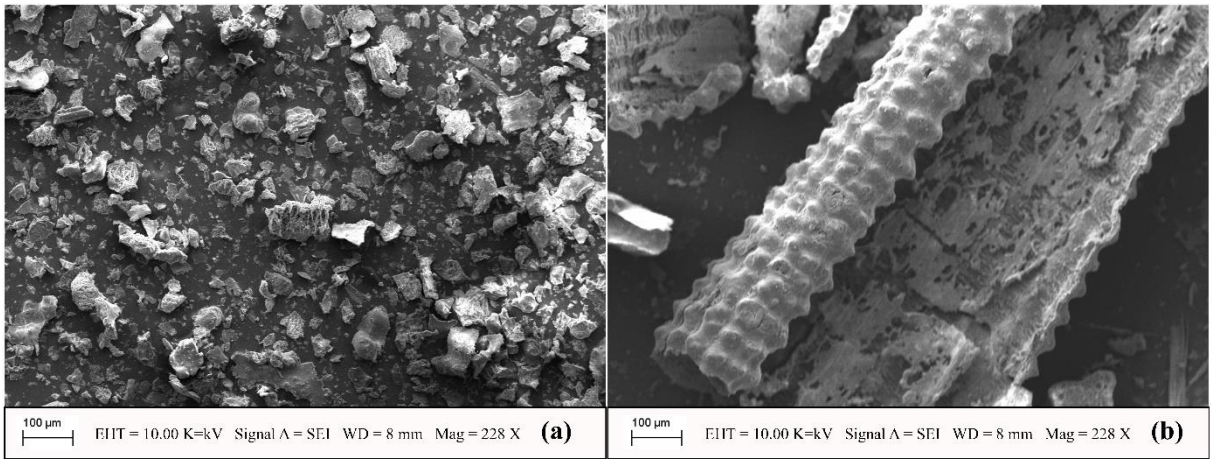

Figure 2.3. RHA morphology (a) after processing and (b) *in natura*.

Tables 2.3 and 2.4 show the leached and solubilized extracts for RHA. As for the classification, annex F of NBR 10004 (ABNT, 2004a) classifies the materials in Hazardous Waste or Non-Hazardous while annex G (ABNT, 2004a) the Non-Hazardous Inert or Non-Hazardous Non-inert characteristics. The leached extracts for RHA (Table 2.3) were all below the maximum limit of annex F, while solubilized extracts were higher than limits of annex G (Table 2.4) only for manganese (Mn). Therefore, this material is classified as Class II A – Non-Hazardous Non-inert, e.g. it may present biodegradability, combustibility, or water-solubility properties.

Table 2.3. Chemical composition of the leached extract.

Element	RHA ($mg.L^{-1}$)	Limits (ABNT, 2004a - Annex F)
Ag	< 0.005	5
As	< 0.001	1
Ba	0.692	70
Cd	< 0.05	0.5
Cr	< 0.003	5
Hg	< 0.00015	0.1
Pb	< 0.005	1
Se	< 0.008	1
Fluorides	0.04	1

Table 2.4. Chemical composition of the solubilized extract.

Element	RHA ($mg.L^{-1}$)	Limits (ABNT, 2004a - Annex G)
Ag	< 0.005	0.05
Al	0.103	0.2
As	< 0.0015	0.01
Ba	0.071	0.7
Cd	< 0.005	0.005
Cr	< 0.003	0.05
Cu	< 0001	2
Fe	0.001	0.3
Hg	< 0.0001	0.001
Mn	1.2	0.1
Na	45	200
Pb	< 0.005	0.01
Se	< 0.008	0.01
Zn	0.668	5
Cl	29.7	250
Surfactants	0.066	0.5
Nitrates	2.512	10
Cyanides	<0.001	0.07
Sulfates	159.1	400
Chlorides	29.7	250
Fluorides	0.05	1.5

2.2 Production of the alkali-activated binder

For the production of the alkali-activated binder (AA), the liquid alkaline activator was previously prepared by dissolving the RHA in a solution of sodium hydroxide (NaOH) at a 10 M concentration and kept at temperature of 80 °C for 12 hours. The mixing procedure, concentration of the solution, and SiO_2/Al_2O_3 = 4 ratio were kept constant and selected based on previous studies (Bernal et al., 2012; Davidovits, 1989). After the dissolution time and upon reaching room temperature, the solution was then mixed with the solid aluminosilicate source (MK) and latter with the materials to be stabilized (RAP and virgin aggregates).

2.3 Compaction test

The Proctor compaction test was performed using standard effort, in accordance with the guidelines of ASTM D698 (ASTM, 2012). The method involves placing (in a specified manner) a soil sample at a known water content in a mold of given dimensions, subjecting it to a compactive effort of controlled magnitude, and determining the resulting unit weight. The procedure is repeated for various water contents sufficient to establish a relation between water content and unit weight; through this process is possible to define the maximum dry unit weight (γ_{dmax}) and the optimum water content (OWC) of the studied mixtures.

2.4 Unconfined compression tests

Unconfined compression strength (UCS) tests were executed in accordance with ASTM D2166 (ASTM, 2016), using an automatic loading machine, with a maximum load capacity of 50kN. The rate of displacement adopted was 1.14mm per minute, to produce an axial strain at a rate between 0.5%/min and 2%/min, as recommended by ASTM D2166 (ASTM, 2016).

2.5 Mineralogical and microstructural analysis of the cemented mixtures

The mineralogical analysis consisted of X-ray Diffraction (XRD) tests performed in a Shimadzu equipment, XRD – 6000 model (CuKa radiation, 40 kV, 30 mA, 2h range of 10-80°, step size of 0.02°, 1 s/step, and COD database). The microstructure of the mixtures was evaluated by a scanning electron microscopy (SEM). SEM analysis was performed in the following conditions: backscattered electrons (BSE) with magnification of 4000 times, electron beam of voltage of 20 kV, with gold-coated samples (Quorum Q150). For the study the XRD e SEM analysis were performed for the two extremes of the experimental matrix (RAP: AA = 30: 20 and 50:40), for samples at 7 and 28 days and at room temperature and 60°C.

2.6 Molding and curing procedures

To explore the influence of the reclaimed asphalt pavement content on the behavior of the mixtures, three distinctive RAP levels (30%, 40% and 50%) were studied. The virgin aggregates (SP and G) were added to the RAP contents in different quantities, so the particle size limits for pavement applications, established by the WIRTGEN technical manual (Wirtgen GmbH, 2012), were respected. Table 2.5 shows the proportions of the non-cemented compositions.

Table 2.5. Proportions of the non-cemented compositions.

Reclaimed asphalt pavement content (%)	Stone powder content (%)	Gravel 3/4'' content (%)	Gravel 3/8'' content (%)
30	50	10	10
40	40	10	10
50	40	4	6

For the study of the influence of the alkali-activated cement, mixtures from Table 2.5 were stabilized by adding 20%, 30%, and 40%. Thus, the RAP:AA ratios evaluated were 30:0, 30:20, 30:30, 30:40, 40:0, 40:20, 40:30, 40:40, 50:0, 50:20, 50:30 and 50:40. Table 2.6 shows an overview of the studied variables of the experimental design for the mechanical tests.

Table 2.6. Variables of the experimental design.

Test	Reclaimed asphalt pavement (%)	Alkali-activated cement (%)	Curing period (days)	Curing temperature (°C)
UCS	30, 40, 50	0, 20, 30, 40	7, 28	23, 60

For UCS tests triplicates of cylindrical specimens of 10mm in diameter and 127mm in height were utilized. The molding procedure starts by the mixing of the air-dried materials (RAP, virgin aggregates and metakaolin) with the liquid alkaline activator (prepared by dissolving the RHA in a solution of sodium hydroxide) and water until homogenization is achieved. Then, specimens are molded at the optimum moisture content (OMC) and maximum dry unit weight (γ_{dmax}) from the compaction curves. After specimens were molded and had their dimensions taken, they were sealed in hermetic bags before being stored in a humid room with controlled moisture (95 ± 2%) at two distinctive temperatures (23 ± 2°C and 60 ± 2°C) for 7- and 28-days curing. Specimens were considered suitable for testing if the following criteria was met: degree of compaction between 99% and 101%; water content within 0.5% of the target value; diameter within 0.5 mm of the target value; and height within 1 mm of the target value.

2.7 Porosity/binder index (η/Biv)

The mechanical behavior of the cemented mixtures was also expressed in relation to the porosity/binder index (Consoli, Winter, et al., 2018) and calculated by Equations 1 and 2.

$$\eta = 100 - 100\left\{\left[\frac{\gamma_d}{\frac{RAP}{100}+\frac{SP}{100}+\frac{G}{100}+\frac{MK}{100}+\frac{RHA}{100}}\right]\left[\frac{\frac{RAP}{100}}{\gamma_{s_{RAP}}}+\frac{\frac{SP}{100}}{\gamma_{s_{SP}}}+\frac{\frac{G}{100}}{\gamma_{s_G}}+\frac{\frac{MK}{100}}{\gamma_{s_{MK}}}+\frac{\frac{RHA}{100}}{\gamma_{s_{RHA}}}\right]\right\} \quad (1)$$

$$Biv = \frac{V_{RHA}+V_{MK}}{V} = \frac{m_{RHA}/\gamma_{s_{RHA}}+m_{MK}/\gamma_{s_{MK}}}{V} \quad (2)$$

Porosity (η) is a function of the dry unit weight (γ_d) and unit weight of solids (γs_{RAP}, γs_{SP}, γs_G, γs_{MK}, and γs_{RHA}) of the reclaimed asphalt pavement, stone powder, gravel, metakaolin, rice husk ash. The binder content (Biv) results from the volume occupied by MK and RHA divided by the total volume of the specimen. Also, RAP is the reclaimed asphalt pavement content of the mixture; SP is the stone powder content of the mixture; G is the gravel content of the mixture; MK is the metakaolin content of the mixture; and RHA is the rice husk ash content of the mixture. This index allows the unification of all experiments in a single relation, resulting

in a rational dosage methodology for any cemented soil mixture, replacing trial and error conventional strategies that are laborious and time consuming. However, such equations are only valid for the cemented mixtures studied herein and functional if the boundary conditions of the applied variables are ensured.

3. Results and discussion

3.1 Compaction tests

Figure 2.4 presents the relationship between the dry unit weight (γd) and the water content of mixtures with RAP and virgin aggregates (Figure 2.4a), as well as for the same mixtures compacted with AA (Figure 2.4b, Figure 2.4c and Figure 2.4d).

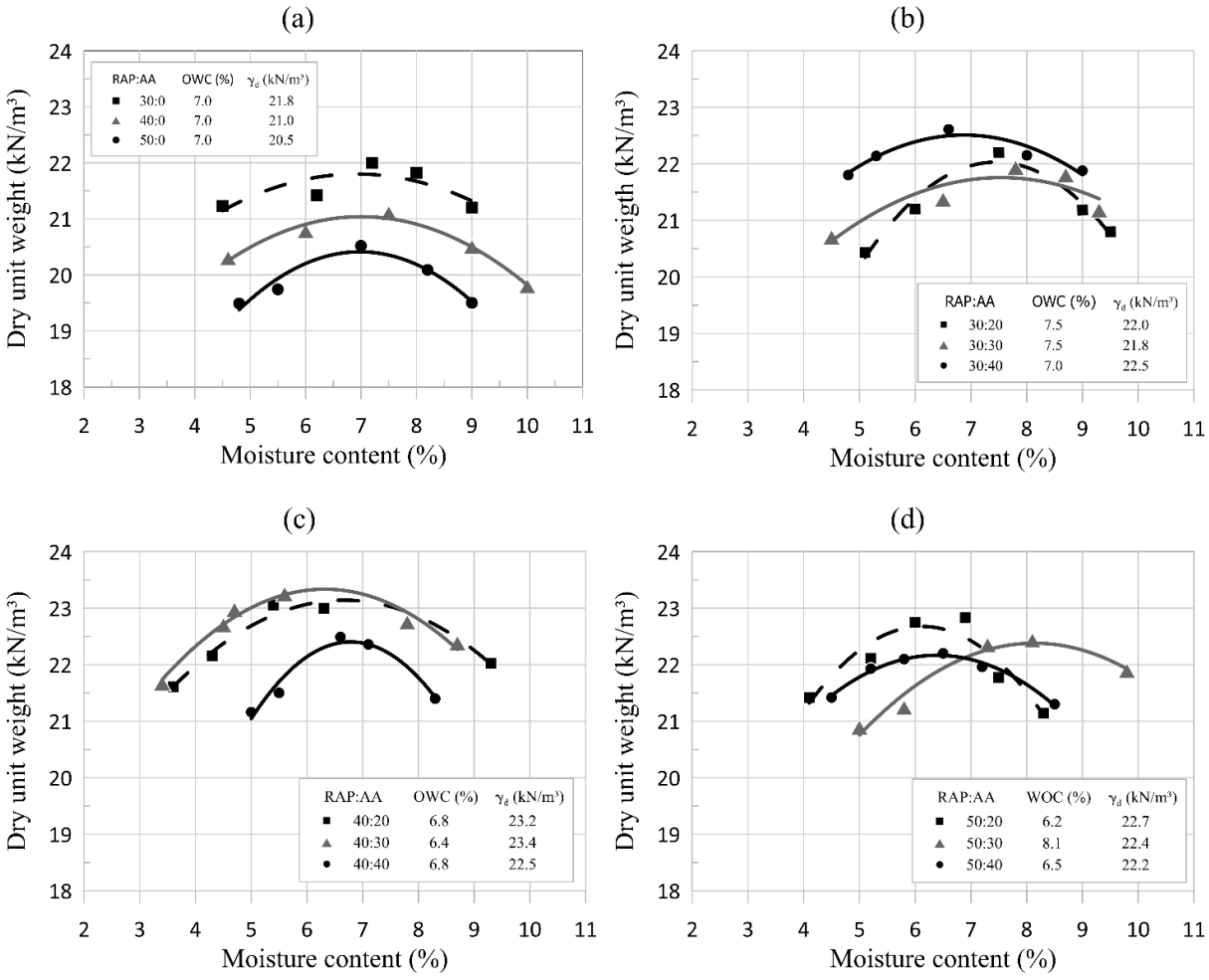

Figure 2.4. Compaction test results: (a) RAP without AA, (b) RAP with 30% AA, (c) RAP with 40% AA e (d) RAP with 50% AA.

For mixtures of 0% AA (Figure 2.4a), the dry unit weight parameter was more sensitive than the OWC; as RAP content increased, dry unit weight decreased for all RAP contents. This

behavior is supported by the fact that most RAP particles are coated with bitumen, reducing moisture absorption and making the added water improve workability (Mohammadinia et al., 2018; Mousa, El-Badawy e Azam, 2021; Taha et al., 1998). However, for the incorporation of different AA contents the opposite behavior was evidenced; in which the dry unit weight presented no expressive variation and the OMW varied non-linearly. AA improved the compaction properties, mainly for the replacement percentages of 40% and 50% of RAP, in which the largest dry unit weight increases were observed. Although the highest dry unit weight was expected for mixtures with 30% RAP, when adding AA this increase was less expressive than in the other mixtures. For the proportion of 30% RAP, the largest amount of fine virgin aggregates was added among all mixtures (50% of stone powder), showing that AA improves the workability (or packaging) mainly of materials with larger particles. This fact can also be explained by the difficulty in homogenizing fine materials with AA that have a higher viscosity than water. Thus, although the addition of fine virgin aggregates improves the packing of the mixtures, this behavior is not reproduced efficiently in mixtures with AA.

3.2 Unconfined compressive strength

Figure 2.5 presents the unconfined compressive strength (UCS) results for the stabilized RAP mixtures. The increase in AA content led to an increase in UCS for all evaluated mixtures; the increase in AA content reduces porosity aiding on strength development. Porosity reduction induces a greater contact area between the particles, intensifying the interlocking and mobilizing friction between particles. In addition, the increase in AA content is linked to the increase in cementitious reactions, also contributing for strength development (Pereira dos Santos et al., 2022). Similar results have been found for RAP stabilized with alkali-activated binders (Hoy et al., 2018; Hoy, Horpibulsuk e Arulrajah, 2016; Mohammadinia et al., 2016), cement stabilized RAP (Mohammadinia et al., 2016; Suebsuk e Suksan, 2014; Taha et al., 2002) and other cement-stabilized geotechnical materials (Consoli et al., 2007; Diambra et al., 2017; Festugato et al., 2018).

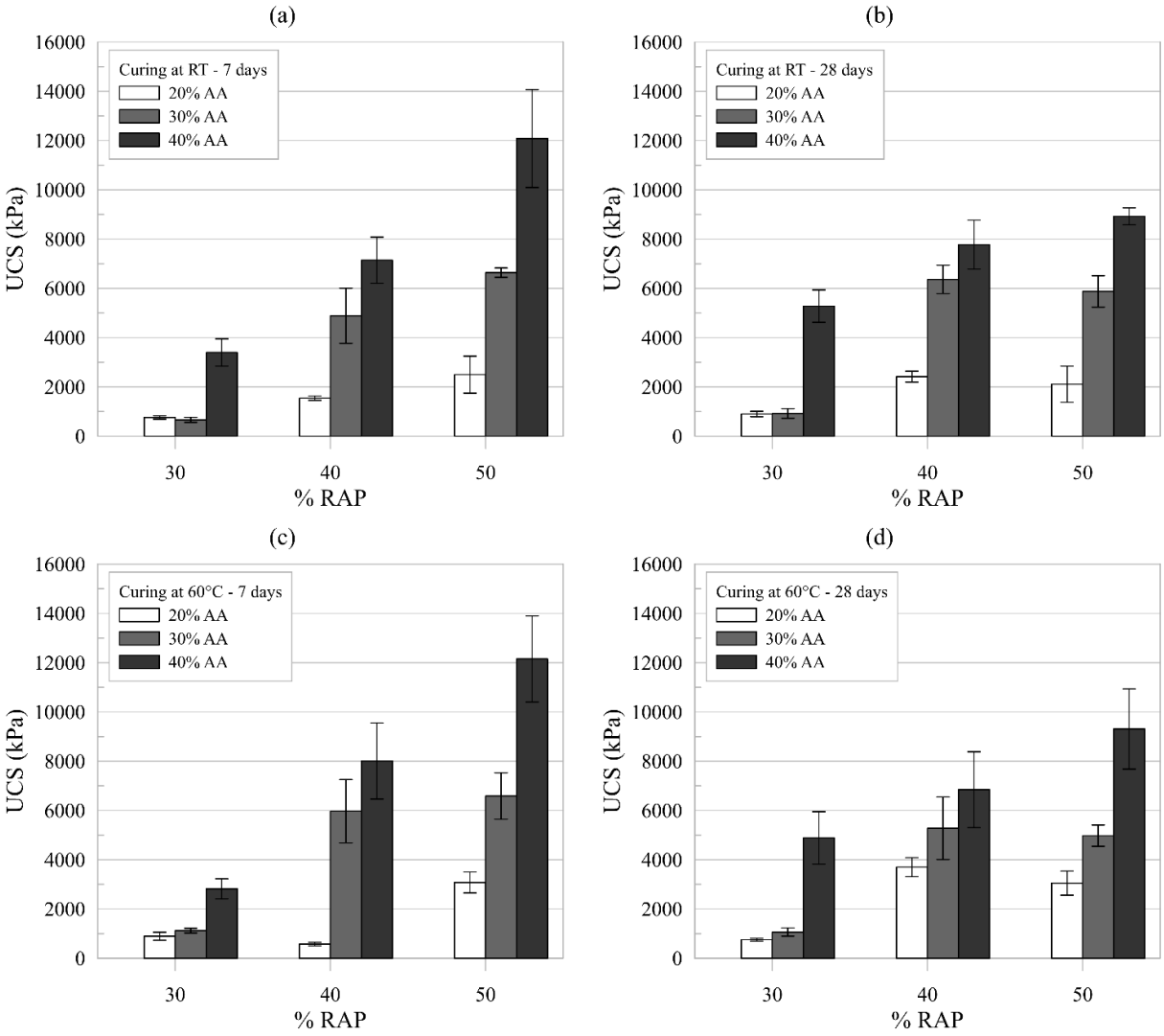

Figure 2.5. Compressive strength of RAP and RAP-AA blends cured at: and 28 days: (a) at room temperature at 7 days (b) at room temperature at 28 days (c) at 60°C at 7 days and (b) at 60°C at 28 days.

Considering that AA additions were carried out in relation to the dry weight of RAP, the increase in strength is less expressive in RAP:AA ratios of 30:20 and 30:30. This implies that, for applications that require high initial strength, a greater incorporation of AA is indicated. Although the highest UCS values were observed for the highest AA contents, it was observed that the strength decreases over time for these same mixtures. This loss in strength was also observed in alkali pastes activated by both commercial sodium silicate and alternative RHA silicate, at curing periods greater than 28 days (Longhi et al., 2014), evidencing that the alternative silicate is not the triggering phenomenon of strength reduction over time. Metakaolin-based geopolymers undergo a major microstructural reorganization, in which amorphous geopolymer gels are able to convert into crystalline zeolites after aging, resulting in

binder densification and the formation of large pores, accompanied by a large reduction in strength (Lloyd, 2009). For the curing condition of 60°C the reduction in mechanical performance can occur because the activated alkali ash hydration products are generally amorphous, but higher temperatures lead to the formation of crystalline hydration products (Wang, Li e Yan, 2005). In addition, the alkali-activated products undergo changes in the gel microstructure formed during longer curing times, suggesting that the continuous reorganization and polymerization of the aluminosilicate gel may be causing autogenous shrinkage, and a reduction in strength (Longhi et al., 2016). The loss of strength may also be related to the beginning of crystallization of the products formed by hydration, resulting in a thermodynamic instability of the amorphous reaction of the products (Lloyd, 2009; Takeda et al., 2013). Finally, except for the ratio RAP:AA = 30:20, 30:30 at 7 days and 28 days and RAP:AA = 40:20 at 7 days, the blends have minimal resistance for use as road construction material in accordance with the requirements of the National Department of Infrastructure and Transport of Brazil.

3.3 Mineralogical and microstructural analysis of the cemented mixtures

XRD results of 30:20 RAP:AA mixtures are presented in Figure 2.6. Results show that some peaks of Quartz (SiO_2) from the raw precursor materials are maintained in the alkali-activated mixtures, indicating that these minerals were not dissolved and remained within their original structures throughout the studied curing periods. Nevertheless, new chemical products rich in silica and alumina were also generated: Anorthoclase [$(Na,K)AlSi_3O_8$], Bytownite [$(Na,Ca)Al1\text{-}2Si_{3}\text{-}_2O_8$], Albite ($NaAlSi_3O_8$), Oligoclase [$(Na,Ca)Al2Si_2O_8$], Ye'eemite ($Ca_4Al_6(SO_4)O1_2$) and Labradorite [$(Ca,Na)(Al,Si)_4O_8$]. Several studies report that the main product of the alkali-activation process is a sodium aluminosilicate gel (N-A-S-H) (Fernandez-Jimenez e Palomo, 2009; Gartner e MacPhee, 2011; Juenger et al., 2011) with subsequent formation of some type of zeolite (Gartner e MacPhee, 2011), as seen in the XRD results of RAP:AA = 30:20 (Figure 2.6) where the peaks formed are part of the zeolite family.

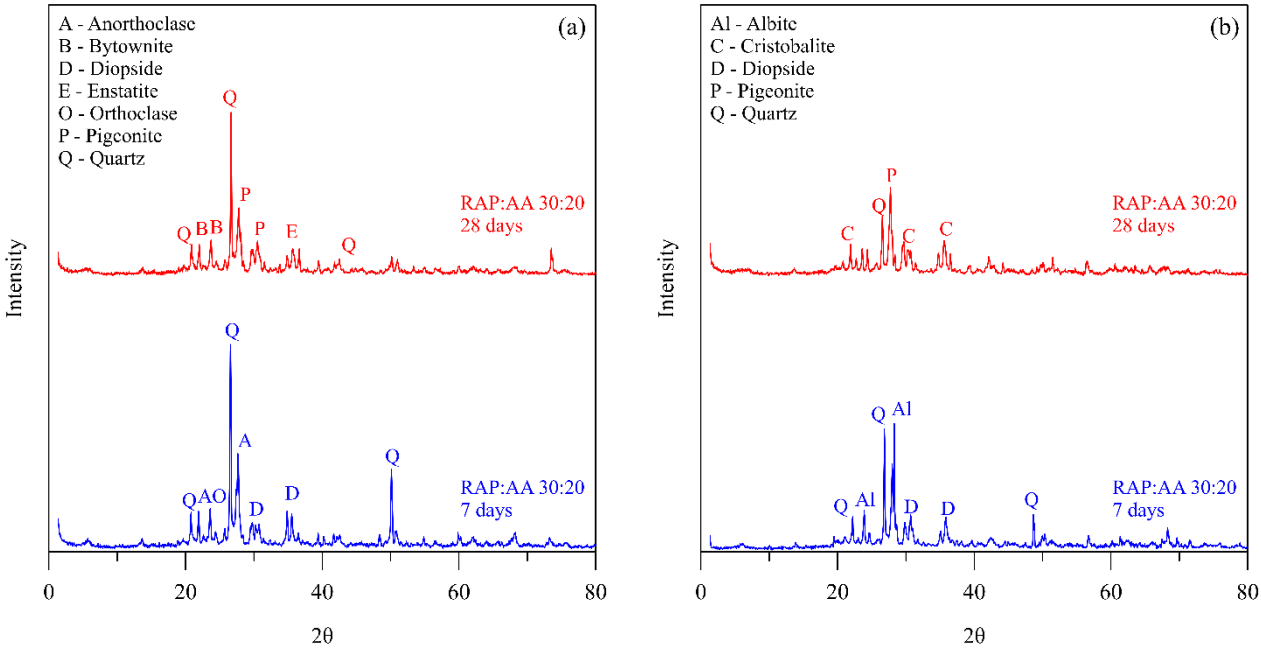

Figure 2.6. XRD patterns for RAP:AA of 30:20 for (a) 23°C curing temperature; and (b) 60°C curing temperature.

For the room temperature samples (Figure 2.6a), a reduction on the peaks of the metakaolin minerals was observed; this phenomenon results in the release of silicate and aluminate species in the solution, represented by the minerals Quartz (SiO_2) and Anorthoclase [$(Na,K)AlSi_3O_8$] respectively. In addition, this process resulted in a new alkali-activated matrix, including Bytownite [$(Na,Ca)Al1\text{-}_2Si_3\text{-}_2O_8$] and Pigeonite [$(Mg,Fe,Ca)(Mg,Fe)Si_2O_6$], as observed in the range between 20° and 30°. As for the 60°C curing temperature samples (Figure 2.6b), XRD analyzes show a reduction in the peaks corresponding to the cementitious products (Quartz and Albite) between 25° and 30°; indicating an acceleration in the reactions caused by the increase in temperature and the total dissolution and consumption of the alumina. This resulted in the formation of alumina-free products such as Cristobalite (SiO_2), Quartz (SiO_2) and Pigeonite [$(Mg,Fe,Ca)(Mg,Fe)Si_2O_6$]. The reduced strength at elevated temperatures can be attributed to the breakdown of the mixture structure during geopolymer synthesis, resulting in dehydration and excessive shrinkage as the gel contracts to a more semi-crystalline form (Khalil e Merz, 1994).

SEM images of 30:20 RAP:AA mixtures are shown in Figure 2.7. For both curing temperatures, a denser cementation matrix is formed with the increase in curing period. However, for the 60°C curing temperature samples, small cracks are evidenced with the increase in curing period, corroborating the reduction in strength over time, evidenced in the UCS results.

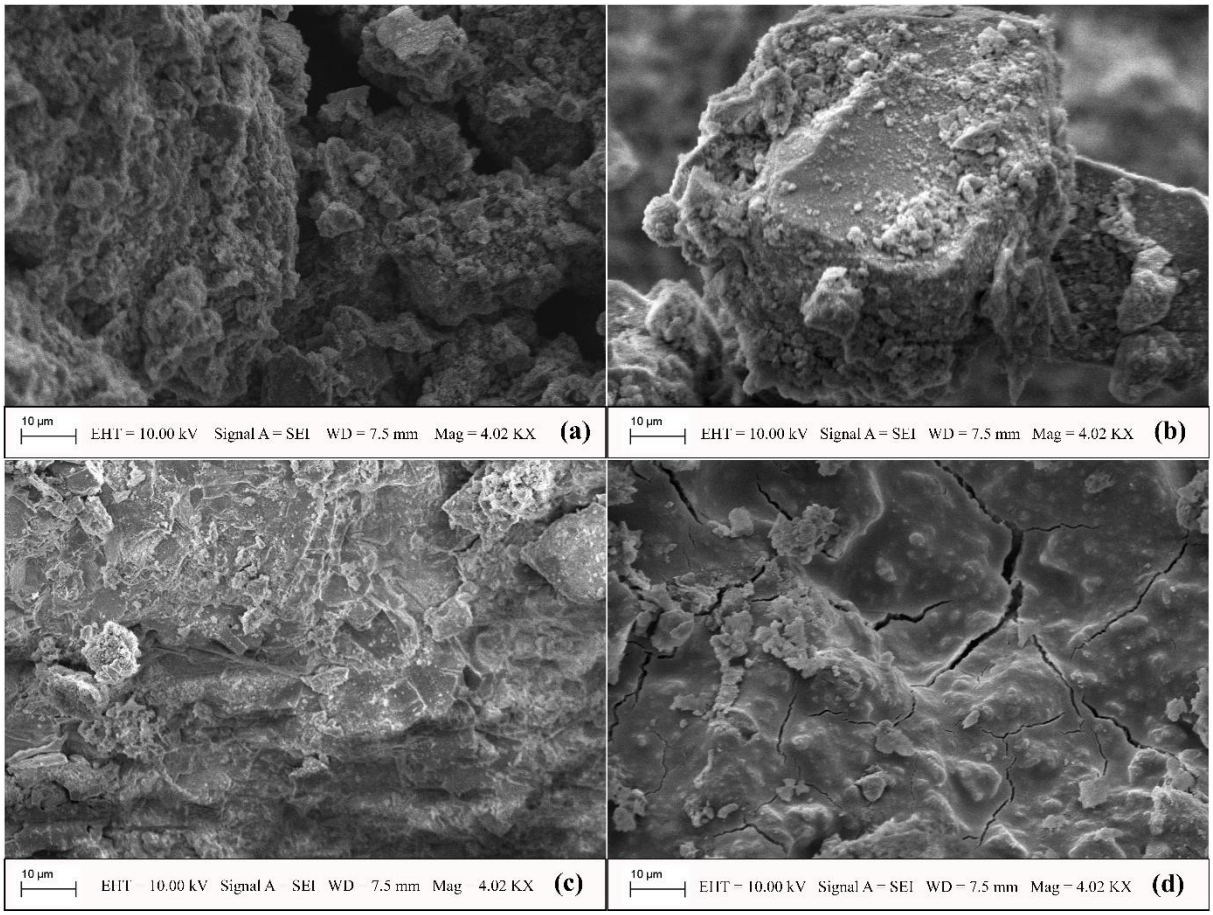

Figure 2.7. SEM images of RAP:AA = 30:20 cured for: (a) 7 days at room temperature, (b) 28 days at room temperature, (c) 7 days at 60°C and (d) 28 days at 60°C.

XRD results of 50:40 RAP:AA mixtures are presented in Figure 2.8. Results show that, for the specimens cured at 60°C, a large part of the alumina was consumed and the silica peaks increased (i.e. alumina was quickly consumed while silica remained unreacted in the system). This behavior indicates that by subjecting the specimens to high temperatures the material becomes more amorphous. At room temperature, it was observed that the labradorite [$(Ca,Na)(Al,Si)_4O_8$] peak is converted into Quartz (SiO_2) and undergoes a crystallization process over time, consistent with UCS results, which showed a reduction in strength from 7 to 28 days. Furthermore, for room temperature samples, higher AA contents made the material more susceptible to the formation of efflorescence (which is associated with a process of degradation of the binder), resulting in a decrease in strength. The efflorescence phenomenon is characterized by the excess of unreacted sodium oxide, causing the product surface to be enriched with this alkaline material, which can react with the CO_2 present in the air forming a

white carbonate surface (Kani, Allahverdi e Provis, 2012). In XRD analyzes at room temperature (Figure 2.8a), the occurrence of efflorescence can also be identified through the appearance of the mineral Bytownite [(Na,Ca)Al1-2$Si_{3-2}O_8$] and Oligoclase [(Na,Ca)$Al_2Si_2O_8$] in the curing period of 28 days.

The increase in RAP and AA content (represented by the higher ratio RAP:AA = 50:40 and the increase in temperature to 60°C) also showed a change in the mineralogical composition that indicates the development of geopolymerization products over time. The XRD analyses (Figure 2.8c and Figure 2.8d) indicate a reduction in the intensity of the peaks related to the formation of geopolymerization gels (N-A-S-H), suggesting a certain reactivity provided by the temperature increase. Furthermore, as a result of alkaline activation, new products including Anorthoclase [(Na,K)$AlSi_3O_8$] and Bywtonite [(Na,Ca)Al1-2$Si_{3-2}O_8$] are detected at peaks between 20° and 35°. As in most chemical reactions, temperature accelerates the alkaline activation process (Alonso e Palomo, 2001), favoring the compounds' dissolution, thus generating greater mechanical strength (Bernal et al., 2011).

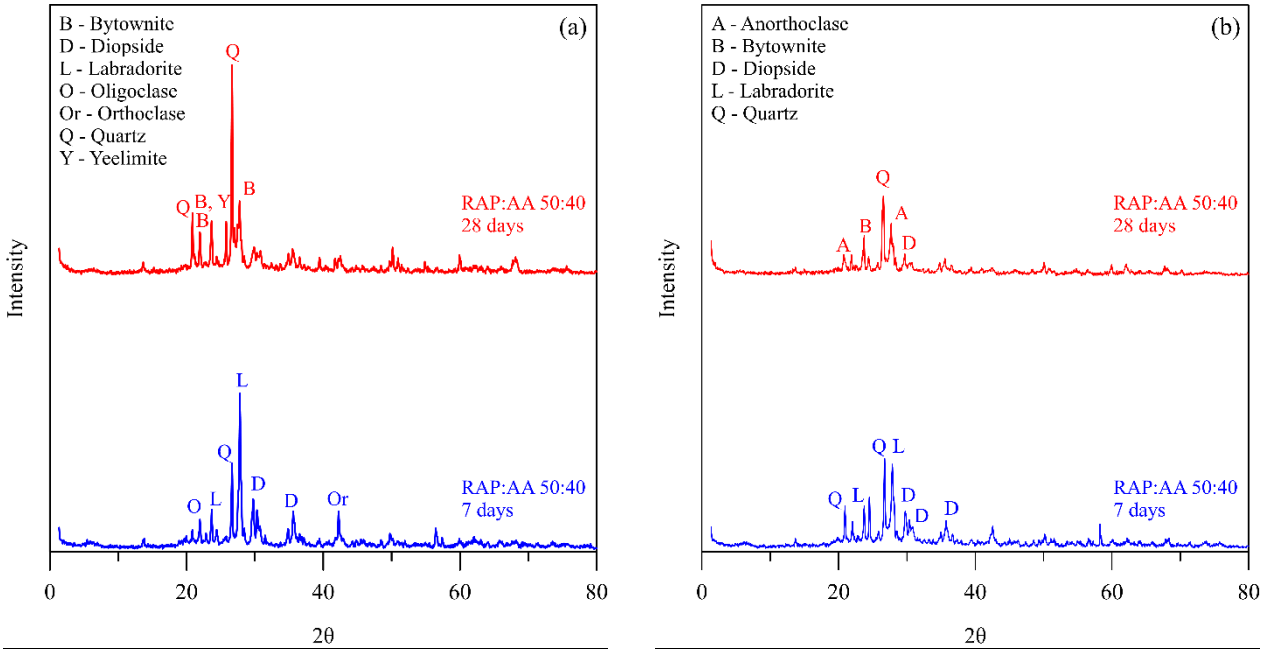

Figure 2.8. XRD patterns for RAP: AA of 50:40 for (a) 23°C curing temperature; and (b) 60°C curing temperature.

SEM images of 50:40 RAP:AA mixtures are shown in Figure 2.9. The increase in curing period led to a denser structure for both curing temperatures. However, high curing temperatures also result in the appearance of cracks in the surface of the mixture, negatively impacting the development of strength (Jaarsveld, Deventer e Lukey, 2002).

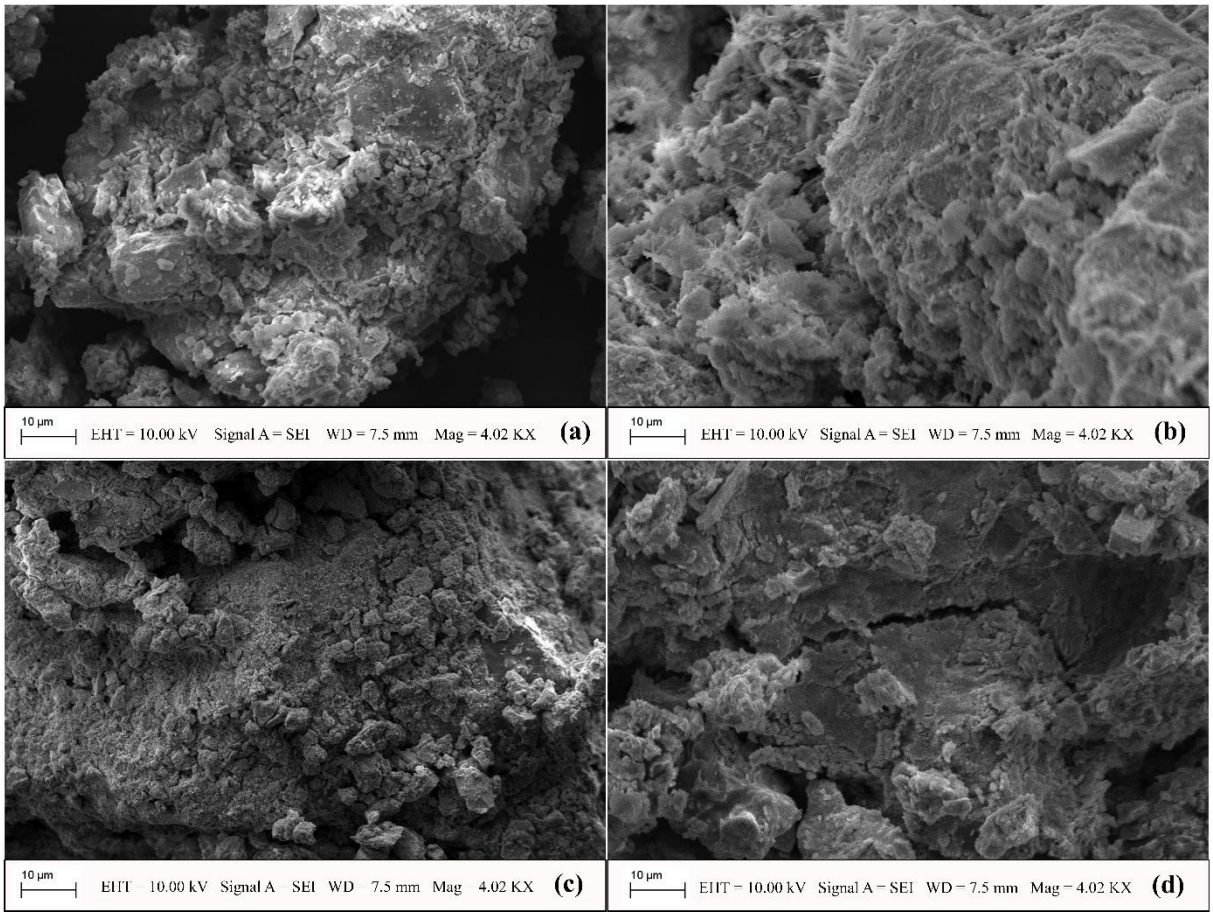

Figure 2.9. SEM images of RAP:AA = 50:40 cured for: (a) 7 days at room temperature, (b) 28 days at room temperature, (c) 7 days at 60°C and (d) 28 days at 60°C.

Finally, it is important to highlight that the final product is the same regardless of the synthesis temperature. As shown by the XRD results, there is only a change in the dissolution rate of the aluminosilicates, but the later phases are not affected by the temperature increase and therefore no significant differences in the final strength are observed.

3.4 Porosity/binder index (η/Biv)

The UCS results were correlated with the porosity/binder index, aiming to unify the experiments in a single relation; this unification results in equations that allow the prediction of strength of the cemented mixtures. Figure 2.10 shows the UCS results for 7-days curing period and 23°C curing temperature. For all RAP contents (30%, 40%, and 50%) the increase in binder content and decrease in porosity led to higher unconfined compressive strength values. The increase in binder content (from 20% to 30% and latter to 40%) increases the amount of alkali-activated reactions occurring in the mixtures, directly influencing the evidenced development

of strength. Regarding the porosity effect, its reduction increases the contact area between particles, enhancing the interlocking phenomenon and friction mobilization resulting in an increase in strength. This physical-chemical phenomenon has also been evidenced in different cemented geotechnical materials, like stabilized RAP (Consoli et al., 2020; Consoli, Giese, et al., 2018; Consoli, Pasche, et al., 2018; Consoli, Scheuermann Filho, et al., 2018; Consoli, Tebechrani Neto, et al., 2021), stabilized soils (Consoli, Daassi-Gli, et al., 2021; Consoli, Tonini de Araújo, et al., 2021; Consoli, Rosa e Saldanha, 2011; Festugato et al., 2018; Lotero et al., 2021; Piuzzi et al., 2021; Quiñónez Samaniego et al., 2021; Saldanha et al., 2021; Tonini de Araújo et al., 2021), and even stabilized mining tailings (Bruschi, Santos, dos, et al., 2021; Bruschi, Santos, et al., 2021; Consoli et al., 2017; Consoli, Silva, et al., 2018; Pereira dos Santos et al., 2022).

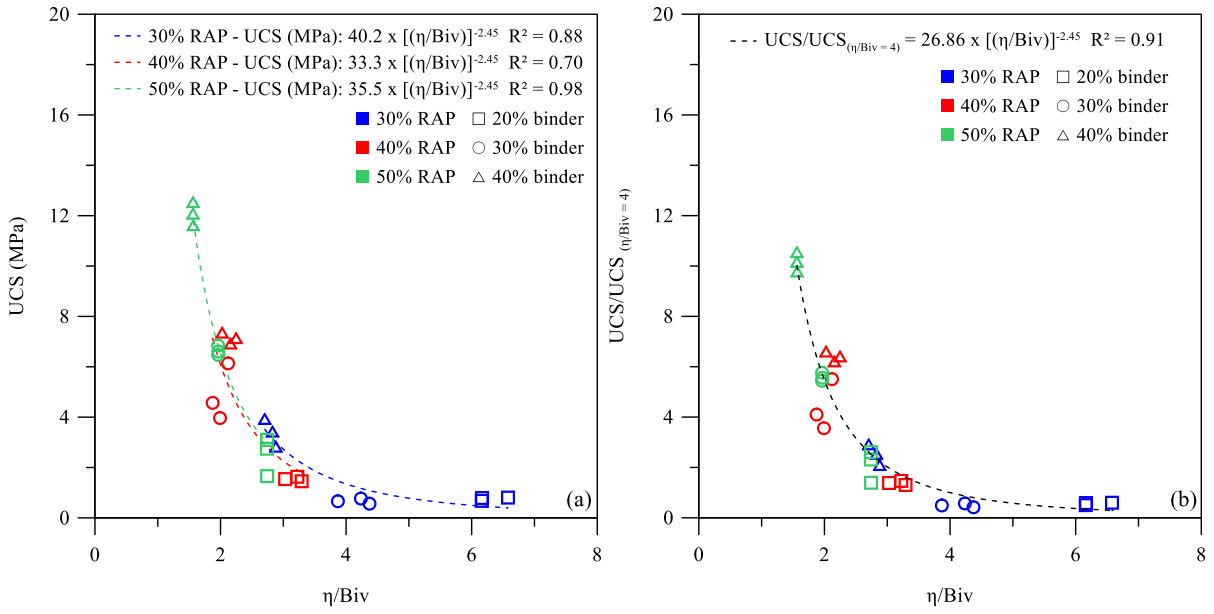

Figure 2.10. UCS versus η/Biv index 7-days curing period and 23°C curing temperature (a) non-normalized (b) normalized by RAP content

Considering that different RAP contents represent different geotechnical materials, three different Equations (Eqs. 3-5) were generated through the η/Biv index. Adequate correlations between the UCS of the mixtures and the η/Biv index were evidenced for all RAP contents (30%, 40%, and 50%); with determination coefficients (R^2) between 0.70 and 0.98. The elevated determination coefficients suggest the viability of the index on the prediction of the UCS behavior of cemented RAP mixtures; this behavior has also been corroborated by several

other research (Consoli et al., 2020; Consoli, Giese, et al., 2018; Consoli, Pasche, et al., 2018; Consoli, Tebechrani Neto, et al., 2021).

$$30\%\ \text{RAP: UCS (MPa)}_{7\text{days}/23°\text{C}} = 40.2 \times \left[\left(\eta/_{\text{Biv}}\right)\right]^{-2.45} \quad (3)$$

$$40\%\ \text{RAP: UCS (MPa)}_{7\text{days}/23°\text{C}} = 33.3 \times \left[\left(\eta/_{\text{Biv}}\right)\right]^{-2.45} \quad (4)$$

$$50\%\ \text{RAP: UCS (MPa)}_{7\text{days}/23°\text{C}} = 35.5 \times \left[\left(\eta/_{\text{Biv}}\right)\right]^{-2.45} \quad (5)$$

From the analysis of Eqs. 3 to 5, it is possible to notice that the external exponents of the equations are the same, however, the initial constants present different values. Consoli et al. (2018) proposed that the mechanical behavior of soil-cement mixtures, for the same stabilizing agent, can be normalized over several pre-established variables (e.g. curing time, temperature, type of soil, moisture content) if the external exponent of the analyzed equations is the same. Thus, it becomes possible to generate a single mathematical correlation despite different initial variables. Considering that different equations (Eqs. 3-5) were generated for each RAP content (30%, 40%, and 50%), the data was normalized over the variable RAP content of the mixtures. This normalization was achieved through the division of UCS results (Figure 10a) by a specific value of UCS (corresponding to a η/Biv = 4), as shown by Eq. 6 (R^2 of 0.91).

$$\text{UCS}/\text{UCS}_{\left(\eta/_{\text{Biv}}=4\right)\ 7\text{days}/23°\text{C}} = 26.86 \times \left[\left(\eta/_{\text{Biv}}\right)\right]^{-2.45} \quad (6)$$

The UCS results for the remaining curing periods and temperatures are shown in Figure 2.11 (28 days and 23°C), Figure 2.12 (7 days and 60°C), and Figure 13 (28 days and 60°C). As in the case of Figure 10a (7-days curing period and 23°C curing temperature), the increase in binder content and decrease in porosity led to higher unconfined compressive strength values for all curing conditions. This was once more to the greater contact area between the mixtures particles, alongside the increase in alkali-activated reactions, that contributed to strength development (Consoli et al., 2020; Consoli, Giese, et al., 2018; Consoli, Scheuermann Filho, et al., 2018; Consoli, Tebechrani Neto, et al., 2021).

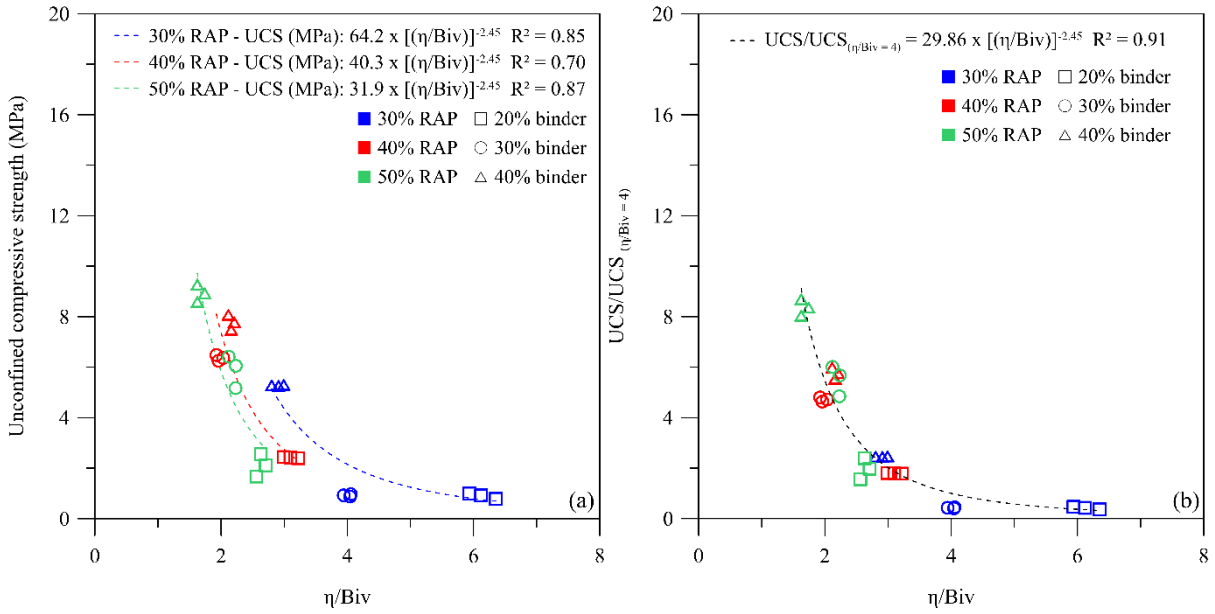

Figure 2.112. UCS versus η/Biv index 28-days curing period and 23°C curing temperature (a) non-normalized (b) normalized by RAP content

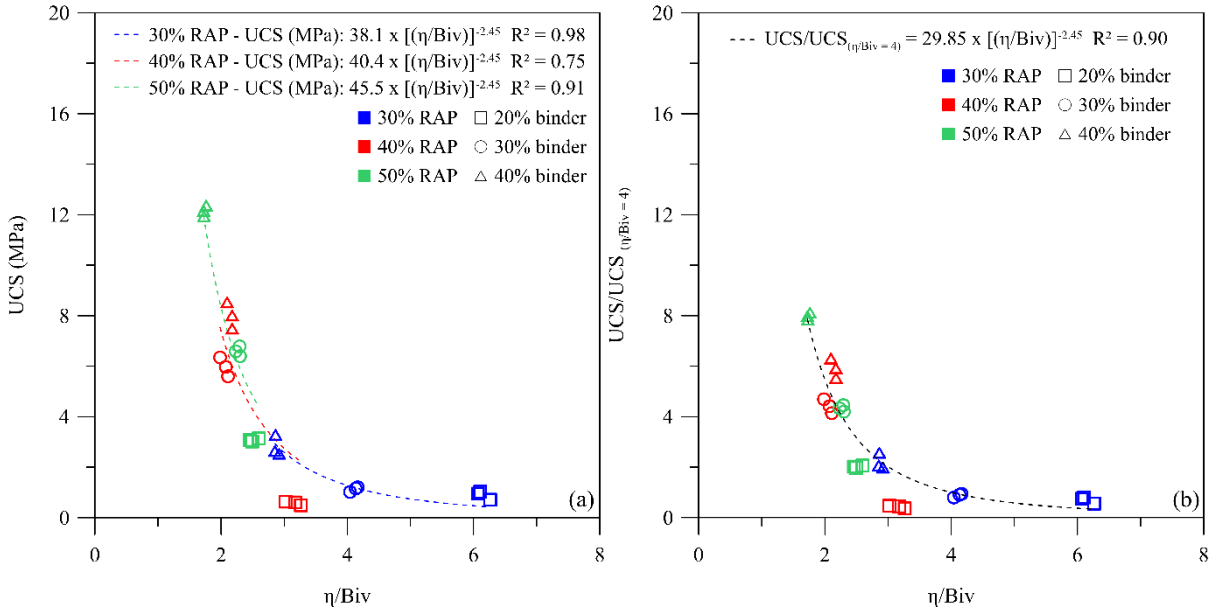

Figure 2.123. UCS versus η/Biv index 7-days curing period and 60°C curing temperature (a) non-normalized (b) normalized by RAP content

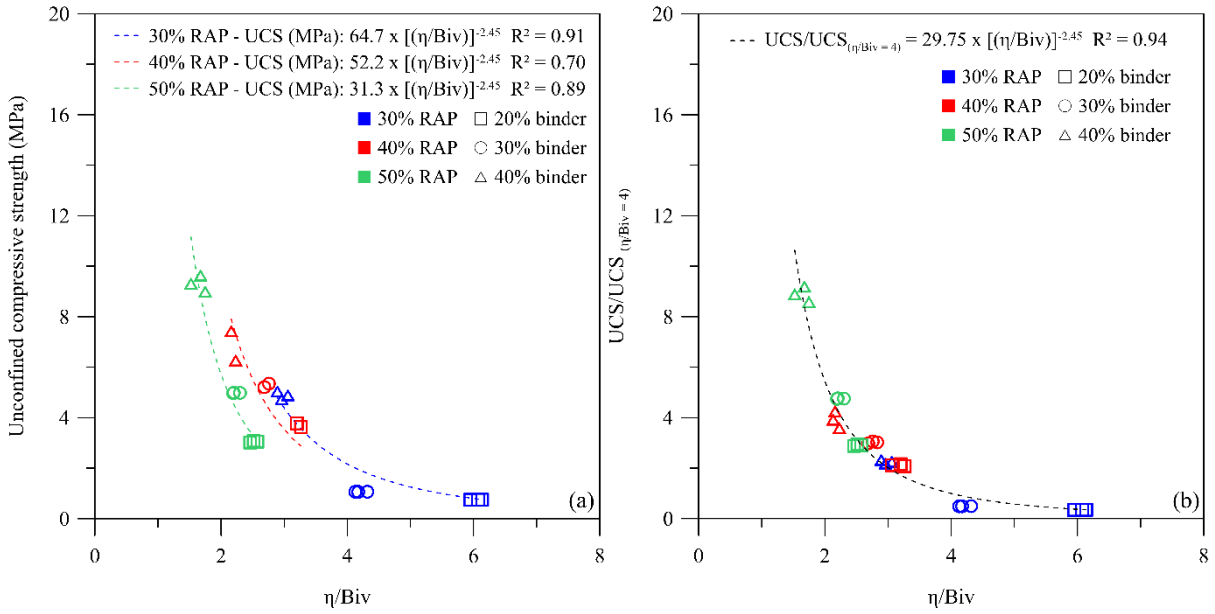

Figure 4. UCS versus η/Biv index 28-days curing period and 60°C curing temperature (a) non-normalized (b) normalized by RAP content

Fair correlations (Eqs. 7-15) were also identified for the remaining curing conditions; with determination coefficients (R^2) ranging from 0.70 to 0.98. These elevated determination coefficients again suggest the viability of the index on the prediction of the UCS behavior of cemented RAP mixtures for all analyzed curing periods (7 and 28 days) and curing temperatures (23°C and 60°C) at different RAP contents (30%, 40%, and 50%).

$$30\%\ \text{RAP: UCS (MPa)}_{28\text{days}/23^{\circ}\text{C}} = 64.2\times\left[\left(\eta/_{\text{Biv}}\right)\right]^{-2.45} \quad (7)$$

$$40\%\ \text{RAP: UCS (MPa)}_{28\text{days}/23^{\circ}\text{C}} = 40.3\times\left[\left(\eta/_{\text{Biv}}\right)\right]^{-2.45} \quad (8)$$

$$50\%\ \text{RAP: UCS (MPa)}_{28\text{days}/23^{\circ}\text{C}} = 31.9\times\left[\left(\eta/_{\text{Biv}}\right)\right]^{-2.45} \quad (9)$$

$$30\%\ \text{RAP: UCS (MPa)}_{7\text{days}/60^{\circ}\text{C}} = 38.1\times\left[\left(\eta/_{\text{Biv}}\right)\right]^{-2.45} \quad (10)$$

$$40\%\ \text{RAP: UCS (MPa)}_{7\text{days}/60^{\circ}\text{C}} = 40.4\times\left[\left(\eta/_{\text{Biv}}\right)\right]^{-2.45} \quad (11)$$

$$50\%\ \text{RAP: UCS (MPa)}_{7\text{days}/60^{\circ}\text{C}} = 45.5\times\left[\left(\eta/_{\text{Biv}}\right)\right]^{-2.45} \quad (12)$$

$$30\%\ \text{RAP: UCS (MPa)}_{28\text{days}/60^{\circ}\text{C}} = 64.7\times\left[\left(\eta/_{\text{Biv}}\right)\right]^{-2.45} \quad (13)$$

$$40\%\ \text{RAP: UCS (MPa)}_{28days/60°C} = 52.2\times\left[\left(\eta/_{Biv}\right)\right]^{-2.45} \quad (14)$$

$$50\%\ \text{RAP: UCS (MPa)}_{28days/60°C} = 31.3\times\left[\left(\eta/_{Biv}\right)\right]^{-2.45} \quad (15)$$

Considering that the external exponents the equations are the same, with only different scalars, the data can be once more normalized (Consoli, Scheuermann Filho, et al., 2018). As for the case of Figure 2.10b (7-days curing period and 23°C curing temperature), the normalization was made over the RAP content of the mixtures. This normalization was once more achieved through the division of UCS results (Figures 2.11a, 2.12a, and 2.13a) by a specific value of UCS (corresponding to a η/Biv = 4), as shown by Eq. 16-18 (R^2 ranging from 0.90-0.94).

$$UCS/UCS_{\left(\eta/_{Biv}=4\right)\ 28days/23°C} = 29.86\times\left[\left(\eta/_{Biv}\right)\right]^{-2.45} \quad (16)$$

$$UCS/UCS_{\left(\eta/_{Biv}=4\right)\ 7days/60°C} = 26.85\times\left[\left(\eta/_{Biv}\right)\right]^{-2.45} \quad (17)$$

$$UCS/UCS_{\left(\eta/_{Biv}=4\right)\ 28days/60°C} = 29.75\times\left[\left(\eta/_{Biv}\right)\right]^{-2.45} \quad (18)$$

With basis on Equations 3-5 and 7-15, it becomes feasible to choose the best combination of porosity and binder content for a specific engineering design, without trial-and-error experiments for a soil-cement dosage. For example, according NBR 12253 (ABNT, 2012) the UCS of cemented soils should be at least 2.1 MPa for application in pavement layers; it is possible to insert the 2.1MPa value on the proposed equations and obtain a minimum η/Biv that fulfills the requirements of NBR 12253 (ABNT, 2012) for any of the analyzed mixtures. By using this minimum η/Biv value, the engineer can determine the best and most economic combination (varying porosity and binder content) for practical applications. In addition, the minimum strength value of any standard [e.g. American Association of State Highway and Transportation Officials (AASHTO), 2008; AUSTROADS, 2017; Portland Cement Association (PCA), 1992; United States Army Corps of Engineers (USACE), 1984] could also be inserted in the equations. Besides the clear applicability of the mixtures as a pavement layer according to NBR 12253 (ABNT, 2012), other applications can be foreseen, such as pipe bedding, slope protection, and facing for earth-fill dams (Pereira dos Santos *et al.*, 2022).

4. Conclusions

This study investigated the stabilization of RAP with a metakaolin-based binder alkali-activated by rice husk ash synthetized sodium silicate. In addition, a rational dosage methodology (porosity/binder index) was also investigated. Based on the findings of this study, the following conclusions can be disclosed:

a) Compaction results showed that the increase in RAP content leads to a linear decrease in dry unit weight for non-stabilized samples. However, the incorporation of the alkali-activated binder resulted in a more expressive increase in the dry unit weight of the samples with lower percentages of fine virgin aggregates, due to the better homogenization conditions.
b) The increase in AA content led to an increase in UCS for all mixtures. This was mainly attributed to two phenomena, decrease in porosity (increasing contact area between particles while providing greater friction mobilization) and increase in cementitious reactions in the mixtures.
c) High initial curing temperatures showed no significant difference when compared to room temperature curing. Subjecting specimens to higher curing temperatures tends to avoid the efflorescence phenomenon. However, this increase in temperature can also result in cracks that, in turn, hinder the mechanical behavior of specimens over time;
d) Microstructural analyzes of the stabilized mixtures depicted minerals rich in silica and alumina, indicating the formation of geopolymerization structures (N-A-S-H). Furthermore, it can be stated that the final product is the same regardless of the synthesis temperature, only with different the dissolution rates;
e) The porosity/binder index was shown to be a viable dosage method to predict the strength of RAP stabilized with a metakaolin-based binder alkali-activated by rice husk ash synthetized sodium silicate. The index allowed the unification of the mechanical behavior in a single relation, replacing trial and error conventional strategies that normally are laborious and time-consuming; Several equations were presented throughout this paper, notwithstanding it is important to consider that such equations are only functional if the boundary conditions are ensured.

3.3 Curing conditions effect on the stabilization of recycled asphalt pavement with alkali-activated metakaolin and rice husk ash-derived activator

Abstract

The stabilization of reclaimed asphalt pavement (RAP) with alkali-activated cement (AAC) is a topic of growing interest for sustainable engineering, especially those containing alternative activators produced from waste. This study evaluated the effect of curing temperature on the stabilization of RAP with a metakaolin AAC and rice husk ash-derived activator. Unconfined compressive strength (UCS), X-ray diffraction, and scanning electron microscopy tests were performed. Analysis of variance was applied to statistically investigate the impact of curing temperature, curing oven time, and curing time. Higher strength values were associated with higher temperatures and curing times. Curing oven time presented no influence over UCS and mineralogy. Blends cured at 20°C exhibited efflorescence formation and prolonged curing time at high temperatures negatively affected the mechanical performance. Curing temperature of 80°C up to 24h promoted the formation and uniform distribution of cementing gels and a dense and compact structure, improving the compressive strength.

Keywords: Reclaimed asphalt pavement; alkali-activated cement; alternative alkaline activator; strength development; mineralogy; microstructure.

1. Introduction

Natural aggregates are essential elements of pavement layers, composing up to 90% weight total of asphalt mixtures and 100% of unbound layers; pavement construction is currently associated with the utilization of millions of tons of these non-renewable materials (Pourkhorshidi et al., 2020; Radević et al., 2020). Thus, emerging environmental issues have led to the search for alternative materials that may decrease the impact of the infrastructure sector.

Recycled asphalt pavement (RAP) is a waste obtained in the rehabilitation of roads, constituted by aged bituminous aggregates and additives. RAP can be utilized as an alternative material for pavements base and subbase layers, reducing global costs of pavement sections up to 40% (Debbarma et al., 2019; Singh et al., 2018) while benefiting society in the optimization of natural sources and reduction of construction waste (Yang et al., 2020). Even though this material has been extensively utilized, the lack of adhesion between its grains (due to the presence of aged bitumen coating) needs to be compensated by using cementing agents (Cihlářová et al., 2018).

Portland cement (PC) has been widely applied as a stabilizing material in pavements design and reclamation (Fedrigo et al., 2020; Ma et al., 2016; Nemati & Uhlmeyer, 2021; Pasche et al., 2022). However, PC utilization is linked to high consumption of energy and non-renewable resources. For the production of one ton of cement, approximately one ton of carbon dioxide (CO_2) is emitted (Garcia-Lodeiro et al., 2015; Qin et al., 2018), which corresponds to 7-8% of global anthropogenic CO_2 emissions (Miller & Myers, 2020). Current methods of reducing the amount of embodied carbon in cement (e.g. partial replacements with fly ash, ground granulated blast furnace slag, condensed silica fume, limestone dust, cement kiln dust) are still limited. Nevertheless, promising alternatives are being developed to meet these environmental challenges.

Alkali-activated materials are swiftly turning into a sustainable alternative to PC (Miller & Myers, 2020). Alkali-activation consists in a chemical process that allows the transformation of vitreous structures (partially or totally amorphous and/or metastable) into cementing materials. This process occurs in a highly alkaline media through the use of an activator (e.g. sodium or potassium hydroxides and/or silicates) (Provis, 2018). As for the precursors (aluminosilicate source), several industrial by-products/waste can be incorporated, reducing the consumption of raw-materials for cement production. In this sense, a wide variety of materials can be utilized, such as ground blast furnace slag (Duży et al., 2022; Mavroulidou et al., 2021; Zhang et al., 2021), stone waste (Queiróz, Souza, et al., 2022), alternative limes (Queiróz, Miguel, et al., 2022; Queiróz, Souza, et al., 2022), sugarcane bagasse ash (Bruschi et al., 2022; Bruschi, dos Santos, et al., 2021; Bruschi, Santos, et al., 2021; Pereira dos Santos et al., 2022).

Even though alkali-activated materials may incorporate industrial waste, conventional activators are still linked to high carbon dioxide emissions (Mendes et al., 2021); considering that temperatures ranging from 1000-1400°C are still involved in their manufacturing process (Hervé Kouamo Tchakouté et al., 2016; Turner & Collins, 2013). For instance, sodium silicate depicts elevated energy and environmental impact, generating 1.514 kg CO_2 per produced kg of sodium silicate glass (Na2SiO3) (Turner & Collins, 2013) or 0.67 kg CO_2 eq/kg sodium silicate solution (Davidovits, 2018). In such a way, alternative silica sources for the synthetization of sodium silicate are emerging as an attractive choice (Alnahhal et al., 2021; Mendes et al., 2021). Rice husk ash (RHA) has the potential to become a competitive option for this synthetization process, as this material is majorly composed of silica in an amorphous state (Alnahhal et al., 2021; Consoli et al., 2019). Several studies have been carried out with RHA as a material in the development of activating solutions (S. A. Bernal et al., 2015; Bouzón

et al., 2014; Hervé K. Tchakouté et al., 2016; Villaquirán-Caicedo et al., 2017); results were shown to be similar to commercial silicates, both in terms of strength and microstructure.

As for paving applications, alkali-activated binders were already utilized as a stabilizing agent in combination with RAP (Adhikari et al., 2020; Al-Hdabi, 2016; Avirneni et al., 2016; Edeh et al., 2012; Horpibulsuk et al., 2017; Hoy et al., 2018; Jallu et al., 2020; Kang, Ge, et al., 2015; Kang, Kang, et al., 2015; Saride et al., 2016; Sukprasert et al., 2021; Syed et al., 2022; Tabyanga et al., 2021). However, the utilization of RAP alongside alternative activators for the alkali-activation process is still a research-gap, especially regarding temperature influence. The development of lower carbon emission activators is highly desirable and could lead to a significant reduction in the global warming potential of alkali-activated binders. Thus, the objective of this research was to stabilize RAP blends with a metakaolin-based binder, alkali-activated by rice husk ash synthetized sodium silicate, while evaluating the influence of curing temperature of the blends. To that extent, unconfined compressive strength, X-ray diffraction, and scanning electron microscopy tests were conducted. In addition, an analysis of variance was applied to investigate the statistical significance of curing temperature, curing oven time and curing time on the compressive strength of the blends.

2. Materials and Methods

2.1 Materials

Reclaimed asphalt pavement (RAP), stone powder (SP), gravel (G), metakaolin (MK), rice husk ash (RHA), and sodium hydroxide (NaOH) were utilized in this research. Materials physical characterization (Table 3.1 and Figure 3.1) was determined through grain size distribution (ASTM, 2017b) and specific weight of grains (ASTM, 2014) tests. In addition, bitumen content (ASTM, 2018) and specific gravity for coarse (ABNT, 2009b) and fine aggregate (ABNT, 2009a) tests were executed for RAP.

X-ray diffraction (XRD) technique was utilized to determine the mineralogical composition of RAP, MK, and RHA. The tests were performed in a Shimadzu X-ray diffractometer, model XRD-6000 (θ-2θ), operating at 40 kV and 30 mA in the primary beam and curved graphite monochromator in the secondary beam. The elemental composition was determined through X-ray fluorescence spectrometry (XRF) technique, through a quantitative analysis with a calibration curve based on tabulated patterns of a data library from Bruker. The scanning electron microscopy (SEM) analysis were performed in a scanning electron microscope, Zeiss brand, model EVO LS25, using secondary electrons (SE) with magnification of 228 times and electron beam of 10 kV voltage, and gold-coated samples (Quorum SC7620).

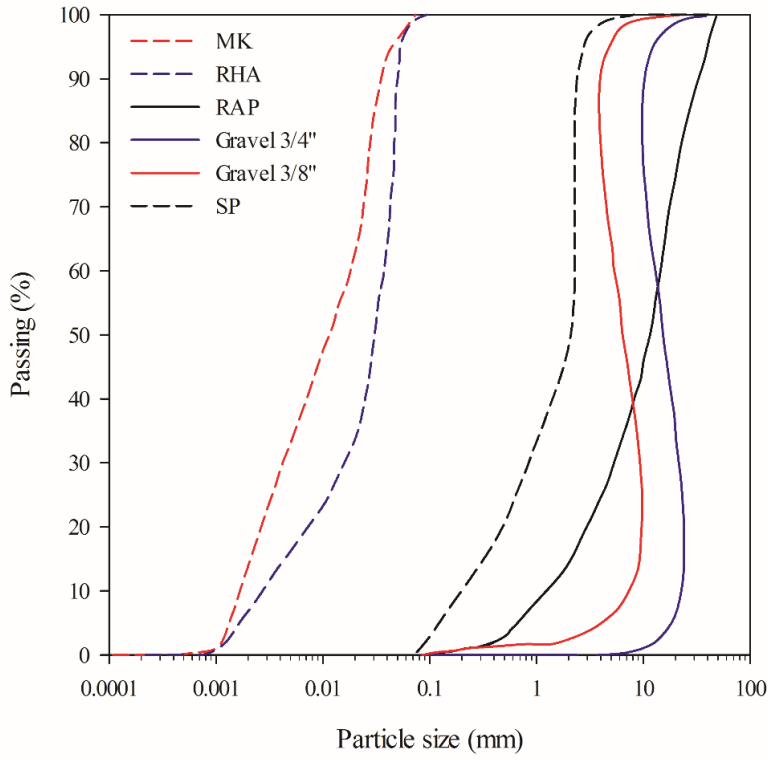

Figure 3.1. Materials grain size distribution.

As shown in Table 3.1, materials were classified following the Unified Soil Classification System (USCS) (ASTM, 2017a); with RAP being a well-graded gravel (GW), and MK and RHA a sand with fines (SW). RAP depicted a crystalline structure, mainly composed by potassium silicate ($K_6Si_3O_9$), quartz (SiO_2), bytownite ($(Ca,Na)(Si,Al)_4O_8$) and labradorite [$(Ca,Na)(Al,Si)_4O_8$]; both MK and RHA presented a semi-crystalline structure, with the first being composed by mica, berlinite ($AlPO_4$) and quartz (SiO_2), and the later by cristobalite (SiO_2) (Figure 3.2). Cristobalite is a polymorphic silica phase, obtained at temperatures up to 990°C, as the case of the RHA of this research. RAP and MK majorly consisted of silica and alumina, while RHA was mainly composed of silica (Table 3.2). Figure 3.3 depicts the morphology of RHA before and after processing; in its natural state, RHA presents a non-uniform particle size, while after processing (milling for 1 hour and sieving at 150 μm) particles present an irregular, porous and finer shape.

Table 3.1. Materials physical properties.

Property	RAP	MK	RHA	SP	Gravel 3/4''	Gravel 3/8"
Specific unit weight of grains (g/cm^3)	2.42	2.64	2.23	2.80	2.85	2.8
Bitumen content (%)	5.8	-	-	-	-	-
Gravel (4.75mm < diameter) (%)	72	0	0	0	100	94
Sand (0.06mm < diameter < 4.75mm) (%)	28	0	10	88	0	6
Silt (0.002mm < diameter < 0.06mm) (%)	0	86	82	22	0	0
Clay (diameter < 0.002mm) (%)	0	14	8	0	0	0
USCS classification	GW	SM	SM	SW	GP	GP

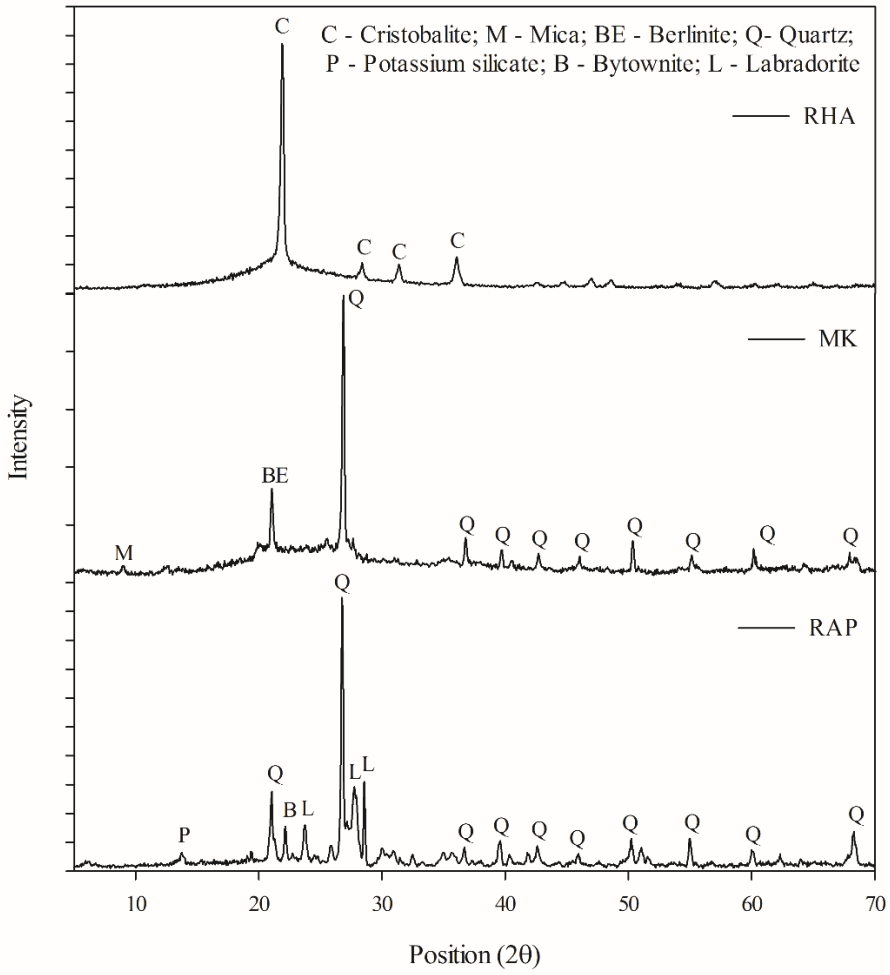

Figure 3.2. Mineralogical composition of RAP, MK and RHA.

Table 3.2. Materials chemical composition.

Oxides (%)	SiO_2	Al_2O_3	Fe_2O_3	CaO	MgO	SO_2	Na_2O	K_2O	P_2O_5	TiO_2	ZnO
RAP	64.39	14.65	1.16	4.10	<0.10	7.68	-	5.55	1.65	<0.10	<0.10
MK	54.72	40.80	1.80	0.10	0.10	-	0.18	0.21	-	2.09	-
RHA	89.33	0.62	1.53	3.84	2.51	-	-	2.18	-	-	-

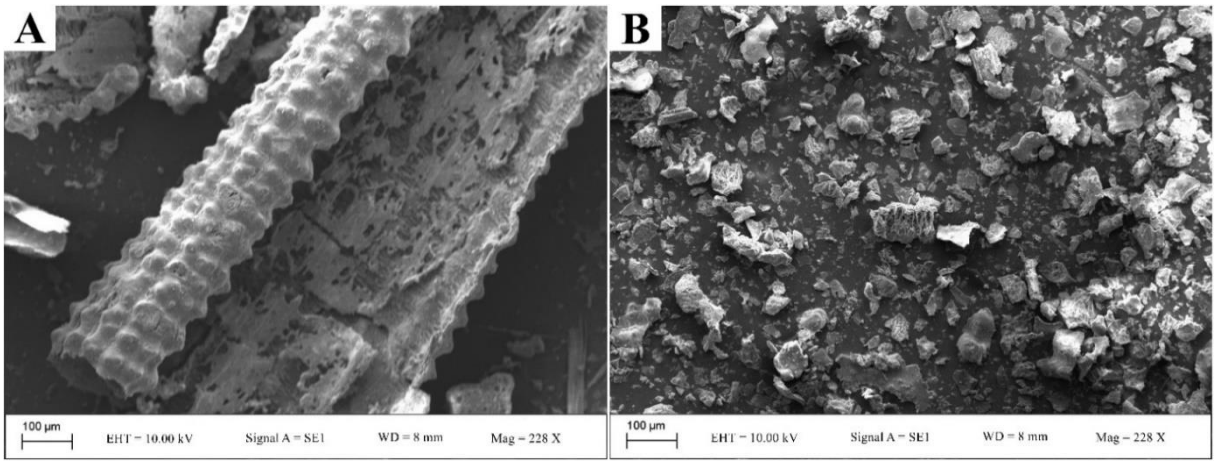

Figure 3.3. RHA morphology (a) in natura and (b) after processing.

2.2 Alkali-activated cement

The alternative alkaline activator was produced through the dissolution of RHA in 10M sodium hydroxide solution (maintaining $SiO_2/Al_2O_3 = 4$), in a thermostatic bath at 80°C for 12h (Susan A. Bernal et al., 2012; Davidovits, 1989). After the dissolution time and upon reaching room temperature (25°C), the solution was then mixed with the solid precursor (MK) and later with the rest of the materials.

2.3 Molding and curing procedures

Virgin aggregates (stone powder and gravel) were added to RAP in order to correct particle size limits for pavement applications, as indicated in WIRTGEN technical manual (Wirtgen GmbH, 2012); Table 3.3 shows the proportions of the non-cemented specimens.

Table 3.3. Proportions of the non-cemented compositions (%).

Reclaimed asphalt pavement content	Stone powder content	Gravel 3/4'' content	Gravel 3/8'' content
40	40	10	10

For the study of the influence of the alkali-activated cement, mixtures from Table 3.3 were stabilized by adding 30% of alkali-activated cement (AAC). Proctor test was performed for RAP-AAC (recycled asphalt pavement-alkali-activated cement) blends following standard D698 methodology (ASTM, 2021).

Cylindrical specimens of 100mm in diameter and 127.3mm in height were utilized for the strength tests. The molding procedure started by the mixing of the air-dried materials (RAP, virgin aggregates and metakaolin) with the liquid alkaline activator (prepared by dissolving the RHA in a solution of sodium hydroxide) and water until homogenization is achieved. Then, RAP-AAC specimens are molded at the optimum moisture content (5.6%) and maximum dry unit weight (22.8 $kN.m^3$) from the compaction curve (Figure 3.4). Curing procedures were conducted as follows: initially specimens were cured for 24 or 48 hours at different temperatures (20, 60, 40, 80°C), in oven, and then maintained at room temperature (25°C) for the rest of the curing period (7 and 28 days). Specimens were considered suitable for testing if the following criteria was met: degree of compaction between 99% and 101%; water content within 0.5% of the target value; diameter within 0.5 mm of the target value; and height within 1 mm of the target value.

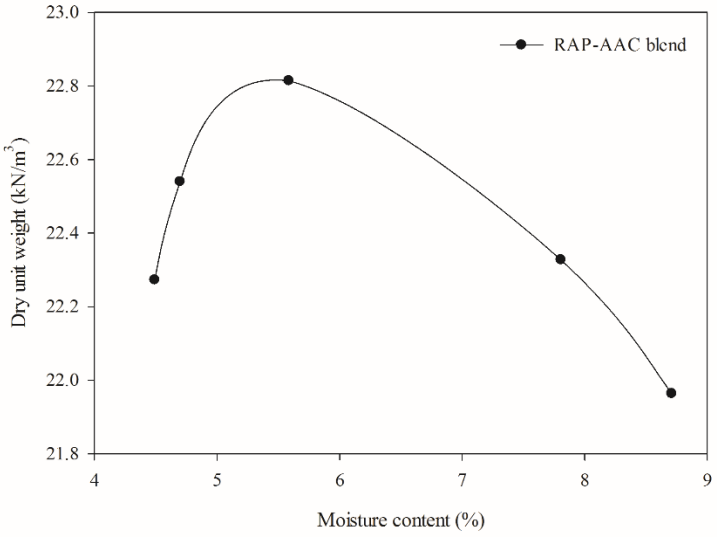

Figure 3.4. Compaction curve of RAP-AAC blend.

2.4 Experimental design

A three factors full factorial design with duplicates, resulting in 32 experiments, was used throughout this research. Analyzed controlled factors were: curing temperature (A); curing oven time (B) and curing time (C). Unconfined compressive strength (UCS) was the response variable. Factors and their respective levels can be seen in Table 3.4. Analysis of variance (ANOVA) was used to determine the statistical significance of controlled factors over the mechanical response.

Table 3.4. Controlled factors and levels of the experimental design.

Factors	Unit	Symbol	Levels			
			1	2	3	4
Curing temperature	°C	A	20	40	60	80
Curing oven time	hours	B	24	48	-	-
Curing time	days	C	7	28	-	-

2.5 Unconfined compressive strength

Unconfined compressive strength (UCS) tests were executed in accordance with ASTM D2166 (ASTM, 2016), using an automatic loading machine, with a maximum load capacity of 50kN. The rate of displacement adopted was 1.14mm per minute, to produce an axial strain at a rate between 0.5%/min and 2%/min, as recommended by ASTM D2166 (ASTM, 2016).

2.6 Mineralogical and microstructural analysis

The mineralogical composition and microstructure of the RAP-AA blends cured for 28 days were evaluated by XRD and SEM techniques, respectively. XRD analysis were carried out in

a Shimadzu X-ray diffractometer, model XRD-6000 (θ-2θ) (40 kV, 30 mA, in the primary beam and curved graphite monochromator in the secondary beam, and COD database). The SEM analysis were performed in a scanning electron microscope, Zeiss brand, model EVO LS25, using secondary electrons (SE) with magnification of 2500 times, electron beam of 10 kV voltage, and gold-coated samples (Quorum SC7620).

3 Results and discussions

3.1 Unconfined compressive strength

Figure 5 presents the unconfined compressive strength (UCS) results for the RAP-AAC blends at temperatures of 20, 40, 60, and 80°C for 24 and 48h (in oven) and cured at room temperature for 7 and 28 days. The increase in curing temperature, curing time and oven time led to RAP-AAC blends with higher strength (Figure 3.5). The blend cured at 80°C for 24h after 7 days showed a 27% increase in strength compared to the blend cured at 20°C in the same period (from 2.2 to 2.8 MPa); this increment was approximately 124% (from 2.1 to 4.7 MPa) after 28 days. The high temperature (especially 80°C) acted as a catalyzer for geopolymerization reactions (dissolution, polymerization and reprecipitation), accelerating the formation of cementitious products and contributing to the increase in strength of the RAP-AAC. Similarly, other studies verified that 80°C is the optimum curing temperature for ashes-based geopolymers and copper tailing-based geopolymers, respectively (Nazari et al., 2011; Tian et al., 2020).

As expected, a longer curing period improved the polymerization process and enabled the formation of a hard and denser structure, resulting in higher UCS for all blends. RAP-AAC blends cured at higher temperatures showed higher strength than those cured at lower temperatures for the same curing period. Nevertheless, the highest strength achieved (4.7 MPa) corresponds to the blend cured for 24h at 80°C, 28 days. Prolonged curing periods at high temperatures (i.e. 80°C for 48h) can cause the contraction of the cementitious gel, resulting in dehydration and excessive shrinkage of the blend and consequently reduced strength (Nazari et al., 2011).

The UCS of RAP-AAC blends cured at 40 and 60°C, were mostly higher than those cured at 20°C. This behavior occurs due to the moderately high temperatures (40 and 60°C) promoting sufficient geopolymer gel formation to bind metakaolin particles in the early-age of geopolymerization (Mo et al., 2014). In general, curing temperatures from 30°C to 90°C increase the compressive strength of geopolymers; curing at 70°C improved the mechanical response compared to 30°C for the same curing periods (Khale & Chaudhary, 2007). RAP-

AAC blends cured at 60°C exhibit higher strength than those treated at 40°C for both curing periods (7 and 28 days), which corroborates the temperature increase effect described in the abovementioned study. Besides, blends cured at temperatures of 40 and 60°C presented no significant difference in strength compared to the periods of 24 and 48h.

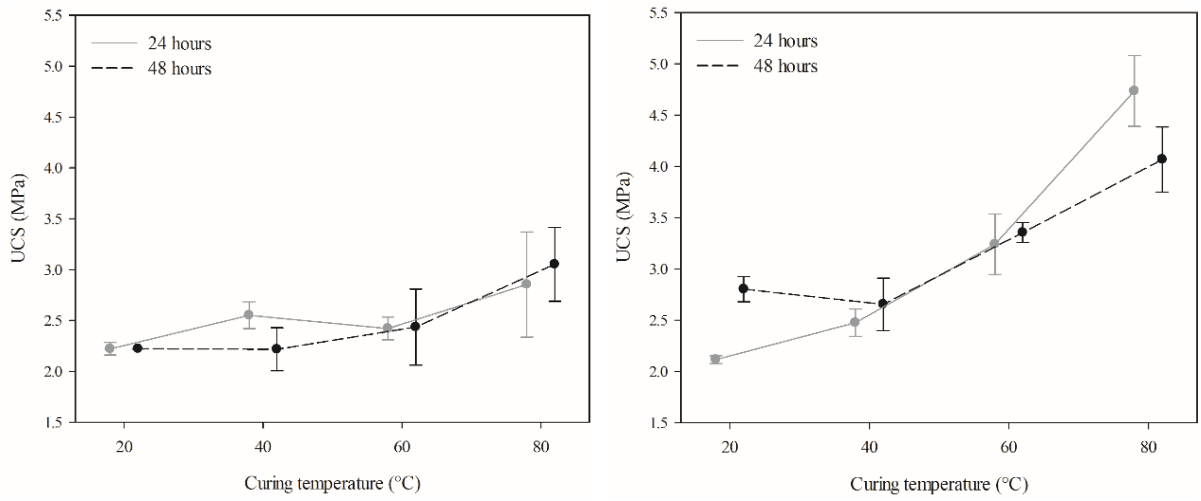

(a) (b)

Figure 3.5. UCS of RAP-AAC blends cured at 20, 40, 60 e 80 °C for 24 and 48h (a) at 7 days (b) and 28 days.

At lower curing temperatures (20°C), the dissolution of amorphous aluminosilicates from metakaolin and the formation of cementitious gels is slow, which explains their inferior mechanical performance. Similar behavior was identified in metakaolin-based geopolymer cured at different temperatures (20-100°C) (Mo et al., 2014). Also, RAP-AAC blends after oven periods of 24 and 48h at 20°C exhibited efflorescence formation. The crystalline deposit of salts (Figure 3.6) consists of sodium carbonate from the reaction between residual excess alkaline solution in the RAP-AAC (due to low dissolution rates) and the carbon dioxide of the atmosphere, when the blends were exposed to humid air. This pathological manifestation was also observed in several geopolymers cured at 20-25°C (Allahverdi et al., 2010; Temuujin et al., 2009; Xie & Ozbakkaloglu, 2015; S. Zhou et al., 2020).

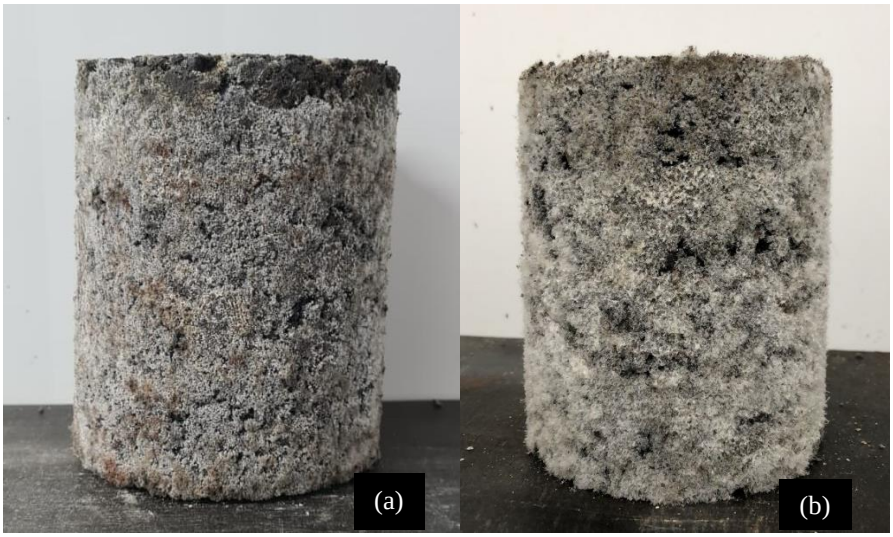

Figure 3.6. Efflorescence in RAP-AAC blends cured at 20°C (in oven) for (a) 24 and (b) 48h.

There is a higher tendency toward efflorescence formation in alkali-activated materials with a high concentration of sodium-based activator (Allahverdi et al., 2015). Efflorescence can be controlled by different methods such as addition of alumina-rich admixtures, hydrothermal curing (Najafi Kani et al., 2012); silane surface treatment (Xue et al., 2018), and decreasing Na_2O/Al_2O_3 molar ratio (Simão et al., 2021). In this study, efflorescence formation in RAP-AAC blends was controlled by accelerating the dissolution rates on curing at higher temperatures (40, 60, and 80°C) (Figure 3.7).

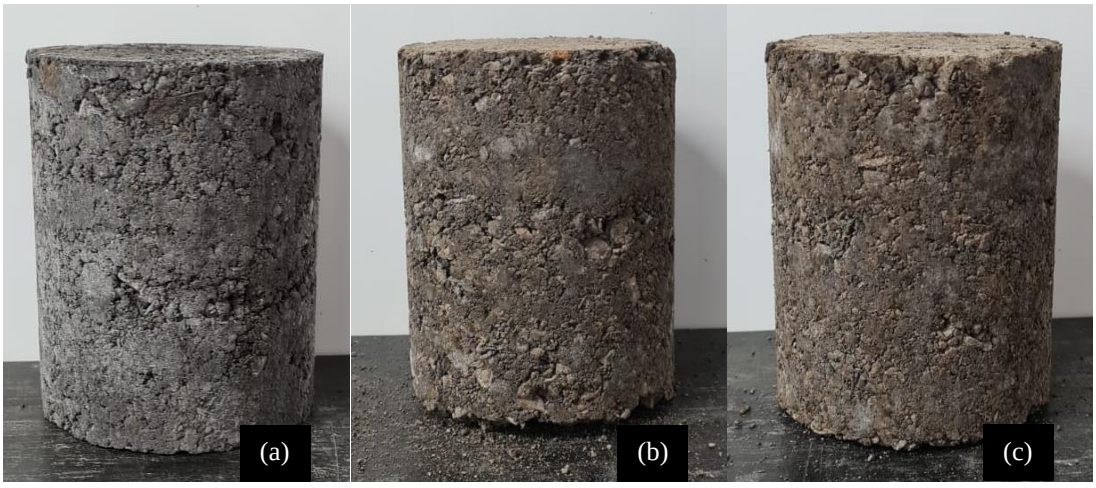

Figure 3.7. RAP-AAC blends cured for 48h (in oven) at (a) 40°C, (b) 60°C and (c) 80°C: no visible efflorescence.

Finally, all RAP-AAC blends presented the minimum strength (i.e. 2.1 MPa after 7 days) for utilization as road construction materials (base and sub-base), according to the requirements of the National Department of Infrastructure and Transport of Brazil (DNIT,

2010). In addition, depending on the local climate, RAP-AAC blends at higher temperatures can be applied in practice, without the need for a large amount of energy. For example, in hottest months in Rio Grande do Sul (Brazil), RAP-AAC can be applied at 40°C as this is the maximum average temperature in the state (SEPLAG, 2021).

The abovementioned mechanical behavior corroborates the statistical results; that show the significantly positive effect of two controlled factors on the UCS response. The Pareto chart (Figure 3.8) shows that both factors significantly affected the blends strength, from the highest to the lowest magnitude: curing temperature and curing time. Curing oven time presented no significant influence on UCS. Curing temperature governs fly ash-based geopolymer strength as compared to other factors (alkaline-activator concentration and curing time) (Sajan et al., 2021). The interaction between curing temperature and curing time presented a significant influence on UCS; with that in mind, the designer can choose between producing RAP-AAC blends at higher temperatures for shorter curing times, or at lower temperatures for longer curing periods. Although three-factor interaction effect was significant, it presents no practical interest as its prediction is complex due to variability caused by uncontrollable factors in the field. Also, the two significant factors (curing temperature and curing time) influenced the mechanical behavior in a positive way, i.e., the increase in the level of the factor resulted in an increase in strength, as shown in Figure 3.9.

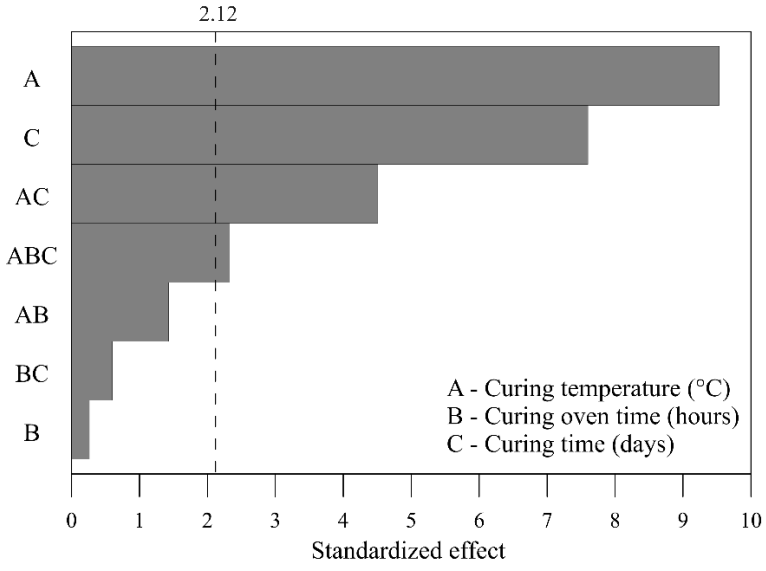

Figure 3.8. Pareto chart of UCS for RAP-AAC blends.

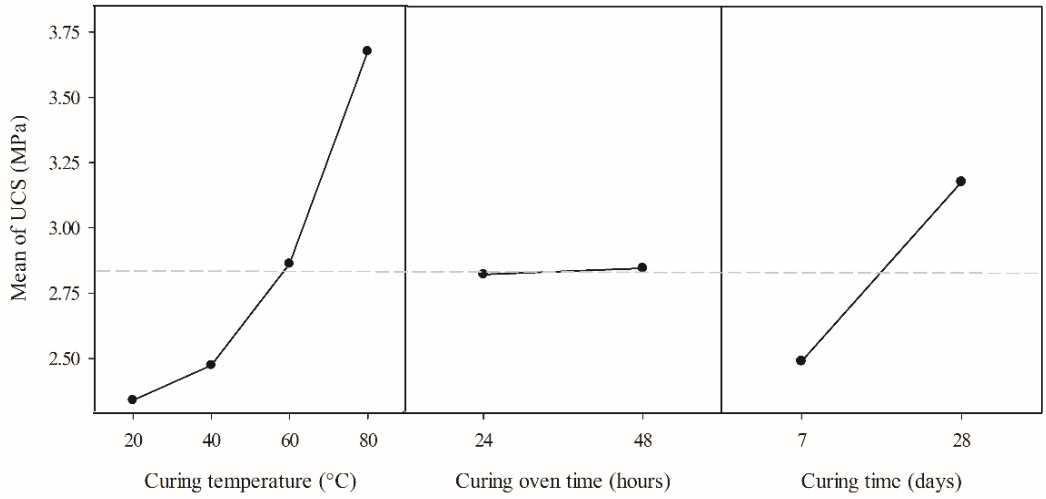

Figure 3.9. Main effects plot (factors).

3.2 Mineralogy and microstructure

Figure 3.10 shows the diffractograms of the RAP-AAC blends at different temperatures (20, 40, 60 and 80°C) for 24 and 48h (in an oven) and cured at room temperature for 28 days. All samples share the presence of quartz, labradorite, diopside and amorphous phases. Quartz (SiO_2) and labradorite ($(Ca,Na)(Al,Si)_4O_8$) are minerals from the precursor (metakaolin) and stabilized material (RAP) respectively. Some blends presented bytownite ($(Ca,Na)(Al,Si)_4O_8$) and berlinite ($AlPO_4$), which are minerals from RAP and metakaolin. Diopside ($CaMgSi_2O$), a calcium-based aluminosilicate, was produced from the chemical reactions between metakaolin, ash and CaO (oxide present in RAP and RHA). Berlinite, a mineral characteristic of metakaolin, was identified in only one of the RAP-AAC blends. Finally, fervanite ($Fe^{3+}4V^{5+}4O16{\cdot}5H_2O$) was found in one of the blends, possibly originated from RAP as petroleum asphalt cement (PAC) contains chemical elements such as iron and vanadium. The punctual observations mentioned above and the different degrees of crystallinity of quartz in the diffractograms suggest great heterogeneity of the asphalt waste, as shown by several authors (W. Ferreira et al., 2022; W. L. G. Ferreira et al., 2021; Lo Presti et al., 2020; Vislavičius & Sivilevičius, 2013).

The curing temperature effect on the cementitious products formation is mainly noted by the different amorphous phases in the XRD pattern of RAP-AAC cured at 20°C and RAP-AAC cured at 80°C, as seen in Figure 3.10.

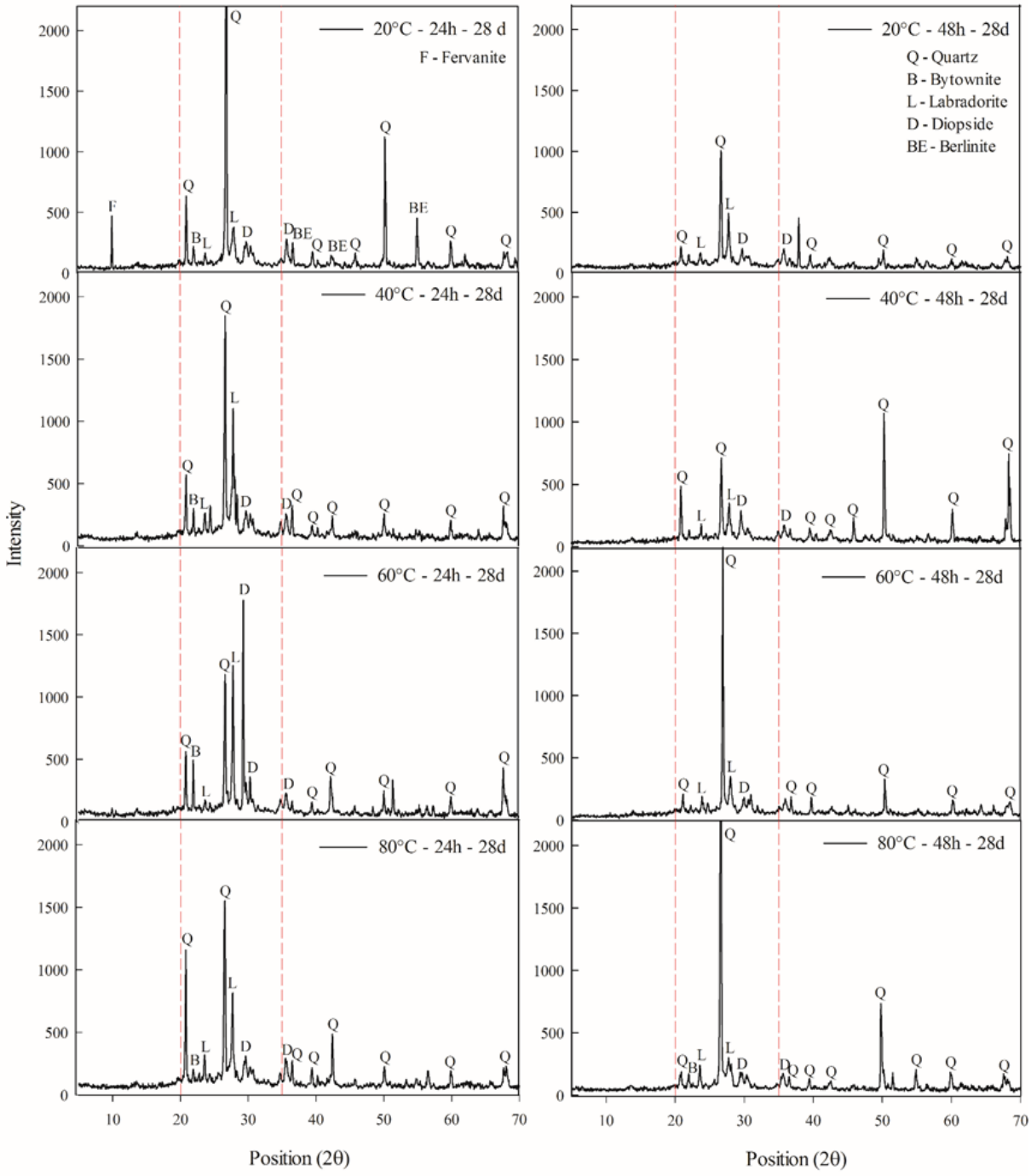

Figure 3.10. XRD patterns for RAP-AAC cured at different temperatures (20, 40, 60 and 80°C) for 24 and 48h.

XRD results show that increasing the curing time from 24h to 48h presented no effect on the mineralogical composition of the RAP-AAC blends. Considering that the precipitates from a low-calcium system present an amorphous halo at 2θ of 20-35° (Garcia-Lodeiro et al., 2011), it is possible to identify the presence of N-A-S-H gel (hydrated sodium aluminosilicate) in amorphous phases within the characteristic angular range (i.e. 20-35°) in the RAP-AAC blends. In addition, due to amorphous properties of C-A-S-H gel (hydrated calcium

aluminosilicate), the phases form broad diffraction peaks at 2θ of 28-30° and 34-35° (H. Zhou et al., 2021). A small amount of CaO from metakaolin participates in the reactions to form the C-A-S-H gel (Dai et al., 2022; H. Zhou et al., 2021), which appears as "featureless peaks" (28-30° and 34-35°) in the RAP-AAC blends. The N-A-S-H and C-A-S-H gels formed from geopolymeric reactions fill the voids of the RAP-AAC structures, resulting in improved mechanical behavior of the material.

XRD analysis provided qualitative information about the cementitious products developed in the RAP-AAC systems. SEM images of RAP-AAC blends were examined to support the mineralogical results. Figure 3.11 presents SEM images of the RAP-AAC cured at different temperatures for 24 and 48h. In general, blends cured at higher temperatures presented denser and more homogeneous structures, indicating a higher degree of geopolymerization than lower temperatures ones. RAP-AAC blends cured at 20°C were characterized by a more heterogeneous structure with loose particles and many voids (interpreted as black areas) (Figure 3.11-a,b), making them more susceptible to early-failure in the UCS test. Also, the presence of crystals corresponding to the efflorescence formation is evidenced. These characteristics are due to the incomplete dissolution of aluminossilicates in the matrices at lower curing temperature.

The blends cured at 40°C present a relatively more homogeneous structure with fewer voids (Figure 3.11-c,d) than those exposed to 20°C, corroborating the reported improvement in strength. RAP-AAC cured at 40°C for 48h (Figure 3.11-d) presented an irregular surface with a gap, due to the RAP heterogeneity and insufficient gel formation to fill these voids. In general, blends cured at 60°C resulted in a denser structure (Figure 3.11-e) than blends exposed to lower temperatures (20 and 40°C), positively impacting the mechanical response (Figure 3.5). In all SEM images of Figure 3.11, clusters of different sizes and shapes were observed; these clusters are normally encountered in RAP (Ferreira et al., 2021a) and RAP-AAC blends. Furthermore, cementing gels can be inside the RAP-AAC matrices and in the surface of RAP clusters (interpreted as lighter areas). The blends cured at 60°C for 48h showed microcracks in the surface (Figure 3.11-f); however, these cracks resulted in no detrimental effect in the strength of the material. The gap and microcracks observed in the blends cured at 40°C-48h and 60°C-48h explain the lower strength gains compared to the blends cured at the same temperatures for 24h (as seen in Figure 3.5).

RAP-AAC cured at 80°C for 24h exhibited a highly homogeneous, dense and compact structure (Figure 3.11-g), confirming the reported UCS. A heterogeneous structure alongside

cracks in the surface were observed in RAP-AAC exposed at 80°C for 48h (Figure 3.11-h). These cracks form from the breakage of the gels structures due to the excessive curing temperature, resulting in dehydration and shrinkage of the blend and strength reduction. This behavior was also reported on copper tailings-based geopolymers cured at temperatures above 80°C (Tian et al., 2020). In the study, prolonged curing time at high temperatures (i.e. 80°C for 48h) affected gels formation and mechanical performance. Curing at higher temperature (80°C) up to 24h promotes the formation and uniform distribution of gels, filling the matrix voids and improving compressive strength of the RAP-AAC.

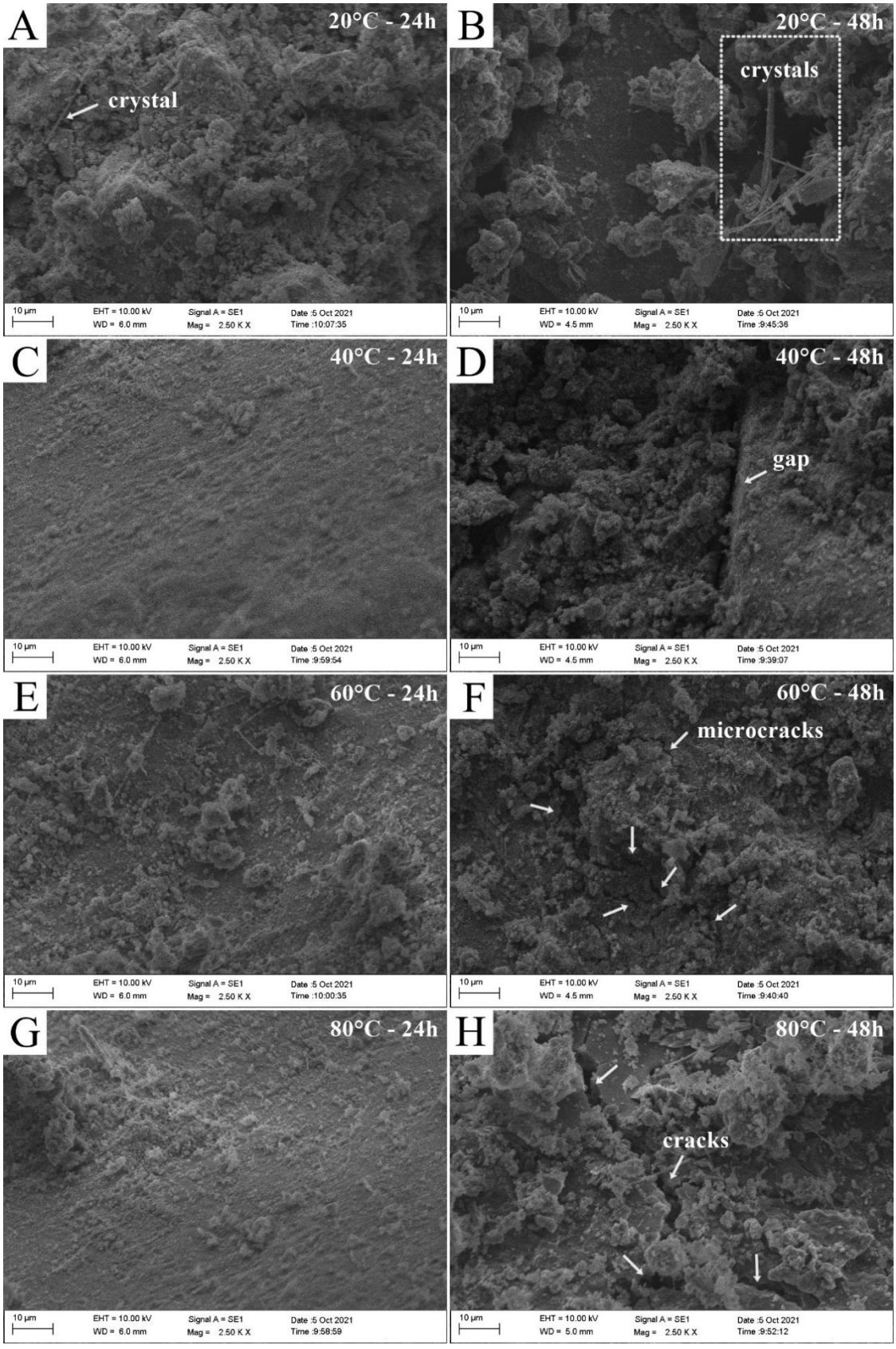

Figure 3.11. SEM images of RAP-AAC blends cured at (a) 20°C-24h, (b) 20°C-48h, (c) 40°C-24h, (d) 40°C-48h, (e) 60°C-24h, (f) 60°C-48h, (g) 80°C-24h and (h) 80°C-48h.

Although all RAP-AAC blends presented satisfactory UCS for application in pavement bases and sub-bases, their macro and microstructures should be considered. Blends cured at 20°C developed fluorescence that could affect the long-term behavior of the material. RAP-AAC exposed to high temperature for a long period of time resulted in cracks and lower strength values; while improved results were obtained for shorter exposure time at 80°C. Therefore, it is important to focus on curing temperature combined with curing time to produce RAP-AAC blends with general microstructure and compressive strength that can meet pavement design requirements.

4 Conclusions

Based on the findings of this study, the following conclusions can be drawn:

- In general, RAP-ACC blends cured at higher temperatures and curing periods resulted in better mechanical behavior with denser structures;
- Low curing temperature (20°C) in the first 24 to 48h is not recommended as it negatively affected the dissolution rates of aluminosilicates and consequently the strength of RAP-AAC;
- Curing temperature was the factor that governed the compressive strength of RAP-AAC blends, followed by curing time. Curing oven time presented no statistical influence on UCS;
- Curing oven time resulted in no mineralogical changes. Also, curing temperature and curing time conditions were responsible for the development of cementing gels, microstructure, and UCS;
- XRD results depicted the presence of amorphous phases within the characteristic angular ranges of N-A-S-H and C-A-S-H gels, indicating the viability of the proposed alkali-activated process;
- Higher curing temperatures promoted the formation of more homogeneous and denser structures due to the filling of voids by the cementing gels from the alkali-activation process;
- Prolonged curing periods at high temperatures (i.e. 80°C for 48h) negatively affected the formation and distribution of cementitious gels, as well as the structure and mechanical response of the material. Curing RAP-AAC at 80°C for up to 24h is recommended to obtain a dense and compact structure, with higher compressive strength.

3.4 Durability, long-term and environmental evaluation of alkali-activated alternative soluble silica source for recycled asphalt pavement stabilization

Abstract

The preservation of natural resources has been gaining considerable space in recent decades, encouraging the use of industrial and civil construction waste. In this work, the recycled asphalt pavement (RAP), from the milling of the pavements, was used to replace virgin aggregates for the construction of road base layers. Due to the large amounts of materials involved in road construction, it is necessary to develop alternative binders. Particularly when it comes to alkali-activated materials, the use of residues in the production of sodium silicate has not yet been investigated for RAP stabilization for the stabilization of RAP. Therefore, in this study rice husk ash (RHA) was activated in an alkaline environment, playing the role of an alternative source of silica, for the formation of an alkali-activated binder (AAB). The exposure of these mixtures to seasonal variations in humidity and temperature was evaluated through durability tests from wet/dry cycles and the unconfined compressive strength (UCS) retained in the samples after the cycles. AAB permanence was also verified through long-term mechanical performance and its environmental impact through leaching tests. The results indicated that mixtures with RAP:AAB ratio = 40:40, 50:30, and 50:40 reached the minimum design strength (2.1 MPa) even after wet/dry cycles, however the mixture with RAP:AAB = 40:40 ratio is potentially superior for better performance in field conditions, possibly without premature failure. In addition, this mixture has no environmental impact as the results of environmental tests do not show any significant risk or hazardous characteristics.

Keywords: Recycled asphalt pavement; alkali-activated binder; alternative silica source; durability; longevity; environmental impact.

1 Introduction

Concerning about traffic loads over pavement structures, it is common to observe a progressive deterioration, which demands continuous maintenance operations. These activities are normally focused on repairing rut, potholes and cracked areas and frequently results a reasonable amount of waste materials. In that regard, during the road rehabilitation process, a residue, composed mainly of aged bituminous aggregates and additives (Hoy et al. 2016a), named Recycled Asphalt Pavement (RAP) is generated (Rahman et al. 2014). In order to reduce

the cost of the base and subbase layers of pavements, RAP can be introduced to replace virgin aggregates (Debbarma et al. 2019; Singh et al. 2018), also providing a reduction in the environmental impacts caused by the construction of highways (Costa et al. 2020).

The RAP mechanical performance has already been studied by several authors, with or without stabilizing agents (Arulrajah et al. 2015; Consoli et al. 2018b; Grilli et al. 2018; Pasche et al. 2018). In the same way, several studies have addressed its influence on the durability performance of mortars and concretes (Abraham and Ransinchung 2019, 2018; Singh et al. 2017) or when reapplied to pavements (Mullapudi et al. 2020; Saride and Jallu 2020; Singh and R.N. 2020). Despite already being used for several applications, RAP still presents an application problem that is related to the presence of a binder that reduces the contact between the grains and induces the use of cementing materials to compensate for the loss of adhesion.

Several studies suggest that RAP stabilized with lime or cement can be successfully adopted in the base layers of flexible pavements (Arulrajah et al. 2013; Puppala et al. 2011; Saride et al. 2010). However, between 2005 and 2017, global cement production grew by more than 77%, and this growth is a global trend (de Oliveira et al. 2022). In Brazil, cement production increased from 39.4 million tons in 2001 to 88.5 million tons in 2017, making it the fifth largest in the world (de Lorena Diniz Chaves et al. 2021). In that regard, new cementitious materials, with a more sustainable footprint, are necessary to sustain a less aggressive development. Currently, alkali-activated materials (AAM) are considered a viable alternative for obtaining construction materials and adding value to waste, as they reuse by-products and industrial waste, which in most cases do not have an environmentally suitable destination (Tayeh et al. 2021). Alkaline activation can be defined as the chemical reaction between an amorphous/semicrystalline aluminosilicate source and an activator, generating cementitious structures similar to those found in OPC. Several residues from industry and agriculture can be used as a source of aluminosilicate such as: fly ash (Phoo-ngernkham et al. 2015; Zhuang et al. 2016), blast furnace slag (Awoyera and Adesina 2019), water treatment sludge (Geraldo et al. 2017), sugarcane bagasse ash (Bruschi et al. 2021a; b; Pereira dos Santos et al. 2022), carbide lime (Bruschi et al. 2022; Queiróz et al. 2022), eggshell lime (Consoli et al. 2021b; Tonini de Araújo et al. 2021) and rice husk ash (Bernal et al. 2012; Tong et al. 2018). Metakaolin is one of the most used precursors, due to its high rate of dissolution in alkaline medium and the simplicity in terms of controlling the SiO_2/Al_2O_3 ratio, in addition to the fact that alkali activation with metakaolin is seen as a model system, not involving the complexity of industrial by-products, which may vary depending on how they are obtained and possible contamination.

As for activators, the most common include sodium or potassium hydroxides and/or silicates, while aluminosilicates can include suitable raw materials and by-products/waste produced from various industrial processes (Torres-Carrasco et al. 2014).

Although alkali-activated binders (AAB) have reduced CO_2 emissions when compared to OPC, there is still a point that makes the practical application of these materials unfeasible: the high temperatures used in the production of alkaline activators also generate significant CO_2 emissions into the atmosphere. (Villaquirán-Caicedo et al. 2017). Some studies indicate that the production of 1 kg of sodium silicate can generate an emission of 1.5 kg of CO_2 into the atmosphere (Tchakouté et al. 2016). Therefore, the importance of developing sodium silicates using alternative sources of silica is highlighted. In this context, rice husk ash (RHA) is an interesting alternative due to its high silica content (Consoli et al. 2019). The literature reports good results in terms of strength and microstructure for activators developed with RHA as a silica source, even showing similar performance to commercially available silicates (Bernal et al. 2015; Bouzón et al. 2014; Tchakouté et al. 2016; Villaquirán-Caicedo et al. 2017).

AAB already have application in the paving area for RAP stabilization purposes (Adhikari et al. 2020; Al-Hdabi 2016; Avirneni et al. 2016; Edeh et al. 2012; Hoy et al. 2016b, 2018; Jallu et al. 2020; Kang et al. 2015; Saride et al. 2016; Sukprasert et al. 2021; Syed et al. 2022; Tabyanga et al. 2021). However, all works reported in the literature make use of commercial activators, suggesting a research gap that encompasses the use of alternative alkaline activators. In addition, the long-term behavior and efficiency of any stabilization/activation technique must be evaluated, as it may happen that the luting agent leaks or disappears during the service period. This is possible when rainwater infiltration occurs or when reactions change due to variations in temperature and humidity (Avirneni et al. 2016). In that regard, durability assessment is a definite prerequisite before adopting any stabilization or field activation technique.

In order to reduce greenhouse gas emissions due to the production of activators, activators with reduced environmental impact are desired. Thus, the objective of this research was to evaluate the use of RHA for the development of an alternative binder produced for RAP stabilization. Durability tests were performed through the evaluation of mass loss through wetting/drying cycles and after the cycles the residual unconfined compressive strength (UCS) was also evaluated. The sustenance and permanence of the cement in the mixtures were studied using the long-term UCS at curing periods of 7, 28, 56, 112 and 224 days. Potential risks to the environment and public health were also estimated through leaching tests. This study aims to

assist in the promotion of an innovative and sustainable system using RAP stabilized with a metakaolin-based binder, alkaline activated by sodium silicate synthesized with RHA in the construction of pavement without premature failures.

2 Materials and methods

2.1 Materials

For the development of this research, RAP, stone powder (SP) and gravel (G) were used as aggregates, metakaolin (MK) as precursor and a solution from the dissolution of rice husk ash (RHA) in sodium hydroxide (NaOH) as activator. The RAP was collected on a highway in Rio Grande do Sul - Brazil, while the RHA was supplied by an industry in the same state.

For the characterization of the materials, granulometric distribution tests were carried out (NBR 7181) (ABNT 2016) (ASTM 2017a), RAP bitumen content (NBR 16208) (ABNT 2013), specific weight of coarse aggregate (NBR NM 53) (ABNT 2009a) were carried out for the characterization of the materials. and fine aggregate (NBR NM 52) (ABNT 2009b) (Figure 4.1 and Table 4.1).

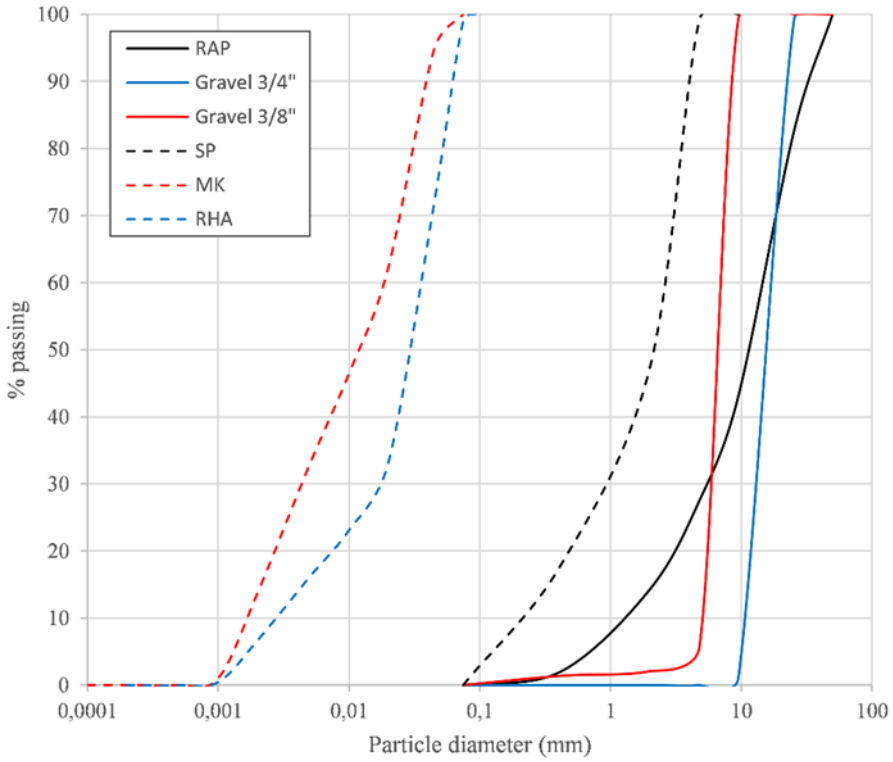

Figure 4.1. Materials grain size distribution.

Table 4.1. Materials physical properties.

Property	RAP	MK	RHA	SP	Gravel 3/4''	Gravel 3/8"
Specific unit weight of grains (g/cm^3)	2.42	2.64	2.23	2.80	2.85	2.8
Bitumen content (%)	5.8	-	-	-	-	-
Gravel (4.75mm < diameter) (%)	72	0	0	0	100	94
Sand (0.06mm < diameter < 4.75mm) (%)	28	0	10	88	0	6
Silt (0.002mm < diameter < 0.06mm) (%)	0	86	82	22	0	0
Clay (diameter < 0.002mm) (%)	0	14	8	0	0	0
USCS classification	GW	SM	SM	SW	GP	GP

X-ray diffraction (XRD) tests were carried out to determine the mineralogical composition of the materials (Figure 4.2). A Shimadzu X-ray diffractometer, model XRD-6000 (θ-2θ), operating at 40 kV and 30 mA in the primary beam and curved graphite monochromator in the secondary beam was used. For the determination of the elemental composition, X-ray fluorescence spectrometry (XRF) was used through a quantitative analysis with a calibration curve based on tabulated patterns from a data library of the Bruker ® equipment (Table 4.2). The microstructural characteristics of the materials were determined by scanning electron microscopy (SEM) analysis (4,000 times magnification). Finally, the RHA was evaluated according to its environmental classification according to the norms NBR 10004 (ABNT 2004a), NBR 10005 (ABNT 2004b) and NBR 10006 (ABNT 2009c) and the results of leached and solubilized extracts indicated that RHA is classified as Class II A – Non-Hazardous Non-Inert.

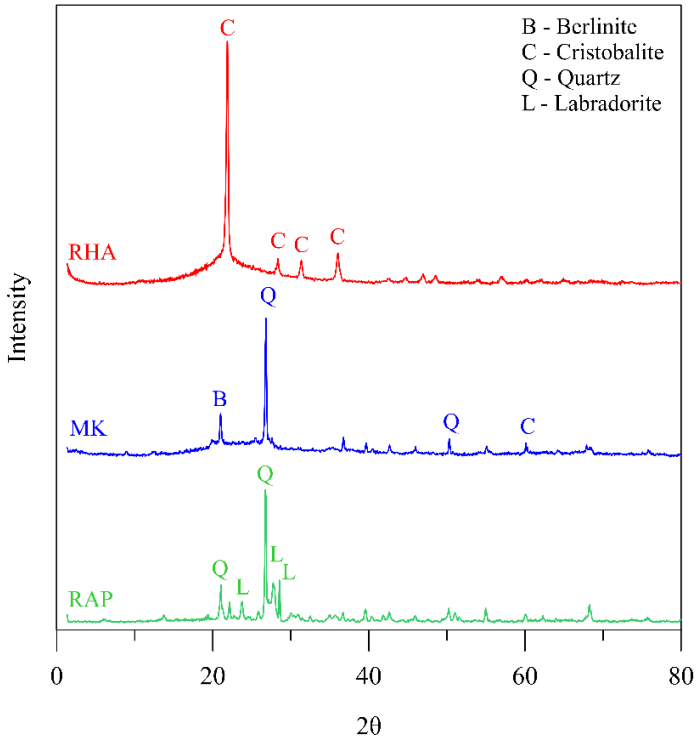

Figure 4.2. Mineralogical composition of RAP, MK and RHA.

Table 2.2. Materials chemical composition.

	SiO_2 (%)	Al_2O_3 (%)	Fe_2O_3 (%)	CaO (%)	MgO (%)	SO_2 (%)	Na_2O (%)	K_2O (%)	P_2O_5 (%)	TiO_2 (%)	ZnO (%)
RAP	64.39	14.65	1.16	4.10	<0.10	7.68	-	5.55	1.65	<0.10	<0.10
MK	54.72	40.80	1.80	0.10	0.10	-	0.18	0.21	-	2.09	-
RHA	89.33	0.62	1.53	3.84	2.51	-	-	2.18	-	-	-

According to the granulometric distribution, through the Unified Soil Classification System (USCS) (ASTM 2017b), the RAP was categorized as GW (well-graded gravel) and the other materials as SM (sand with fines). The XRD and XRF results (Figure 4.2 and Table 4.2) showed minerals rich in silica and alumina for all materials used, demonstrating their potential as raw materials for alkali-activated materials.

2.2 Production of the alkali-activated binder

The production of the alkali-activated binder (AAB) starts by grinding the RHA in ball mills for a predetermined period of one hour and then it was subjected to sieving (sieve with an opening of 150 μm). After preparing the RHA, it is dissolved in a solution of sodium hydroxide (NaOH) and water at a molarity of 10 M. This process lasts 12 hours and the solution is kept at the temperature that NaOH reaches when mixed with water (80°C). The molarity of the solution (10 M) and SiO_2/Al_2O_3 ratio = 4 were used in this work based on the good results presented in the literature (Bernal et al. 2012; Davidovits 1989).

2.3 Experimental design and molding procedures

The proportions of the materials were based on previous studies and only mixtures that met the normative requirements for mechanical strength for cemented base layers (ABNT 2012a) (Pelissaro et al. 2023) were chosen. The dry materials (aggregates and MK) were previously mixed and then the AAB was added at room temperature. Table 4.3 shows the proportions of the materials used in this experimental study design. It is important to emphasize that the amounts of aggregates totaled 100% of the mixtures and the amount of activated alkali binder was added in relation to the weight of RAP. It is also worth noting that all mixtures meet the criteria established by the WIRTGEN technical manual (Wirtgen GmbH 2012) regarding particle size limitations for flooring applications.

Table 4.3. Proportions of materials compositions.

Reclaimed asphalt pavement content (%)	Alkali-activated binder (%)	Stone powder content (%)	Gravel 3/4'' content (%)	Gravel 3/8'' content (%)
40	20, 30, 40	40	10	10
50	20, 30, 40	40	4	6

After mixing the materials, specimens were molded using the standard proctor compaction energy in order to reach the optimum moisture content (OMC) and the maximum dry unit weight (γdmax). For each mixture, three specimens of 100mm in diameter and 200mm in height were molded. The curing process consisted of preserving the specimens in airtight bags at an ambient temperature of 23 ± 2°C and humidity of 95 ± 2%. After curing, the specimens were submitted to the respective tests for which they were produced, following a control criterion that established the following requirements: to reach a degree of compaction between 99% and 101%; OMC variation of a maximum of 0.5%; variation in the diameter of the specimen of up to 0.5 mm and variation in the height of the specimen of up to 1 mm.

2.4 Durability test

The durability tests (wetting-drying cycles) of the RAP-AAB mixtures followed the recommendations of DNER-ME 203 (DNER 1994). Mass loss was measured in 12 wetting-drying cycles, which consisted of submerging the specimens in water for 5 h at 23 °C, then in an oven at 71 °C for 42 h, and finally being brushed.

2.5 Leaching tests

Environmental performance evaluation of the samples was done by conducting batch leaching test in according to NBR 10005 (ABNT 2004b), using extracting solution from glacial acetic acid. An amount of 2000mL of extracting solution were added to a set of 100 grams of each sample making a ratio liquid to solid of 20:1. Samples were prepared by crushing to fine powder and sieved through sieve 9,5 mm and then placed on polyethylene bottles under 30 revolutions per minute (RPM) in a rotary tumbler. At the conclusion of the leaching test period the aqueous and solid components were separated using a 45μm pore size filter paper. ICP-AES technique was utilized to determine the concentrations of metals. The pattern solution used was multi element standard for ICP with elements in dilute nitric acid-HNO3. pH was also determined by pH meter, model HI 2221, Hanna brand, glass body Ag/AgCl electrode with a ceramic junction, diameter 9.5 mm, pH range 0 to 13, and temperature 20–40 °C. Metal concentrations from the leaching test were compared with distinctive standards, being annex F of NBR 10004 (ABNT 2004a) and EPA (USEPA 2022).

2.6 Longevity studies

The behavior of RAP stabilized with AAB in longer curing periods was also investigated, since preliminary work indicated a trend of reduction in strength over time (Pelissaro et al. 2023). It is important to assess whether the resistance obtained in the initial curing times is preserved in the long term. Thus, unconfined compressive strength (UCS) tests were carried out, following the recommendations of NBR 12770 (ABNT 2022), for curing periods of 7, 28, 56, 112 and 224 days. These cure times were chosen based on other studies that also investigated the long RAP stabilization time performance through alkali-activated binders (Avirneni et al. 2016).

3 Results and discussions

3.1 Durability tests

The effect of cycling on the outer surface of the mixtures after 1, 3, 6, 9 and 12 cycles for the samples with 40% and 50% RAP are shown in Figures 4.3 and 4.4 respectively. It can be seen that the mixtures with higher AAB contents are more intact in all cycles, indicating that they have a stronger bonding structure. On the other hand, large cracks and greater deterioration are observed in mixtures with lower percentages of AAB (RAP:AAB = 40:20, 40:30 and 50:20 shown in Figures 4.3a, 4.3b and 4.4a, respectively), leading to loss of strength mechanics. In addition, it is important to emphasize that the RAP has an asphalt coating on its surface, which

impairs the adherence of the cementing material and that, for this reason, it was observed that the greatest material losses occurred at the interface with the RAP.

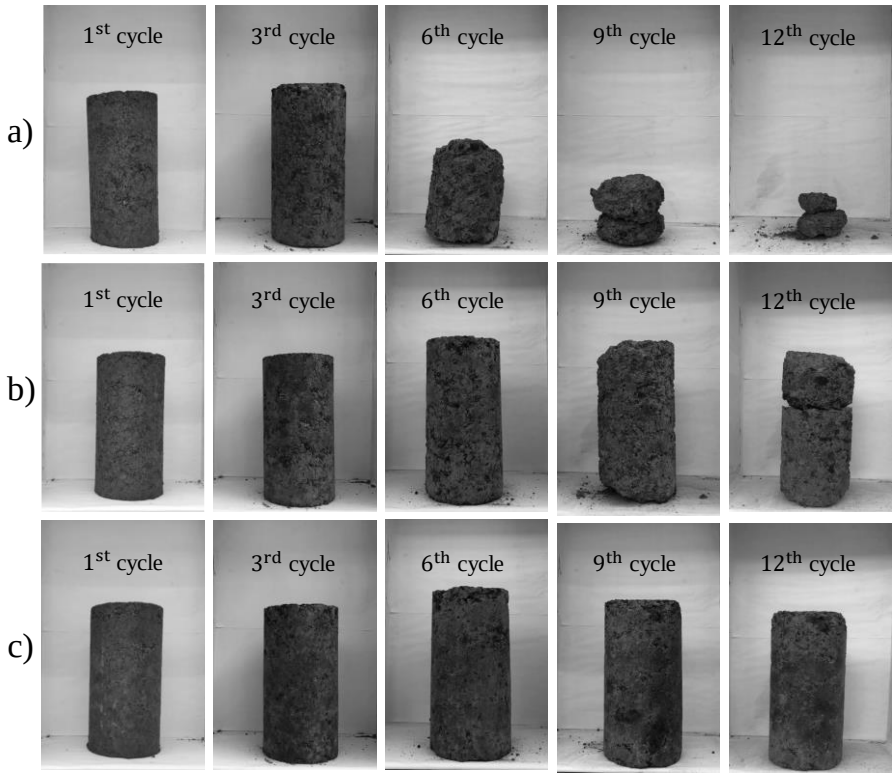

Figure 4.3. Typical samples after 1, 3, 6, 9 and 12 wet/dry cycles for RAP:AAB (a) 40:20 (b) 40:30 and (c) 40:40

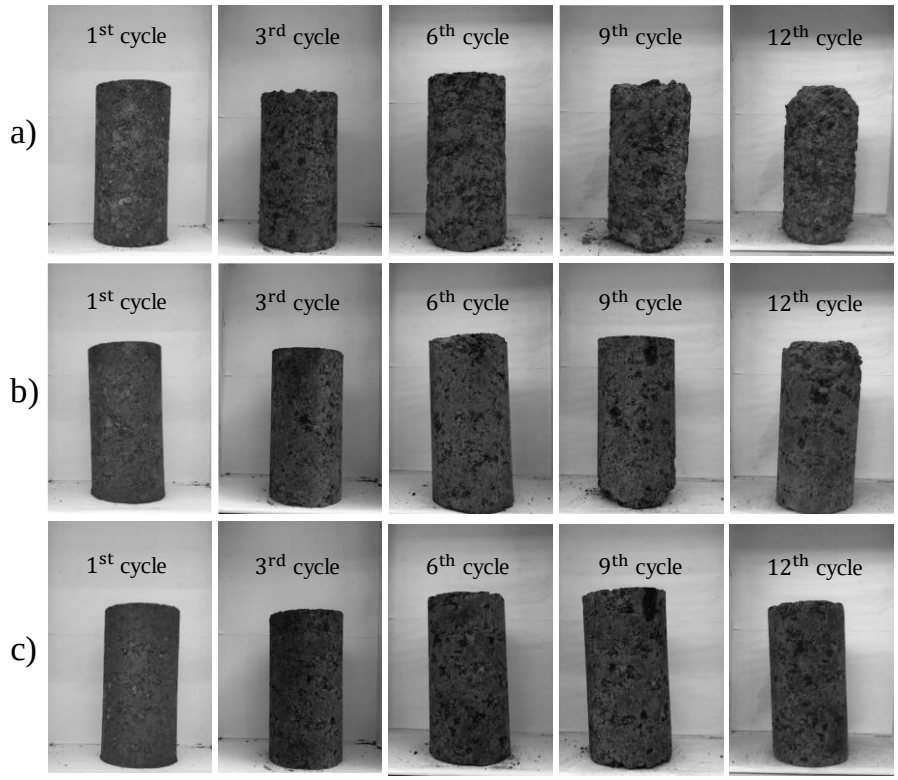

Figure 4.4. Typical samples after 1, 3, 6, 9 and 12 wet/dry cycles for RAP:AAB (a) 50:20 (b) 50:30 and (c) 50:40

To account for seasonal variations in humidity and temperature, samples cured for 7 days were subjected to 12 wet/dry cycles and the relationship between accumulated loss of mass (ALM) and the number of cycles is shown in Figure 4.5.

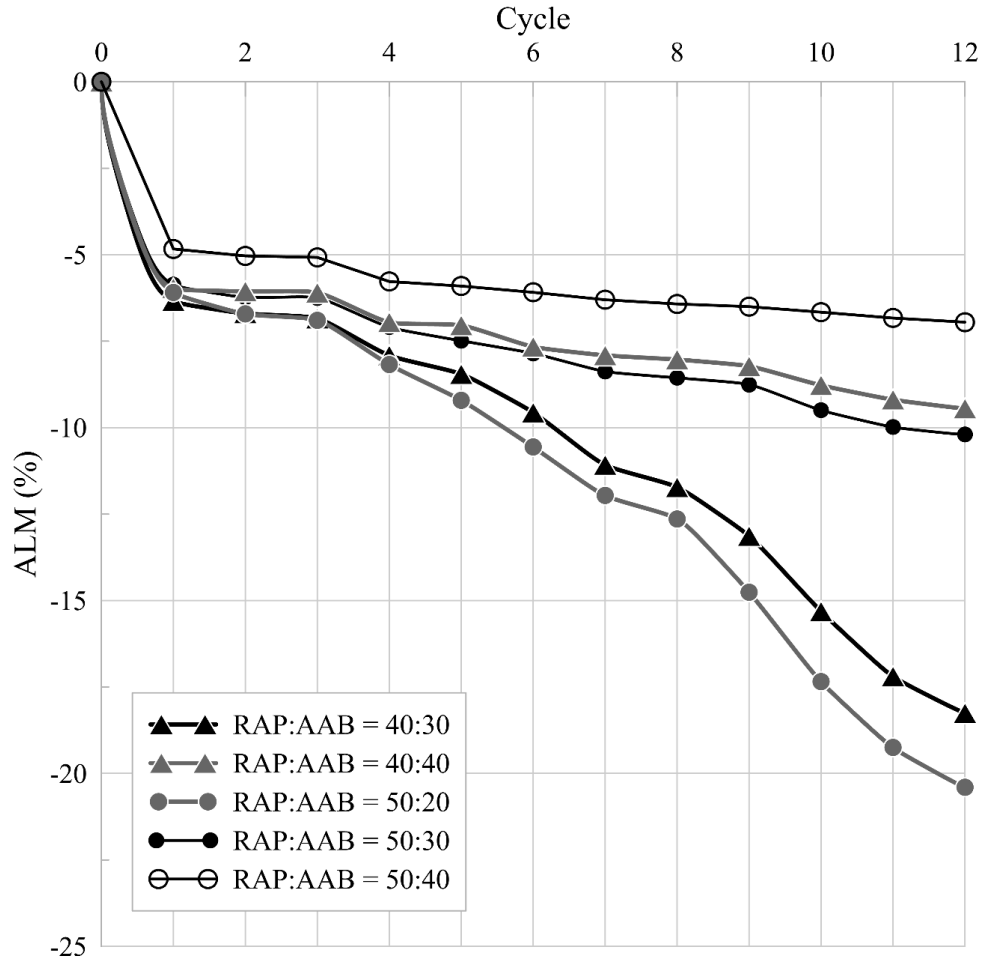

Figure 4.5. Accumulated loss of mass after wet-dry cycles for alkali-activated CCA binder stabilized RAP

The ALM results for the RAP:AAB = 40:20 sample were not shown in Figure 4.5 because it presented ALM greater than 50% from the sixth cycle onwards, as can be seen in Figure 3a. In general, it is noted that the ALM are more significant in the first cycle, as there is a higher percentage of surface grains that have not yet fully adhered to the main body of the sample. Higher ALM were also observed for samples with a lower percentage of AAB (RAP:AAB ratio = 40:30 and 50:20) from the sixth cycle onwards, possibly due to the low amount of binder that did not involve most of the aggregates and, therefore, showed low cementation. The increase in the AAB content resulted in more durable specimens, corroborating the behavior found in the other mechanical tests and indicating that durability is directly linked to strength. In addition, higher percentages of AAB are associated with a reduction in porosity, as observed in similar studies that evaluated soils stabilized with Portland cement (Consoli and Tomasi 2018); stabilized dispersive soils (Consoli et al. 2016); soils stabilized with ash and limestone (Consoli et al. 2018c, 2020); reclaimed asphalt paving

stabilized (Consoli et al. 2018a, 2021a) and gold tailings stabilized with Portland cement (Consoli et al. 2018d).

For the results of the present study, only mixtures with a RAP:AAB ratio of 40:40, 50:30 and 50:40 met the request of the Portland Cement Association (PCA 1956), in which the maximum ALM after 12 cycles of wet drying should be 14% for stony soils, cured at room temperature for 7 days. Furthermore, the ALM found in the present study was higher than mixtures of alkali-activated fly ash binder stabilized RAP (Avirneni et al. 2016; Horpibulsuk et al. 2017).

From the results of the w-d cycles and the photos, it is apparent that the mixtures with higher AAB contents provide a very good durability when subjected to seasonal variations in humidity and temperature. The alternative binder produced from RHA can increase the durability of the RAP, especially for the RAP:AAB = 50:40 sample.

Based on the performance of these mixtures against the 12 aggressive cycles and accelerated wet/dry cycles, more than 12 years project life in the field can be estimated. However, the field life of these mixtures can be much longer than 12 years, as all consecutive years may not receive heavy rainfall and higher temperatures than were maintained in the trial (Avirneni et al. 2016).

The mechanical strength of the mixtures after the wetting/drying cycles was also evaluated to verify the strength after mass loss. Although there are no regulations that provide any specification for the strength retained after the cycles, it is valid to verify the loss of strength, especially when alternative materials are used, as is the case of RAP and RHA in this work.

The loss of strength after the 12 cycles was high for all mixtures (64% on average) as shown in Figure 4.6. Therefore, only the mixtures with a RAP:AAB ratio = 40:40, 50:30 and 50:40 met the minimum strength requirements, being 25%, 45% and 114% higher, respectively, than the DNIT specifications of UCS 2.1 MPa for cemented pavement bases (DNIT 2022). These three blends are potentially superior for better performance in field conditions, possibly without premature failure.

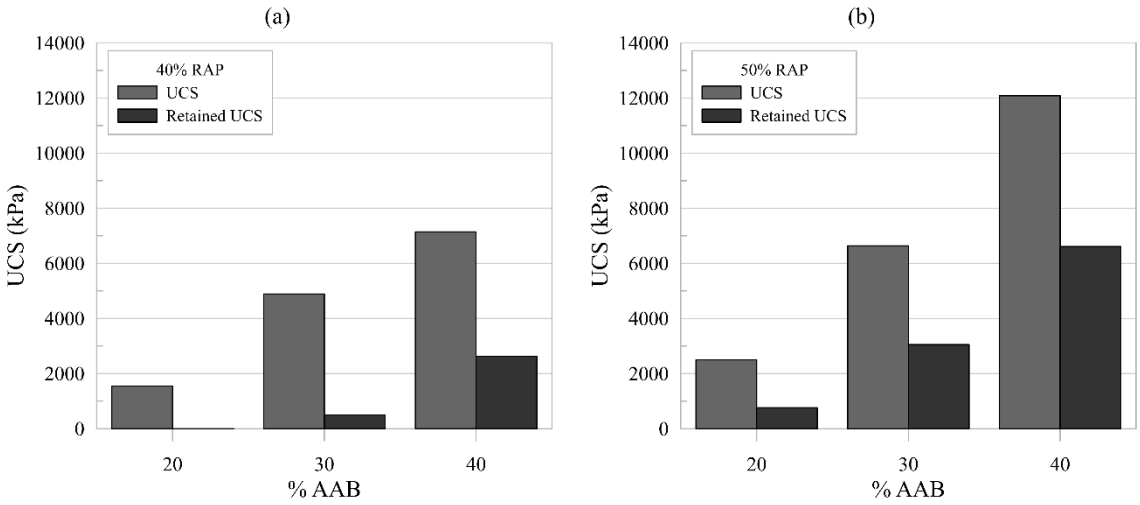

Figure 4.6. Variation of UCS and retained strength after 12 wet-dry cycles for different mixes (a) 40% RAP (b) 50% RAP

Several researchers report the loss of stabilizers from the base layers after a certain period of service. It has been noticed that secondary chemical reactions during the stabilization process may result a strength loss over the long performance evaluation and in many cases this change is associated with the absorption of moisture in the stabilized materials (Avirneni et al. 2016). Previous studies have also reported that the infiltration of moisture through the subgrade results in variations in pH and in the Ca/Mg ratios, which may influence the permanence of chemical modifiers (Puertas et al. 2000).

3.2 Longevity studies

Long-term UCS tests were performed to verify the longevity of RAP stabilized with AAB produced from RHA. Figures 4.7a and 4.7b show the variation of mechanical strength over the evaluated period (7, 28, 56, 112 and 224 days) for mixtures with 40% and 50% RAP, respectively. It is observed that the UCS values do not show significant variations for the lowest AAB content (20%) for both proportions of RAP in the evaluated curing periods. This AAB content is not recommended because in several curing times evaluated, the minimum resistance is not reached as recommended by Brazilian road standards. Increasing the AAB content to 30% did not show a significant increase in the UCS of the mixtures in the first curing times (7 and 28 days) and resulted in a reduction in the mechanical performance in the long term. This decrease in resistance causes the mixture RAP:AAB = 40:30 to reach values below the mixture with the lowest AAB content (RAP:AAB = 40:20) and which do not meet the DNIT regulations (ABNT, 2012). Similar behavior was observed in activated alkali pastes, which also reduced

strength for curing times greater than 28 days, both for pastes produced with commercial sodium silicate and for those produced with RHA-based sodium silicate (Longhi et al. 2014). This fact leads to the conclusion that sodium silicate is not the material responsible for this drop in resistance. Some studies show that the metakaolin used as a precursor may be responsible for this behavior, since metakaolin-based activated alkali systems undergo a microstructure reorganization process, where amorphous gels are converted into zeolites after a certain period of curing. This microstructural change results in denser binders and pore formation that can affect mechanical performance over time (Lloyd 2009). Some authors also state that the formation of crystals during hydration results in thermodynamic instability of the amorphous reaction of the products, which may also be responsible for the reduction in strength (Lloyd 2009; Takeda et al. 2013). A preliminary investigation, which evaluated the microstructure of RAP stabilized with AAB produced from RHA, showed that when these mixtures are cured at room temperature, they are subject to the occurrence of efflorescence and that this phenomenon was responsible for the reduction in resistance (Pelissaro et al. 2023).

Concerning the mixtures UCS, highest AAB content evaluated (40%) has resulted a strength reduction. This behavior tendency continues to occur for the highest percentage of RAP (50%), indicating once again that this content is not suitable for application on highways. However, for 40% RAP, the material behaves similarly to the other AAB contents, even though the reduction in mechanical performance over time, the values stabilize or even increase in the longest curing time evaluated (224 days). Similarly observed in this study, no reduction in strength long-term evaluation has been observed over, other studies, (Avirneni et al. 2016) shown that after 56 days, the alkali activation reactions nearly stabilize to the point of not significantly affecting the mechanical performance of the stabilized RAP.

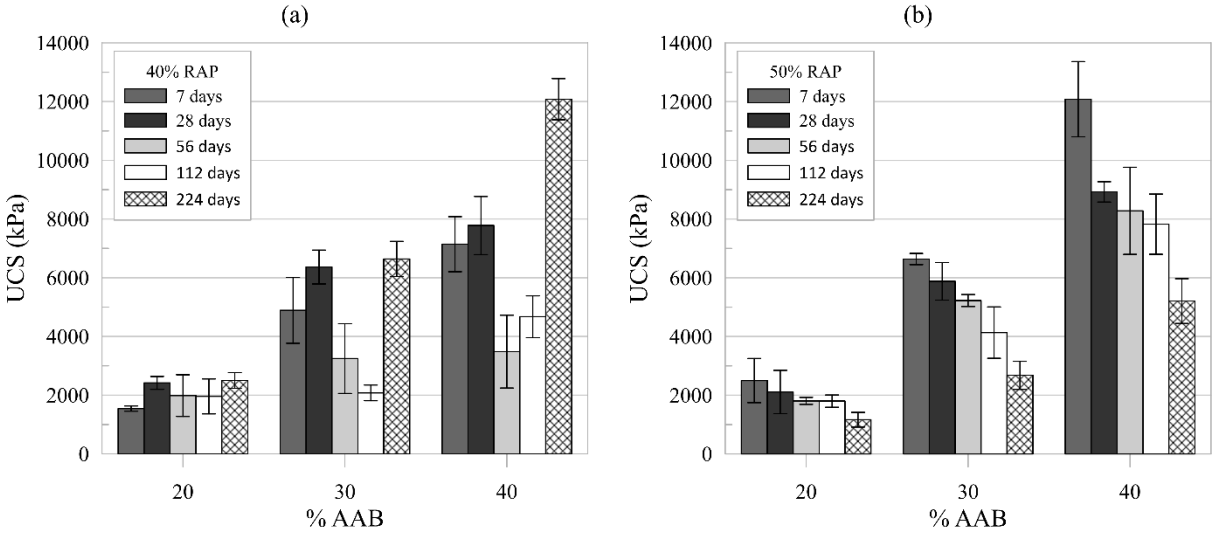

Figure 4.7. Variation of UCS with curing period for (a) 40% RAP (b) 50% RAP

3.3 Leachate studies

Leaching tests were performed to evaluate the environmental performance from leachate studies of RAP stabilized with AAB produced from RHA. Table 4.4 present concentration results, in which shaded cells represent concentrations of RAP stabilized with AAB that exceeded the limits of the standards in comparation with RHA concentrations. Due to durability results, samples with RAP:AAB ratio = 40:20 were not evaluated according to environmental criteria. For all mixtures with 40% and 50% RAP limits of standards NBR 10004 (ABNT 2004a) and EPA (USEPA 2022) were not exceeded for Ag, As, Cd, Cu, Hg and Na. Besides, none of the metals exceeded the leaching limit of annex F for the Brazilian standard NBR 10004 (ABNT 2004a), demonstrating the Non-Hazardous characteristics. For EPA limit (USEPA 2022) only Pb and Se exceeded concentrations for mixture RAP:AAB = 40:30, which represents an error of determination. In general, no relationship was observed between the leached concentrations of metals with the different RAP:AAB ratios, indicating that the origin is not related to AAB and RAP.

Table 4.4. Metals concentration from leaching tests for mixtures with different RAP:AAB rations

Element	40F30G	40F40G	50F20G	50F30G	50F40G	NBR 10004 limit (Annex F)	EPA limit
Ag	0	0	0	0	0	5	-
Al	12.2	11	8.9	15.4	11.45	-	-
As	0	0	0	0	0	1	0.01
Ba	0.1	0.05	0.07	0.08	0.05	70	2
Cd	0	0	0	0	0	0.5	0.0005
Cr	0.03	0.03	0.03	0.03	0.03	5	0.1
Cu	0	0	0	0	0	-	1.3
Fe	5.2	0	0	3.91	3.05	-	-
Hg	0	0	0	0	0	0.1	0.002
Mn	1.47	1.49	1.78	1.58	0.97	-	-
Na	46.8	62.25	44.37	57.5	65.6	-	
Pb	0	1	0	0	0	1	0.015
Se	0	1	0	0	0	1	0.05
Zn	0.04	-	0.18	0.12	0.01	-	-

4 Conclusions

This study investigated the stabilization of RAP with a metakaolin-based binder alkali-activated by rice husk ash synthetized sodium silicate. The following conclusions are drawn from the combined analysis of durability results from wet/dry cycles, leachate analysis and long-term studies:

a) Durability studies in terms of aggressive wet/dry cycles indicated that only mixtures with a RAP:AAB ratio = 40:40, 50:30 and 50:40 satisfactorily met the normative specifications for mass loss;

b) Retained strength after aggressive wet/dry cycles was higher than the minimum design strength only for mixtures with RAP:AAB ratio = 40:40, 50:30 and 50:40;

c) From the results of the long-term UCS tests, it was observed that the mechanical performance decreases for the highest concentrations of AAB. However, after 56 days of curing for 40% RAP, there is a stabilization in the alkaline activation reactions, making to return to increase resistance over time;

d) Environmental performance of RAP stabilized with AAB produced from RHA demonstrated mixtures that did not exceed EPA limit and leaching limit of annex F for the Brazilian standard NBR 10004 resulting in Non-Hazardous characteristic

e) From a geotechnical engineering point of view, the survey results indicate that RAP is mechanically and environmentally viable for use in pavement base application when stabilized mainly at RAP:AAB = 40:40 ratio. In addition to having a high UCS, these blends exhibit good durability and long-term performance. In addition, these mixtures have no environmental impact as the results of environmental tests do not show any significant risk or hazardous characteristics.

f) Besides the clear applicability of the mixtures as a pavement layer according to NBR 12253 (ABNT 2012a), the results presented in this study can help to attend a new law established in Brazil that provides that all restoration engineering projects, adaptation of capacity and expansion of road works by the National Department of Transport Infrastructure - DNIT, must include the reuse of the RAP eventually produced in the undertaking.

Finally, it is worth mentioning that in addition to the properties evaluated in this study, there is a significant lack of research on the fatigue performance in flexion of RAP pavement

bases cemented by alkali activation. Fatigue cracking is one of the main failure mechanisms in mixtures with high RAP content, resulting from the brittle behavior of the material associated with accumulated damage due to traffic.

3.5 Flexural fatigue behavior of reclaimed asphalt pavement stabilized with alkali-activated rice husk ash

Fatigue cracking is one of the main failure mechanisms in cemented base/subbase layers with a high content of Reclaimed Asphalt Pavement (RAP). Thus, it is essential to evaluate the behavior of pavements in terms of flexural fatigue under traffic load. Therefore, this study focuses on investigating the static and dynamic flexural behavior of mixtures of RAP with metakaolin-based binder, alkali activated by sodium silicate synthesized from RHA. The experimental program included tests: unconfined compression strength, diametral compression, bending tensile strength and fatigue life analysis based on four-point bending test. The results showed that the use of alkali-activated binder (AAB) provided more flexible mixtures for higher RAP contents and that flexible pavements with base and sub-base layers with high RAP content can be recycled without compromising the mechanical resistance to wear over time. In addition, depending on the RAP and AAB content used, when subjected to cyclic loading, the mixtures may exhibit brittle behavior or break when reaching approximately 50% of its initial modulus.

Keywords: Reclaimed asphalt pavement; Flexural strength; Fatigue modulus; alkali-activated binder.

1. Introduction

The construction industry is an important sector that serves other sectors and contributes to global socio-economic growth (Olukolajo et al. 2022). However due to rapid population growth, estimated to be over 6 billion by 2045 (Čuček et al. 2012; Zheng et al. 2016) and the development of infrastructure in countries with emerging economies, the generation of industrial waste has increased significantly (Bordoloi et al. 2022). The construction industry consumes up to 40% of global raw materials (Darko and Chan 2016), generates around 40% of waste (Nasir et al. 2017) and emits around 25% of carbon dioxide (Mahpour 2018). This scenario puts the construction industry in the position of one of the largest generators of waste globally (Bilal et al. 2020), indicating a sign of unsustainability of the sector (Núñez-Cacho et al. 2018) and representing environmental challenges (Esa et al. 2017a; b; Menegaki and Damigos 2018).

Particularly in the paving sector, roads present constant problems that require continuous maintenance. In cases of road rehabilitation, a fully recyclable material called Reclaimed Asphalt Pavement (RAP) is generated (AAPA 2018; EAPA 2014), composed

mainly of aged bituminous aggregates and additives (Hoy et al. 2016). This material can be reused in new asphalt mixes, reducing the demand for virgin aggregates and asphalt binder, or as recycled aggregates to produce unbound pavement layers (SABITA, 2019). Its use in base and sub-base layers of pavements reduces the total cost of pavement sections by up to 46% (Debbarma et al. 2019; Singh et al. 2018).

Although the amount of reused RAP has gradually grown in many countries around the world (SABITA, 2019), the lack of adhesion between its grains needs to be compensated for by the use of cementing agents such as Portland cement. However, the production of this type of cement has a high carbon footprint, with cement factories responsible for around 8% of global CO_2 emissions (Cadavid-Giraldo et al. 2020).

Thus, given the emphasis on sustainability and environmental factors, RAP stabilized with Portland cement may not be considered as a possible solution for long-lasting sustainable pavements (Jallu et al. 2020). In this context, alkali-activated materials have gained significant attention in recent decades as high-quality cementing agents, since in addition to reducing carbon emissions, they also allow the use of waste (Athira et al. 2021). These materials come from the alkali activation of aluminosilicate precursors from alkaline solutions.

Various industrial by-products/waste can be incorporated as a source of aluminosilicate, such as: fly ash (Phoo-ngernkham et al. 2015; Zhuang et al. 2016), blast furnace slag (Awoyera and Adesina 2019), water treatment sludge (Geraldo et al. 2017), sugar cane bagasse ash (Bruschi et al. 2021a; b; Pereira dos Santos et al. 2022b), lime carbide (Bruschi et al. 2022; Queiróz et al. 2022), eggshell (Consoli et al. 2021; Tonini de Araújo et al. 2021) and rice husk ash (Bernal et al. 2012; Luukkonen et al. 2018; Mejía et al. 2013; Sturm et al. 2016; Tchakouté et al. 2016; Tong et al. 2018). As for activators, the most common ones include sodium or potassium hydroxides and/or silicates (Torres-Carrasco et al. 2015). However, one of the biggest obstacles to the large-scale application of alkali-activated materials is that the commercial alkaline activators used for their activation are expensive and have a high carbon footprint. As a result, the cost and environmental sustainability of the final product is drastically affected, although the overall cost and carbon footprint is lower than that of Portland cement (Mohapatra et al. 2022). Therefore, to obtain maximum cost optimization, several researchers have advocated the use of waste-based alkaline activators (Abdulkareem et al. 2021; Adesanya et al. 2021).

The interest in processing agro-industrial waste, as well as the need to reduce the cost of producing alkali-activated materials, has motivated researchers to develop alternative alkaline activators based on amorphous silica sources derived from waste (Mohapatra et al. 2022). In this context, properly burned and ground rice husk ash (RHA) has significant potential due to the compound rich in reactive silica (SiO_2) (Khan et al. 2015), being considered the agricultural waste with the highest amount of silica (Athira et al. 2021), reaching SiO_2 contents of up to 80-85% (Siddique 2008). When RHA is applied in cementitious systems, it improves the properties of the systems through a double effect: chemical or pozzolanic effect and physical or filler effect (Khan et al. 2015).

As for paving applications, alkali activated binders are already evaluated as a stabilizing agent in combination with RAP (Al-Hdabi 2016; Edeh et al. 2012; Kang et al. 2015; Syed et al. 2022; Tabyanga et al. 2021). However, the use of RAP with alternative activators for the alkaline activation process has research gaps. In addition, there is a significant lack of research on the flexural fatigue performance of alkali activation cemented RAP pavement bases. Fatigue cracking is one of the main failure mechanisms in mixtures with high RAP content, resulting from the brittle behavior of the material associated with accumulated damage due to traffic (Subhy et al. 2019).

Therefore, this research aims to investigate the development of low-cost activators in alkali-activated materials for the stabilization of RAP under the condition of repetitive heavy traffic load for use in base and sub-base layers of pavements. Thus, the present study is mainly focused on evaluating the static and dynamic flexural behavior of mixtures of RAP with a binder based on metakaolin, alkali activated by sodium silicate synthesized from RHA. The discussion focuses on the analysis of compaction results, resistance to simple compression, diametral compression, tensile strength and analysis of fatigue life based on bending and tensile tests at load points.

2. Materials and Methods

2.1 Materials

The materials utilized in this research were reclaimed asphalt pavement (RAP), stone powder (SP), gravel (G), metakaolin (MK), rice husk ash (RHA), and sodium hydroxide (NaOH). RAP was acquired from ERS - 135 highway, located in city of Coxilha in southern Brazil. RHA is the waste of a rice processing industry and was collected directly from the

company in Rio Grande do Sul, Brazil. On the other hand, SP, G, MK, and NaOH were all purchased from local manufacturers in Rio Grande do Sul, Brazil.

Materials physical characterization (Figure 5.1 and Table 5.1) was evaluated by determining their grain size distribution (ASTM 2017a) and specific weight of grains (ASTM 2014). For RAP, the bitumen content was determined in accordance with ASTM D 2172 (ASTM 2018); the specific gravity for coarse aggregate of RAP was determined according to NBR NM 53 (ABNT 2009a), while for the fine aggregate NBR NM 52 (ABNT 2009b).

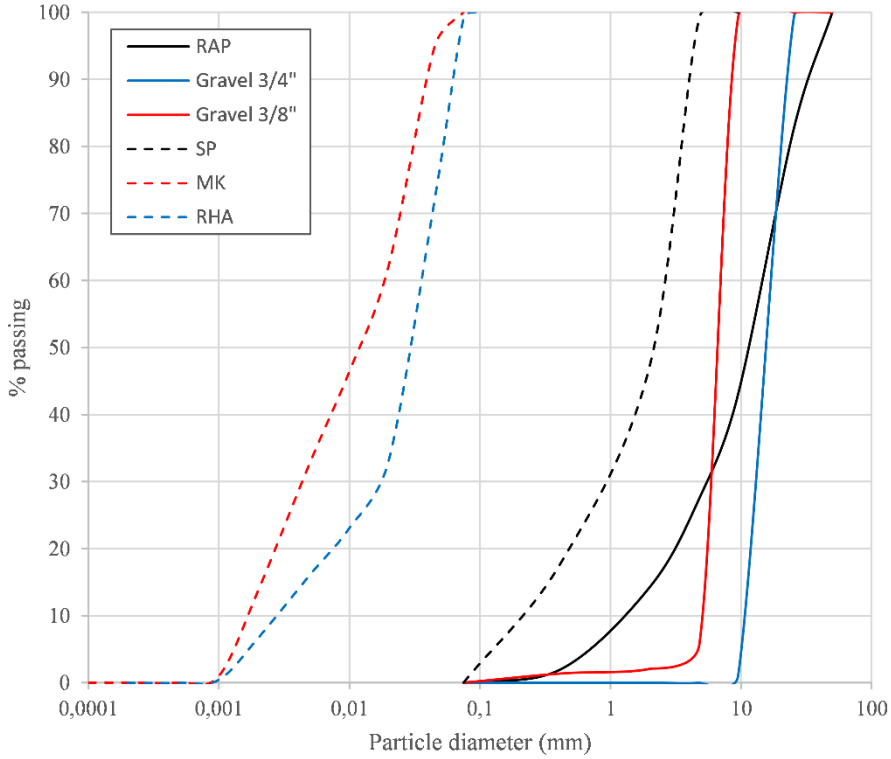

Figure 5.1. Materials grain size distribution.

Table 5.1. Materials physical properties.

Property	RAP	MK	RHA	SP	Gravel 3/4''	Gravel 3/8"
Specific unit weight of grains (g/cm^3)	2.42	2.64	2.23	2.80	2.85	2.8
Bitumen content (%)	5.8	-	-	-	-	-
Gravel (4.75mm < diameter) (%)	72	0	0	0	100	94
Sand (0.06mm < diameter < 4.75mm) (%)	28	0	10	88	0	6
Silt (0.002mm < diameter < 0.06mm) (%)	0	86	82	22	0	0
Clay (diameter < 0.002mm) (%)	0	14	8	0	0	0
USCS classification	GW	SM	SM	SW	GP	GP

The mineralogical composition (Figure 5.2) was determined through an X-ray diffraction (XRD) test, the analysis was performed on a Shimadzu X-ray diffractometer, model XRD-6000 (θ-2θ), operating at 40 kV and 30 mA in the primary beam and curved graphite monochromator in the secondary beam. X-ray fluorescence spectrometry (XRF) was utilized to determine the elemental composition (Table 5.2), through a quantitative analysis with a calibration curve based on tabulated rock patterns from Geostandards. Scanning electron microscopy (SEM) analysis (magnifications of 4000 times) was utilized to study the microstructural characteristics of the raw materials. In addition, an environmental classification was carried out on the RHA, following the procedures of NBR 10004 (ABNT 2004a), NBR 10005 (ABNT 2004b), and NBR 10006 (ABNT 2009c). Metal concentrations were measured by inductively coupled plasma atomic emission spectrometry (Shimadzu-branded ICP-AES).

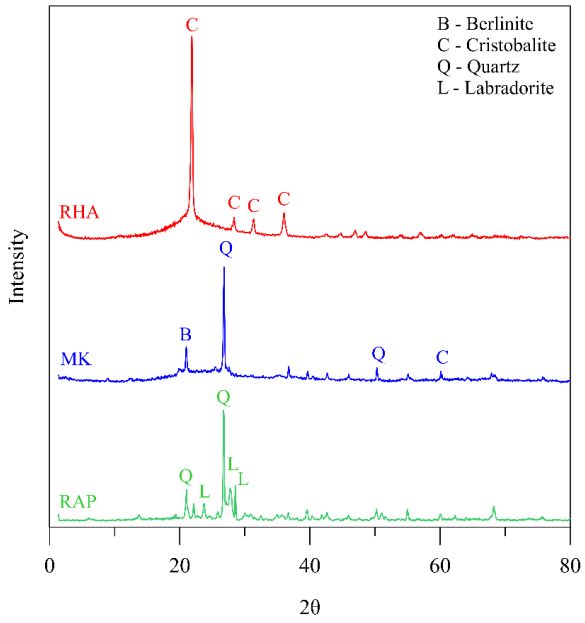

Figure 5.2. Mineralogical composition of RAP, MK and RHA.

Table 5.2. Materials chemical composition.

	SiO_2 (%)	Al_2O_3 (%)	Fe_2O_3 (%)	CaO (%)	MgO (%)	SO_2 (%)	Na_2O (%)	K_2O (%)	P_2O_5 (%)	TiO_2 (%)	ZnO (%)
RAP	64.39	14.65	1.16	4.10	<0.10	7.68	-	5.55	1.65	<0.10	<0.10
MK	54.72	40.80	1.80	0.10	0.10	-	0.18	0.21	-	2.09	-
RHA	89.33	0.62	1.53	3.84	2.51	-	-	2.18	-	-	-

RAP was classified as GW (well-graded gravel), while MK and RHA as SM (sand with fines) in accordance with the Unified Soil Classification System (USCS) (ASTM 2017b).

Regarding the mineralogical composition (Figure 5.2), RAP exhibit a crystalline structure composed by quartz (SiO_2) and labradorite [$(Ca,Na)(Al,Si)_4O_8$]; MK presented quartz (SiO_2), cristobalite (SiO_2), and berlinite ($AlPO_4$); and RHA was predominantly amorphous, with few sharp diffraction peaks of cristobalite (SiO_2). Crystalline silica has three polymorphic forms, cristobalite being obtained when subjected to burning temperatures between 981-991°C, as in the case of the RHA of this research. As for the chemical composition, RAP and MK majorly consisted of silica and alumina, while RHA was mainly composed of silica. It is important to highlight that in its natural condition, RHA presents non-uniform particle size and therefore in this research it was subjected to grinding in a laboratory ball mill for 1 hour and then sieved in a sieve with an opening of 150 μm. RHA morphology after processing and in natura is shown in Figure 5.3a e Figure 5.3b respectively, indicating that the particles have an irregular, porous and finer shape after processing.

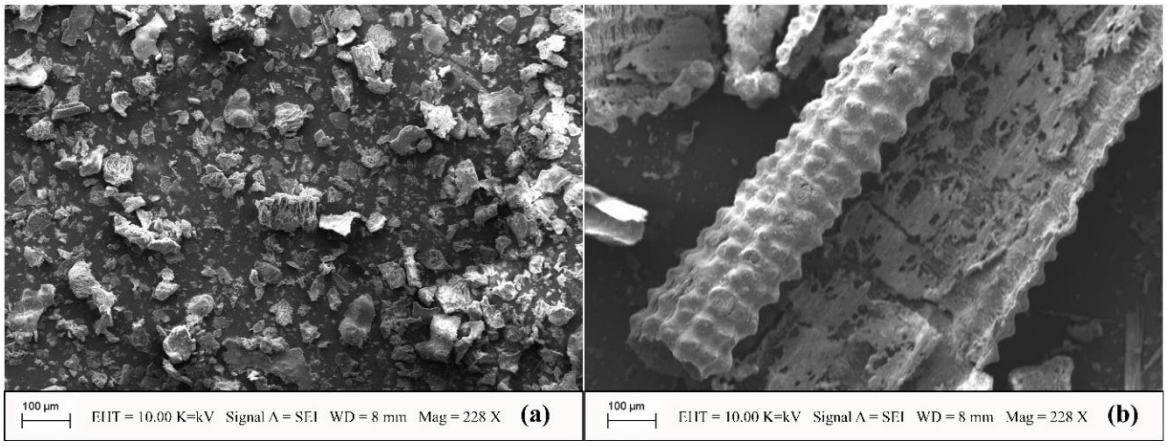

Figure 3. RHA morphology (a) after processing and (b) in natura.

2.2 Specimens preparation and molding procedures

Two distinctive RAP levels (40% and 50%) were studied. The virgin aggregates (SP and G) were added to the RAP contents in different quantities, so the particle size limits for pavement applications, established by the WIRTGEN technical manual (Wirtgen GmbH 2012), were respected. Table 5.3 shows the proportions of the non-cemented compositions.

Table 5.3. Proportions of the non-cemented compositions.

Reclaimed asphalt pavement content (%)	Stone powder content (%)	Gravel 3/4'' content (%)	Gravel 3/8'' content (%)
40	40	10	10
50	40	4	6

The aggregates were stabilized using an alkali-activated cement by adding 30% and 40% in relation to the weight of RAP. Thus, the RAP:AA ratios evaluated were 40:30, 40:40, 50:30 and 50:40 and this relation has been used to identify the different mixtures.

2.3 Compaction test

The Proctor compaction test was performed using standard effort, in accordance with the guidelines of ASTM D698 (ASTM 2012). The method involves placing (in a specified manner) a soil sample at a known water content in a mold of given dimensions, subjecting it to a compactive effort of controlled magnitude, and determining the resulting unit weight. The procedure is repeated for various water contents sufficient to establish a relation between water content and unit weight; through this process is possible to define the maximum dry unit weight (γ_{dmax}) and the optimum water content (OWC) of the studied mixtures.

2.2 Molding procedures

Initially, for the production of the alkali-activated binder (AA), the liquid alkaline activator was previously prepared by dissolving the RHA in a solution of sodium hydroxide (NaOH) at a 10 M concentration and kept at temperature of 80 °C for 12 hours. During the mixing procedure, concentration of the solution, and SiO_2/Al_2O_3 = 4 ratio were kept constant and selected based on previous studies (Bernal et al. 2012; Davidovits 1989). After the dissolution time and upon reaching room temperature, the solution was then mixed with the solid aluminosilicate source (MK) and latter with the materials to be stabilized (RAP and virgin aggregates).

The molding procedure starts by the mixing of the air-dried materials (RAP, virgin aggregates and metakaolin) with the liquid alkaline activator (prepared by dissolving the RHA in a solution of sodium hydroxide) and water until homogenization is achieved. Then, specimens are molded at the optimum moisture content (OMC) and maximum dry unit weight (γ_{dmax}) from the compaction curves. After specimens were molded and had their dimensions taken, they were sealed in hermetic bags before being stored in a humid room with controlled moisture (95 ± 2%). Specimens were considered suitable for testing if the following criteria

was met: degree of compaction between 99% and 101%; water content within 0.5% of the target value; diameter within 0.5 mm of the target value; and height within 1 mm of the target value.

For unconfined compression strength (UCS) and diametral strength tests triplicates of cylindrical specimens of 100mm in diameter and 200mm in height were utilized. For flexural tests the beam samples had a rectangular cross section with 450 mm (L) x 150 mm (B) x 150 mm (H), and the beam supports were set to be 150 mm apart.

2.4 Unconfined compression tests

UCS tests were executed in accordance with ASTM D2166 (ASTM 2016), using an automatic loading machine, with a maximum load capacity of 50kN. The rate of displacement adopted was 1.14mm per minute, to produce an axial strain at a rate between 0.5%/min and 2%/min, as recommended by ASTM D2166 (ASTM 2016). The specimens were maintained at 23 ± 2°C for 7- and 28-days curing.

2.5 Indirect tensile strength

The procedures for the indirect tensile strength tests by diametral compression (q_t) followed the Brazilian standard (ABNT 2011) based on the American standard (ASTM n.d.). An automatic press with a capacity of 50 kN was used to carry them out. The tests were carried out with an automated system, at a speed of (0.05 ± 0.02) MPa/s until the specimen ruptured. The tensile strength (qt) is adopted according to Eq. 1, when, in the axial stress-strain curve test, a maximum peak is observed:

$$q_t = \frac{2F}{\pi DL} \quad (1)$$

Where, q_t is the tensile strength by diametral compression (MPa), F is the breaking load at the peak of the diametral stress-strain curve (N), D and L are the diameter (mm) and height (mm) of the specimens, respectively.

2.6 Flexural strength tests

The four-point bending test method is quite often used to assess the flexural strength of asphalt concrete/cement-treated materials in the laboratory. The flexural strength of the beam specimens was evaluated using Eq. (2).

$$\sigma_t = \frac{P_{max}L}{BH^2} \quad (2)$$

where, σ_t = flexural strength of the beam specimen (MPa); P = maximum load applied by the actuator (N); L = span length (mm); B = average specimen width (mm); and H = average specimen height (mm).

2.5. Flexural fatigue modulus

The flexural fatigue modulus testing in this study used a similar experimental test setup used to obtain the flexural strength. The flexural modulus of the beam specimens was obtained under stress-controlled mode with stress levels of 70%, 80% e 90% of peak load from the flexural testing. It is noteworthy that the stress levels applied in this study are lower than those often used for fatigue tests of cement-treated materials, which are between 60% and 100% (Alvaro et al. 2013; Arulrajah et al. 2015; Disfani et al. 2014; Jia et al. 2018; Jitsangiam et al. 2016; Mandal et al. 2016, 2018). However, due to the press load limitation (max 10kN), and it was not possible to reach these tension levels. Furthermore, only the mixtures with the most satisfactory results obtained in the flexural strength were submitted to fatigue tests, after 7 days of curing. The flexural modulus tests were performed under haversine cyclic loading of 500 ms (250 ms of loading followed by 250 ms of rest), featuring a frequency of 2 Hz. Pulse calibration and its control are carried out by means of solenoid valves. In this way, the opening time and the way air is introduced into the system determine the pulse shape and time.

3. Results and discussions

Figure 5.4 presents the relationship between the dry unit weight (γd) and the water content of mixtures with RAP, virgin aggregates and AA. It is observed that for the mixtures with 40% of RAP, the addition of AA showed the parameter dry unitary weight more sensitive than the OWC; as the AA content increased, the dry specific weight decreased and the OWC practically did not change. On the other hand, for mixtures with 50% RAP, the opposite behavior was observed. Despite this difference in behavior, both OWC and dry unit weight were in the range of typical values reported for RAP mixes, virgin aggregates and AA (Avirneni et al. 2016; Jallu et al. 2020; Saride et al. 2016).

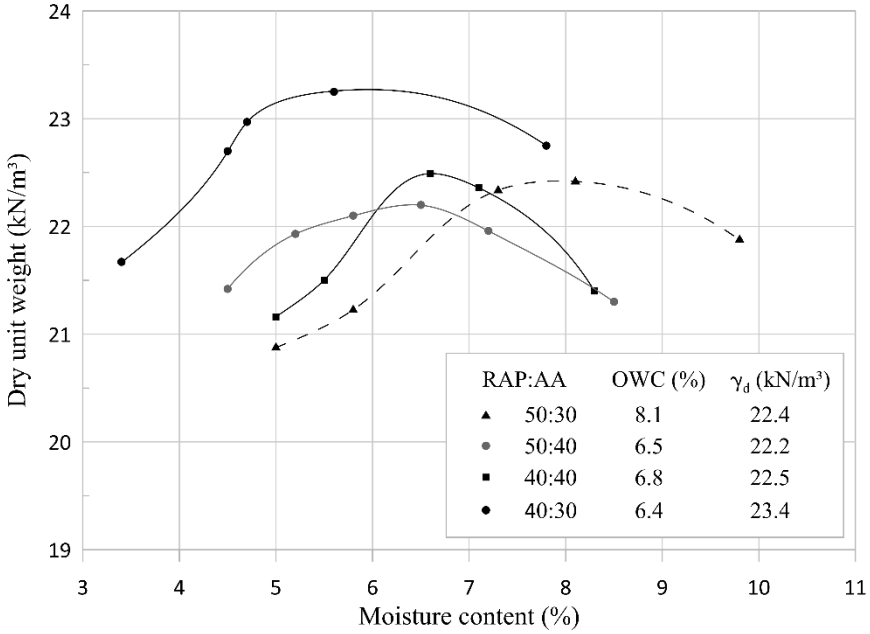

Figure 5.4. Compaction test results

Figure 5.5 presents the results of unconfined compressive strength (UCS) for stabilized RAP mixes. The increase in AA content for mixtures with 40% RAP led to an increase in UCS at 7 days and did not show significant differences at 28 days. Increasing the AA content reduces porosity helping to develop strength. The reduction in porosity induces a larger contact area between the particles, intensifying the entanglement and mobilizing the friction between the particles. In addition, the increase in the AA content is related to the increase in cementitious reactions, also contributing to the development of resistance (Pereira dos Santos et al. 2022a). Similar results were found for RAP stabilized with alkali activated binders (Hoy et al. 2016, 2018; Mohammadinia et al. 2018), cement stabilized RAP (Mohammadinia et al. 2018; Suebsuk and Suksan 2014; Taha et al. 2002) and other cement stabilized geotechnical materials (Consoli et al. 2007; Diambra et al. 2017; Festugato et al. 2018).

Although the mixture with RAP:AA ratio = 50:30 presented the highest UCS value, a significant reduction in strength was observed over time. This loss of resistance was also observed in alkaline pastes activated both by commercial sodium silicate and by alternative RHA silicate, in curing times greater than 28 days (Longhi et al. 2014), evidencing that the alternative silicate is not the triggering phenomenon of the resistance reduction over time. Metakaolin-based geopolymers undergo major microstructural reorganization, in which amorphous geopolymer gels are able to convert to crystalline zeolites after aging, resulting in binder densification and formation of large pores, accompanied by a large reduction in strength

(Lloyd 2009). In addition, alkali-activated products undergo changes in the microstructure of the gel formed during longer curing times, suggesting that continuous reorganization and polymerization of the aluminosilicate gel may be causing autogenous shrinkage and reduced strength (Longhi et al. 2016). The loss of resistance can also be related to the beginning of the crystallization of the products formed by hydration, resulting in a thermodynamic instability of the amorphous reaction of the products (Lloyd 2009; Takeda et al. 2013).

Finally, despite the different mechanical behavior observed in the evaluated mixtures, it is important to highlight that all RAP:AA proportions present minimum resistance for use as a road construction material, in accordance with the requirements of the National Department of Infrastructure and Transport of Brazil (DNIT) (ABNT 2012).

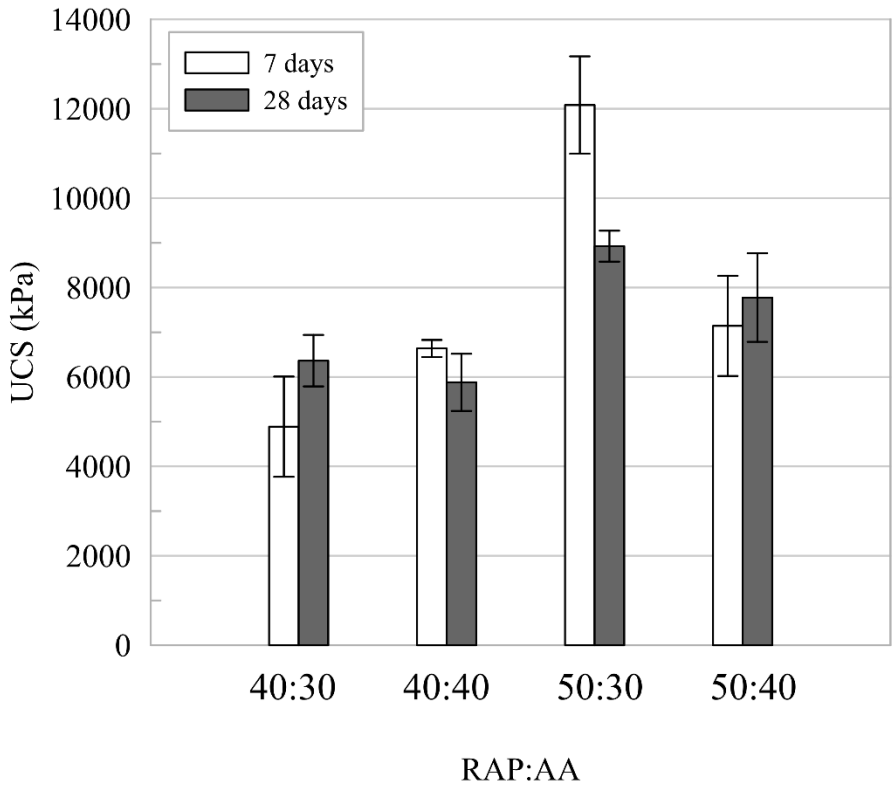

Figure 5.5. Compressive strength of RAP-AA blends cured for 7 and 28 days

Figure 5.6 presents the results of resistance to diametral compression for the mixtures evaluated. Observing the results, it is possible to affirm that the increase in the consumption of AA provides an increase in the tensile strength by diametral compression, regardless of the percentage of RAP evaluated. When evaluating the influence of the RAP content, it is observed that there is a significant influence only for low levels of AA; increasing RAP from 40% to

50% RAP increased tensile strength by 44% for blends with 30% AA. The greater stiffness of mixtures with high levels of milled material may be related to the presence of aged binder (Barreto Torres et al. 2022). However, the presence of aged asphalt binder and its incorporation in high amounts can create mixtures with high rigidity. As a result, such mixtures may present a reduction in workability, weakening them and reducing their resistance, especially to fatigue (Al-Qadi et al. 2012; Rocha Segundo et al. 2016).

Another interesting behavior to be mentioned is that during the tests, the specimens had subtle ruptures, that is, the cylinders did not separate and continued to support some load after the initial fracture. This behavior during failure can be attributed to the fact that the milled aggregate is a fractured aggregate due to the nature of its extraction in the field (Sachet et al. 2011). Therefore, the failure probably occurred in the fractured aggregate and not in the binder.

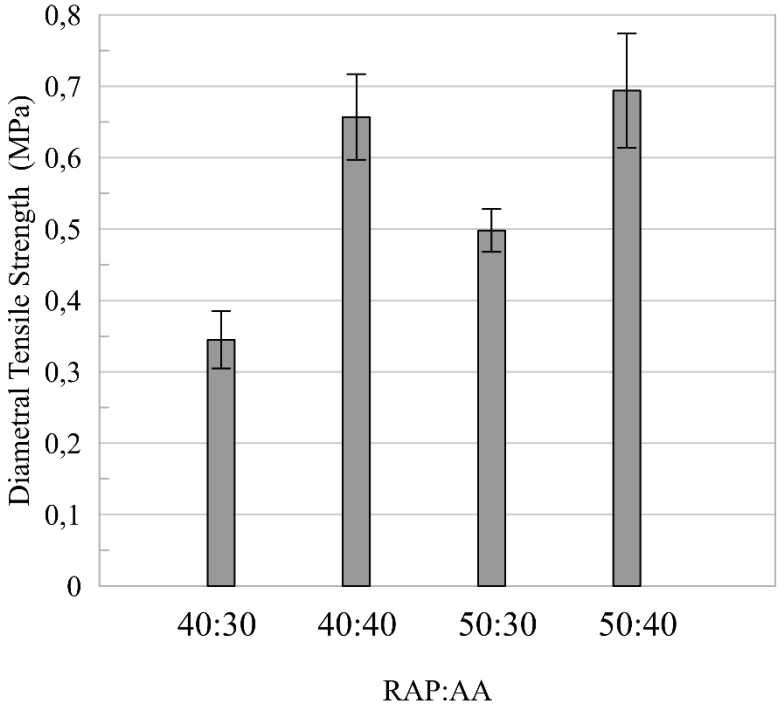

Figure 5.6. Diametral compressive strength of RAP-AA blends cured for 7 days

Although most recommendations and testing regimes are focused on UCS testing to determine the suitability of geomaterials for construction activities, flexural stresses and tensile stresses are often overlooked (Mohammadinia et al. 2019). To investigate the performance of alkali-activated RAP under bending and tensile forces, the four-point bending test was performed under both monotonic forces and cyclic loading conditions. The flexural strength

calculated from the maximum peak load before failure for the different RAP:AA ratios are shown in Fig. 5.7. Mean tensile stress values at rupture ranged from 0.09 MPa to 0.93 MPa and increased with higher binder contents. For the AA content of 30%, mixtures with 50% RAP were more flexible than those with 40% RAP. This behavior is contrary to that of RAP stabilized with cement, in which the materials tend to lose strength with the addition of RAP. However, other authors have also observed similar behavior for RAP stabilized with cement and explain that RAP possibly has agglomerates of fine grains bonded together with an asphalt binder (mastic), forming a type of "aggregate" that has low rigidity (Fedrigo et al. 2021).

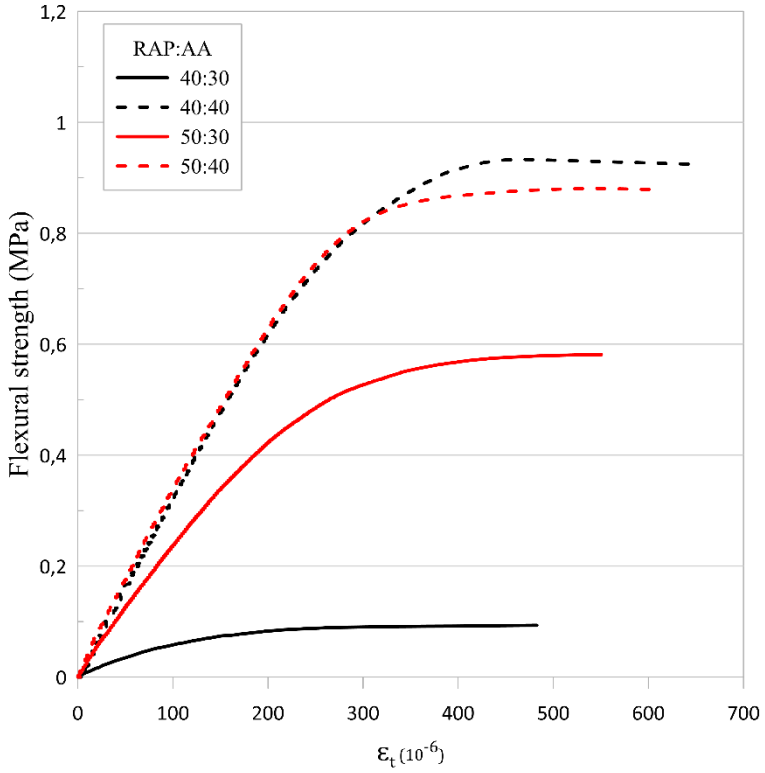

Figure 5.7. Flexural strength - displacement curves of RAP-AA blends

Figures 5.8, 5.9 and 5.10 show the results of the fatigue test on prismatic samples subjected to flexion-tension tested at 70%, 80% and 90% of peak load, respectively, at controlled room temperature (23 ± 2 °C). It is observed that the samples with RAP:AA ratio = 50:40 presented the highest modules and resisted the highest load cycles for all evaluated stress ranges. On the other hand, in the same way as in the results of UCS and diametral resistance, the samples with RAP:AA = 50:30 presented lower fatigue life than the other samples for all the evaluated load ranges. As can be seen in Figs 5.8, 5.9 and 5.10, the fatigue life for samples

with RAP:AA = 50:40 is significantly higher compared to samples with RAP:AA = 50:30, withstanding 11, 15 and 7 times more cycles, respectively.

Samples with RAP:AA ratio = 50:40 and 40:40 showed similar initial modulus, however, over the cycles these mixtures showed different fatigue life behavior. Thus, it can be observed that there is a RAP:AA ratio that can be considered better from the point of view of increasing tensile strength due to a longer service life to fatigue in the recycling of layers cemented by alkali activation.

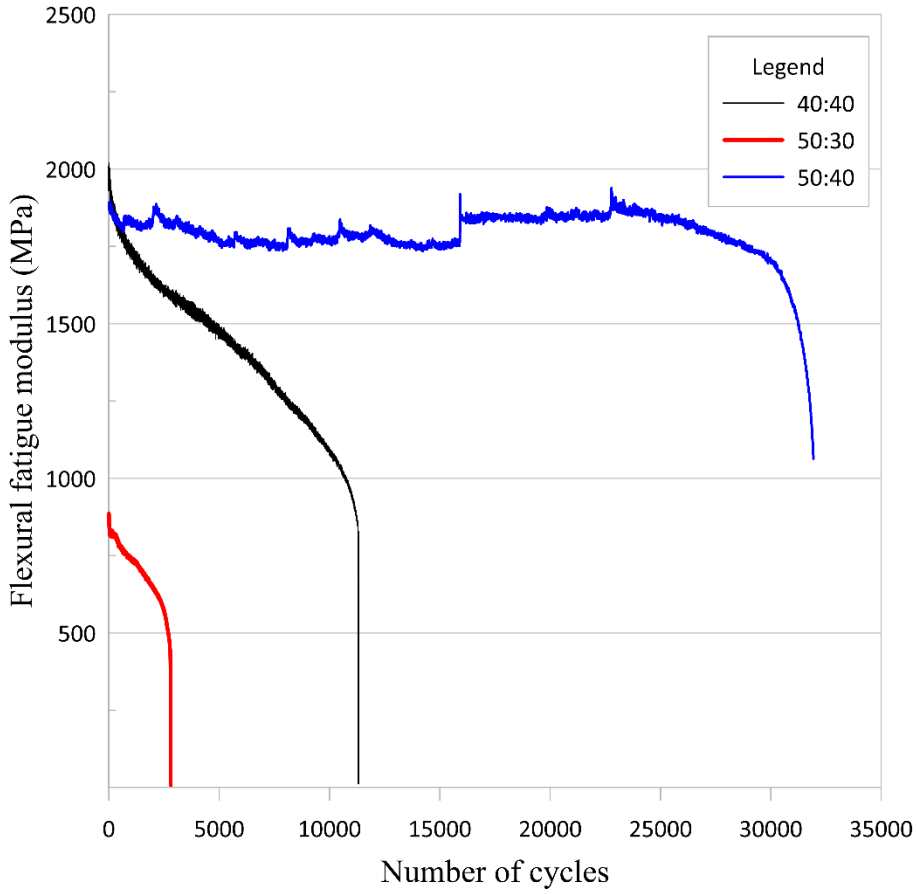

Figure 5.8. Variation of flexural fatigue modulus for RAP-AA blends with stress level of 70% of peak load from the flexural testing

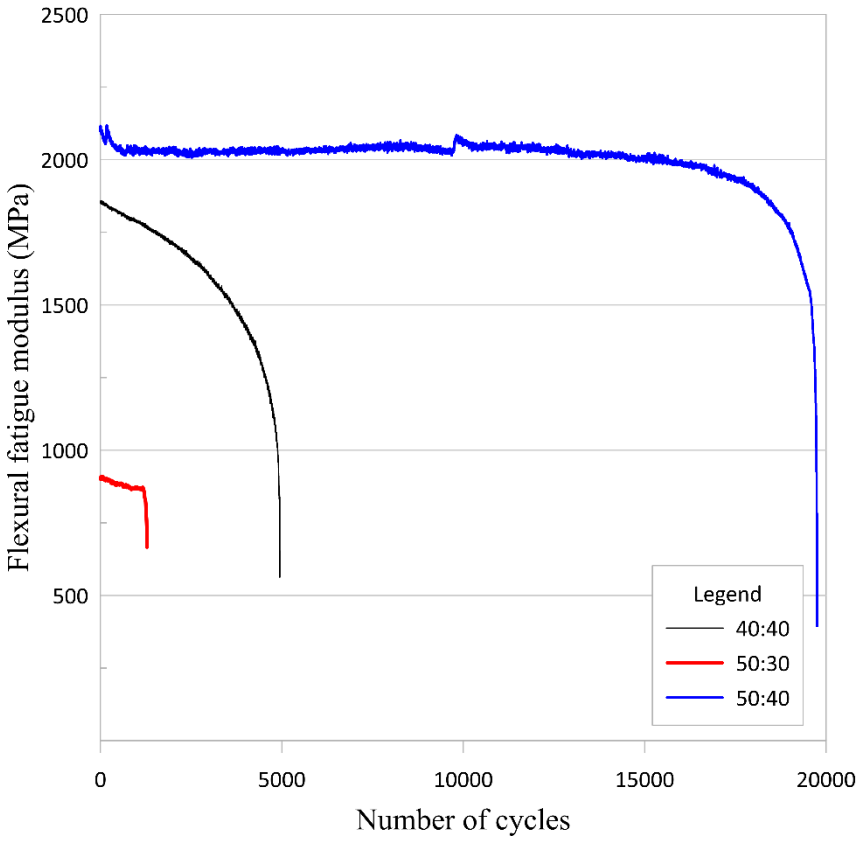

Figure 5.9. Variation of flexural fatigue modulus for RAP-AA blends with stress level of 80% of peak load from the flexural testing

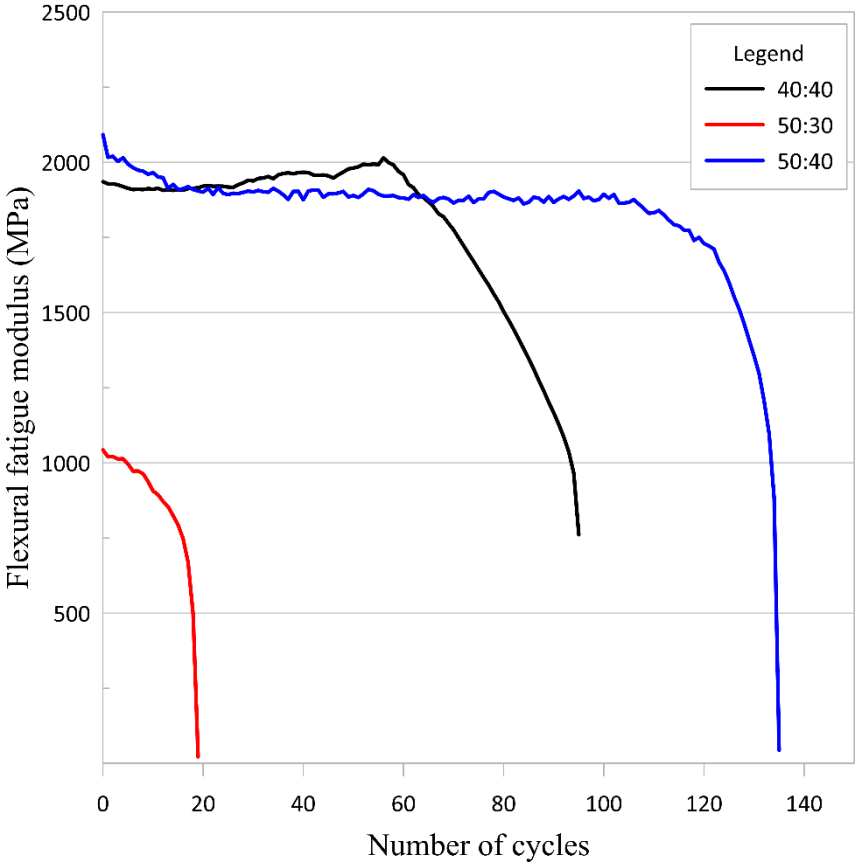

Figure 5.10. Variation of flexural fatigue modulus for RAP-AA blends with stress level of 90% of peak load from the flexural testing

Typical pattern of conventional cement-treated materials showing three stages of damage (Alvaro et al. 2013; Jia et al. 2018; Mandal et al. 2016, 2018) was not observed in the present study. For samples with RAP:AA ratio = 50:40, when subjected to cyclic loading, it is observed that the modulus remains approximately constant for most of the test, followed by a rapid reduction of this parameter shortly before the failure stress, associated with the formation of greater damage to the cementitious structure. Similar results of alkali-activated stabilized RAP also identified high flexural fatigue strength and highly brittle behavior for both high and low calcium systems (Mohammadinia et al. 2019). The samples with RAP:AA ratio = 40:40 and 50:30 showed a tendency of degradation of the modulus similar to each other. As in other studies (Jallu et al. 2020), for these RAP:AA ratios, the modulus decreased over the cycles until it reached approximately half of the initial modulus, and then suffered rupture. It is also worth mentioning that no visible cracks were observed in the specimens until the imminence of rupture.

4. Conclusions

This research aimed to investigate the development of low-cost activators in alkali-activated materials for the stabilization of RAP under the condition of repetitive heavy traffic load for use in base and sub-base layers of pavements. Based on the analyzed data, the conclusions of this article are:

a) The evaluation of simple compressive strength for different RAP:AA ratios showed that all evaluated mixtures meet the resistance requirements for use as base material and sub-bases for pavements in accordance with the criteria established by DNIT;

b) The flexural tensile strength of RAP mixtures treated with activated alkali binders increased for higher binder contents. Unlike cement-stabilized RAP, in which there is a tendency for strength loss as more RAP is added, the use of activated alkali binder provided more flexible mixes for higher RAP contents;

c) The fatigue failure of the mixtures was shown to be affected by the applied stress level. Mixtures subjected to high stress levels tend to fail with fewer cycles;

d) It can be observed that the samples with RAP:AA ratio = 50:40 showed the highest indirect tensile strength and the highest modulus of fatigue in bending and resisted the highest load cycles for all ranges of stresses evaluated. Therefore, flexible pavements with base and sub-base layers with high RAP contents can be recycled without compromising mechanical resistance over time;

e) Two distinct behaviors were observed for the mixtures when subjected to cyclic loading: the RAP:AA ratio = 50:40 showed brittle behavior and longer fatigue life, while for the other mixtures failure occurred when approximately 50% of the modulus value was reached initial;

4. CONSIDERAÇÕES FINAIS

Os resultados dessa pesquisa foram divididos em capítulos específicos, os quais foram apresentados na forma de artigos e cada um representa um dos objetivos específicos. Em cada artigo foram apresentados a revisão bibliográfica, os materiais e o métodos experimentais utilizados, bem como os resultados, discussões e principais conclusões de cada etapa. Desta forma, nesse capítulo se faz um fechamento destas etapas individuais indicando as conclusões de cada artigo, as principais contribuições da tese e recomendações para novas pesquisas.

4.1 Conclusões

Sobre a revisão da literatura a respeito do uso de álcali ativação na reciclagem profunda de RAP:

- A técnica é estudada em uma quantidade bastante limitada de trabalhos e pode ser considerada bem recente. Apesar das excelentes contribuições e dos resultados promissores das pesquisas já realizadas até então, vale ressaltar que todos os trabalhos utilizam uma solução ativadora composta por hidróxido ou silicato de sódio, ou ainda uma combinação dos dois. Tendo em vista a considerável contribuição na emissão de CO_2 na fabricação desses produtos, identificou-se uma lacuna de pesquisa voltada para o desenvolvimento de ativadores alcalinos com menor impacto ambiental e sua possível aplicação na reciclagem profunda de pavimento asfáltico fresado.

Em relação a influência dos parâmetros na produção de pastas álcali ativadas utilizando ligante álcali ativado alternativo a partir da dissolução de CCA:

- O tempo de moagem da CCA e o tempo de cura em temperatura elevada não afetaram significativamente o desempenho mecânico das pastas álcali ativadas, sendo utilizados, portanto, menores tempos (moagem de 30 min e cura por 20 horas) de forma a promover uma redução de energia no processo de produção. A avalição do tempo de dissolução indicou que a partir de 6 horas também não se obtém melhoras significativas na resistência, indicando ser esse o tempo de dissolução ideal. Em relação a temperatura de cura foi identificada uma faixa de temperatura que apresentou melhor desempenho mecânico, sendo adotado o extremo inferior (40°C) como a temperatura de cura ideal. As pastas álcali ativadas produzidas a partir desse processo de produção apresentaram uma taxa de reação mais lenta e resistências mais altas do que as pastas produzidas com silicato de sódio comercial.

Sobre a influência das diferentes proporções de agregados e solução álcali ativadora no comportamento mecânico e microestrutural das misturas de RAP e ligante álcali ativado alternativo:

- As propriedades mecânicas relacionadas a resistência a compressão simples resultaram em uma relação direta entre o teor de ligante álcali ativado e RAP, onde o aumento no teor de ligante álcali ativado proporcionou melhor comportamento mecânico para todas as misturas avaliadas. As análises microestruturais também confirmaram esses resultados evidenciando a presença de minerais ricos em sílica e alumina, que indicam a formação de estruturas de geopolimerização (N-A-S-H). A temperatura de cura não afetou os resultados mecânicos para mesmos períodos de cura, no entanto aparenta inibir a formação de eflorescência. No entanto a exposição a temperaturas maiores levou a formação de trincas que resultaram em redução no desempenho mecânico das misturas.

A respeito da influência das condições de cura no comportamento mecânico e microestrutural das misturas de RAP e ligante álcali ativado alternativo:

- A temperatura de cura foi o fator que governou a resistência à compressão simples das misturas, seguida pelo tempo de cura. Particularmente o tempo de cura em estufa não apresentou influência estatística significativa. De um modo geral, as misturas curadas em temperaturas e tempos de cura mais elevados resultaram em melhor comportamento mecânico devido a formação de estruturas mais homogêneas e densas devido ao preenchimento de vazios pelos géis cimentantes do processo de ativação alcalina. No entanto, períodos prolongados de cura em altas temperaturas afetaram negativamente na resposta mecânica do material.

Se tratando da durabilidade, comportamento mecânico a longo prazo e lixiviação de álcalis das misturas de RAP e ligante álcali ativado (LAA) alternativo:

- Apenas as misturas com relação RAP: LAA = 40:40, 50:30 e 50:40 atenderam satisfatoriamente às especificações normativas para perda de massa, atendendo também a resistência mínima de projeto para bases e sub-bases de rodovias após os ciclos de molhagem e secagem. A longo prazo foi evidenciado uma redução no comportamento mecânico para a maiores concentrações de ligante. Além disso, essas misturas não têm impacto ambiental, pois os resultados dos testes ambientais.

Por fim são apresentadas as conclusões baseadas na resistência a tração e o comportamento flexural estático e dinâmico das misturas das misturas de RAP e ligante álcali ativado (LAA) alternativo:

- Os resultados mostraram que o uso de LAA proporcionou misturas mais flexíveis para maiores teores de RAP e que pavimentos flexíveis com camadas de base e sub-base com alto teor de RAP podem ser reciclados in situ sem comprometer a resistência mecânica ao longo do tempo. Além disso, dependendo do teor de RAP e LAA utilizados, quando submetidas a carregamento cíclico, as misturas podem apresentar comportamento frágil ou romper ao atingir aproximadamente 50% do seu modulo inicial. Por fim os modelos probabilísticos de vida de fadiga mostraram uma tendência bem definida onde os dados ficaram muito próximos da curva de regressão ajustada.

4.2 Principais contribuições ao conhecimento

Esta pesquisa avançou no conhecimento cientifico em relação a viabilidade técnica de um sistema álcali ativado de cinza de casca de arroz, metacaulim e hidróxido de sódio na reciclagem profunda de pavimentos. A seguir são resumidas as descobertas mais significativas deste pesquisar:

a) A avalição das diversas variáveis envolvidas no processo de produção de um silicato de sódio alternativo é relevante para a obtenção de um melhor desempenho mecânico dos materiais álcali ativados, mas ainda mais importante no sentido de reduzirem os custos, consumo energético e impactos ambientais;
b) As proporções de RAP e ligante álcali ativado afetam no comportamento mecânico das misturas devendo ser levantadas em consideração no processo de reciclagem de pavimentos;
c) A avaliação das condições de cura demonstrou que apesar de existirem temperaturas em que o desempenho das misturas recicladas de RAP e ligante álcali ativado é melhor quando expostos a temperaturas mais altas, essas misturas atendem aos requisitos normativos para uso em base e sub-base de rodovias mesmo a temperatura ambiente;
d) O ligante álcali ativado alternativo mostrou-se eficiente para reciclagem de RAP, tanto em termos de comportamento mecânico, quanto do ponto de vista ambiental por não apresentar nenhum risco significativo ou características perigosas e principalmente por reduzir as emissões de CO2 resultantes da produção de silicato de sódio;

e) É possível reciclar pavimentos com RAP e ligante álcali ativado sem comprometer o comportamento mecânico e à fadiga da camada reciclada.

4.3 Recomendações para pesquisas futuras

Com base nos resultados e conclusões apresentados nesse documento, as seguintes recomendações são sugeridas para novas pesquisas:

a) Avaliar o comportamento de outros precursores, provenientes de resíduos por exemplo, na reciclagem de RAP por meio da técnica de álcali ativação;
b) Avaliar o impacto ambiental, social e econômico do ligante álcali-ativado e das misturas de RAP recicladas por meio de uma Análise de Ciclo de Vida (ACV);
c) Investigar se as características do ligante asfáltico presente no RAP afetam o comportamento mecânico das misturas de RAP recicladas por álcali ativação;
d) Avaliar o desenvolvimento de um material álcali ativado pelo método “one-part mix” que também utilize uma fonte alternativa de silicato de sódio.

REFERÊNCIAS

AHMED, A.T., KHALID, H.A. Effectiveness of Novel and Traditional Treatments on the Performance of Incinerator Bottom Ash Waste. **Waste Management**, n. 31, p. 2431 – 2439, 2011.

AIELLO R., CREA, F., NASTRO, A., SUBOTIÉ, B., TESTA, F. Zeolites 11:767, 1991.

ALAM, Q., HENDRIX, Y., THIJS, L., LAZARO, A., SCHOLLBACH, K., BROUWERS, H. Novel low temperature synthesis of sodium silicate and ordered mesoporous silica from incineration bottom ash. **Journal of Cleaner Production**, v. 211, p. 874–883, 2019.

ALANAZI, H., YANG, M., ZHANG, D., GAO, Z.J. Bond strength of PCC pavement repairs using metakaolin- based geopolymer mortar. **Cement and Concrete Composites**, v. 65, p. 75–82, 2016.

AL BAKRI, A.M.M., ABDULKAREEM, O.A., RAFIZA, A.R., ZARINA, Y., NORAZIAN, M.N., KAMARUDIN, H. Review on Processing of Low Calcium Fly Ash Geopolymer, **Concrete**, v. 7, p. 342–349, 2013.

ALDRED, J., DAY, J. Is geopolymer concrete a suitable alternative to traditional concrete. **37th Conference on Our World in Concrete & Structures**, Singapore, pp. 29–31, 2012.

ALNAHHAL, M.F., ALENGARAM, U.J., JUMAAT, M.Z., ALQEDRA, M.A., MO, K.H., SUMESH, M. Evaluation of industrial by-products as sustainable pozzolanic materials in recycled aggregate concrete. **Sustainability**, v. 9, n. 5, p. 767, 2017.

ALNAHHAL, M.F., KIM, T., HAJIMOHAMMADI, A. Waste-derived activators for alkali-activated materials: A review. **Cement and Concrete Composites**, v. 118, , p. 103980, 2021.

AL-QADI, I.L., ELSEIFI, M., CARPENTER, S.H. Reclaimed Asphalt Pavement - A Literature Review, FHWA:Washington, DC, USA, 2007.

AL-SHATHR, B.S., AL-ATTAR, T.S., HASAN, Z.A. Optimization of Geopolymer Concrete Based on Local Iraqi Metakaolin, **The 2nd International Conference of Buildings, Construction and Environmental Engineering**, 2015.

ANDREOLA, F., BARBIERI, L., LANCELLOTTI, I. The environmental friendly route to obtain sodium silicate solution from rice husk ash: a comparative study with commercial silicates deflocculating agents, **Waste Biomass Valorization**, p. 1–11, 2019.

ANTIOHOS, S., PAPADAKIS, V., TSIMAS, S. Rice husk ash (RHA) effectiveness in cement and concrete as a function of reactive silica and fineness. **Cement and Concrete Research**, v. 61, p. 20–27, 2014.

ANTONI, S. WIJAYA, W., HARDJITO, D. Compressive Strength of Geopolymer using Fly Ash from Various Sources. **Materials Science Forum**, v. 841, n. 1, p. 0-5, 2016.

ANTONI, S. WIJAYA, W., HARDJITO, D. Factors Affecting the Setting Time of Fly Ash - Based Geopolymer. **Materials Science Forum**, v. 841, p. 90- 97, 2016.

AMARH, E. A., FERNANDEZ-GÓMEZ, W., FLINTSCH, G., DIEFENDERFER, B. K., e BOWERS, B. F. Nondestructive in situ characterization of elastic moduli of full-depth reclamation base mixtures. **Transportation Research Record: Journal of the Transportation Research Board**, v. 2641, p. 1–11, 2017.

AMERICAN SOCIETY FOR TESTING AND MATERIALS – ASTM. **D 559**: Standard test methods for wetting and drying compacted soil-cement mixtures, ASTM International, Philadelphia, 2015.

APOLÔNIO, P. H. **Produção de geopolímeros usando cinza de casca de arroz como fonte complementar de sílica**. Dissertação. Universidade Federal de Pernambuco, 2017.

ARULRAJAH, A., DISFANI, M. M., HAGHIGHI, H., MOHAMMADINIA, A., HORPIBULSUK, S. Modulus of rupture evaluation of cement stabilized recycled glass/recycled concrete aggregate blends. **Construction and Building Materials**, v. 84, p. 146–155, 2015.

ARULRAJAH, A., PIRATHEEPAN, J., DISFANI, M.M. Reclaimed asphalt pavement and recycled concrete aggregate blends in pavement subbases: laboratory and field evaluation. **Journal of Materials in Civil Engineering**, v. 26, p. 349–357, 2014. https://doi.org/10.1061/(ASCE)MT.1943-5533.0000850

ASSOCIAÇÃO BRASILEIRA DE NORMAS TÉCNICAS - ABNT. NBR 13554: Solo-cimento – Ensaio de durabilidade por molhagem e secagem, Rio de Janeiro, 1996.

ASSOCIATION OF AUSTRALASIAN ROAD TRANSPORT AND TRAFFIC AGENCIES. **Preliminary Investigation of the Influence of Micro-cracking on Fatigue Life of Cemented Materials**: *Austroads* Publication AP-T198. Sydney, 65p. 2012.

AUSTRALIAN ASPHALT PAVEMENT ASSOCIATION - AAPA. Reclaimed Asphalt Pavement (RAP) Management Plan; **National Technology & Leadership Committee**: Port Melbourne, Australia, 2018.

AVILA, T. C. **Estudo da utilização da mistura de cinza da casca de arroz com hidróxido de sódio na produção de argamassas ativadas alcalinamente**. Dissertação. Faculdade de Engenharia – UNESP, 2018.

AVIRNENI, D., PEDDINTI, P.R.T.T., SARIDE, S. Durability and long term performance of geopolymer stabilized reclaimed asphalt pavement base courses. **Construction and Building Materials**, v. 121, p. 198–209, 2016. https://doi.org/10.1016/j.conbuildmat.2016.05.162

AYDIN, S., BARADAN, B. Mechanical and microstructural properties of heat cured alkali-activated slag mortars, **Materials and Design**, v. 35, p. 374–383, 2012.

BABASHAMSI, P., NUR, I.M.Y, HALIL, C., NOR, G.M.N, HASHEM, S.J. Evaluation of pavement life cycle cost analysis: Review and analysis. **International Journal of Pavement Research and Technology**, v. 9, n. 4, p. 241 - 254, 2016.

BABURAMANI, P. Asphalt Fatigue Life Prediction Models – A Literature Review. **ARRB Transport Research Ltd., Research Report ARR 334**, pp. 40, Vermont South, Victoria, 1999.

BEHAK, L. **Análise estrutural de Pavimentos de Baixo Volume de Tráfego Revestidos com Solo Modificado com Cal Considerando Ensaios Laboratoriais e Monitoramento de Trechos Experimentais**. Tese de Doutorado (Engenharia Civil). Universidade Federal do Rio Grande do Sul, Porto Alegre, 2013, 298p.

BERNAL, S.A., RODRÍGUEZ, E.D., MEJÍA DE GUTIERREZ, R., GORDILLO, M., PROVIS, J.L. Mechanical and thermal characterisation of geopolymers based on silicate-activated metakaolin/slag blends. **Journal of Materials Science**, v. 46, p. 5477–5486, 2011.

BERNAL, S.A., RODRÍGUEZ, E.D., MEJIA DE GUTIÉRREZ, R., PROVIS, J.L., DELVASTO, S. Activation of metakaolin/slag blends using alkaline solutions based on chemically modified silica fume and rice husk ash. **Waste and Biomass Valorization**, v. 3, n. 1, p. 99–108, 2012.

BERNAL, S.A., RODRÍGUEZ, E.D., DE GUTIÉRREZ, R.M., PROVIS, J.L. Performance at high temperature of alkali-activated slag pastes produced with silica fume and rice husk ash based activators. **Materiales de Construcción**, v. 65, p. 1–10, 2015. https://doi.org/10.3989/mc.2015.03114

BERNUCCI, L.B., MOTTA, L.M.G., CERATTI, J.A.P., SOARES, J.B. **Pavimentação Asfáltica: Formação Básica para Engenheiros**. Rio de Janeiro. PETROBRAS: ABEDA, 2008. 475 p.

BESSA, I.S., ARANHA, A.L., VASCONCELOS, K.L., SILVA, A.H.M., e BERNUCCI, L.L.B. Laboratory and field evaluation of recycled unbound layers with cement for use in asphalt pavement rehabilitation. **Materials and Structures**, v. 49, n. 7, p. 2669–2680, 2016.

BONDAR, D., LYNSDALE, C.J., MILESTONE, N.B., HASSANI, N., RAMEZANIANPOUR, A.A. Effect of type, form, and dosage of activators on strength of alkali-activated natural pozzolans. **Cement and Concrete Composites**, v. 33, p. 251-260, 2011. https ://doi.org/10.1016/j.cemco ncomp .2010.10.021

BONFIM, V. **Fresagem de pavimentos asfálticos**. 3ª ed. São Paulo: Exceção Editorial, 123 p., 2007.

BOUZÓN, N., PAYÁ, J., BORRACHERO, M.V., SORIANO, L., TASHIMA, M.M., MONZÓ, J. Refluxed rice husk ash/NaOH suspension for preparing alkali activated binders. **Materials Letters**, v. 115, p. 72–74, 2014. https://doi.org/10.1016/j.matlet.2013.10.001

BOYCE, J.R. **The Behaviour of Granular Material under Repeated Loading**. Tese de Doutorado em Filosofia, Department of Civil Engineering, University of Nottingham, Reino Unido, 1976.

BRAHAM, A. Comparing life-cycle cost analysis of full-depth reclamation versus traditional pavement maintenance and rehabilitation strategies, **Transportation Research Record: Journal of the Transportation Research Board**, v. 2573, p. 49–59, 2016. https://doi.org/10.3141/2573-07

BRAND, A.S. e ROESLER, J.R. Bonding in cementitious materials with asphaltcoated particles: Part I - the interfacial transition zone. **Construction and Building Materials,** v. 130, p. 171–181, 2017.https://doi.org/10.1016/j.conbuildmat.2016.10.019

BRETT, A.W., WILLIS, J.R., ROSS, T.C. Asphalt Pavement Industry Survey on Recycled Materials and Warm-Mix Asphalt Usage. **National Asphalt Pavement Association,** 2018, 9th ed.; IS 138, Greenbelt, MD, USA, 2019.

BUMANIS, G., VITOLA, L., BAJARE, D., PUNDIENE, I. Impact of Reactive SiO2/Al2O3 ratio in precursor on durability of porous álcali activated materials. **Ceramics International**, v. 43, n. 7, p. 5471-5477, 2017. https ://doi.org/10.1016/j.ceram int.2017.01.060

CARDOSO, S. H., CABRAL, A. A. A., SEIXAS, S., TINOCO, G. J. R. e SANTOS, C. A. Influence of Compactive Effort and Soaking Period on the CBR of Base Course Lateritic Soils Improved with Cement for Low Volume Roads. **1° Simpósio Internacional de**

Pavimentos de Rodovias de Baixo Volume de Tráfego, Rio de Janeiro, RJ, v. 1, p. 297-308, 1997.

CERATTI, J. A. e CASANOVA, F. J. Um Método Físico-Químico para Dosagem de Solo-cimento. **Simpósio sobre Novos Conceitos em Ensaios de Campo e Laboratório em Geotecnia**, Rio de Janeiro, RJ, p. 191-200, 1988.

CHATTI, K., ZABAAR, I. Estimating the Effects of Pavement Condition on Vehicle Operating Costs, NCHRP: Washington, DC, USA, 2012.

CNT – CONFEDERAÇÃO NACIONAL DE TRANSPORTES. **Pesquisa CNT de rodovias 2019**. Brasília: CNT: SEST SENAT, 2019.

CRIADO, M., PALOMO, A., FERNÁNDEZ-JIMÉNEZ, A. Alkali activation of fly ashes. Part 1: Effect of curing conditions on the carbonation of the reaction products. **Fuel**, v. 84, p. 2048–2054, 2005.

DALLA ROSA, F., JORGE, F.S., BRITO, L.A.T., e CERATTI, J.A.P. Análise do comportamento mecânico de um pavimento reciclado com adição de diferentes agentes estabilizadores. **Transportes**, v. 23, n. 2, p. 95–104, 2015.

DAVIDOVITS, J. **Geopolymer Chemistry and Applications**, third ed., Geopolymer Institute, 2014.

DAVIDOVITS, J. **Geopolymer Chemistry and Applications**, 4ª edição, Institut Géopolymère, Saint-Quentin, 2008.

DAVIDOVITS, J. Geopolymers - Inorganic polymeric new materials. **Journal of Thermal Analysis and Calorimetry**, v. 37, p. 1633-1656, 1991. doi:10.1007/BF01912193

DAVIDOVITS, J. Geopolymeric Reactions in Archaeological Cements and in Modern Blended Cements. In: Davidovits, J., Orlinski, J. (Eds.), **Proceedings of the 1st International Conference on Geopolymer '88**, vol. 1, Compiegne, France, pp. 93–106, 1987.

DELLABIANCA, L.M.A. **Estudo do Comportamento de Material Fresado de Revestimento Asfáltico Visando sua Aplicação em Reciclagem de Pavimentos**. Tese (Doutorado em Engenharia), Faculdade de Tecnologia, Universidade de Brasília, Brasília, 2004, 110p.

DELLA, V.P., KÜHN, I., HOTZA, D. Rice husk ash as an alternate source for active silica production. **Materials Letters**, v. 57, p. 818–821, 2002. https://doi.org/10.1016/S0167-577X(02)00879-0

DEPARTAMENTO NACIONAL DE INFRAESTRUTURA DE TRANSPORTE – DNIT. **Manual de restauração de pavimentos asfálticos**. 2ª ed. Rio de Janeiro, 2006, 310 p.

DEPARTAMENTO NACIONAL DE INFRAESTRUTURA DE TRANSPORTES. **Pavimentação – Reciclagem de Profunda de Pavimentos "in situ" com adição de cimento Portland ‑ Especificação de serviço**: DNIT 167/2013. Rio de Janeiro, 11p. 2013.

DEPARTAMENTO NACIONAL DE INFRAESTRUTURA DE TRANSPORTES. DNIT 134/2010 – ME: **Pavimentação - Solos - Determinação do Módulo de Resiliência - Método de Ensaio**. Rio de Janeiro, 2010.

DETPHAN, S. E CHINDAPRASIRT, P. Preparation of fly ash and rice husk ash geopolymer. **International Journal of Minerals, Metallurgy and Materials**, v. 16, n. 6, p. 720, 2009.

DIAZ–LOYA, E.I., ALLOUCHE, E.N., VAIDYA, S. Mechanical properties of fly–ash–based geopolymer concrete. **ACI Materials Journal**, v. 108, n. 3, p. 300–306, 2011.

DIXON, P.A., GUTHRIE, W.S. e EGGETT, E.L. Factors affecting strength of road base stabilized with cement slurry or dry cement in conjunction with full-depth reclamation. **Transportation Research Record: Journal of the Transportation Research Board**, v. 2310, p. 113–120, 2012.

DUAN P., YAN C., ZHOU, W. Influence of partial replacement of fly ash by metakaolin on mechanical properties and microstructure of fly ash geopolymer paste exposed to sulfate attac. Ceramics International, v. 42, p. 1–14, 2015. http://dx.doi.org/10.1016/j.ceramint.2015.10.154

DUXSON, P., FERNÁNDEZ-JIMÉNEZ, A., PROVIS, J.L., LUKEY, G.C., PALOMO, A., VAN DEVENTER, J.S.J. Geopolymer technology: The current state of the art, **Journal of Materials Science**, v. 42, p. 2917-2933, 2007. doi:10.1007/s10853-006-0637-z

DUXSON, P., PROVIS, J.L., LUKEY, G.C., MALLICOAT, S.W., KRIVEN, W.M., VAN DEVENTER, J.S.J. Understanding the relationship between geopolymer composition, microstructure and mechanical properties. **Colloids and Surfaces**, v. 269, p. 47-58, (2005). doi: 10.1016/j.colsurfa.2005.06.060

EDUOK, E. I, **Thermal Properties of Geopolymer Materials**, Master thesis, University of Stavanger, Norway, 2016.

EPPS, J.A.; MONISMITH, C.L. Influence of Mixture Variables on the Flexural Fatigue Properties of Asphaltic Concrete. **Journal of the Association of Asphalt Paving Technologists**, v. 38, p. 423 – 464, Lino Lakes, Minnesota, 1969.

EUROPEAN ASPHALT PAVEMENT ASSOCIATION - EAPA. Asphalt the 100% Recyclable Construction Product - **EAPA Position Paper**, EAPA: Brussels, Belgium, 2014.

FAO: Organizacion de las Naciones Unidas para la Alimentacion y la Agricultura. FAO, Rome, 2019.

FARHAN, K. Z.; JOHARI, M. A. M.; DEMIRBOĞA, R. Assessment of important parameters involved in the synthesis of geopolymer composites: A review. **Construction and Building Materials**, v. 264, 2020.

FAWER, M., CONCANNON, M., RIEBER, W. Life cycle inventories for the production of sodium silicates. **The International Journal of Life Cycle Assessment**, n. 207, 1999.

FEDRIGO, W., NÚÑEZ, W. P., KLEINERT, T. R., MATUELLA, M. F., e CERATTI, J. A. P. Strength, shrinkage, erodibility and capillary flow characteristics of cement-treated recycled pavement materials. **International Journal of Pavement Research and Technology**, v. 10, n. 5, p. 393–402, 2017a.

FEDRIGO, W., NÚÑEZ, W. P., SCHREINERT, G. G., KLEINERT, T. R., MATUELLA, M. F., LÓPEZ, M. A. C. e CERATTI, J. A. P. Flexural strength, stiffness and fatigue of cement-treated mixtures of reclaimed asphalt pavement and lateritic soil. **Road Materials and Pavement Design**, v. 22, n. 5, p. 1004-1022, 2021. Doi: 10.1080/14680629.2019.1660207

FERNÁNDEZ-JIMÉNEZ, A., PALOMO, A., CRIADO, M. Microstructure development of alkali-activated fly ash cement: a descriptive model. **Cement and Concrete Research**, v. 35, p. 1204-1209, 2005

FERNÁNDEZ-JIMÉNEZ, A., PALOMO, A., SOBRADOS, I., SANZ, J. The role played by the reactive alumina content in the alkaline activation of fly ashes. **Microporous and Mesoporous Materials**, v. 91, p. 111-119, 2006.

FERDOUS, W., MANALO, A., KHENNANE, A., KAYALI, O. Geopolymer concrete-filled pultruded composite beams – Concrete mix design and application. **Cement and Concrete Composites**, v. 58, p. 1–13, 2015.

GARCÍA-LODEIRO, I., FERNÁNDEZ-JIMÉNEZ, A., PALOMO, A. Variation in hybrid cements over time. Alkaline activation of fly ash–portland cement blends. **Cement and Concrete Research**, v. 52, P. 112–122. 2013.

FOLETTO, E.L., GRATIERI, E., OLIVEIRA, L.H., JAHN, S.L. Conversion of Rice Hull Ash into Soluble Sodium Silicate. **Materials Research**, v. 9, n. 3, p. 335–338, 2006.

GARCÍA-LODEIRO, I., PALOMO, A., FERNÁNDEZ-JIMÉNEZ, A., MACPHEE, D.E. Compatibility studies between N–A–S–H and C–A–S–H gels. Study in the ternary diagram Na2O–CaO–Al2O3–SiO2–H2O. **Cement and Concrete Research**, v. 41, p. 923–931, 2011.

GARTNE, R.E.M., MACPHEE, D.E. A physico-chemical basis for novel cementitious binders. **Cement and Concrete Research**, v. 41, p. 736–749, 2011.

GERALDO, R. H., FERNANDES, L. F. R., CAMARINI, G. Water treatment sludge and rice husk ash to sustainable geopolymer production. **Journal of Cleaner Production**, v. 149, p. 146–155, 2017.

GEORGE, A. M., BANERJEE, A., PUPPALA, A. J., E SALADHI, M. Performance Evaluation of Geocell-reinforced Reclaimed Asphalt Pavement (RAP) Bases in Flexible Pavements. **International Journal of Pavement Engineering**, v. 22, n. 2, p. 1-11, 2019.

CHINDAPRASIRT, P., DE SILVA, P., SAGOE-CRENTSIL, K., HANJITSUWAN, S. Effect of SiO2 and Al2O3 on the setting and hardening of high calcium fly ash-based geopolymer systems, **Journal of Materials Science**, v. 47, n. 12, p. 4876–4883, 2012.

GIANNOPOULOU, I., PANIAS, D. Structure, Design and Applications of Geopolymeric Materials. **3rd International Conference on Deformation Processing and Structure of Materials**, p. 5-15, 2007.

GIASUDDIN, H.M., SANJAYAN, J.G., RANJITH, P.G. Strength of geopolymer cured in saline water in ambient conditions, **Fuel**, v. 107, p. 34–39, 2013.

GLASBY, T., DAY, J., GENRICH, R., ALDRED, J. EFC geopolymer concrete aircraft pavements at Brisbane West Wellcamp Airport. **Concrete**, p. 1–9, 2015.

GLUKHOVSKY, V.D. Soil silicates. Gosstroyizdat, Kiev, 1959, 154pp

GNANENDRAN, C. T., PIRATHEEPAN, J. Determination of fatigue life of a granular base material lightly stabilized with slag lime from indirect diametral tensile testing. **Journal of Transportation Engineering**, v. 136, n. 8, p. 736–745, 2010.

GODENZONI, C., GRAZIANI, A., BOCCI, E., e BOCCI, M. The evolution of the mechanical behaviour of cold recycled mixtures stabilised with cement and bitumen: Field and laboratory study**. Road Materials and Pavement Design**, v. 19, n. 4, p. 856–877, 2018.

GOURLEY, J.T. Geopolymers; opportunities for environmentally friendly construction materials, **Conference: Adaptive materials for modern society**, Sydney, Institute of Materials Engineering Australia, 2003.

GRILLI, A., BOCCI, E., e TARANTINO, A.M. Experimental investigation on fibre-reinforced cementtreated materials using reclaimed asphalt. **Construction and Building Materials**, v. 38, p. 491–496, 2013a.

GUNASEKARA, C., LAW, D.W., SETUNGE, S. Effect of Composition of Fly Ash On Compressive Strength of Fly Ash Based Geopolymer Mortar. **23rd Australasian Conference on the Mechanics of Structures and Materials**, vol. 3, n. 1, 168-177, 2014.

GUTHRIE, W.S., BROWN, A.V., e EGGETT, D.L. Cement stabilization of aggregate base material blended with reclaimed asphalt pavement. **Transportation Research Record: Journal of the Transportation Research Board**, v. 2026, p. 47–53, 2007.

HABEEB, G.A., MAHMUD, H. B. Study on properties of rice husk ash and its use as cement replacement material. **Materials Research**, v. 13, p. 185–190, 2010. https://doi.org/10.1590/s1516-14392010000200011

HAJIMOHAMMADI, A., PROVIS, J.L., VAN DEVENTER, J.S. One-part geopolymer mixes from geothermal silica and sodium aluminate. **Industrial & Engineering Chemistry Research**, v. 47, n. 23, p. 9396–9405, 2008.

HAJIMOHAMMADI, A., VAN DEVENTER, J.S.J. Solid reactant-based geopolymers from rice hull ash and sodium aluminate. **Waste Biomass Valorization**, v. 8, n. 6, p. 2131–2140, 2017.

HE, J., JIE, Y., ZHANG, J., YU, Y., ZHANG, G. Synthesis and characterization of red mud and rice husk ash-based geopolymer composites. **Cement and Concrete Composites**, v. 37, p. 108–118, 2013. https://doi.org/10.1016/j.cemconcomp.2012.11.010

HE, J., ZHANG, J., YU, Y., ZHANG, G. The strength and microstructure of two geopolymers derived from metakaolin and red mud-fly ash admixture: a comparative study, **Construction and Building Materials**, v. 30, p. 80–91, 2012.

HORPIBULSUK, S., HOY, M., WITCHAYAPHONG, P., RACHAN, R., ARULRAJAH, A. Recycled asphalt pavement - fly ash geopolymer as a sustainable stabilized pavement material. **IOP Conference Series: Materials Science and Engineering**, v. 273, 2017. https://doi.org/10.1088/1757-899X/245/1/012005

HORPIBULSUK, S., C. PHETCHUAY, A. UDOMCHAI, A. ARULRAJAH. Calcium Carbide Residue-A Cementing Agent for Sustainable Soil Stabilization. **Geotechnical Engineering Journal of the SEAGS and AGSSEA**, v. 46, pp. 22-27, 2015.

HOY, M., HORPIBULSUK, S., ARULRAJAH, A. Strength development of recycledasphalt pavement - fly ash geopolymer as a road construction material, **Construction and Building Materials**, v. 117, p. 209–219, 2016. https://doi.org/10.1016/j.conbuildmat.2016.04.136

HOY, M., HORPIBULSUK, S., ARULRAJAH, A., MOHAJERANI, A. Strength and microstructural study of recycled asphalt pavement: slag geopolymer as a pavement base material. **Journal of Materials in Civil Engineering**, v. 30, 2018. https://doi.org/10.1061/(ASCE)MT.1943-5533.0002393

HOY, M., HORPIBULSUK, S., RACHAN, R., CHINKULKIJNIWAT, A., ARULRAJAH, A. Recycled asphalt pavement – fly ash geopolymers as a sustainable pavement base material: strength and toxic leaching investigations. **Science of The Total Environment**, v. 573, p. 19–26, 2016. https://doi.org/10.1016/j.scitotenv.2016.08.078

HU, M., ZHU, X., LONG, F. Alkali-activated fly ash-based geopolymers with zeolite or bentonite as aditives. **Cement and Concrete Composites**. v. 31, n. 10, p. 762– 768, 2009.

HUANG, Y.S. **Pavement Analysis and Design**. Ed. Prentice Hall, pp. 805, New Jersey, 1993.

IBRAHIM, D.M., EL-HEMALY, S.A., ABDEL-KERIM, F.M. Study of rice-husk ash silica by infrared spectroscopy. **Thermochim Acta**, v. 37, n. 3, p. 307–314, 1980.

INGLES, O G., METCALF, J. B. Soil Stabilization – Principles and Practice. **Australia: Butterworth's Pty. Limited**, 366p, 1972.

INSTITUTO ESPAÑOL DEL CEMENTO Y SUS APLICACIONES (IECA). Reciclado de firmes in situ con cemento: Guías técnicas, Madrid, Spain, 2013.

IVANOVA, I.I., AIELLO, R., NAGY, J.B., CREA, F., DEROUANE, E.G., DUMONT, N., NASTRO, A., SUBOTIC, B., TESTA, F. Influence of Cations on the Physicochemical and Structural Properties of Aluminosilicate Gel Precursors. **Multinuclear Magnetic Resonance Characterization**. **Microporous and Mesoporous Materials**, v. 3, n. 3, p. 245-257, 1994.

JALLU, M., ARULRAJAH, A., SARIDE, S., EVANS, R. Flexural fatigue behavior of fly ash geopolymer stabilized-geogrid reinforced RAP bases. **Construction and Building Materials**, v. 254, 2020. https://doi.org/10.1016/j.conbuildmat.2020.119263 119263

JASIENSKI, A. RENS L. In situ recycling with cement: The Belgian experience. **Proceedings of the 1st International Symposium on Subgrade Stabilization and In Situ Pavement Recycling Using Cement**, Salamanca, Spain, 2001.

JUNAID, M.T., KHENNANE, A., KAYALI, O., SADAOUI, A., PICARD, D., FAFARD, M. Aspects of the deformational behaviour of alkali activated fly ash concrete at elevated temperatures. **Cement and Concrete Research**, v. 60, p. 24-29, 2014. https://doi.org/10.1016/j.cemconres.2014.01.026

KALAPATHY, U., PROCTOR, A., SHULTZ, J. A simple method for production of pure silica from rice hull ash. **Bioresource Technology**, v. 73, n. 3, p. 257-262, 2000.

KAMSEU, E., BELEUK, L.M., MOUNGAM, A., CANNIO, M., BILLONG, N., CHAYSUWAN, D., MELO, U.C., LEONELLI, C. Substitution of sodium silicate with rice husk ash-NaOH solution in metakaolin based geopolymer cement concerning reduction in global warming. **Journal of Cleaner Production**, v. 142, n. 4, p. 3050-3060, 2016. https://doi.org/10.1016/j.jclepro. 2016.10.164.

KANI, E.N., ALI, A. Effects of curing time and temperature on strength development of inorganic polymeric binder based on natural pozzolan. **Journal of Materials Science**, v. 44, p. 3088–3097, 2009.

KATSAKOU, M., e KOLIAS, S. Mechanical properties of cement-bound recycled pavements. **Proceedings of the Institution of Civil Engineers - Construction Materials**, v. 160, n. 4, p. 171-179, 2007.

KENNEDY, W. O. TAM E M. SOLAIMANIAN. Optimizing Use of Reclaimed Asphalt Pavement with the SuperPave System. **Journal of the Association of Asphalt Paving Technologists**, v. 67, p. 311-333, 1998.

KEULEN, A., VAN ZOMEREN, A., DIJKSTRA, J.J. Leaching of monolithic and granular alkali activated slag-fly ash materials, as a function of the mixture design. **Waste Management**, v. 78, p. 497–508, 2018. https://doi.org/10.1016/j.wasman.2018.06.019

KHALID, H.A. A Comparison Between Bending and Diametral Fatigue Tests for Bituminous Materials. **Materials and Structures**, v. 33, n. 7, p. 457 - 465, 2000.

KOLIAS, S., KATSAKOU, M., e KALOIDAS, V. Mechanical properties of flexible pavement materials recycled with cement. **Proceedings of the 1st international symposium on subgrade stabilization and in situ pavement recycling using cement**, Salamanca, 2001.

KIM, H., KIM, Y. Relationship between compressive strength of geo-polymers and pre-curing conditions. **Applied Microscopy**, v. 43, p. 155–163, 2013.

KINGERY, W.D., BOWEN, H.K., UHLMANN, D.R. Introduction to ceramics. 2 ed. **Nova York: John Wiley & Sons**, xii, 1032 p, 1976.

KOMNITSAS, K., ZAHARAKI, D. Geopolymerisation: A review and prospects for minerals industry. **Minerals Engineering**, n. 20, p. 1261-1277, 2007.

KRIVENKO, P.V., SKURCHINSKAYA, J.V. Fly Ash Containing Geocements. 91 Shanghai International Conference on the Utilisation of Fly Ash and other Coal Combustion By-Products (1991) 64-1.

KUA, T.-A., IMTEAZ, M.A., ARULRAJAH, A. HORPIBULSUK, S. Environmental and economic viability of Alkali Activated Material (AAM) comprising slag, fly ash and spent coffee ground. **International Journal of Sustainable Engineering**, v. 12, p. 223-232, 2019. doi:10.1080/19397038.2018.1492043

KUEHL, H. US900939 A. Germany, 1908.

KUMAR, S., KUMAR, R. Mechanical activation of fly ash: Effect on reaction, structure and properties of resulting geopolymer. **Ceramics International**, v. 37, n. 2, p. 533–541, 2011.

KUSBIANTORO, A., NURUDDIN, M.F., SHAFIQ, N., QAZI, S.A. The effect of microwave incinerated rice husk ash on the compressive and bond strength of fly ash based geopolymer concrete, **Construction and Building Materials**, v. 36, p. 695–703, 2012.

LIMA, J.S. **Efeito da relação molar sio2/al2o3 e das condições de cura nas propriedades de geopolímeros obtidos com silicato de cinza da casca de arroz**. Dissertação, Centro Acadêmico do Agreste da Universidade Federal de Pernambuco, 2018.

LLOYD, N., RANGAN, B. Geopolymer Concrete with Fly Ash. **Proceedings of the Second International Conference on Sustainable Construction Materials and Technologies**, v. 3, p. 1493-1504, 2010.

LITTLE, D.N., YUSUF, F.A.M.S. Example Problem Illustrating the Application of the National Lime Association Mixture Design and Testing Protocol (MDTP) to Ascertain Engineering Properties of Lime-Treated Subgrades for Mechanistic Pavement Design/Analysis. **National Lime Association**, pp. 29, 2001.

LIU, Y., SHI, C., ZHANG, Z., LI, N. An overview on the reuse of waste glasses in alkali-activated materials. **Resources Conservation and Recycling**, v. 144, p. 297–309, 2019. doi:10.1016/j.resconrec.2019.02.007

LONGHI, M. A. **Álcali-ativação de lodo de caulim calcinado e cinza pesada com ativadores convencionais e silicato de sódio alternativo**. Dissertação de Mestrado. Universidade Federal do Rio Grande do Sul, 2015.

LÓPEZ, M.A.C. **Reciclagem de pavimentos flexíveis com adição de cimento Portland: estudo de fadiga através do ensaio de flexão em viga quatro pontos**. Dissertação de Mestrado. Universidade Federal do Rio Grande do Sul, 2016.

LUUKKONEN, T., ABDOLLAHNEJAD, Z., YLINIEMI, J., KINNUNEN, P., ILLIKAINEN, M. Comparison of alkali and silica sources in one-part alkali-activated blast furnace slag mortar, **Journal of Cleaner Production**, v. 187, p. 171–179, 2018.

LUUKKONEN, T., ABDOLLAHNEJAD, Z., YLINIEMI, J., KINNUNEN, P., ILLIKAINEN, M. One-part alkali-activated materials: a review. **Cement and Concrete Research**, v. 103, p. 21–34, 2018.

MEJÍA, J., GUTIÉRREZ, R.M., PUERTAS, F. Rice husk ash as a source of silica in alkaliactivated fly ash and granulated blast furnace slag systems. **Materiales de Construcción**, v. 63, p. 361–375, 2013.

MA, C.K., AWANG, A.Z., OMAR, W. Structural and material performance of geopolymer concrete: A review. **Construction and Building Material**, v. 186, p. 90-102, 2018. doi:10.1016/j.conbuildmat.2018.07.111

MAJIDI, B. Geopolymer technology, from fundamentals to advanced applications: a review. **Materials technology**, v. 24, p. 79-87, 2009.

MALLICK, R.B., BONNER, D.S., BRADBURY, R.L., ANDREWS, J.O., KANDHAL, P.S., e KEARNEY, E.J. Evaluation of performance of full-depth reclamation mixes. **Transportation Research Record: Journal of the Transportation Research Board**, v. 1809, p. 199–208, 2002a.

MALLICK, R.B., VEERARAGAVAN, A. Sustainable pavements in India-the time to start is now. **New Building Materials and Construction World Magazine**, v. 16, p. 128-140, 2010.

MALLICK, R.B., TETO, M.R., KANDHAL, P.S., BROWN, E.R., BRADBURY, R.L., e KEARNEY, E.J. Laboratory study of full-depth reclamation mixes. **Transportation Research Record: Journal of the Transportation Research Board**, v. 1813, p. 103-110, 2002b.

MARAGHECHI, H., RAJABIPOUR, F., PANTANO, C.G., BURGOS, W.D. Effect of calcium on dissolution and precipitation reactions of amorphous silica at high alkalinity. **Cement and Concrete Research**, v. 87, p. 1–13, 2016.

MEDINA, J. e MOTTA, L.M.G. **Mecânica dos Pavimentos**. 3ª ed. Editora Interciências. Rio de Janeiro, RJ, 2015.

MEDINA, J. **Mecânica dos Pavimentos**. Ed. UFRJ, pp. 380, Rio de Janeiro, 1997.

MEHTA, P.K. Reducing the environmental impact of concrete. **Concrete International**, v. 23, n.10, p. 61-66, 2001.

MEHTA, P. Properties of blended cements made from rice husk ash. **Journal of American Concrete Institute**, v. 74, n. 9, p. 440-442, 1977.

MEHTA, P.K. Rice husk as: a unique supplementary cementing material. **Proceedings of the International Symposium on Advances in Concrete Technology**, Athens, Greece, p. 407-430, 1992.

MEJÍA, J.M., MEJÍA DE GUTIÉRREZ, R., MONTES, C. Rice husk ash and spent diatomaceous earth as a source of silica to fabricate a geopolymeric binary binder. **Journal of Cleaner Production**, v. 118, p. 133–139, 2016. https://doi.org/10.1016/j.jclep ro.2016.01.057

MENDES, B.C., PEDROTI, L.G., VIEIRA, C.M.F., MARVILA, M.T., AZEVEDO, A.R.G., CARVALHO, J.M.F., RIBEIRO, J.C.L. Application of eco-friendly alternative activators in alkali-activated materials: A review. **Journal of Building Engineering**, v. 35, p. 102010, 2021.

MILAD, A., TAIB, A.M., AHMEDA A.G.F., SOLLA, M., YUSOFF, N.I.M. A review of the use of reclaimed asphalt pavement for road paving applications. **Jurnal Teknologi**, v. 82, n. 3, p. 35-45, 2020.

MINGUELA, J.D. El estudio del comportamiento de los firmes reciclados in situ con cemento. Tese de doutorado, University of Burgos, Spain, 2011.

MOHAMMADINIA, A., ARULRAJAH, A., SANJAYAN, J., DISFANI, M. M., BO, M. W., e DARMAWAN, S. Laboratory evaluation of the use of cement-treated construction and demolition materials in pavement base and subbase applications. **Journal of Materials in Civil Engineering**, v. 27, n. 6, 2015.

MOHAMMADINIA, A., ARULRAJAH, A., SANJAYAN J.G., DISFANI, M.M., BO, M.W., DARMAWAN, S. Strength development and microfabric structure of construction and demolition aggregates stabilized with fly ash-based geopolymers. **Journal of Materials in Civil Engineering**, v. 28, 2016. https://doi.org/10.1061/(ASCE)MT.1943-5533.0001652

MOHAMMADINIA, A., ARULRAJAH, A., SANJAYAN J.G., DISFANI, M.M., WIN BO, M., DARMAWAN, S. Stabilization of demolition materials for pavement base/subbase applications using fly ash and slag geopolymers: laboratory investigation, **Journal of Materials in Civil Engineering**, v. 28, n. 7, 2016. https://doi.org/10.1061/(asce)mt.1943-5533.0001526

MUÑIZ-VILLARREAL, M.S., MANZANO-RAMÍREZ, A., SAMPIERI-BULBARELA, S., GASCA-TIRADO, J. R., REYES-ARAIZA, J. L., RUBIO-ÁVALOS, J.C., PÉREZBUENO, J.J., APATIGA, L.M., ZALDIVAR, C., AMIGÓ-BORRÁS, A.V. The effect of temperature on the geopolymerization process of a metakaolin-based geopolymer. **Materials Letters**, v. 65, n. 6, p. 995-998, 2011.

NAZARI, A., BAGHERI, A., RIAHI, S. Properties of geopolymer with seeded fly ash and rice husk bark ash, **Materials Science and Engineering: A**, v. 528, n. 24, p. 395–401, 2011.

NÚÑEZ, W.P. **Estabilização Físico-Química de um Solo Residual de Arenito Botucatu, Visando seu Emprego na Pavimentação**. Dissertação de Mestrado (UFRS), Porto Alegre, 1991, 150 p.

OH, J.E., MONTEIRO, P.J.M., JUN, S.S., CHOI, S., CLARK, S.M. The evolution of strength and crystalline phases for alkali-activated ground blast furnace slag and fly ash-based geopolymers. **Cement and Concrete Research**, v. 40, p. 189–196, 2010.

OWOEYE, S. Effects of extraction temperature and time on the physical properties of soluble sodium silicate from rice husk ash. **Science Journal of Chemistry**, v. 5, n. 1, p. 8-11, 2017.

PACHECO-TORGAL, F., LABRINCHA, J.A., LEONELLI, C., PALOMO, A., CHINDAPRASIRT, P. Handbook of Alkali-Activated Cements, Mortars and Concretes, **Woodhead Publishing**, Oxford, pp. 663-686, 2015.

PALOMO, A., KRIVENKO, P., GARCIA-LODEIRO, I., KAVALEROVA, E., MALTSEVA, O., FERNÁNDEZ-JIMÉNEZ, A. A review on alkaline activation: new analytical perspectives. **Materiales de Construcción**. v. 64, n. 315, 2014.

PALOMO, A., GRUTZECK, M.W., BLANCO, M.T. Alkali-activated fly ashes: A cement for the future. **Cement and Concrete Research**, v. 29, p. 1323–1329,1999. doi:10.1016/S0008-8846(98)00243-9

PAIGE-GREEN, P. e WARE, C. Some Material and Construction Aspects Regarding in situ Recycling of Road Pavements in South Africa. **Road Materials and Pavement Design**, v. 7, n. 3, p. 273–287, 2006.

PAIVA, C.E.L., OLIVEIRA, P.C.A, BONFIM, V. As perspectivas de reabilitação de pavimentos no estado de São Paulo – Brasil: Enquadramento e técnicas usuais, **Revista Construção**, v. 53, p. 34-38, 2013.

PANGDAENG, S., SATA, V., AGUIAR, J.B., PACHECO-TORGAL, F., CHINDAPRASIRT, P. Apatite forming on calcined kaolin-white Portland cement geopolymer, **Materials Science and Engineering C**, v. 51, p. 1–6, 2015.

PASSUELLO, A., RODRIGUEZ, E.D., HIRT, E., LONGHI, M., BERNAL, S.A., PROVIS, J.L., KIRCHHEIM, A.P. Evaluation of the potential improvement in the environmental footprint of geopolymers using waste-derived activators. **Journal of Cleaner Production**, v. 166, p. 680–689, 2017.

PERERA, D., UCHIDA, O., VANCE, E., FINNIE K. Influence of curing schedule on the integrity of geopolymers. **Advances in Geopolymer Science & Technology**, v. 42, p. 3099–3106, 2007.

PORTLAND CEMENT ASSOCIATION (PCA), Guide to Full Depth Reclamation (FDR) with Cement, Skokie, USA, 2005.

POUEY, M.T.F. **Beneficiamento da cinza de casca de arroz residual com vistas à produção de cimento composto e/ou pozolânico**. Tese de doutorado. Universidade Federal do Rio Grande do Sul, Porto Alegre, 2006.

PROVIS, J.L. Alkali-activated materials. **Cement and Concrete Research,** v. 114, p. 40-48, 2018. doi:10.1016/j.cemconres.2017.02.009

PROVIS, J.L. **Modelling the formation of geopolymers**. PhD thesis, Chemical & Biomolecular Engineering, University of Melbourne, 2006, 310pp.

PROVIS, J.L. Geopolymers and other alkali activated materials: Why, how, and what?, **Materials and Structures**, v. 47, p. 11–25, 2014. doi:10.1617/s11527-013-0211-5

PROVIS, J.L., BERNAL, S.A. Geopolymers and Related Alkali-Activated Materials. **Annual Review of Materials Research**, v. 44, p. 299-327, 2014. doi:10.1146/annurev-matsci-070813-113515.

PROVIS, J.L., DUXSON, P., VAN DEVENTER, J.S.J, LUKEY, G.C. The Role of Mathematical Modelling and Gel Chemistry in Advancing Geopolymer Technology. **Chemical Engineering Research and Design**, v. 83, n. 7, p. 853-860, 2005.

PROVIS, J.L., LUKEY, G.C., VAN DEVENTER, J.S.J. Do Geopolymers Actually Contain Nanocrystalline Zeolites? A Reexamination of Existing Results. **Chemistry of Materials**, v. 17, n. 12, p. 3075-3085, 2005.

PROVIS, J.L., VAN DEVENTER, J.S.J. **Alkali-Activated Materials: State-of-the-Art Report**, RILEM TC 224-AAM, Springer/RILEM, Dordrecht, 2014.

PUPPALA, A.J., HOYOS, L.R., e POTTURI, A.K. Resilient moduli response of moderately cementtreated reclaimed asphalt pavement aggregates. **Journal of Materials in Civil Engineering**, v. 23, n. 7, p. 990 - 998, 2011.

RAHEEM, M., OTUOSE, H.S., ABDULHAFIZ, U. Properties of Rice Husk Ash Stabilized Laterite Roof Tiles. **Leonardo Electronic Journal of Practices and Technologies**, v. 23, p. 41–50, 2013.

RAHIM, R.H.A., RAHMIATI, T., AZIZ,I A.K., MAN, Z., NURUDDIN, M.F., ISMAIL, L. Comparison of using NaOH and KOH activated fly ash-based geopolymer on the mechanical properties. **Materials Science Forum**, v. 803, 2015.

RANJBAR, N., MEHRALI, M., BEHNIA, A., JOHNSON, A.U., JUMAAT, M.Z. Graphene nanoplatelet-fly ash based geopolymer composites. **Cement and Concrete Research**, v. 59, p. 532–539, 2014.

RIVERA, J., CASTRO, F., FERNÁNDEZ-JIMÉNEZ, A., CRISTELO, N. Alkali-Activated Cements from Urban, Mining and Agro-Industrial Waste: State-of-the-art and Opportunities. **Waste and Biomass Valorization**, v. 12, n. 5, p. 2665–2683, 2021.

ROBAYO-SALAZAR, R. A., DE GUTIÉRREZ, R. M. Natural volcanic pozzolans as an available raw material for alkali-activated materials in the foreseeable future: A review. **Construction and Building Materials**, v. 189, p. 109-118, 2018.

ROSCHAT, W., SIRITANON, T., YOOSUK, B., PROMARAK, V. Rice husk-derived sodium silicate as a highly efficient and low-cost basic heterogeneous catalyst for biodiesel production. **Energy Conversion and Management**, v. 119, p. 453–462, 2016.

SAMARAKOON, M.H., RANJITH, P.G., RATHNAWEERA, T.D., PERERA, M.S.A. Recent advances in alkaline cement binders: A review, **Journal of Cleaner Production,** v. 227, p. 70–87, 2019.doi:10.1016/j.jclepro.2019.04.103.

SANTOS, R.O.G., REZENDE, L.R., SILVA JR., V.M., COSTA, L.C.S., e HÓMEZ, J.H.G. Monitoramento do desempenho da técnica de reciclagem profunda em pavimentos do estado de Goiás, **Transportes**, v. 25, n. 4, p. 27-41, 2017.

SAID, S.F. Variability in Roadbase Layer Properties Conducting Indirect Tensile Test. 8th. **International Conference on Asphalt Pavements**, v. II, p. 977-986, Seattle, Washington, 1997

SANJAYAN, J.G., NAZARI, A., POURALIAKBAR, H. FEA modelling of fracture toughness of steel fibre-reinforced geopolymer composites. **Materials & Design**, v. 76, p. 215–222, 2015.https://doi.org/10.1016/j.matdes.2015.03.029

SARAVANAN, M., SIVARAJA, M. Mechanical Behavior of Concrete Modified by Replacement of Cement by Rice Husk Ash. **Brazilian Archives of Biology and Technology**, 2016.

SARIDE, S., AVIRNENI, D., CHALLAPALLI, S. Micro-mechanical interaction of activated fly ash mortar and reclaimed asphalt pavement materials, **Construction and Building Materials**, v. 123, p. 424–435, 2016. https://doi.org/10.1016/j.conbuildmat.2016.07.016

SARIDE, S., JALLU, M. Effect of Fly Ash Geopolymer on Layer Coefficients of Reclaimed Asphalt Pavement Bases. **Journal of Transportation Engineering, Part B: Pavements**, v. 146, n. 3, 2020.

SARIDE, S.; PUPPALA, A. J.; WILLIAMMEE, R. Assessing recycled/secondary materials as pavement bases. **Proceedings of the Institution of Civil Engineers: Ground Improvement**, v. 163, n. 1, p. 3–12, 2010.

SARIDE, S., AVIRNENI, D., CHALLAPALLI, S. Micro-mechanical interaction of activated fly ash mortar and reclaimed asphalt pavement materials, **Construction and Building Materials**, v. 123, p. 424–435, 2016. https://doi.org/10.1016/j.conbuildmat.2016.07.016

SARIDE, S. AVIRNENI, D., JAVVADI, S.C.P., PUPPALA A., HOYOS, L.R. Evaluation of Fly ash Treated Reclaimed Asphalt Pavement for Base/Subbase Applications. **Indian Geotechnical Journal**, v. 45, n. 4, p. 401-411, 2015.

SCRIVENER, K.L., JOHN, V.M., GARTNER, E.M. Eco-efficient cements: potential economically viable solutions for a low-CO2 cement-based materials industry. **Cement and Concrete Research**, v. 114, p. 2–26, 2018.

SHALINI, A., GURUNARAYANAN, G., KUMAR, R., PRAKASH, V., SAKTHIVEL, S. Performance of Rice Husk Ash in Geopolymer Concrete. **International Journal for Innovative Research in Science & Technology**, v. 2, n. 12, p. 73–77, 2016.

SERRES, N.; BRAYMAND, S.; FEUGEAS, F. Environmental evaluation of concrete made from recycled concrete aggregate implementing life cycle assessment. **Journal of Building Engineering**, v. 5, p. 24–33, 2016.

SEVERO, C.G.S., COSTA D.L., BEZERRA, I.M.T., MENEZES, R.R., NEVES, G.A. Características, particularidades e princípios científicos dos materiais ativados alcalinamente. **Revista Eletrônica de Materiais e Processos**, v. 8, n. 2, p. 55-67, 2013.

SHI, C., KRIVENKO, P.V., ROY, D.M. **Alkali-Activated Cements and Concretes**, Taylor & Francis, Abingdon, UK, 2006.

SHI, C., JIMÉNEZ, A.F., PALOMO, A. New cements for the 21st century: The pursuit of an alternative to Portland cement. **Cement and Concrete Research**, v. 41, p. 750-763, 2011. doi:10.1016/j.cemconres.2011.03.016

SHU, X., HUANG, B., VUKOSAVLJEVIC, D. Laboratory evaluation of fatigue characteristics of recycled asphalt mixture. **Constrution and Building Materials**, v. 22, p. 1323–1330, 2008.

SILVA, H.M.R.D., OLIVEIRA, J.R.M., JESUS, C.M.G. Are totally recycled hot mix asphalts a sustainable alternative for road paving? **Resources, Conservation and Recycling**, v. 60, p. 38–48, 2012.

SILVEIRA, A. A. **Contribuição ao estudo do efeito da incorporação de cinza de casca de arroz em concretos submetidos à reação álcali-agregado**. Tese. Universidade Federal do Rio Grande do Sul, Porto Alegre, 2007.

SINGH, S., RANSINCHUNG, G.D., KUMAR, P. An economical processing technique to improve RAP inclusive concrete properties, **Construction and Building Materials**, v. 148, p. 734–747, 2017. https://doi.org/10.1016/j.conbuildmat.2017.05.030

SINGH, N. B., MIDDENDORF, B. Geopolymers as an alternative to Portland cement: An overview. **Construction and Building Materials**, v. 237, 2020.

SINGH, S., RANSINCHUNG, G.D.R.N., MONU, K., KUMAR, P. Laboratory investigation of RAP aggregates for dry lean concrete mixes. **Construction and Building Materials**, v. 166, p. 808–816, 2018. https://doi.org/10.1016/j.conbuildmat.2018.01.131

SINULINGGA, K., AGUSNAR, H., WIRJOSENTONO, B., AMIN, Z.M. The Effect of Mixing Rice Husk Ash and Palm Oil Boiler Ash on Concrete Strength, **American Journal of Physical Chemistry**, v. 3, p. 9–14, 2014. http://dx.doi.org/10.11648/j.ajpc.20140302.11

SOMNA, K., JATURAPITAKKUL, C., KAJITVICHYANUKUL, P., CHINDAPRASIRT, P. NaOH activated ground fly ash geopolymer cured at ambient temperature, **Fuel**, v. 90, n. 6, p. 2118–2124, 2011.

SONG, W., HUANG, B., e SHU, X. Influence of Warm-mix Asphalt Technology and Rejuvenator on Performance of Asphalt Mixtures Containing 50% Reclaimed Asphalt Pavement. **Journal of Cleaner Production**, v. 192, p. 191-198, 2018.

SOUTHERN AFRICAN BITUMEN ASSOCIATION - SABITA. Use of Reclaimed Asphalt in the Production of Asphalt, **Manual36/trh 21**:Western Cape, South Africa, 2019.

ŠPAK, M., RASCHMAN, P. Influence of different mineral precursors on the properties of fly ash based alkali-activated mortars. **Key Engineering Materials**. v. 761, p. 73–78, 2018. https ://doi.org/10.4028/www.scien tific.net/KEM.761.73

STURM, P., GLUTH, G.J.G., BROUWERS, H.J.H., KÜHNE, H.-C. Synthesizing one-part geopolymers from rice husk ash. **Construction and Building Materials**, v. 124, p. 961–966, 2016.

SU, Y.M., HOSSINEY, N., TIA, M., BERGIN, M. Mechanical properties assessment of concrete containing reclaimed asphalt pavement using the superpave indirect tensile strength test. **Journal of Testing and Evaluation**, v. 42, n. 4, p. 912-920, 2014. https://doi.org/10.1520/jte20130093

SUDDEEPONG, A., INTRA, A., HORPIBULSUK, S., SUKSIRIPATTANAPONG, C., ARULRAJAH, A., e SHEN, J. S. Durability against wetting-drying cycles for cement-stabilized reclaimed asphalt pavement blended with crushed rock. **Soils and Foundations**, v. 58, p. 333–343, 2018.

TAKEDA, M.C.A. **Influência da variação da umidade pós-compactação no comportamento mecânico de solos de rodovias do interior paulista**. Tese de Doutorado, USP. São Paulo, SP, 2006

TARSI, G., TATARANNI, P., SANGIORGI, C. The challenges of using reclaimed asphalt pavement for new asphalt mixtures: A review. **Materials**, v. 13, n. 18, 2020.

TATARANNI, P., SANGIORGI, C., SIMONE, A., VIGNALI, V., LANTIERI, C., e DONDI, G. A laboratory and field study on 100% recycled cement bound mixture for base layers. **International Journal of Pavement Research and Technology**, v. 11, n. 5, p. 427-434, 2017.

TCHAKOUTÉ H.K., RÜSCHER, C.H., KONG, S., KAMSEU, E., LEONELLI, C. Geopolymer binders from metakaolin using sodium waterglass from waste glass and rice husk ash as alternative activators: A comparative study. **Construction and Building Materials**, v. 114, p. 276–289, 2016.

TCHAKOUTÉ, H. K., RÜSCHER, C. H., KONG, S., RANJBAR, N. Synthesis of sodium waterglass from white rice husk ash as an activator to produce metakaolin-based geopolymer cements. **Journal of Building Engineering**, v. 6, p. 252–261, 2016.

TEMUUJIN, J., WILLIAMS, R., VAN RIESSEN, A. Effect of mechanical activation of fly ash on the properties of geopolymer cured at ambient temperature. **Journal of Materials Processing Technology**, v. 209, p. 5276–5280, 2009.

TEOREANU, I. The interaction mechanism of blast-furnace slags with water: the role of activating agents. **Cemento**, v. 8, n. 2, p. 91–97, 1991.

TONG, K.T., VINAI, R., SOUTSOS, M.N. Use of Vietnamese rice husk ash for the production of sodium silicate as the activator for alkali-activated binders. **Journal of Cleaner Production**, v. 201, p. 272–286, 2018.

TSEN, T.J., KONG, D., ZEIMARAN, E., SOUTSOS, M. Rice husk ash derived sodium silicate using hydrothermal and convection heating methods. **Proceedings of AICCE'19: Transforming the Nation for a Sustainable Tomorrow**, v. 53, p. 629-646, 2020. https://doi.org/10.1007/978-3-030-32816-0_44

TURNER, L.K., COLLINS, F.G. Carbon dioxide equivalent (CO2-e) emissions: A comparison between geopolymer and OPC cement concrete. **Construction and Building Materials**, v. 43, p. 125-130, 2013. doi:10.1016/j.conbuildmat.2013.01.023

United Nations Transforming Our World: The 2030 Agenda for Sustainable Development; United Nations: New York, NY, USA, 2015.

United States Department of Agriculture – **USDA**. World Agricultural Production. 2020. Disponível em: <https://apps.fas.usda.gov/psdonline/circulars/production.pdf>

VAKILI, M., RAFATULLAH, M., IBRAHIM, M.H., SALAMATINIA, B., GHOLAMI, Z., ZWAIN, H.M. A review on composting of oil palm biomass, **Environment, Development and Sustainability**, v. 17, n. 4, p. 691–709, 2015. https://doi.org/10.1007/s10668-014-9581-2

VAN DEVENTER, J.S.J., PROVIS, J.L., DUXSON, P., LUKEY, G.C. J Hazard Mater (in press), 2006. Doi: 10.1016/j.jhazmat.2006.02.044

VAN JAARSVELD, J.G.S., VAN DEVENTER, J.S.J., LUKEY, G.C. The effect of composition and temperature on the properties of fly ash and kaolinite based geopolymers. **Chemical Engineering Journal**, v. 89, p. 63–73, 2002.

VARGAS, A.S., DAL MOLIN, D.C.C., VILELA, A.C.F., SILVA, F.J.D., PAVAO, B., VEIT, H. The effects of Na2O/SiO2 molar ratio, curing temperature and age on compressive strength, morphology and micro structure of alkali-activated fly ash-based geopolymers, **Cement and Concrete Composites**, v. 33, n. 6, p. 653–660, 2011.

VILLAQUIRÁN-CAICEDO, M.A., MEJÍA DE GUTIÉRREZ, R., GALLEGO, N.C. A novel MK-based geopolymer composite activated with rice husk ash and KOH: performance at high temperature. **Materiales de Construcción**, v. 67, p. 1–13, 2017. https://doi.org/10.3989/mc.2017.02316

VINAI, R., SOUTSOS, M. Production of sodium silicate powder from waste glass cullet for alkali activation of alternative binders. **Cement and Concrete Research**, v. 116, p. 45–56, 2019.

WANG, A., SUN, D., HU, P., REN, X. Experimental research on preparing geopolymeric cement with metakaolin activated by alkali activators, **Journal of Hefei University of Technology**, v. 31, n. 4, p. 617–621, 2008.

WANG, T., LEE, I.-S., KENDALL, A., HARVEY, J., LEE, E.-B., KIM, C. Life cycle energy consumption and GHG emission from pavement rehabilitation with diferent rolling resistance. **Journal of Cleaner Production**, v. 33, p. 86-96, 2012.

WANG, Y. The effects of using reclaimed asphalt pavements (RAP) on the long-term performance of asphalt concrete overlays. **Constrution and Building Materials**, v. 120, p. 335-348, 2016.

WENG, L., SAGOE-CRENTSIL, K., BROWN, T. Speciation and hydrolysis kinetics of aluminates in inorganic polymer systems, **Geopolymer International Conference**, Melbourne, Australia 28–29 October, 2002.

WENG, L., SAGOE-CRENTSIL, K. Dissolution processes, hydrolysis and condensation reactions during geopolymer synthesis: Part I-Low Si/Al ratio systems. **Journal of Materials Science**, v. 42, p. 2997–3006, 2007.

WERK. S.M.S. **Estudo da influência dos métodos de compactação no comportamento resiliente de solos**. Dissertação de Mestrado. Universidade Federal do Rio Grande do Sul. Programa de Pós-Graduação em Engenharia Civil, 2000.

WIRTGEN. **Tecnologia de Reciclagem a Frio**. 1. ed. Windhagen, Alemanha, 2012.

WONGPA, J., KIATTIKOMOL, K., JATURAPITAKKUL, C., CHINDAPRASIRT, P. Compressive strength, modulus of elasticity, and water permeability of inorganic Polymer concrete. **Materials & Design**, v. 31, n. 10, p. 4748–4754, 2010.

WU, R., LOUW, S., e JONES, D. Effects of binder, curing time, temperature, and trafficking on moduli of stabilized and unstabilized full-depth reclamation materials. **Transportation Research Record: Journal of the Transportation Research Board**, v. 2524, p. 11–19, 2015.

YANG, K., SONG, J. Workability Loss and Compressive Strength Development of Cementless Mortars Activated by Combination of Sodium Silicate and Sodium Hydroxide. **Journal of Materials in civil Engineering**, v. 21, n. 3, 2009.

YE, N., CHEN, Y., YANG, J., LIANG, S., HU, Y., XIAO, B., HUANG, Q., SHI, Y., HU, J., WU, X. Co-disposal of MSWI fly ash and Bayer red mud using an one-part geopolymeric system. **Journal of Hazardous Materials**, v. 318, p. 70–78, 2016. https://doi.org/10.1016/j.jhazmat. 2016.06.042

YODER, E. J., WITCZACK, M.W. **Principles of Pavement Design**. New York: John Wiley & Sons Inc., ed. 2, 1975. 711p.

YUAN, D., NAZARIAN, S., HOYOS, L. R., e PUPPALA, A. J. Evaluation and mix design of cement-treated base materials with high content of reclaimed asphalt pavement. **Transportation Research Record: Journal of the Transportation Research Board**, v. 2212, p. 110–119, 2011.

YUN-MING, L., CHENG-YONG, H., AL BAKRI, M.M., HUSSIN, K. Structure and properties of clay-based geopolymer cements: A review Progress in Materials, **Science**, v. 83, p. 595–629, 2016.

YUSUF, M.O., JOHARI M.A.M., AHMAD, Z.A., MASLEHUDD, M. Influence of curing methods and concentration of NaOH on strength of the synthesized alkaline activated ground slag-ultrafine palm oil fuel ash mortar/concrete. **Construction and Building Materials**, v. 66, p. 541–548, 2014.

ZAIN, M.F.M., ISLAM, M.N., MAHMUD, F., JAMIL, M. Production of rice husk ash for use in concrete as a supplementary cementitious material. **Construction and Building Materials**, v. 25, n. 2, p. 798-805, 2011. https://doi.org/10.1016/j.conbuildmat.2010.07.003

ZHANG, M., GUO, H., EL-KORCHI, T., ZHANG, G., TAO, M. Experimental feasibility study of geopolymer as the next-generation soil stabilizer. **Construction and Building Materials**, v. 47, p. 1468-1478, 2013.

ZHANG, Z., WANG, H., PROVIS, J.L. Quantitative study of the reactivity of fly ash in geopolymerization by FTIR. **Journal of Sustainable Cement-Based Materials**, v.1, n. 4, p. 154–166, 2012.

ZHANG, Z.H., ZHUB, H.J., ZHOUA, C.H., WANG, H. Geopolymer from kaolin in China: An overview, Applied Clay Science, v. 119, p. 31–4, 2016.

ZHUANG, X.Y., CHEN, L., KOMARNENI, S., ZHOU, C.H., TONG, D.S., YANG, H.M., YU, W.H., WANG, H. Fly ash-based geopolymer: Clean production, properties and applications. **Journal of Cleaner Production**, v. 125, p. 253–267, 2016. doi:10.1016/j.jclepro.2016.03.019

ZHANG, Z., YAO, X., ZHU, H. Activating process of geopolymer source material: kaolinite, Journal of Wuhan University of Technology. Materials Science Edition, v. 24, n. 1, p. 132–136, 2009.

ZIEGLER, D., FORMIA, A., TULLIANI, J.-M., PALMERO, P. Environmentally Friendly Dense, Porous Geopolymers, Using fly ash and rice husk ash as raw materials, **Materials**, v. 9, n. 6, p. 466, 2016.

ŽIVICA, V. Effectiveness of new silica fume alkali activator. **Cement and Concrete Composites**, v. 28, n. 1, p. 21–25, 2006.

ZUHUA, Z., XIAO, Y., HUAJUN, Z., YUE, C. Role of water in the synthesis of calcined kaolin-based geopolymer, **Applied Clay Science**, v. 43, n. 2, p. 218–223, 2009.

XU, H. The geopolymerisation of alumino-silicate minerals. **International Journal of Mineral Processing**, v. 59, p. 247–266, 2000.

XU, H., LI, Q., SHEN, L., ZHANG, M., ZHAI, J. Low-reactive circulating fluidized bed combustion (CFBC) fly ashes as source material for geopolymer synthesis. **Waste management**, v. 30, p. 57–62, 2010.

XU, H., VAN DEVEVENTER, J. The geopolymerization of alumino-silicate mínerals. **International Journal of Mineral Processing**, v. 59, p. 247 – 266, 2000.

XU, H., VAN DEVENTER, J.S.J., LUKEY, G.C. The Effect of Alkali Metals on the Preferential Geopolymerisation of Stilbite/ Kaolinite Mixtures. **Industrial & Engineering Chemistry Research**, v. 40, n. 17, p. 3749, 2001.

REFERÊNCIAS ITEM 3.1

APOLONIO, P.H., LIMA, J.S., MARINHO, E.P., NOBREGA, A.C. V., FREITAS, J.C.O., MARTINELLI, A.E., 2020. Produção de geopolímeros utilizando cinza da casca de arroz como fonte complementar de sílica. **Cerâmica** 66, 172–178.

BERNAL, S.A., RODRÍGUEZ, E.D., DE GUTIÉRREZ, R.M., PROVIS, J.L., 2015. Performance at high temperature of alkali-activated slag pastes produced with silica fume and rice husk ash based activators. **Materiales de Construcción**. 65.

BERNAL, S.A., RODRÍGUEZ, E.D., MEJIA DE GUTIÉRREZ, R., PROVIS, J.L., DELVASTO, S., 2012. Activation of metakaolin/slag blends using alkaline solutions based on chemically modified silica fume and rice husk ash. **Waste and Biomass Valorization** 3, 99–108.

BOUZÓN, N., PAYÁ, J., BORRACHERO, M. V., SORIANO, L., TASHIMA, M.M., MONZÓ, J., 2014. Refluxed rice husk ash/NaOH suspension for preparing alkali activated binders. **Materials Letters**. 115, 72–74.

CHENG, Y., HONGQIANG, M., HONGYU, C., JIAXIN, W., JING, S., ZONGHUI, L., MINGKAI, Y., 2018. Preparation and characterization of coal gangue geopolymers. **Construction and Building Materials.** 187, 318–326.

Chindaprasirt, P., Kanchanda, P., Sathonsaowaphak, A., Cao, H.T., 2007. Sulfate resistance of blended cements containing fly ash and rice husk ash. Constr. Build. Mater. 21, 1356–1361.

CHINDAPRASIRT, P., RUKZON, S., 2008. Strength, porosity and corrosion resistance of ternary blend Portland cement, rice husk ash and fly ash mortar. **Construction and Building Materials**. 22, 1601–1606.

CISSE, I.K., LAQUERBE, M., 2000. Mechanical characterization of filler sandcretes with rice husk ash additions. Study applied to Senegal. **Cement Concrete Research** 30, 13–18.

DAVIDOVITS, J., 2020. Geopolymer Chemistry and Applications. 5-th edition, J. Davidovits.–Saint-Quentin, France.

DETPHAN, S., CHINDAPRASIRT, P., 2009. Preparation of fly ash and rice husk ash geopolymer. **International Journal of Minerals, Metallurgy and Materials**. 16, 720–726.

DUXSON, P., MALLICOAT, S.W., LUKEY, G.C., KRIVEN, W.M., VAN DEVENTER, J.S.J., 2007. The effect of alkali and Si/Al ratio on the development of mechanical properties of metakaolin-based geopolymers. **Colloids Surfaces A Physicochem. Eng. Asp**. 292, 8–20.

FOLETTO, E.L., GRATIERI, E., DE OLIVEIRA, L.H., JAHN, S.L., 2006. Conversion of rice hull ash into soluble sodium silicate. **Materials Research**. 9, 335–338.

GANESAN, K., RAJAGOPAL, K., THANGAVEL, K., 2008. Rice husk ash blended cement: Assessment of optimal level of replacement for strength and permeability properties of concrete. **Construction and Building Materials**. 22, 1675–1683.

GERALDO, R.H., FERNANDES, L.F.R., CAMARINI, G., 2017. Water treatment sludge and rice husk ash to sustainable geopolymer production. **Journal of Cleaner Production**. 149, 146–155.

HABEEB, G.A., FAYYADH, M.M., 2009. Rice Husk Ash concrete: The effect of RHA average particle size on mechanical properties and drying shrinkage. **Australian Journal of Basic and Applied Sciences**. 3, 1616–1622.

HAJIMOHAMMADI, A., VAN DEVENTER, J.S.J., 2017. Solid Reactant-Based Geopolymers from Rice Hull Ash and Sodium Aluminate. **Waste and Biomass Valorization** 8, 2131–2140.

HE, J., JIE, Y., ZHANG, J., YU, Y., ZHANG, G., 2013. Synthesis and characterization of red mud and rice husk ash-based geopolymer composites. **Cement and Concrete Composites**. 37, 108–118.

JAARSVELD, J.G.S. VAN, DEVENTER, J.S.J. VAN, LUKEY, G.C., 2002. The effect of composition and temperature on the properties offly ash- and kaolinite-based geopolymers. **Chemical Engineering Journal**. 89, 63–73.

JUENGSUWATTANANON, K., WINNEFELD, F., CHINDAPRASIRT, P., PIMRAKSA, K., 2019. Correlation between initial SiO2/Al2O3, Na2O/Al2O3, Na2O/SiO2 and H2O/Na2O ratios on phase and microstructure of reaction products of metakaolin-rice husk ash geopolymer. **Construction and Building Materials**. 226, 406–417.

KALAPATHY, U., PROCTOR, A., SHULTZ, J., 2001. A simple method for production of pure silica from rice hull ash. **Bioresource Technology**. 42, 45.

KAMSEU, E., BELEUK À MOUNGAM, L.M., CANNIO, M., BILLONG, N., CHAYSUWAN, D., MELO, U.C., LEONELLI, C., 2017. Substitution of sodium silicate with rice husk ash-NaOH solution in metakaolin based geopolymer cement concerning reduction in global warming. **Journal of Cleaner Production**. 142, 3050–3060.

KHALIL, M.Y., MERZ, E., 1994. Immobilization of intermediate-level wastes in geopolymers 211, 141–148.

KUENZEL, C., VANDEPERRE, L.J., DONATELLO, S., BOCCACCINI, A.R., CHEESEMAN, C., 2012. Ambient temperature drying shrinkage and cracking in metakaolin-based geopolymers. **Journal of the American Ceramic Society**. 95, 3270–3277.

LIMA, J.S., APOLONIO, P.H., MARINHO, E.P., VASCONCELOS, E.A., NÓBREGA, A.C.V., FREITAS, J.C.O., 2021. Use of rice husk ash to produce alternative sodium silicate for geopolymerization reactions. **Ceramica** 67, 58–64.

LUUKKONEN, T., ABDOLLAHNEJAD, Z., YLINIEMI, J., KINNUNEN, P., ILLIKAINEN, M., 2018. Comparison of alkali and silica sources in one-part alkali-activated blast furnace slag mortar. **Journal of Cleaner Production**. 187, 171–179.

MCLELLAN, B.C., WILLIAMS, R.P., LAY, J., VAN RIESSEN, A., CORDER, G.D., 2011. Costs and carbon emissions for geopolymer pastes in comparison to ordinary portland cement. **Journal of Cleaner Production**. 19, 1080–1090.

MEHTA, P.K., 1998. Role of pozzolanic and cementitious material in sustainable development of the concrete industry. **American Concrete Institute**. 1, 1–20.

MEJÍA, J.M., MEJÍA DE GUTIÉRREZ, R., MONTES, C., 2016. Rice husk ash and spent diatomaceous earth as a source of silica to fabricate a geopolymeric binary binder. **Journal of Cleaner Production**. 118, 133–139.

MEJÍA, J.M., MEJÍA DE GUTIÉRREZ, R., PUERTAS, F., 2013. Ceniza de cascarilla de arroz como fuente de sílice en sistemas cementicios de ceniza volante y escoria activados alcalinamente. **Materiales de construcción**. 63, 361–375.

MENDES, B.C., PEDROTI, L.G., VIEIRA, C.M.F., MARVILA, M.T., AZEVEDO, A.R.G., FRANCO DE CARVALHO, J.M., RIBEIRO, J.C.L., 2021. Application of eco-friendly alternative activators in alkali-activated materials: A review. **Journal of building**

engineering. 35.

PASSUELLO, A., RODRÍGUEZ, E.D., HIRT, E., LONGHI, M., BERNAL, S.A., PROVIS, J.L., KIRCHHEIM, A.P., 2017. Evaluation of the potential improvement in the environmental footprint of geopolymers using waste-derived activators. **Journal of Cleaner Production**. 166, 680–689.

RAHIM, R.H.A., RAHMIATI, T., AZIZ, I.A.K., MAN, Z., NURUDDIN, M.F., ISMAIL, L., 2015. Comparison of using NaOH and KOH activated fly ash-based geopolymer on the mechanical properties. **Materials Science Forum 803**.

RAMADHANSYAH, P.J., MAHYUN, A.W., SALWA, M.Z.M., ABU BAKAR, B.H., MEGAT JOHARI, M.A., WAN IBRAHIM, M.H., 2012. Thermal Analysis and Pozzolanic Index of Rice Husk Ash at Different Grinding Time. **Procedia Engineering**. 50, 101–109.

ROSAS-CASAREZ, C.A., ARREDONDO-REA, S.P., GÓMEZ-SOBERÓN, J.M., ALAMARAL-SÁNCHEZ, J.L., CORRALHIGUERA, R., CHINCHILLAS-CHINCHILLAS, M.J., ACUÑA-AGÜERO, O.H., 2014. Experimental study of XRD, FTIR and TGA techniques in geopolymeric materials. **International Journal for Housing Science and Its Applications**. 4, 25-30.

ROSCHAT, W., SIRITANON, T., YOOSUK, B., PROMARAK, V., 2016. Rice husk-derived sodium silicate as a highly efficient and low-cost basic heterogeneous catalyst for biodiesel production. **Energy Conversion and Management**. 119, 453–462.

SAMUEL OWOEYE, S., 2017. Effects of Extraction Temperature and Time on the Physical Properties of Soluble Sodium Silicate from Rice Husk Ash. **Science Journal of Chemistry**. 5, 8.

STURM, P., GLUTH, G.J.G., BROUWERS, H.J.H., KÜHNE, H.C., 2016. Synthesizing one-part geopolymers from rice husk ash. **Construction and Building Materials**. 124, 961–966.

TCHAKOUTÉ, HERVÉ K, RÜSCHER, C.H., KONG, S., KAMSEU, E., LEONELLI, C., 2016. Geopolymer binders from metakaolin using sodium waterglass from waste glass and rice husk ash as alternative activators: A comparative study. **Construction and Building Materials**. 114, 276–289.

TCHAKOUTÉ, HERVÉ KOUAMO, RÜSCHER, C.H., KONG, S., RANJBAR, N., 2016. Synthesis of sodium waterglass from white rice husk ash as an activator to produce metakaolin-based geopolymer cements. **Journal of Building Engineering**. 6, 252–261.

TONG, K.T., VINAI, R., SOUTSOS, M.N., 2018. Use of Vietnamese rice husk ash for the production of sodium silicate as the activator for alkali-activated binders. **Journal of Cleaner Production**. 201, 272–286.

TSEN, T.J., KONG, D., ZEIMARAN, E., SOUTSOS, M., 2020. Rice husk ash derived sodium silicate using hydrothermal and convection heating methods. **Proceedings of AICCE'19 Transform. Nation a Sustain**. Tomorrow 53, 629–646.

VAN JAARSVELD, J.G.S., VAN DEVENTER, J.S.J., LORENZEN, L., 1998. Factors affecting the immobilization of metals in geopolymerized flyash. Metall. **Metallurgical and Materials Transactions B** 29, 283–291.

VILLAQUIRÁN-CAICEDO, M.A., MEJÍA DE GUTIÉRREZ, R., GALLEGO, N.C., 2017. A novel MK-based geopolymer composite activated with rice husk ash and KOH: Performance at high temperature. **Materiales de Construcción**. 67, 1–13.

VINAI, R., SOUTSOS, M., 2019. Production of sodium silicate powder from waste glass

cullet for alkali activation of alternative binders. **Cement and Concrete Research**. 116, 45–56.

XU, H., VAN DEVENTER, J.S.J., 2000. The geopolymerisation of alumino-silicate minerals. **International Journal of Mineral Processing**. 59, 247–266.

XU, W., LO, Y.T., OUYANG, D., MEMON, S.A., XING, F., WANG, W., YUAN, X., 2015. Effect of rice husk ash fineness on porosity and hydration reaction of blended cement paste. **Construction and Building Materials**. 89, 90–101.

ZHANG, M.H., MALHOTRA, V.M., 1996. High-performance concrete incorporating rice husk ash as a supplementary cementing material. **ACI Mateials. Journal**. 93, 629–636.

ŽIVICA, V., 2006. Effectiveness of new silica fume alkali activator. **Cement and Concrete Composites**. 28, 21–25.

REFERÊNCIAS ITEM 3.2

ABNT. NBR 10004: Resíduos sólidos - Classificação. **Associação Brasileira de Normas Técnicas**, 2004a.

NBR 10005: Procedimento para obtenção de extrato de lixiviado de resíduos sólidos. **Associação Brasileira de Normas Técnicas**, p. 16, 2004b.

NBR NM 53 : Agregado graúdo - Determinação de massa específica, massa específica aparente e absorção de água. **Associação Brasileira de Normas Técnicas**, 2009a.

NBR NM 52: Agregados miúdo - Determinação da massa específica e massa específica aparente. **Associação Brasileira de Normas Técnicas**, 2009b.

NBR 10006: Procedimento para obtenção de extreto de solubilizado de resíduos sólidos. **Associação Brasileira de Normas Técnicas**, p. 1–14, 2009c.

NBR 12253: Solo-cimento - Dosagem para emprego como camada de pavimento. **Associação Brasileira de Normas Técnicas**, 2012.

ADHIKARI, S.; KHATTAK, M. J.; ADHIKARI, B. Mechanical characteristics of Soil-RAP-Geopolymer mixtures for road base and subbase layers. **International Journal of Pavement Engineering**, v. 21, n. 4, p. 483–496, 2020.

AL-HDABI, A. Laboratory investigation on the properties of asphalt concrete mixture with Rice Husk Ash as filler. **Construction and Building Materials**, v. 126, p. 544–551, 2016.

ALONSO, S.; PALOMO, A. Alkaline activation of metakaolin and calcium hydroxide mixtures: Influence of temperature, activator concentration and solids ratio. **Materials Letters**, v. 47, n. 1–2, p. 55–62, 2001.

ASTM. D698-12: Standard Test Methods for Laboratory Compaction Characteristics of Soil Using Standard Effort (12 400 ft-lbf/ft3 (600 kN-m/m3)). **American Society for Testing and Materials**, 2012.

D854: Standard Test Methods for Specific Gravity of Soil Solids by Water Pycnometer. **American Society for Testing and Materials**, p. 1–8, 2014.

D2166/D2166M: Standard Test Method for Unconfined Compressive Strength of Cohesive Soil. **American Society for Testing and Materials**, p. 1–7, 2016.

D7928: Standard Test Method for Particle-Size Distribution (Gradation) of Fine-Grained Soils Using the Sedimentation (Hydrometer) Analysis. **ASTM International**, 2017a.

D2487: Standard Practice for Classification of Soils for Engineering Purposes (Unified Soil Classification System). **American Society for Testing and Materials**, p. 1–5, 2017b.

D2172/D2172M: Standard Test Methods for Quantitative Extraction of Bitumen From Bituminous Paving Mixtures. **American Society for Testing and Materials**, 2018.

AVIRNENI, D.; PEDDINTI, P. R. T.; SARIDE, S. Durability and long term performance of geopolymer stabilized reclaimed asphalt pavement base courses. **Construction and Building Materials**, v. 121, p. 198–209, 2016.

AWOYERA, P.; ADESINA, A. A critical review on application of alkali activated slag as a sustainable composite binder. **Case Studies in Construction Materials**, v. 11, p. e00268, 2019.

BERNAL, S. A. *et al.* Mechanical and thermal characterisation of geopolymers based on

silicate-activated metakaolin/slag blends. **Journal of Materials Science**, v. 46, n. 16, p. 5477–5486, 2011.

___. Activation of metakaolin/slag blends using alkaline solutions based on chemically modified silica fume and rice husk ash. **Waste and Biomass Valorization**, v. 3, n. 1, p. 99–108, 2012.

BERNAL, S. A. *et al.* Performance at high temperature of alkali-activated slag pastes produced with silica fume and rice husk ash based activators. **Materiales de Construccion**, v. 65, n. 318, 2015.

BOUZÓN, N. *et al.* Refluxed rice husk ash/NaOH suspension for preparing alkali activated binders. **Materials Letters**, v. 115, p. 72–74, 2014.

BRUSCHI, G. J.; SANTOS, C. P. DOS; *et al.* Parameters controlling loss of mass and stiffness degradation of green stabilized bauxite tailings. **Proceedings of the Institution of Civil Engineers - Geotechnical Engineering**, p. 1–21, set. 2021.

BRUSCHI, G. J.; SANTOS, C. P. DOS; *et al.* Green Stabilization of Bauxite Tailings: Mechanical Study on Alkali-Activated Materials. **Journal of Materials in Civil Engineering**, v. 33, n. 11, p. 06021007, nov. 2021.

BRUSCHI, G. J. *et al.* Leaching assessment of cemented bauxite tailings through wetting and drying cycles of durability test. **Environmental Science and Pollution Research**, n. 0123456789, abr. 2022.

CARVALHO QUEIRÓZ, L. *et al.* Macro–Micro Characterization of Green Stabilized Alkali-Activated Sand. **Geotechnical and Geological Engineering**, n. April, abr. 2022.

CONSOLI, N. C. *et al.* Key Parameters for Strength Control of Artificially Cemented Soils. **Journal of Geotechnical and Geoenvironmental Engineering**, v. 133, n. 2, p. 197–205, fev. 2007.

___. Durability and strength of fiber-reinforced compacted gold tailings-cement blends. **Geotextiles and Geomembranes**, v. 45, n. 2, p. 98–102, 2017.

CONSOLI, N. C.; SILVA, A. P. DA; *et al.* Durability, strength, and stiffness of compacted gold tailings – cement mixes. **Canadian Geotechnical Journal**, v. 55, n. 4, p. 486–494, abr. 2018.

CONSOLI, N. C.; GIESE, D. N.; *et al.* Sodium chloride as a catalyser for crushed reclaimed asphalt pavement – Fly ash – Carbide lime blends. **Transportation Geotechnics**, v. 15, p. 13–19, jun. 2018.

CONSOLI, N. C.; SCHEUERMANN FILHO, H. C.; *et al.* Durability of RAP-Industrial Waste Mixtures Under Severe Climate Conditions. **Soils and Rocks**, v. 41, n. 2, p. 149–156, ago. 2018.

CONSOLI, N. C.; WINTER, D.; *et al.* Durability, Strength, and Stiffness of Green Stabilized Sand. **Journal of Geotechnical and Geoenvironmental Engineering**, v. 144, n. 9, p. 04018057, set. 2018.

CONSOLI, N. C.; PASCHE, E.; *et al.* Key parameters controlling dynamic modulus of crushed reclaimed asphalt paving–powdered rock–Portland cement blends. **Road Materials and Pavement Design**, v. 19, n. 8, p. 1716–1733, nov. 2018.

CONSOLI, N. C. *et al.* The effects of curing time and temperature on stiffness, strength and durability of sand-environment friendly binder blends. **Soils and Foundations**, v. 59, n. 5, p. 1428–1439, 2019.

___. Durability of reclaimed asphalt pavement–coal fly ash–carbide lime blends under severe environmental conditions. **Road Materials and Pavement Design**, v. 21, n. 2, p. 557–569, fev. 2020.

CONSOLI, N. C.; TEBECHRANI NETO, A.; *et al.* Durability evaluation of reclaimed asphalt pavement, ground glass and carbide lime blends based on unconfined compression tests. **Transportation Geotechnics**, v. 27, p. 100461, mar. 2021.

CONSOLI, N. C.; TONINI DE ARAÚJO, M.; *et al.* Increasing density and cement content in stabilization of expansive soils: Conflicting or complementary procedures for reducing swelling? **Canadian Geotechnical Journal**, v. 58, n. 6, p. 866–878, jun. 2021.

CONSOLI, N. C.; DAASSI-GLI, C. A. P.; *et al.* Lime–Ground Glass–Sodium Hydroxide as an Enhanced Sustainable Binder Stabilizing Silica Sand. **Journal of Geotechnical and Geoenvironmental Engineering**, v. 147, n. 10, p. 06021011, out. 2021.

CONSOLI, N. C.; ROSA, A. D.; SALDANHA, R. B. Variables Governing Strength of Compacted Soil–Fly Ash–Lime Mixtures. **Journal of Materials in Civil Engineering**, v. 23, n. 4, p. 432–440, abr. 2011.

COSTA, J. O. *et al.* Cementitious binders and reclaimed asphalt aggregates for sustainable pavement base layers: Potential, challenges and research needs. **Construction and Building Materials**, v. 265, p. 120325, 2020.

DAVIDOVITS, J. Geopolymers and geopolymeric materials. **Journal of thermal analysis**, v. 35, p. 429–441, 1989.

DEBBARMA, S.; RANSINCHUNG, G. D.; SINGH, S. Feasibility of roller compacted concrete pavement containing different fractions of reclaimed asphalt pavement. **Construction and Building Materials**, v. 199, p. 508–525, 2019.

DIAMBRA, A. *et al.* Theoretical Derivation of Artificially Cemented Granular Soil Strength. **Journal of Geotechnical and Geoenvironmental Engineering**, v. 143, n. 5, 2017.

EDEH, J. E.; ONCHE, O. J. J.; OSINUBI, K. J. Rice Husk Ash Stabilization of Reclaimed Asphalt Pavement Using Cement As Additive. n. January 2015, p. 3863–3872, 2012.

FERNANDEZ-JIMENEZ, A.; PALOMO, A. Nanostructure/microstructure of fly ash geopolymers. *In*: **Geopolymers: Structure, processing, properties and industrial applications**. [s.l: s.n.]. p. 89–117.

FESTUGATO, L. *et al.* Modelling tensile/compressive strength ratio of fibre reinforced cemented soils. **Geotextiles and Geomembranes**, v. 46, n. 2, p. 155–165, abr. 2018.

GARTNER, E. M.; MACPHEE, D. E. A physico-chemical basis for novel cementitious binders. **Cement and Concrete Research**, v. 41, n. 7, p. 736–749, 2011.

GERALDO, R. H.; FERNANDES, L. F. R.; CAMARINI, G. Water treatment sludge and rice husk ash to sustainable geopolymer production. **Journal of Cleaner Production**, v. 149, p. 146–155, abr. 2017.

HORPIBULSUK, S. *et al.* Recycled asphalt pavement ◆ fly ash geopolymer as a sustainable stabilized pavement material. **IOP Conference Series: Materials Science and Engineering**, v. 273, p. 012005, 2017.

HOY, M. *et al.* Strength and Microstructural Study of Recycled Asphalt Pavement: Slag Geopolymer as a Pavement Base Material. **Journal of Materials in Civil Engineering**, v. 30, n. 8, p. 04018177, 2018.

HOY, M.; HORPIBULSUK, S.; ARULRAJAH, A. Strength development of Recycled Asphalt Pavement - Fly ash geopolymer as a road construction material. **Construction and Building Materials**, v. 117, p. 209–219, 2016.

JAARSVELD, J. G. S. VAN; DEVENTER, J. S. J. VAN; LUKEY, G. C. <Vanjaarsveld2002.Pdf>. **Chemical Engineering Journal**, v. 89, p. 63–73, 2002.

JALLU, M. *et al.* Flexural fatigue behavior of fly ash geopolymer stabilized-geogrid reinforced RAP bases. **Construction and Building Materials**, v. 254, p. 119263, 2020.

JUENGER, M. C. G. *et al.* Advances in alternative cementitious binders. **Cement and Concrete Research**, v. 41, n. 12, p. 1232–1243, 2011.

KANG, X.; GE, L.; *et al.* Laboratory investigation of the strength, stiffness, and thermal conductivity of fly ash and lime kiln dust stabilised clay subgrade materials. **Road Materials and Pavement Design**, v. 16, n. 4, p. 928–945, 2015.

KANG, X.; KANG, G.-C.; *et al.* Chemically Stabilized Soft Clays for Road-Base Construction. **Journal of Materials in Civil Engineering**, v. 27, n. 7, p. 04014199, 2015.

KANI, N. E.; ALLAHVERDI, A.; PROVIS, J. L. Efflorescence control in geopolymer binders based on natural pozzolan. **Cement and Concrete Composites**, v. 34, n. 1, p. 25–33, 2012.

KHALIL, M. Y.; MERZ, E. Immobilization of intermediate-level wastes in geopolymers. v. 211, p. 141–148, 1994.

LLOYD, R. R. Accelerated ageing of geopolymers. *In*: **Geopolymers: Structures, Processing, Properties and Industrial Applications**. Geopolymer ed. [s.l: s.n.]. p. 139–166.

LONGHI, M. A. *et al.* **Geopolymers based on calcined kaolin sludge/ bottom ash blends and an alternative sodium silicate activator**34th Cement and Concrete Science Conference. **Anais**...2014

___. Valorisation of a kaolin mining waste for the production of geopolymers. **Journal of Cleaner Production**, 2016.

LOTERO, A. *et al.* Mechanical properties of alkali-activated ground waste glass-carbide lime blends for geotechnical uses. **Journal of Materials in Civil Engineering**, 2021.

LUUKKONEN, T. *et al.* Comparison of alkali and silica sources in one-part alkali-activated blast furnace slag mortar. **Journal of Cleaner Production**, v. 187, n. March, p. 171–179, 2018.

MEJÍA, J. M.; MEJÍA DE GUTIÉRREZ, R.; PUERTAS, F. Ceniza de cascarilla de arroz como fuente de sílice en sistemas cementicios de ceniza volante y escoria activados alcalinamente. **Materiales de Construccion**, v. 63, n. 311, p. 361–375, 2013.

MOHAMMADINIA, A. *et al.* Strength Development and Microfabric Structure of Construction and Demolition Aggregates Stabilized with Fly Ash–Based Geopolymers. **Journal of Materials in Civil Engineering**, v. 28, n. 11, p. 04016141, 2016.

Alkali-activation of fly ash and cement kiln dust mixtures for stabilization of demolition aggregates. **Construction and Building Materials**, v. 186, p. 71–78, 2018.

MOUSA, E.; EL-BADAWY, S.; AZAM, A. Evaluation of reclaimed asphalt pavement as base/subbase material in Egypt. **Transportation Geotechnics**, v. 26, n. August 2020, p. 100414, 2021.

NAWAZ, M.; HEITOR, A.; SIVAKUMAR, M. Geopolymers in construction - recent

developments. **Construction and Building Materials**, v. 260, p. 120472, 2020.

PEREIRA DOS SANTOS, C. *et al.* Stabilization of gold mining tailings with alkali-activated carbide lime and sugarcane bagasse ash. **Transportation Geotechnics**, v. 32, n. November 2021, p. 100704, jan. 2022.

PHOO-NGERNKHAM, T. *et al.* Compressive strength, Bending and Fracture Characteristics of High Calcium Fly Ash Geopolymer Mortar Containing Portland Cement Cured at Ambient Temperature. **Arabian Journal for Science and Engineering**, v. 41, n. 4, p. 1263–1271, 2015.

PIUZZI, G. P. *et al.* The effects of porosity, asphalt content and fiberglass incorporation on the tensile strength and resilient modulus of asphalt concrete blends. **Geotextiles and Geomembranes**, v. 49, n. 3, p. 864–870, jun. 2021.

PUERTAS, F.; TORRES-CARRASCO, M. Use of glass waste as an activator in the preparation of alkali-activated slag. Mechanical strength and paste characterisation. **Cement and Concrete Research**, v. 57, p. 95–104, mar. 2014.

QUEIRÓZ, L. C. *et al.* Alkali-activated system of carbide lime and rice husk for granular soil stabilization. **Proceedings of the Institution of Civil Engineers - Ground Improvement**, p. 1–37, abr. 2022.

QUIÑÓNEZ SAMANIEGO, R. A. *et al.* Key parameters controlling strength and resilient modulus of a stabilised dispersive soil. **Road Materials and Pavement Design**, n. December, p. 1–16, dez. 2021.

RAHMAN, A. *et al.* Suitability of recycled construction and demolition aggregates as alternative pipe back fi lling materials. **Journal of Cleaner Production**, v. 66, p. 75–84, 2014.

SALDANHA, R. B. *et al.* Technical and environmental performance of eggshell lime for soil stabilization. **Construction and Building Materials**, v. 298, p. 123648, set. 2021.

SARIDE, S.; AVIRNENI, D.; CHALLAPALLI, S. Micro-mechanical interaction of activated fly ash mortar and reclaimed asphalt pavement materials. **Construction and Building Materials**, v. 123, p. 424–435, 2016.

SINGH, S. *et al.* Utilization of reclaimed asphalt pavement aggregates containing waste from Sugarcane Mill for production of concrete mixes. **Journal of Cleaner Production**, v. 174, p. 42–52, 2018.

STURM, P. *et al.* Synthesizing one-part geopolymers from rice husk ash. **Construction and Building Materials**, v. 124, p. 961–966, 2016.

SUEBSUK, J.; SUKSAN, A. Strength assessment of cement treated soil-reclaimed asphalt pavement (RAP) mixture. **International Journal of GEOMATE**, v. 6, n. 2, p. 878–884, 2014.

SUKPRASERT, S. *et al.* Fly ash based geopolymer stabilisation of silty clay/blast furnace slag for subgrade applications. **Road Materials and Pavement Design**, v. 22, n. 2, p. 357–371, 2021.

SYED, M.; GUHARAY, A.; GOEL, D. Strength characterisation of fiber reinforced expansive subgrade soil stabilized with alkali activated binder. **Road Materials and Pavement Design**, v. 23, n. 5, p. 1037–1060, 2022.

TABYANGA, W. *et al.* Evaluation of municipal solid waste incineration fly ash based geopolymer for stabilised recycled concrete aggregate as road material. **Road Materials and**

Pavement Design, 2021.

TAHA, R. *et al.* Evaluation of reclaimed asphalt pavement aggregate in road bases and subbases. **Transportation Research Record**, n. 1652, p. 264–269, 1998.

Cement Stabilization of Reclaimed Asphalt Pavement Aggregate for Road Bases and Subbases. **Journal of Materials in Civil Engineering**, v. 14, n. 3, p. 239–245, 2002.

TAKEDA, H. *et al.* Characterization of Zeolite in Zeolite-Geopolymer Hybrid Bulk Materials Derived from Kaolinitic Clays. **Materials**, v. 6, n. 5, p. 1767–1778, 2013.

TCHAKOUTÉ, H. K. *et al.* Geopolymer binders from metakaolin using sodium waterglass from waste glass and rice husk ash as alternative activators: A comparative study. **Construction and Building Materials**, v. 114, p. 276–289, 2016.

TONG, K. T.; VINAI, R.; SOUTSOS, M. N. Use of Vietnamese rice husk ash for the production of sodium silicate as the activator for alkali-activated binders. **Journal of Cleaner Production**, v. 201, p. 272–286, 2018.

TONINI DE ARAÚJO, M. *et al.* Mechanical and Environmental Performance of Eggshell Lime for Expansive Soils Improvement. **Transportation Geotechnics**, v. 31, n. November, p. 100681, 2021.

TORRES-CARRASCO, M.; PALOMO, J. G.; PUERTAS, F. Sodium silicate solutions from dissolution of glasswastes. Statistical analysis. **Materiales de Construcción**, v. 64, n. 314, p. e014, mar. 2014.

TORRES-CARRASCO, M.; PUERTAS, F. Waste glass in the geopolymer preparation. Mechanical and microstructural characterisation. **Journal of Cleaner Production**, v. 90, p. 397–408, mar. 2015.

VILLAQUIRÁN-CAICEDO, M. A.; MEJIA DE GUTIÉRREZ, R.; GALLEGO, N. . A novel MK-based geopolymer composite activated with rice husk ash and KOH: performance at high temperature. **Materiales de Construcción**, v. 67, p. 1–13, 2017.

WANG, H.; LI, H.; YAN, F. Synthesis and mechanical properties of metakaolinite-based geopolymer. **Colloids and Surfaces A: Physicochemical and Engineering Aspects**, v. 268, n. 1–3, p. 1–6, 2005.

WIRTGEN GMBH. Wirtgen Cold Recycling Technology. 2012.

ZHANG, G. *et al.* Novel selection of environment-friendly cementitious materials for winter construction: Alkali-activated slag/Portland cement. **Journal of Cleaner Production**, v. 258, p. 120592, jun. 2020.

ZHUANG, X. Y. *et al.* Fly ash-based geopolymer: Clean production, properties and applications. **Journal of Cleaner Production**, v. 125, p. 253–267, 2016.

REFERÊNCIAS ITEM 3.3

ABNT. (2009A). NBR NM 52: Agregados miúdo - Determinação da massa específica e massa específica aparente. **Associação Brasileira de Normas Técnicas**.

ABNT. (2009b). NBR NM 53 : Agregado graúdo - Determinação de massa específica, massa específica aparente e absorção de água. **Associação Brasileira de Normas Técnicas**.

ADHIKARI, S., KHATTAK, M. J., & ADHIKARI, B. (2020). Mechanical characteristics of Soil-RAP-Geopolymer mixtures for road base and subbase layers. **International Journal of Pavement Engineering**, 21(4), 483–496. https://doi.org/10.1080/10298436.2018.1492131

AL-HDABI, A. (2016). Laboratory investigation on the properties of asphalt concrete mixture with Rice Husk Ash as filler. **Construction and Building Materials**, 126, 544–551. https://doi.org/10.1016/j.conbuildmat.2016.09.070

ALLAHVERDI, A., NAJAFI KANI, E., HOSSAIN, K. M. A., & LACHEMI, M. (2015). Methods to control efflorescence in alkali-activated cement-based materials. **In Handbook of Alkali-Activated Cements, Mortars and Concretes**. Woodhead Publishing Limited. https://doi.org/10.1533/9781782422884.3.463

ALLAHVERDI, A., SHAVERDI, B., & KANI, E. N. (2010). Influence of sodium oxide on properties of fresh and hardened paste of alkali-activated blast-furnace slag. International **Journal of Civil Engineering**, 8(4), 304–314.

ALNAHHAL, M. F., HAMDAN, A., HAJIMOHAMMADI, A., & KIM, T. (2021). Effect of rice husk ash-derived activator on the structural build-up of alkali activated materials. **Cement and Concrete Research**, 150(September), 106590. https://doi.org/10.1016/j.cemconres.2021.106590

ASTM. (2014). D854: Standard Test Methods for Specific Gravity of Soil Solids by Water Pycnometer. **American Society for Testing and Materials**, 1–8.

ASTM. (2016). D2166/D2166M: Standard Test Method for Unconfined Compressive Strength of Cohesive Soil. **American Society for Testing and Materials**, 1–7.

ASTM. (2017a). D2487: Standard Practice for Classification of Soils for Engineering Purposes (Unified Soil Classification System). **American Society for Testing and Materials**, 1–5.

ASTM. (2017b). D7928: Standard Test Method for Particle-Size Distribution (Gradation) of Fine-Grained Soils Using the Sedimentation (Hydrometer) Analysis. **ASTM International**.

ASTM. (2018). D2172/D2172M: Standard Test Methods for Quantitative Extraction of Bitumen From Bituminous Paving Mixtures. **American Society for Testing and Materials**. https://doi.org/10.1520/D2172-11.2

ASTM. (2021). D698: Standard Test Methods for Laboratory Compaction Characteristics of Soil Using Standard Effort (12,400 ft-lbf/ft3 (600 kN-m/m3)). **American Society for Testing and Materials**.

AVIRNENI, D., PEDDINTI, P. R. T., & SARIDE, S. (2016). Durability and long term performance of geopolymer stabilized reclaimed asphalt pavement base courses. **Construction and Building Materials**, 121, 198–209. https://doi.org/10.1016/j.conbuildmat.2016.05.162

BERNAL, S. A., RODRÍGUEZ, E. D., DE GUTIÉRREZ, R. M., & PROVIS, J. L. (2015). Performance at high temperature of alkali-activated slag pastes produced with silica fume and rice husk ash based activators. **Materiales de Construccion**, 65(318).

https://doi.org/10.3989/mc.2015.03114

BERNAL, SUSAN A., RODRÍGUEZ, E. D., MEJIA DE GUTIÉRREZ, R., PROVIS, J. L., & DELVASTO, S. (2012). Activation of metakaolin/slag blends using alkaline solutions based on chemically modified silica fume and rice husk ash. **Waste and Biomass Valorization**, 3(1), 99–108. https://doi.org/10.1007/s12649-011-9093-3

BOUZÓN, N., PAYÁ, J., BORRACHERO, M. V., SORIANO, L., TASHIMA, M. M., & MONZÓ, J. (2014). Refluxed rice husk ash/NaOH suspension for preparing alkali activated binders. **Materials Letters**, 115, 72–74. https://doi.org/10.1016/j.matlet.2013.10.001

BRUSCHI, G. J., DOS SANTOS, C. P., TONINI DE ARAÚJO, M., FERRAZZO, S. T., MARQUES, S. F. V., & CONSOLI, N. C. (2021). Green Stabilization of Bauxite Tailings: Mechanical Study on Alkali-Activated Materials. **Journal of Materials in Civil Engineering**, 33(11), 06021007. https://doi.org/10.1061/(ASCE)MT.1943-5533.0003949

BRUSCHI, G. J., SANTOS, C. P. DOS, FERRAZZO, S. T., ARAÚJO, M. T. DE, & CONSOLI, N. C. (2021). Parameters controlling loss of mass and stiffness degradation of green stabilized bauxite tailings. **Proceedings of the Institution of Civil Engineers - Geotechnical Engineering,** 1–21. https://doi.org/10.1680/jgeen.21.00119

BRUSCHI, G. J., SECCO, M. P., SOUSA, L., BRIGA-SÁ, A., & CRISTELO, N. (2022). Development of facade panels with optimised thermal performance from alkali-activated stone-cutting waste. **Environmental Earth Sciences,** 81(12), 1–15. https://doi.org/10.1007/s12665-022-10452-3

CIHLÁŘOVÁ, D., FENCL, I., CÁPAYOVÁ, S., & POSPÍŠIL, P. (2018). Use of Adhesion Promoters in Asphalt Mixtures. **Slovak Journal of Civil Engineering**, 26(1), 19–24. https://doi.org/10.2478/sjce-2018-0003

CONSOLI, N. C., LEON, H. B., DA SILVA CARRETTA, M., DARONCO, J. V. L., & LOURENÇO, D. E. (2019). The effects of curing time and temperature on stiffness, strength and durability of sand-environment friendly binder blends. **Soils and Foundations**, 59(5), 1428–1439. https://doi.org/10.1016/j.sandf.2019.06.007

DAI, S., WANG, H., AN, S., & YUAN, L. (2022). Mechanical Properties and Microstructural Characterization of Metakaolin Geopolymers Based on Orthogonal Tests. **Materials,** 15(8).

DAVIDOVITS, J. (1989). Geopolymers and geopolymeric materials. **Journal of Thermal Analysis**, 35, 429–441.

DAVIDOVITS, J. (2018). False Values on CO2 Emission for Geopolymer Cement / Concrete published in Scientific Papers How to cite this paper : False Values on CO_2 Emission for Geopolymer Cement / Concrete published in **Scientific Papers**. January 2015.

DEBBARMA, S., RANSINCHUNG, G. D., & SINGH, S. (2019). Feasibility of roller compacted concrete pavement containing different fractions of reclaimed asphalt pavement. **Construction and Building Materials**, 199, 508–525.

DNIT. (2010). DNIT 143: Pavimentação – Base de solo-cimento - Especificação de serviço. **Departamento Nacional de Infraestrutura de Transportes**, 1–10.

DUŻY, P., CHOINSKA, M., HAGER, I., AMIRI, O., & CLAVERIE, J. (2022). Mechanical Strength and Chloride Ions' Penetration of Alkali-Activated Concretes (AAC) with Blended Precursor. **Materials**, 15(13). https://doi.org/10.3390/ma15134475

EDEH, J. E., ONCHE, O. J. J., & OSINUBI, K. J. (2012). Rice Husk Ash Stabilization of Reclaimed Asphalt Pavement Using Cement As Additive. **January** 2015, 3863–3872.

FEDRIGO, W., NÚÑEZ, W. P., & VISSER, A. T. (2020). A review of full-depth reclamation of pavements with Portland cement: Brazil and abroad. **Construction and Building Materials**, 262, 120540.

FERREIRA, W., CASTELO BRANCO, V., & VASCONCELOS, K. (2022). The Impact of the RAP cluster dissociation on gradation and shape properties of aggregates from recycled asphalt mixtures. **Journal of Testing and Evaluation**, 50(2), 20210155.

FERREIRA, W. L. G., CASTELO BRANCO, V. T. F., VASCONCELOS, K., BHASIN, A., & SREERAM, A. (2021). The impact of aging heterogeneities within RAP binder on recycled asphalt mixture design. **Construction and Building Materials**, 300(March).

GARCIA-LODEIRO, I., PALOMO, A., & FERNÁNDEZ-JIMÉNEZ, A. (2015). An overview of the chemistry of alkali-activated cement-based binders. **Handbook of Alkali-Activated Cements, Mortars and Concretes**, April 2016, 19–47.

GARCIA-LODEIRO, I., PALOMO, A., FERNÁNDEZ-JIMÉNEZ, A., & MACPHEE, D. E. (2011). Compatibility studies between N-A-S-H and C-A-S-H gels. Study in the ternary diagram Na2O-CaO-Al2O3-SiO 2-H2O. **Cement and Concrete Research**, 41(9), 923–931.

HORPIBULSUK, S., HOY, M., WITCHAYAPHONG, P., RACHAN, R., & ARULRAJAH, A. (2017). Recycled asphalt pavement ﬂy ash geopolymer as a sustainable stabilized pavement material. **IOP Conference Series: Materials Science and Engineering**, 273, 012005.

HOY, M., HORPIBULSUK, S., ARULRAJAH, A., & MOHAJERANI, A. (2018). Strength and Microstructural Study of Recycled Asphalt Pavement: Slag Geopolymer as a Pavement Base Material. **Journal of Materials in Civil Engineering**, 30(8), 04018177.

JALLU, M., ARULRAJAH, A., SARIDE, S., & EVANS, R. (2020). Flexural fatigue behavior of fly ash geopolymer stabilized-geogrid reinforced RAP bases. **Construction and Building Materials**, 254, 119263.

KANG, X., GE, L., KANG, G. C., & MATHEWS, C. (2015). Laboratory investigation of the strength, stiffness, and thermal conductivity of fly ash and lime kiln dust stabilised clay subgrade materials. **Road Materials and Pavement Design**, 16(4), 928–945.

KANG, X., KANG, G.-C., CHANG, K.-T., & GE, L. (2015). Chemically Stabilized Soft Clays for Road-Base Construction. **Journal of Materials in Civil Engineering**, 27(7), 04014199.

KHALE, D., & CHAUDHARY, R. (2007). Mechanism of geopolymerization and factors influencing its development: A review. **Journal of Materials Science**, 42(3), 729–746. https://doi.org/10.1007/s10853-006-0401-4

LO PRESTI, D., VASCONCELOS, K., OREŠKOVIĆ, M., PIRES, G. M., & BRESSI, S. (2020). On the degree of binder activity of reclaimed asphalt and degree of blending with recycling agents. **Road Materials and Pavement Design** (Vol. 21, Issue 8).

MA, F., SHA, A., YANG, P., & HUANG, Y. (2016). The greenhouse gas emission from portland cement concrete pavement construction in China. **International Journal of Environmental Research and Public Health**, 13(7).

MAVROULIDOU, M., GRAY, C., GUNN, M. J., & PANTOJA-MUÑOZ, L. (2021). A Study of Innovative Alkali-Activated Binders for Soil Stabilisation in the Context of Engineering Sustainability and Circular Economy. **Circular Economy and Sustainability**.

MENDES, B. C., PEDROTI, L. G., VIEIRA, C. M. F., MARVILA, M., AZEVEDO, A. R.

G., FRANCO DE CARVALHO, J. M., & RIBEIRO, J. C. L. (2021). Application of eco-friendly alternative activators in alkali-activated materials: A review. **Journal of Building Engineering,** 35(November 2020).

MILLER, S. A., & MYERS, R. J. (2020). Environmental Impacts of Alternative Cement Binders. **Environmental Science and Technology**, 54(2), 677–686.

MO, B. H., ZHU, H., CUI, X. M., HE, Y., & GONG, S. Y. (2014). Effect of curing temperature on geopolymerization of metakaolin-based geopolymers. **Applied Clay Science**, 99, 144–148.

NAJAFI KANI, E., ALLAHVERDI, A., & PROVIS, J. L. (2012). Efflorescence control in geopolymer binders based on natural pozzolan. **Cement and Concrete Composites**, 34(1), 25–33.

NAZARI, A., BAGHERI, A., & RIAHI, S. (2011). Properties of geopolymer with seeded fly ash and rice husk bark ash. **Materials Science and Engineering A**, 528(24), 7395–7401. https://doi.org/10.1016/j.msea.2011.06.027

NEMATI, K. M., & UHLMEYER, J. S. (2021). Accelerated construction of urban intersections with Portland Cement Concrete Pavement (PCCP). **Case Studies in Construction Materials**, 14, e00499.

PASCHE, E., BRUSCHI, G. J., SPECHT, L. P., ARAGÃO, F. T. S., & CONSOLI, N. C. (2022). Fiber-reinforcement effect on the mechanical behavior of reclaimed asphalt pavement–powdered rock–Portland cement mixtures. **Transportation Engineering, 9**(January).

PEREIRA DOS SANTOS, C., BRUSCHI, G. J., MATTOS, J. R. G., & CONSOLI, N. C. (2022). Stabilization of gold mining tailings with alkali-activated carbide lime and sugarcane bagasse ash. **Transportation Geotechnics**, 32(December).

POURKHORSHIDI, S., SANGIORGI, C., TORREGGIANI, D., & TASSINARI, P. (2020). Using Recycled Aggregates from Construction and Demolition Waste in Unbound Layers of Pavements. **Sustainability** (Switzerland), 12(22), 1–20.

PROVIS, J. L. (2018). Alkali-activated materials. **Cement and Concrete Research**, 114, 40–48.

QIN, L., GAO, X., & LI, Q. (2018). Upcycling carbon dioxide to improve mechanical strength of Portland cement. **Journal of Cleaner Production,** 196, 726–738.

QUEIRÓZ, L. C., MIGUEL, G. D., BRUSCHI, G. J., & LIMA, M. D. S. DE. (2022). Macro-Micro Characterization of Green Stabilized Alkali-Activated Sand. **Geotechnical and Geological Engineering**, 40(7), 3763–3778.

QUEIRÓZ, L. C., SOUZA, L. M. P., LIMA, M. D., DANIELI, S., BRUSCHI, G. J., & BERGMANN, C. P. (2022). Alkali-activated system of carbide lime and rice husk for granular soil stabilisation. **Proceedings of the Institution of Civil Engineers - Ground Improvement**, 175(6), 1–37.

RADEVIĆ, A., ISAILOVIĆ, I., WISTUBA, M. P., ZAKIĆ, D., OREŠKOVIĆ, M., & MLADENOVIĆ, G. (2020). The impact of recycled concrete aggregate on the stiffness, fatigue, and low-temperature performance of asphalt mixtures for road construction. **Sustainability** (Switzerland), 12(10).

SAJAN, P., JIANG, T., LAU, C. K., TAN, G., & NG, K. (2021). Combined effect of curing temperature, curing period and alkaline concentration on the mechanical properties of fly ash-

based geopolymer. **Cleaner Materials**, 1(June), 100002.

SARIDE, S., AVIRNENI, D., & CHALLAPALLI, S. (2016). Micro-mechanical interaction of activated fly ash mortar and reclaimed asphalt pavement materials. **Construction and Building Materials**, 123, 424–435.

SEPLAG. (2021). Clima, temperatura e precipitação - Atlas Socioeconômico do Rio Grande do Sul. **Secretária de Planejamento, Orçamento e Gestão**, 1–5.

SIMÃO, L., FERNANDES, E., HOTZA, D., RIBEIRO, M. J., MONTEDO, O. R. K., & RAUPP-PEREIRA, F. (2021). Controlling efflorescence in geopolymers: A new approach. **Case Studies in Construction Materials**, 15(October).

SINGH, S., RANSINCHUNG, G. D., DEBBARMA, S., & KUMAR, P. (2018). Utilization of reclaimed asphalt pavement aggregates containing waste from Sugarcane Mill for production of concrete mixes. **Journal of Cleaner Production**, 174, 42–52.

SUKPRASERT, S., HOY, M., HORPIBULSUK, S., ARULRAJAH, A., RASHID, A. S. A., & NAZIR, R. (2021). Fly ash based geopolymer stabilisation of silty clay/blast furnace slag for subgrade applications. **Road Materials and Pavement Design**, 22(2), 357–371.

SYED, M., GUHARAY, A., & GOEL, D. (2022). Strength characterisation of fiber reinforced expansive subgrade soil stabilized with alkali activated binder. **Road Materials and Pavement Design**, 23(5), 1037–1060.

TABYANGA, W., SUKSIRIPATTANAPONG, C., PHETCHUAY, C., LAKSANAKIT, C., & CHUSILP, N. (2021). Evaluation of municipal solid waste incineration fly ash based geopolymer for stabilised recycled concrete aggregate as road material. **Road Materials and Pavement Design.**

TCHAKOUTÉ, HERVÉ K., RÜSCHER, C. H., KONG, S., KAMSEU, E., & LEONELLI, C. (2016). Geopolymer binders from metakaolin using sodium waterglass from waste glass and rice husk ash as alternative activators: A comparative study. **Construction and Building Materials**, 114, 276–289.

TCHAKOUTÉ, HERVÉ KOUAMO, RÜSCHER, C. H., KONG, S., & RANJBAR, N. (2016). Synthesis of sodium waterglass from white rice husk ash as an activator to produce metakaolin-based geopolymer cements. **Journal of Building Engineering,** 6, 252–261.

TEMUUJIN, J., VAN RIESSEN, A., & WILLIAMS, R. (2009). Influence of calcium compounds on the mechanical properties of fly ash geopolymer pastes. **Journal of Hazardous Materials**, 167(1–3), 82–88.

TIAN, X., XU, W., SONG, S., RAO, F., & XIA, L. (2020). Effects of curing temperature on the compressive strength and microstructure of copper tailing-based geopolymers. **Chemosphere**, 253, 126754.

TURNER, L. K., & COLLINS, F. G. (2013). Carbon dioxide equivalent (CO2-e) emissions: A comparison between geopolymer and OPC cement concrete. **Construction and Building Materials**, 43, 125–130.

VILLAQUIRÁN-CAICEDO, M. A., MEJIA DE GUTIÉRREZ, R., & GALLEGO, N. . (2017). A novel MK-based geopolymer composite activated with rice husk ash and KOH: performance at high temperature. **Materiales de Construcción**, 67, 1–13.

VISLAVIČIUS, K., & SIVILEVIČIUS, H. (2013). Effect of reclaimed asphalt pavement gradation variation on the homogeneity of recycled hot-mix asphalt. **Archives of Civil and Mechanical Engineering**, 13(3), 345–353.

WIRTGEN GMBH. (2012). Wirtgen Cold Recycling Technology.

XIE, T., & OZBAKKALOGLU, T. (2015). Behavior of low-calcium fly and bottom ash-based geopolymer concrete cured at ambient temperature. **Ceramics International**, 41(4), 5945–5958.

XUE, X., LIU, Y. L., DAI, J. G., POON, C. S., ZHANG, W. D., & ZHANG, P. (2018). Inhibiting efflorescence formation on fly ash–based geopolymer via silane surface modification. **Cement and Concrete Composites**, 94(March), 43–52.

YANG, Q., YIN, H., HE, X., CHEN, F., ALI, A., MEHTA, Y., & YAN, B. (2020). Environmental impacts of reclaimed asphalt pavement on leaching of metals into groundwater. **Transportation Research Part D: Transport and Environment**, 85(June),

ZHANG, S., REN, F., ZHAO, Y., QIU, J., & GUO, Z. (2021). The effect of stone waste on the properties of cemented paste backfill using alkali-activated slag as binder. **Construction and Building Materials**, 283, 122686.

ZHOU, H., WANG, X., WU, Y., & ZHANG, X. (2021). Mechanical properties and micro-mechanisms of marine soft soil stabilized by different calcium content precursors based geopolymers. **Construction and Building Materials**, 305(September), 124722.

ZHOU, S., ZHOU, S., ZHANG, J., TAN, X., & CHEN, D. (2020). Relationship between moisture transportation, efflorescence and structure degradation in fly ash/slag geopolymer. **Materials**, 13(23), 1–16.

REFERÊNCIAS ITEM 3.4

ABNT. 2004a. NBR 10004: Resíduos sólidos - Classificação. **Associação Brasileira de Normas Técnicas.**

ABNT. 2004b. NBR 10005: Procedimento para obtenção de extrato de lixiviado de resíduos sólidos. **Associação Brasileira de Normas Técnicas.**, 16.

ABNT. 2009a. NBR NM 53 : Agregado graúdo - Determinação de massa específica, massa específica aparente e absorção de água. **Associação Brasileira de Normas Técnicas.**.

ABNT. 2009b. NBR NM 52: Agregados miúdo - Determinação da massa específica e massa específica aparente. **Associação Brasileira de Normas Técnicas.**.

ABNT. 2009c. NBR 10006: Procedimento para obtenção de extreto de solubilizado de resíduos sólidos. **Associação Brasileira de Normas Técnicas.**, 1–14.

ABNT. 2012. NBR 12253: Solo-cimento - Dosagem para emprego como camada de pavimento. **Associação Brasileira de Normas Técnicas.**.

ABRAHAM, S. M., AND G. D. RANSINCHUNG. 2019. Effects of Reclaimed Asphalt Pavement aggregates and mineral admixtures on pore structure, mechanical and durability properties of cement mortar. **Construction and Building Materials**, 216: 202–213. Elsevier Ltd.

ABRAHAM, S. M., AND G. D. R. N. RANSINCHUNG. 2018. Influence of RAP aggregates on strength, durability and porosity of cement mortar. **Construction and Building Materials**, 189: 1105–1112. Elsevier Ltd.

ADHIKARI, S., M. J. KHATTAK, AND B. ADHIKARI. 2020. Mechanical characteristics of Soil-RAP-Geopolymer mixtures for road base and subbase layers. **International Journal of Pavement Engineering**, 21 (4): 483–496. Taylor & Francis.

AL-HDABI, A. 2016. Laboratory investigation on the properties of asphalt concrete mixture with Rice Husk Ash as filler. **Construction and Building Materials**, 126: 544–551. Elsevier Ltd.

ARULRAJAH, A., M. M. DISFANI, H. HAGHIGHI, A. MOHAMMADINIA, AND S. HORPIBULSUK. 2015. Modulus of rupture evaluation of cement stabilized recycled glass/recycled concrete aggregate blends. **Construction and Building Materials**, 84: 146–155.

ARULRAJAH, A., J. PIRATHEEPAN, M. M. DISFANI, AND M. W. BO. 2013. Resilient Moduli Response of Recycled Construction and Demolition Materials in Pavement Subbase Applications. **Journal of Materials in Civil Engineering**, 25 (12): 1920–1928.

ASTM. 2012. D559-03: Standard Test Methods for Wetting and Drying Compacted Soil-Cement Mixtures. **American Society for Testing and Materials**.

ASTM. 2014. D854: Standard Test Methods for Specific Gravity of Soil Solids by Water Pycnometer. **American Society for Testing and Materials**, 1–8.

ASTM. 2016. D2166/D2166M: Standard Test Method for Unconfined Compressive Strength of Cohesive Soil. **American Society for Testing and Materials**, 1–7.

ASTM. 2017a. D7928: Standard Test Method for Particle-Size Distribution (Gradation) of Fine-Grained Soils Using the Sedimentation (Hydrometer) Analysis. **American Society for Testing and Materials.**

ASTM. 2017b. D2487: Standard Practice for Classification of Soils for Engineering Purposes

(Unified Soil Classification System). **American Society for Testing and Materials**, 1–5.

AVIRNENI, D., P. R. T. PEDDINTI, AND S. SARIDE. 2016. Durability and long term performance of geopolymer stabilized reclaimed asphalt pavement base courses. **Construction and Building Materials**, 121: 198–209.

AWOYERA, P., AND A. ADESINA. 2019. A critical review on application of alkali activated slag as a sustainable composite binder. **Case Studies in Construction Materials**, 11: e00268.

BERNAL, S. A., E. D. RODRÍGUEZ, R. M. DE GUTIÉRREZ, AND J. L. PROVIS. 2015. Performance at high temperature of alkali-activated slag pastes produced with silica fume and rice husk ash based activators. **Materiales De Construccion**, 65 (318).

BERNAL, S. A., E. D. RODRÍGUEZ, R. MEJIA DE GUTIÉRREZ, J. L. PROVIS, AND S. DELVASTO. 2012. Activation of metakaolin/slag blends using alkaline solutions based on chemically modified silica fume and rice husk ash. **Waste and Biomass Valorization**, 3 (1): 99–108.

BONICELLI, A., P. CALVI, G. MARTINEZ-ARGUELLES, L. FUENTES, AND F. GIUSTOZZI. 2017. Experimental study on the use of rejuvenators and plastomeric polymers for improving durability of high RAP content asphalt mixtures. **Construction and Building Materials**, 155: 37–44.

BOUZÓN, N., J. PAYÁ, M. V. BORRACHERO, L. SORIANO, M. M. TASHIMA, AND J. MONZÓ. 2014. Refluxed rice husk ash/NaOH suspension for preparing alkali activated binders. **Materials Letters**, 115: 72–74.

BRUSCHI, G. J., C. P. DOS SANTOS, S. T. FERRAZZO, M. T. DE ARAÚJO, AND N. C. CONSOLI. 2021a. Parameters controlling loss of mass and stiffness degradation of green stabilized bauxite tailings. **ICE Proceedings Geotechnical Engineering**, 1–21.

BRUSCHI, G. J., C. P. DOS SANTOS, W. M. K. LEVANDOSKI, S. T. FERRAZZO, E. P. KORF, R. B. SALDANHA, AND N. C. CONSOLI. 2022. Leaching assessment of cemented bauxite tailings through wetting and drying cycles of durability test. **Environmental Science and Pollution Research**, 29 (6).

BRUSCHI, G. J., C. P. DOS SANTOS, M. TONINI DE ARAÚJO, S. T. FERRAZZO, S. F. V. MARQUES, AND N. C. CONSOLI. 2021B. Green Stabilization of Bauxite Tailings: Mechanical Study on Alkali-Activated Materials. **Journal of Materials in Civil Engineering**, 33 (11).

CNT. 2019. Confederação Nacional de Transportes. **CNT Highw. Surv**. Brasília CNT SEST Senat. Port.

CONSOLI, N. C., L. FESTUGATO, H. C. S. FILHO, G. D. MIGUEL, A. T. NETO, AND D. ANDREGHETTO. 2020. Durability Assessment of Soil-Pozzolan-Lime Blends through Ultrasonic-Pulse Velocity Test. **Journal of Materials in Civil Engineering**, 32 (8).

CONSOLI, N. C., D. N. GIESE, H. B. LEON, D. M. MOCELIN, R. WETZEL, AND S. F. V. MARQUES. 2018a. Sodium chloride as a catalyser for crushed reclaimed asphalt pavement – Fly ash – Carbide lime blends. **Transportation Geotechnics**, 15: 13–19.

CONSOLI, N. C., H. B. LEON, M. DA SILVA CARRETTA, J. V. L. DARONCO, AND D. E. LOURENÇO. 2019. The effects of curing time and temperature on stiffness, strength and durability of sand-environment friendly binder blends. **Soils and Foundations**, 59 (5): 1428–1439.

CONSOLI, N. C., E. PASCHE, L. P. SPECHT, AND M. TANSKI. 2018b. Key parameters controlling dynamic modulus of crushed reclaimed asphalt paving–powdered rock–Portland cement blends. **Road Materials and Pavement Design**, 19 (8): 1716–1733.

CONSOLI, N. C., R. A. Q. SAMANIEGO, L. E. GONZÁLEZ, AND E. J. BITTAR. 2018c. Impact of Severe Climate Conditions on Loss of Mass, Strength, and Stiffness of Compacted Fine-Grained Soils–Portland Cement Blends. **Journal of Materials in Civil Engineering**, 30 (8).

CONSOLI, N. C., R. A. Q. SAMANIEGO, AND N. M. K. VILLALBA. 2016. Durability, Strength, and Stiffness of Dispersive Clay–Lime Blends. **Journal of Materials in Civil Engineering**, 28 (11).

CONSOLI, N. C., A. P. DA SILVA, H. P. NIERWINSKI, AND J. SOSNOSKI. 2018d. Durability, strength, and stiffness of compacted gold tailings – cement mixes. **Canadian Geotechnical Journal**, 55 (4): 486–494.

CONSOLI, N. C., A. TEBECHRANI NETO, B. R. S. CORREA, R. A. QUIÑÓNEZ SAMANIEGO, AND N. CRISTELO. 2021a. Durability evaluation of reclaimed asphalt pavement, ground glass and carbide lime blends based on unconfined compression tests. **Transportation Geotechnics**, 27 (June 2020).

CONSOLI, N. C., AND L. F. TOMASI. 2018. The impact of dry unit weight and cement content on the durability of sand-cement blends. **Proceedings of the Institution of Civil Engineers Ground Improvement**, 171 (2): 96–102.

CONSOLI, N. C., M. TONINI DE ARAÚJO, S. TONATTO FERRAZZO, V. DE LIMA RODRIGUES, AND C. GRAVINA DA ROCHA. 2021b. Increasing density and cement content in stabilization of expansive soils: Conflicting or complementary procedures for reducing swelling? **Canadian Geotechnical Journal**, 58 (6): 866–878.

COSTA, J. O., P. H. R. BORGES, F. A. DOS SANTOS, A. C. S. BEZERRA, W. VAN DEN BERGH, AND J. BLOM. 2020. Cementitious binders and reclaimed asphalt aggregates for sustainable pavement base layers: Potential, challenges and research needs. **Construction and Building Materials**, 265: 120325.

D2172, A. 2011. Standard Test Methods for Quantitative Extraction of Bitumen From Bituminous Paving Mixtures. **American Society for Testing and Materials**, 1–13.

DAVIDOVITS, J. 1989. Geopolymers and geopolymeric materials. **J. Therm. Anal**., 35: 429–441.

DEBBARMA, S., G. D. RANSINCHUNG, S. SINGH. 2019. Feasibility of roller compacted concrete pavement containing different fractions of reclaimed asphalt pavement. **Construction and Building Materials**, 199: 508–525.

DONG, Q., B. HUANG. 2014. Laboratory Evaluation on Resilient Modulus and Rate Dependencies of RAP Used as Unbound Base Material. **Journal of Materials in Civil Engineering**, 26 (2).

EDEH, J. E., O. J. J. ONCHE, AND K. J. OSINUBI. 2012. Rice Husk Ash Stabilization of Reclaimed Asphalt Pavement Using Cement As Additive. **Journal of ASTM International**, 2015: 3863–3872.

GERALDO, R. H., L. F. R. FERNANDES, AND G. CAMARINI. 2017. Water treatment sludge and rice husk ash to sustainable geopolymer production. **Journal of Cleaner Production**, 149: 146–155.

GODENZONI, C., A. GRAZIANI, E. BOCCI, M. BOCCI. 2018. The evolution of the mechanical behaviour of cold recycled mixtures stabilised with cement and bitumen: field and laboratory study. **Road Materials and Pavement Design**, 19 (4): 856–877.

GODENZONI, C., A. GRAZIANI, D. PERRATON. 2017. Complex modulus characterisation of cold-recycled mixtures with foamed bitumen and different contents of reclaimed asphalt. **Road Materials and Pavement Design**, 18 (1): 130–150.

GÓMEZ-MEIJIDE, B., H. AJAM, P. LASTRA-GONZÁLEZ, A. GARCIA. 2018. Effect of ageing and RAP content on the induction healing properties of asphalt mixtures. **Construction and Building Materials**, 179: 468–476.

GRILLI, A., F. CARDONE, E. BOCCI. 2018. Mechanical behaviour of cement-bitumen treated materials containing different amounts of reclaimed asphalt. **European Journal of Environmental and Civil Engineering**, 22 (7).

HORPIBULSUK, S., M. HOY, P. WITCHAYAPHONG, R. RACHAN, AND A. ARULRAJAH. 2017. Recycled asphalt pavement fly ash geopolymer as a sustainable stabilized pavement material. **IOP Conference Series Materials Science and Engineering**, 273: 012005.

HOY, M., S. HORPIBULSUK, AND A. ARULRAJAH. 2016a. Strength development of Recycled Asphalt Pavement - Fly ash geopolymer as a road construction material. **Construction and Building Materials**, 117: 209–219.

HOY, M., S. HORPIBULSUK, A. ARULRAJAH, AND A. MOHAJERANI. 2018. Strength and Microstructural Study of Recycled Asphalt Pavement: Slag Geopolymer as a Pavement Base Material. **Journal of Materials in Civil Engineering**, 30 (8): 04018177.

HOY, M., S. HORPIBULSUK, R. RACHAN, A. CHINKULKIJNIWAT, A. ARULRAJAH. 2016b. Recycled asphalt pavement – fly ash geopolymers as a sustainable pavement base material: Strength and toxic leaching investigations. **Science of The Total Environment**, 573: 19–26.

JALLU, M., A. ARULRAJAH, S. SARIDE, R. EVANS. 2020. Flexural fatigue behavior of fly ash geopolymer stabilized-geogrid reinforced RAP bases. **Construction and Building Materials**, 254: 119263.

KANG, X., L. GE, G. C. KANG, AND C. MATHEWS. 2015. Laboratory investigation of the strength, stiffness, and thermal conductivity of fly ash and lime kiln dust stabilised clay subgrade materials. **Road Materials and Pavement Design**, 16 (4): 928–945.

LEANDRI, P., M. LOSA, A. DI NATALE. 2015. Field validation of recycled cold mixes viscoelastic properties. **Construction and Building Materials**, 75: 275–282.

LI, P., L. ZHAI, Q. FU, Q. YAN. 2019. Influence of RAP Dispersion Characteristics on Mixture Performance. **Journal of Materials in Civil Engineering**, 31 (9).

LLOYD, R. R. 2009. Accelerated ageing of geopolymers. **Geopolymers: Structure, processing, properties and industrial applications**, 139–166.

LONGHI, M. A., F. GAEDKE, E. D. RODRÍGUEZ, A. PASSUELLO, A. P. KIRCHHEIM, S. A. BERNAL, J. L. PROVIS. 2014. Geopolymers based on calcined kaolin sludge/ bottom ash blends and an alternative sodium silicate activator. **34th Cem. Concr. Sci. Conf**., 182.

LONGHI, M. A., E. D. RODRÍGUEZ, S. A. BERNAL, J. L. PROVIS, A. PAULA. 2016. Valorisation of a kaolin mining waste for the production of geopolymers. **Journal of Cleaner Production**.

DE LORENA DINIZ CHAVES, G., R. R. SIMAN, G. M. RIBEIRO, N. BIN CHANG. 2021. Synergizing environmental, social, and economic sustainability factors for refuse derived fuel use in cement industry: A case study in Espirito Santo, Brazil. **Journal of Environmental Management**, 288 (November 2020).

LUUKKONEN, T., Z. ABDOLLAHNEJAD, J. YLINIEMI, P. KINNUNEN, M. ILLIKAINEN. 2018. Comparison of alkali and silica sources in one-part alkali-activated blast furnace slag mortar. **Journal of Cleaner Production**, 187 (March): 171–179.

MEJÍA, J. M., R. MEJÍA DE GUTIÉRREZ, F. PUERTAS. 2013. Ceniza de cascarilla de arroz como fuente de sílice en sistemas cementicios de ceniza volante y escoria activados alcalinamente. **Materiales de construcción**, 63 (311): 361–375.

MONU, K., G. D. RANSINCHUNG, S. SINGH. 2019. Effect of long-term ageing on properties of RAP inclusive WMA mixes. **Construction and Building Materials**, 206: 483–493.

MULLAPUDI, R. S., P. S. CHOWDHURY, K. S. REDDY. 2020. Fatigue and Healing Characteristics of RAP Binder Blends. **Journal of Materials in Civil Engineering**, 32 (8): 04020214.

NGUYEN, M. L., J. M. BALAY, H. DI BENEDETTO, C. SAUZÉAT, K. BILODEAU, F. OLARD, B. HÉRITIER, H. DUMONT, AND D. BONNEAU. 2017. Evaluation of pavement materials containing RAP aggregates and hydraulic binder for heavy traffic pavement. **Road Materials and Pavement Design**,18 (2): 264–280.

DE OLIVEIRA, L. B., A. R. G. DE AZEVEDO, M. T. MARVILA, E. C. PEREIRA, R. FEDIUK, AND C. M. F. VIEIRA. 2022. Durability of geopolymers with industrial waste. **Case Studies in Construction Materials**, 16 (December 2021): e00839.

PASCHE, E., L. P. SPECHT, M. C. TANSKY, AND N. C. CONSOLI. 2018. Avaliação da rigidez de misturas recicladas cimentadas: Abordagem elástica e viscoelásticas. **Transportes**, 26 (1): 94–107.

PCA. 1956. Soil-cement laboratory handbook. **Portland Cement Association**.

PEREIRA DOS SANTOS, C., G. J. BRUSCHI, J. R. G. MATTOS, AND N. C. CONSOLI. 2022. Stabilization of gold mining tailings with alkali-activated carbide lime and sugarcane bagasse ash. **Transportation Geotechnics**, 32 (November 2021): 100704.

PHOO-NGERNKHAM, T., V. SATA, S. HANJITSUWAN, C. RIDTIRUD, S. HATANAKA, AND P. CHINDAPRASIRT. 2015. Compressive strength, Bending and Fracture Characteristics of High Calcium Fly Ash Geopolymer Mortar Containing Portland Cement Cured at Ambient Temperature. **Arabian Journal for Science and Engineering**, 41 (4): 1263–1271.

PUERTAS, F., S. MARTÍNEZ-RAMÍREZ, S. ALONSO, AND T. VÁZQUEZ. 2000. Alkali-Activated Fly Ash/Slag Cement Strength Behaviour and Hydration Products. **Cement Concrete Research**, 301 (10): 1625–1632.

PUERTAS, F., M. TORRES-CARRASCO. 2014. Use of glass waste as an activator in the preparation of alkali-activated slag. Mechanical strength and paste characterisation. **Cement Concrete Research**, 57: 95–104.

PUPPALA, A. J., L. R. HOYOS, A. K. POTTURI. 2011. Resilient Moduli Response of Moderately Cement-Treated Reclaimed Asphalt Pavement Aggregates. **Journal of Materials in Civil Engineering**, 23 (7).

PUPPALA, A. J., S. SARIDE, AND R. WILLIAMMEE. 2012. Sustainable Reuse of Limestone Quarry Fines and RAP in Pavement Base/Subbase Layers. **Journal of Materials in Civil Engineering**, 24 (4).

QUEIRÓZ, L. C., L. L. S. BATISTA, L. M. P. SOUZA, M. D. LIMA, S. DANIELI, G. J. BRUSCHI, AND C. P. BERGMANN. 2022. Alkali-activated system of carbide lime and rice husk for granular soil stabilization. **Proceedings of the Institution of Civil Engineers Ground Improvement**, 1–37.

RAHMAN, M. A., M. IMTEAZ, A. ARULRAJAH, M. M. DISFANI. 2014. Suitability of recycled construction and demolition aggregates as alternative pipe backfilling materials. **Journal of Cleaner Production**, 66: 75–84.

SARIDE, S., D. AVIRNENI, S. CHALLAPALLI. 2016. Micro-mechanical interaction of activated fly ash mortar and reclaimed asphalt pavement materials. **Construction and Building Materials**, 123: 424–435.

SARIDE, S., M. JALLU. 2020. Effect of Fly Ash Geopolymer on Layer Coefficients of Reclaimed Asphalt Pavement Bases. **Journal of Transportation Engineering Part B Pavements**, 146 (3).

SARIDE, S., A. J. PUPPALA, R. WILLIAMMEE. 2010. Assessing recycled/secondary materials as pavement bases. **Proceedings of the Institution of Civil Engineers Ground Improvement**, 163 (1): 3–12.

SINGH, S., G. D. R. R.N. 2020. Laboratory and Field Evaluation of RAP for Cement Concrete Pavements. **Journal of Transportation Engineering Part B Pavements**, 142 (2).

SINGH, S., G. D. RANSINCHUNG, S. DEBBARMA, AND P. KUMAR. 2018. Utilization of reclaimed asphalt pavement aggregates containing waste from Sugarcane Mill for production of concrete mixes. **Journal of Cleaner Production**, 174: 42–52.

SINGH, S., G. D. RANSINCHUNG, AND P. KUMAR. 2017. Effect of mineral admixtures on fresh, mechanical and durability properties of RAP inclusive concrete. **Construction and Building Materials**, 156: 19–27.

STIMILLI, A., G. FERROTTI, A. GRAZIANI, AND F. CANESTRARI. 2013. Performance evaluation of a cold-recycled mixture containing high percentage of reclaimed asphalt. **Road Materials and Pavement Design**, 14: 149–161.

STURM, P., G. J. G. GLUTH, H. J. H. BROUWERS, H. C. KÜHNE. 2016. Synthesizing one-part geopolymers from rice husk ash. **Construction and Building Materials**, 124: 961–966.

SUKPRASERT, S., M. HOY, S. HORPIBULSUK, A. ARULRAJAH, A. S. A. RASHID, R. NAZIR. 2021. Fly ash based geopolymer stabilisation of silty clay/blast furnace slag for subgrade applications. **Road Materials and Pavement Design**, 22 (2): 357–371. Taylor & Francis.

SYED, M., A. GUHARAY, D. GOEL. 2022. Strength characterisation of fiber reinforced expansive subgrade soil stabilized with alkali activated binder. **Road Materials and Pavement Design**, 23 (5): 1037–1060.

TABYANGA, W., C. SUKSIRIPATTANAPONG, C. PHETCHUAY, C. LAKSANAKIT, N. CHUSILP. 2021. Evaluation of municipal solid waste incineration fly ash based geopolymer for stabilised recycled concrete aggregate as road material. **Road Materials and Pavement Design**.

TAHA, R., A. AL-HARTHY, K. AL-SHAMSI, M. AL-ZUBEIDI. 2002. Cement Stabilization of Reclaimed Asphalt Pavement Aggregate for Road Bases and Subbases. **Journal of Materials in Civil Engineering**, 14 (3): 239–245.

TAKEDA, H., S. HASHIMOTO, H. YOKOYAMA, S. HONDA, Y. IWAMOTO. 2013. Characterization of Zeolite in Zeolite-Geopolymer Hybrid Bulk Materials Derived from Kaolinitic Clays. **Materials (Basel)**., 6 (5): 1767–1778.

TAYEH, B. A., A. M. ZEYAD, I. S. AGWA, M. AMIN. 2021. Effect of elevated temperatures on mechanical properties of lightweight geopolymer concrete. **Case Studies in Construction Materials**, 15 (August): e00673.

TCHAKOUTÉ, H. K., C. H. RÜSCHER, S. KONG, E. KAMSEU, C. LEONELLI. 2016. Geopolymer binders from metakaolin using sodium waterglass from waste glass and rice husk ash as alternative activators: A comparative study. **Construction and Building Materials**, 114: 276–289.

TONG, K. T., R. VINAI, M. N. SOUTSOS. 2018. Use of Vietnamese rice husk ash for the production of sodium silicate as the activator for alkali-activated binders. **Journal of Cleaner Production**, 201: 272–286.

TONINI DE ARAÚJO, M., S. TONATTO FERRAZZO, G. J. JORDI BRUSCHI, N. C. CONSOLI. 2021. Mechanical and Environmental Performance of Eggshell Lime for Expansive Soils Improvement. **Transportation Geotechnics**, 31 (October).

TORRES-CARRASCO, M., J. G. PALOMO, F. PUERTAS. 2014. Sodium silicate solutions from dissolution of glasswastes. Statistical analysis. **Materiales de construcción**, 64 (314).

TORRES-CARRASCO, M., F. PUERTAS. 2015. Waste glass in the geopolymer preparation. Mechanical and microstructural characterisation. **Journal of Cleaner Production**, 90: 397–408.

USEPA. 2022. Ground water and drinking water: national primary drinking water regulations. Accessed July 15, 2022.

VILLAQUIRÁN-CAICEDO, M. A., R. MEJIA DE GUTIÉRREZ, N. GALLEGO. 2017. A novel MK-based geopolymer composite activated with rice husk ash and KOH: performance at high temperature. **Materiales de construcción**, 67: 1–13.

WIRTGEN GMBH. 2012. “Wirtgen Cold Recycling Technology.”

ZHUANG, X. Y., L. CHEN, S. KOMARNENI, C. H. ZHOU, D. S. TONG, H. M. YANG, W. H. YU, AND H. WANG. 2016. Fly ash-based geopolymer: Clean production, properties and applications. **Journal of Cleaner Production**, 125: 253–267.

REFERÊNCIAS ITEM 3.5

AAPA. Reclaimed Asphalt Pavement (RAP) Management Plan. **Australian Asphalt Pavement Association**, 2018.

ABDULKAREEM, M. *et al.* Environmental and economic perspective of waste-derived activators on alkali-activated mortars. **Journal of Cleaner Production**, v. 280, p. 124651, 2021.

ABNT. NBR 10004: Resíduos sólidos - Classificação. **Associação Brasileira de Normas Técnicas**, 2004a.

___. NBR 10005: Procedimento para obtenção de extrato de lixiviado de resíduos sólidos. **Associação Brasileira de Normas Técnicas**, p. 16, 2004b.

___. NBR NM 53 : Agregado graúdo - Determinação de massa específica, massa específica aparente e absorção de água. **Associação Brasileira de Normas Técnicas**, 2009a.

___. NBR NM 52: Agregados miúdo - Determinação da massa específica e massa específica aparente. **Associação Brasileira de Normas Técnicas**, 2009b.

___. NBR 10006: Procedimento para obtenção de extreto de solubilizado de resíduos sólidos. **Associação Brasileira de Normas Técnicas**, p. 1–14, 2009c.

___. NBR 7222: Concreto e argamassa - Determinação da resistência à tração por compressão diametral de corpos de prova cilíndricos. **Associação Brasileira de Normas Técnicas**, 2011.

___. NBR 12253: Solo-cimento - Dosagem para emprego como camada de pavimento. **Associação Brasileira de Normas Técnicas**, 2012.

ADESANYA, E. *et al.* Opportunities to improve sustainability of alkali-activated materials: A review of side-stream based activators. **Journal of Cleaner Production**, v. 286, p. 125558, 2021.

AL-HDABI, A. Laboratory investigation on the properties of asphalt concrete mixture with Rice Husk Ash as filler. **Construction and Building Materials**, v. 126, p. 544–551, 2016.

AL-QADI, I. L.; QAZI, A.; CARPENTER, S. H. Impact of High RAP Content on Structural and Performance Properties of Asphalt Mixtures. **Research Report FHWA-A-ICT-12-002, Illinois Center for Transportation, Rantoul.**, 2012.

ALVARO, G. *et al.* Laboratory fatigue life of cemented materials in Australia. **Road Materials and Pavement Design**, v. 14, n. 3, p. 518–536, 2013.

ARULRAJAH, A. *et al.* Modulus of rupture evaluation of cement stabilized recycled glass/recycled concrete aggregate blends. **Construction and Building Materials**, v. 84, p. 146–155, 2015.

ASTM. ASTM C 496/C 496M - 11 Standard Test Method for Splitting Tensile Strength of Cylindrical Concrete. **ASTM International, West Conshohocken**, [s.d.].

___. D698-12: Standard Test Methods for Laboratory Compaction Characteristics of Soil Using Standard Effort (12 400 ft-lbf/ft3 (600 kN-m/m3)). **American Society for Testing and Materials**, 2012.

___. D854: Standard Test Methods for Specific Gravity of Soil Solids by Water Pycnometer.

American Society for Testing and Materials, p. 1–8, 2014.

___. D2166/D2166M: Standard Test Method for Unconfined Compressive Strength of Cohesive Soil. **American Society for Testing and Materials**, p. 1–7, 2016.

___. D7928: Standard Test Method for Particle-Size Distribution (Gradation) of Fine-Grained Soils Using the Sedimentation (Hydrometer) Analysis. **ASTM International**, 2017a.

___. D2487: Standard Practice for Classification of Soils for Engineering Purposes (Unified Soil Classification System). **American Society for Testing and Materials**, p. 1–5, 2017b.

___. D2172/D2172M: Standard Test Methods for Quantitative Extraction of Bitumen From Bituminous Paving Mixtures. **American Society for Testing and Materials**, 2018.

ATHIRA, V. S. *et al.* Agro-waste ash based alkali-activated binder : Cleaner production of zero cement concrete for construction. **Journal of Cleaner Production**, v. 286, p. 125429, 2021.

AVIRNENI, D.; PEDDINTI, P. R. T.; SARIDE, S. Durability and long term performance of geopolymer stabilized reclaimed asphalt pavement base courses. **Construction and Building Materials**, v. 121, p. 198–209, 2016.

AWOYERA, P.; ADESINA, A. A critical review on application of alkali activated slag as a sustainable composite binder. **Case Studies in Construction Materials**, v. 11, p. e00268, 2019.

BARRETO TORRES, P. R. *et al.* Análise do comportamento mecânico de misturas asfálticas recicladas modificadas com a adição de óleo vegetal residual. **Transportes**, v. 30, n. 1, p. 2585, 2022.

BERNAL, S. A. *et al.* Activation of metakaolin/slag blends using alkaline solutions based on chemically modified silica fume and rice husk ash. **Waste and Biomass Valorization**, v. 3, n. 1, p. 99–108, 2012.

BILAL, M. *et al.* Current state and barriers to the circular economy in the building sector: Towards a mitigation framework. **Journal of Cleaner Production**, v. 276, p. 123250, 2020.

BRUSCHI, G. J.; SANTOS, C. P. DOS; *et al.* Parameters controlling loss of mass and stiffness degradation of green stabilized bauxite tailings. **Proceedings of the Institution of Civil Engineers - Geotechnical Engineering**, p. 1–21, set. 2021.

BRUSCHI, G. J.; SANTOS, C. P. DOS; *et al.* Green Stabilization of Bauxite Tailings: Mechanical Study on Alkali-Activated Materials. **Journal of Materials in Civil Engineering**, v. 33, n. 11, p. 06021007, nov. 2021.

BRUSCHI, G. J. *et al.* Leaching assessment of cemented bauxite tailings through wetting and drying cycles of durability test. **Environmental Science and Pollution Research**, n. 0123456789, 2022.

CADAVID-GIRALDO, N.; VELEZ-GALLEGO, M. C.; RESTREPO-BOLAND, A. Carbon emissions reduction and financial effects of a cap and tax system on an operating supply chain in the cement sector. **Journal of Cleaner Production**, v. 275, p. 122583, 2020.

CONSOLI, N. C. *et al.* Key Parameters for Strength Control of Artificially Cemented Soils. **Journal of Geotechnical and Geoenvironmental Engineering**, v. 133, n. 2, p. 197–205, 2007.

___. Increasing density and cement content in stabilization of expansive soils: Conflicting or complementary procedures for reducing swelling? **Canadian Geotechnical Journal**, v. 58, n. 6, p. 866–878, jun. 2021.

ČUČEK, L.; JIŘÍ, J. K.; ZDRAVKO, K. A Review of Footprint analysis tools for monitoring impacts on sustainability. **Journal of Cleaner Production**, v. 34, p. 9–20, 2012.

DARKO, A.; CHAN, A. P. C. Critical analysis of green building research trend in construction journals. **Habitat International**, v. 57, p. 53–63, 2016.

DAVIDOVITS, J. Geopolymers and geopolymeric materials. **Journal of thermal analysis**, v. 35, p. 429–441, 1989.

DEBBARMA, S.; RANSINCHUNG, G. D.; SINGH, S. Feasibility of roller compacted concrete pavement containing different fractions of reclaimed asphalt pavement. **Construction and Building Materials**, v. 199, p. 508–525, 2019.

DIAMBRA, A. *et al.* Theoretical Derivation of Artificially Cemented Granular Soil Strength. **Journal of Geotechnical and Geoenvironmental Engineering**, v. 143, n. 5, 2017.

DISFANI, M. M. *et al.* Flexural beam fatigue strength evaluation of crushed brick as a supplementary material in cement stabilized recycled concrete aggregates. **Construction and Building Materials**, v. 68, p. 667–676, 2014.

EAPA. Asphalt the 100% Recyclable Construction Product—EAPA Position Paper. **European Asphalt Pavement Association**, 2014.

EDEH, J. E.; ONCHE, O. J. J.; OSINUBI, K. J. Rice Husk Ash Stabilization of Reclaimed Asphalt Pavement Using Cement As Additive. n. January 2015, p. 3863–3872, 2012.

ESA, M. R.; HALOG, A.; RIGAMONTI, L. Strategies for minimizing construction and demolition wastes in Malaysia. **Resources, Conservation and Recycling**, v. 120, p. 219–229, 2017a.

___. Developing strategies for managing construction and demolition wastes in Malaysia based on the concept of circular economy. **Journal of Material Cycles and Waste Management**, v. 19, n. 3, p. 1144–1154, 2017b.

FEDRIGO, W. *et al.* Flexural strength, stiffness and fatigue of cement-treated mixtures of reclaimed asphalt pavement and lateritic soil. **Road Materials and Pavement Design**, v. 22, n. 5, p. 1004–1022, 2021.

FESTUGATO, L. *et al.* Modelling tensile/compressive strength ratio of fibre reinforced cemented soils. **Geotextiles and Geomembranes**, v. 46, n. 2, p. 155–165, 2018.

GERALDO, R. H.; FERNANDES, L. F. R.; CAMARINI, G. Water treatment sludge and rice husk ash to sustainable geopolymer production. **Journal of Cleaner Production**, v. 149, p. 146–155, 2017.

HOY, M. *et al.* Strength and Microstructural Study of Recycled Asphalt Pavement: Slag Geopolymer as a Pavement Base Material. **Journal of Materials in Civil Engineering**, v. 30, n. 8, p. 04018177, 2018.

HOY, M.; HORPIBULSUK, S.; ARULRAJAH, A. Strength development of Recycled Asphalt Pavement - Fly ash geopolymer as a road construction material. **Construction and Building Materials**, v. 117, p. 209–219, 2016.

JALLU, M. *et al.* Flexural fatigue behavior of fly ash geopolymer stabilized-geogrid reinforced RAP bases. **Construction and Building Materials**, v. 254, p. 119263, 2020.

JIA, Y. *et al.* Degradation reliability modeling of stabilized base course materials based on a modulus decrement process. **Construction and Building Materials**, v. 177, p. 303–313, 2018.

JITSANGIAM, P. *et al.* Fatigue Assessment of Cement-Treated Base for Roads: An Examination of Beam-Fatigue Tests. **Journal of Materials in Civil Engineering**, v. 28, n. 10, p. 1–11, 2016.

KANG, X. *et al.* Chemically Stabilized Soft Clays for Road-Base Construction. **Journal of Materials in Civil Engineering**, v. 27, n. 7, p. 04014199, 2015.

KHAN, M. N. N. *et al.* Utilization of rice husk ash for sustainable construction: A review. **Research Journal of Applied Sciences, Engineering and Technology**, v. 9, n. 12, p. 1119–1127, 2015.

LLOYD, R. R. Accelerated ageing of geopolymers. *In*: **Geopolymers: Structures, Processing, Properties and Industrial Applications**. Geopolymer ed. [s.l: s.n.]. p. 139–166.

LONGHI, M. A. *et al.* **Geopolymers based on calcined kaolin sludge/ bottom ash blends and an alternative sodium silicate activator**34th Cement and Concrete Science Conference. **Anais**...2014

___. Valorisation of a kaolin mining waste for the production of geopolymers. **Journal of Cleaner Production**, 2016.

LUUKKONEN, T. *et al.* Comparison of alkali and silica sources in one-part alkali-activated blast furnace slag mortar. **Journal of Cleaner Production**, v. 187, n. March, p. 171–179, 2018.

MAHPOUR, A. Prioritizing barriers to adopt circular economy in construction and demolition waste management. **Resources, Conservation and Recycling**, v. 134, n. January, p. 216–227, 2018.

MANDAL, T. *et al.* Protocol for testing flexural strength, flexural modulus, and fatigue failure of cementitiously stabilized materials using third-point flexural beam tests. **Geotechnical Testing Journal**, v. 39, n. 1, 2016.

MANDAL, T.; EDIL, T. B.; TINJUM, J. M. Study on flexural strength, modulus, and fatigue cracking of cementitiously stabilised materials. **Road Materials and Pavement Design**, v. 19, n. 7, p. 1546–1562, 2018.

MEJÍA, J. M.; MEJÍA DE GUTIÉRREZ, R.; PUERTAS, F. Ceniza de cascarilla de arroz como fuente de sílice en sistemas cementicios de ceniza volante y escoria activados alcalinamente. **Materiales de Construccion**, v. 63, n. 311, p. 361–375, 2013.

MENEGAKI, M.; DAMIGOS, D. A review on current situation and challenges of construction and demolition waste management. **Current Opinion in Green and Sustainable Chemistry**, v. 13, p. 8–15, 2018.

MOHAMMADINIA, A. *et al.* Alkali-activation of fly ash and cement kiln dust mixtures for stabilization of demolition aggregates. **Construction and Building Materials**, v. 186, p. 71–78, 2018.

___. Flexural fatigue strength of demolition aggregates stabilized with alkali-activated

calcium carbide residue. **Construction and Building Materials**, v. 199, p. 115–123, 2019.

MOHAPATRA, S. S. *et al.* A review on waste-derived alkali activators for preparation of geopolymer composite. **Materials Today: Proceedings**, v. 56, p. 440–446, 2022.

NASIR, M. H. A. *et al.* Comparing linear and circular supply chains: A case study from the construction industry. **International Journal of Production Economics**, v. 183, p. 443–457, 2017.

NÚÑEZ-CACHO, P. *et al.* New Measures of Circular Economy Thinking In Construction Companies. **Journal of EU Research in Business**, v. 2018, p. 1–16, 2018.

OLUKOLAJO, M. A.; OYETUNJI, A. K.; OLULEYE, I. B. Covid-19 protocols: assessing construction site workers compliance. **Journal of Engineering Design and Technology**, v. 20, n. 1, p. 115–131, 2022.

PALANKAR, N.; RAVI SHANKAR, A. U.; MITHUN, B. M. Investigations on Alkali-Activated Slag/Fly Ash Concrete with steel slag coarse aggregate for pavement structures. **International Journal of Pavement Engineering**, v. 18, n. 6, p. 500–512, 2017.

PEREIRA DOS SANTOS, C. *et al.* Stabilization of gold mining tailings with alkali-activated carbide lime and sugarcane bagasse ash. **Transportation Geotechnics**, v. 32, n. December 2021, 2022a.

___. Stabilization of gold mining tailings with alkali-activated carbide lime and sugarcane bagasse ash. **Transportation Geotechnics**, v. 32, n. November 2021, p. 100704, jan. 2022b.

PHOO-NGERNKHAM, T. *et al.* Compressive strength, Bending and Fracture Characteristics of High Calcium Fly Ash Geopolymer Mortar Containing Portland Cement Cured at Ambient Temperature. **Arabian Journal for Science and Engineering**, v. 41, n. 4, p. 1263–1271, 2015.

QUEIRÓZ, L. C. *et al.* Alkali-activated system of carbide lime and rice husk for granular soil stabilization. **Proceedings of the Institution of Civil Engineers - Ground Improvement**, p. 1–37, 2022.

ROCHA SEGUNDO, I. G. DA *et al.* Misturas asfálticas recicladas a quente com incorporação de elevado percentual de fresado como alternativa para camada de módulo elevado. **Transportes**, v. 24, n. 4, p. 85, 2016.

S, B.; O. D, A.; C.W.W, N. Feasibility of construction demolition waste for unexplored geotechnical and geo-environmental applications- a review. **Construction and Building Materials**, v. 356, n. June, 2022.

SABITA. Use of Reclaimed Asphalt in the Production of AsphaltMANUAL 36/TRH 21. **Southern African Bitumen Association**, 2019.

SACHET, T. *et al.* Investigation of Resistance and Fracture Parameters for Compacted Concrete with Incorporation of Reclaimed Asphalt Pavement. **International Journal of Pavements**, v. 10, n. 1-2–3, p. 83–94, 2011.

SARIDE, S.; AVIRNENI, D.; JAVVADI, S. C. P. Utilization of Reclaimed Asphalt Pavements in Indian Low-Volume Roads. **Journal of Materials in Civil Engineering**, v. 28, n. 2, p. 1–10, 2016.

SIDDIQUE, R. **Waste Materials and By-Products in Concrete**. Springer P ed. Berlin: [s.n.].

SINGH, S. *et al.* Utilization of reclaimed asphalt pavement aggregates containing waste from Sugarcane Mill for production of concrete mixes. **Journal of Cleaner Production**, v. 174, p. 42–52, 2018.

STURM, P. *et al.* Synthesizing one-part geopolymers from rice husk ash. **Construction and Building Materials**, v. 124, p. 961–966, 2016.

SUBHY, A. *et al.* Binder and mixture fatigue performance of plant-produced road surface course asphalt mixtures with high contents of reclaimed asphalt. **Sustainability (Switzerland)**, v. 11, n. 13, 2019.

SUEBSUK, J.; SUKSAN, A. Strength assessment of cement treated soil-reclaimed asphalt pavement (RAP) mixture. **International Journal of GEOMATE**, v. 6, n. 2, p. 878–884, 2014.

SYED, M.; GUHARAY, A.; GOEL, D. Strength characterisation of fiber reinforced expansive subgrade soil stabilized with alkali activated binder. **Road Materials and Pavement Design**, v. 23, n. 5, p. 1037–1060, 2022.

TABYANGA, W. *et al.* Evaluation of municipal solid waste incineration fly ash based geopolymer for stabilised recycled concrete aggregate as road material. **Road Materials and Pavement Design**, 2021.

TAHA, R. *et al.* Cement Stabilization of Reclaimed Asphalt Pavement Aggregate for Road Bases and Subbases. **Journal of Materials in Civil Engineering**, v. 14, n. 3, p. 239–245, 2002.

TAKEDA, H. *et al.* Characterization of Zeolite in Zeolite-Geopolymer Hybrid Bulk Materials Derived from Kaolinitic Clays. **Materials**, v. 6, n. 5, p. 1767–1778, 2013.

TCHAKOUTÉ, H. K. *et al.* Geopolymer binders from metakaolin using sodium waterglass from waste glass and rice husk ash as alternative activators: A comparative study. **Construction and Building Materials**, v. 114, p. 276–289, 2016.

THEYSE, H. L.; BEER, M. DE; RUST, F. C. Overview of South African mechanistic pavement design method. **Transportation Research Record**, n. 1539, p. 6–17, 1996.

TONG, K. T.; VINAI, R.; SOUTSOS, M. N. Use of Vietnamese rice husk ash for the production of sodium silicate as the activator for alkali-activated binders. **Journal of Cleaner Production**, v. 201, p. 272–286, 2018.

TONINI DE ARAÚJO, M. *et al.* Mechanical and Environmental Performance of Eggshell Lime for Expansive Soils Improvement. **Transportation Geotechnics**, v. 31, n. November, p. 100681, 2021.

TORRES-CARRASCO, M. *et al.* Alkali activated slag cements using waste glass as alternative activators. Rheological behaviour. **Boletin de la Sociedad Espanola de Ceramica y Vidrio**, v. 54, n. 2, p. 45–57, 2015.

WIRTGEN GMBH. Wirtgen Cold Recycling Technology. 2012.

ZHENG, X. *et al.* Review of the application of social network analysis (SNA) in construction project management research. **International Journal of Project Management**, v. 34, n. 7, p. 1214–1225, 2016.

ZHUANG, X. Y. *et al.* Fly ash-based geopolymer: Clean production, properties and applications. **Journal of Cleaner Production**, v. 125, p. 253–267, 2016.

UPF
UNIVERSIDADE
DE PASSO FUNDO

UPF Campus I - BR 285, São José
Passo Fundo - RS - CEP: 99052-900
(54) 3316 7000 - www.upf.br